Extracellular Phosphorylation of the Amyloid β-Peptide Promotes Aggregation

Dissertation

zur

Erlangung des Doktorgrades (Dr. rer. nat.)

der

Mathematisch-Naturwissenschaftlichen Fakultät

der

Rheinischen Friedrich-Wilhelms-Universität Bonn

vorgelegt von

Sathish Kumar H.S.

aus

Chamarajanagar, Indien

– Bonn, 2009 –

Angefertigt mit Genehmigung der Mathematisch-
Naturwissenschaftlichen Fakultät der Rheinischen Friedrich-Wilhelms-
Universität Bonn

Gutachter

1. Prof. Dr. rer. nat. Jochen Walter
2. Prof. Dr. rer. nat. Michael Hoch

Eingereicht am: 08. April 2009

Tag der Promotion: 01. July 2009

Die vorliegende Arbeit wurde in der Zeit von Februar 2005 bis April 2009 in der Klinik und Poliklinik für Neurologie, Molekulare Zellbiologie, Universitätsklinikum Bonn, Sigmund-Freud-Str. 25, Bonn unter Leitung von Prof. Dr. Jochen Walter durchgeführt.

LIST OF FIGURES:

LIST OF TABLES

ABBREVIATIONS

µg	Microgram
µl	Microlitre
µM	Micro mol
α-secretase	Alpha Secretase
[γ^{32}P]ATP	gamma radiolabeled ATP
°C	Grad Celsius
a.u.	Atomic units
aa	Amino acid
AC	Adenylate cyclase
AD	Alzheimer's Disease
ADAM	A disintegrin and metalloprotease
ADDLs	Amyloid Derived Diffusible Ligands
AFM	Atomic force microscopy
AICD	APP intracellular domain
ALS	Amyotrophic lateral sclerosis
AMP	Adenosine monophosphate
APLPs	Amyloid precursor like proteins
Apo E	Apolipoprotein E
APP	β-Amyloid precursor protein
APP-CTFs/CTFs	C-terminal fragments of APP
APPsβ	Soluble APP generated by β-secretase cleavage
APPsβ	Soluble APP generated by β-secretase cleavage
APS	Ammonium persulphate
ATP	Adenosine 5´-Triphosphate
Aβ	Amyloid β peptide
$Aβ_{40}$	Amyloid β peptide 1-40

$A\beta_{42}$	Amyloid β peptide 1-42
BACE-1	β-site APP-cleaving enzyme-1; β-secretase
BSA	Bovine serum albumin
cAMP	Cyclic adenosine mono phosphate
CD	Circular Dichroism
cdc2	Cyclin-dependent protein kinase-2
CDK	Cyclin-dependent kinase
CHO	Chinese Hamster Ovary cell line
CK1	Casein Kinase 1
CK2	Casein Kinase 2
CO_2	Carbon dioxide
CR	Congo Red
CSF	Cerebrospinal fluid
CTFα; C83; α-stub	C-terminal fragment of APP generated by α-secretase cleavage
CTFβ; C99; β-stub	C-terminal fragment of APP generated by β-secretase cleavage
DLS	Dynamic Light Scattering
Ecto-PKs	Ecto-protein kinases
ELISA	Enzyme-linked Immunosorbent Assay
Exo-PKs	Exo-protein kinases
FAD	Familial Alzheimer's Disease
FCS	Foetal calf serum
GFAP	Glial fibrillary acidic protein
GSK-3	Glycogen Synthase Kinase 3
H.M.W.	High Molecular Weight
HD	Huntington's disease
HEK293	Human Embryonic Kidney 293 Cells
hrs	Hours
ICDs	Intracellular C-terminal domains
IF	Immunofluoresence
IHC	Immunohistochemistry
KPI	Kunitz protease inhibition
LC-MS	Liquid Chromatography and Mass spectroscopy
LTD	Long-term depression
LTP	Long-term potentiation
M.W.	Molecular weight
min	Minute
NFTs	Neurofibrillary tangles
nm	Nanometer
NMR	Nuclear Magnetic Resonance
NMR	Nuclear magnetic resonance spectroscopy
npAβ	Non phosphorylated Amyloid β peptide
NPs	Neuritic plaques
NTs	Neurophil threads
p3	Product of APP generated by α- and β- secretase cleavage
pAβ	Phosphorylated Amyloid β peptide
pAβ(Ser-26)	Amyloid β peptide phosphorylated at Serine-26 residue
pAβ(Ser-8)	Amyloid β peptide phosphorylated at Serine-8 residue
PBS	Phosphate buffered saline
PD	Parkinson's disease
PDBu	Phorbol 12,13-dibutyrate
PHFs	Paired helical filaments
PKA	Protein kinases A

PKA-Cα1	PKA catalytic subunit alpha-1
PKA-Cβ1	PKA catalytic subunit beta-1
PKC	Protein kinase C
PKs	Protein kinases
PS-1/2	Presenilin 1/2
R_H	Hydrodynamic Radius
RT	Room temperature
SAP	Shrimp alkaline phosphatase
SDS	Sodium dodecyl sulphate
SDS-PAGE	Sodium dodecyl sulfate-polyacrylamide gel electrophoresis
TEM	Transmission Electron Microscopy
tg	Transgenic
ThT	Thioflavin-T
TMD	Trans-membrane domain
TSE	Transmissible spongiform encephalopathies
WB	Western-blotting
www	World Wide Web
β-secretase	Beta Secretase
γ-secretase	Gamma Secretase

AMINO ACIDS, ABBREVIATIONS AND SINGLE LETTER CODE

Alanine	Ala	A
Arginine	Arg	R
Asparagine	Asn	N
Aspartic acid	Asp	D
Cysteine	Cys	C
Glutamine	Gln	Q
Glutamic acid	Glu	E
Glycine	Gly	G
Histidine	His	H
Isoleucine	Ile	I
Leucine	Leu	L
Lysine	Lys	K
Methionine	Met	M
Phenylalanine	Phe	F
Proline	Pro	P
Serine	Ser	S
Threonine	Thr	T
Tryptophan	Trp	W
Tyrosine	Tyr	Y
Valine	Val	V
Any amino acid		X

Summary/Abstract

The most common characteristics of diverse age-related neurodegenerative diseases are aggregation and accumulation of the misfolded protein in the brain. All of the known neurodegenerative diseases are associated with folding of proteins in fatal ways which finally lead to neuronal death. Alzheimer's disease (AD) is one of these protein conformational diseases characterized by two major neuropathological hallmarks: extracellular accumulation of amyloid-β (Aβ) peptide in the form of plaques and intracellular tangles consisting of hyperphosphorylated tau protein. AD associated extracellular amyloid plaques contain aggregated forms of the Aβ in the brain derived from the proteolytic processing of the amyloid precursor protein (APP) by β- and γ-secretases. The combined activity of β-and γ-secretases results in the secretion of Aβ into conditioned media of cultured cells or extracellular fluids of the brain or the periphery. Secreted Aβ includes two major variants with 40 (Aβ40) or 42 (Aβ42) amino acids. The elongated variant Aβ42 shows an increased aggregation as compared to Aβ40. Aggregation of Aβ is believed to be critical for its neurotoxicity and pathogenesis of AD. This is supported by the identification of mutations in APP and presenilins 1 and 2 that increase Aβ generation or more importantly, the generation of Aβ42 with an increased propensity for aggregation. However, such mutations are very rare and account for only a very small number of cases (<5%). The mechanisms that increase the aggregation and accumulation of Aβ and cause the much more common sporadic forms of AD (>95%) are largely unknown. Thus, one could assume that the aggregation of Aβ in AD is induced by unknown post-translational modification. Therefore, identification of such modifications and molecular mechanisms that promote the aggregation of wild-type Aβ in the brain could play important roles in the pathogenesis of sporadic AD.

The purpose of the thesis work was to investigate whether Aβ could undergo phosphorylation and to study the extracellular phosphorylation of Aβ and its role in Aβ aggregation. I first carried out *in silico* analysis to identify the potential phosphorylation sites in Aβ. *In vitro* phosphorylation experiments were carried out using synthetic Aβ variants and purified kinases to verify the identified phosphorylation sites and the protein kinases (PKs). The results from the *in silico* analysis indicate that Aβ contains two putative phosphorylation sites (Ser-8 and Ser-26) and the neighboring amino acids can conform the consensus sequences for variety of PKs. *In vitro* phosphorylation experiments further confirmed that the Aβ40 and Aβ42 can undergo phosphorylation by the respective PKs.

The second set of experiments were performed to identify the PK expression in human AD brain and to study the mechanism of Aβ phosphorylation by extracellular PKs which are present at the surface of cultured cells. Several PKs are present at the surface of living cells or secreted into extracellular fluids and can phosphorylate cell-surface proteins and soluble extracellular substrates. *In vivo* and *ex vivo* phosphorylation experiments were carried out using intact cultured cells, mouse cerebellar neurons and in cerebrospinal fluid (CSF) of AD patients to identify and characterize the extracellular PKs activity. The extracellular protein kinase A (PKA) activity was identified in cultured cells and primary neurons, which could phosphorylate the extracellular Aβ. In addition, the presence of PKA like kinase activity was identified in CSF of AD patients. These results suggest that Aβ can undergo phosphorylation extracellularly by PKA-like kinase.

The third part of the work elucidates the effect of phosphorylation on Aβ folding, self-assembly and its aggregation. Increasing evidence shows that, despite the generic nature of amyloid structures, the propensity to form aggregates is strongly influenced by the nature of the amino acid side chains along with the properties of the environment in which aggregation occurs. Therefore, it was hypothesized that phosphorylation of Aβ could influence the structural transition resulting in alteration of Aβ folding, assembly and its aggregation. Different biophysical studies were carried out using synthetic phosphorylated and non-phosphorylated variants of Aβ peptides to document the effect of phosphorylation on Aβ misfolding, oligomerization and aggregation. The results indicate that phosphorylation increases the propensity of Aβ to adopt a β-sheet conformation, resulting in faster self-assembly and thereby promoting oligomerization. These small phosphorylated Aβ (pAβ) oligomeric aggregates could serve as a seed or nucleus and increased the rate of aggregation.

The fourth part of the thesis work documents the occurrence of phosphorylated Aβ and its preferential aggregation and deposition *in vivo.* To assess the phosphorylation of Aβ *in vivo*, the polyclonal phosphorylation-state Aβ specific antibody was generated and characterized. Biochemical and immunohistological staining were carried out using brains of AD transgenic (*tg*) mice and human AD patients employing phosphorylation-state Aβ specific antibody. The specific detection of phosphorylated and non-phosphorylated Aβ species in *tg* mice and human AD brain indicates the enrichment of pAβ in oligomeric assemblies and preferential aggregation of phosphorylated Aβ *in vivo*. The quantitative analysis of pAβ in aged *tg* mice revealed that about 20-25% of extracted monomeric Aβ is in a phosphorylated state. This finding is further supported by the detection of pAβ in neuritic plaques of AD patients which could strongly argue in favour of a critical role of pAβ in AD-related neurodegeneration.

In summary, the undertaken study shows that extracellular Aβ is phosphorylated by protein kinases present at the cell surface and in the cerebrospinal fluid of the human brain. The phosphorylation at serine residue 8 increases the propensity of Aβ to adopt β-sheet conformation and promotes the formation of small oligomeric aggregates that could seed aggregation into larger oligomeric and fibrillar assemblies. The specific detection of phosphorylated and non-phosphorylated Aβ species in *tg* mice and human AD brain indicates the preferential aggregation of phosphorylated Aβ *in vivo*. Thus, the present work highlights the importance of extracellular phosphorylation of Aβ which can lead to misfolding and may promote soluble oligomeric and fibrillar aggregate formation and thereby trigger the pathogenesis of sporadic AD. Hence, targeting extracellular phosphorylation of Aβ could be explored for therapeutic or preventive strategies to decrease Aβ aggregation in sporadic AD. In addition, the detection of phosphorylated and non-phosphorylated Aβ in biological fluids could also be explored for evaluation as biomarkers. Finally, the demonstration of protein kinases in human CSF might also stimulate further studies on the physiological and pathophysiological implications of the extracellular phosphorylation of peptides and proteins in the human brain. Based on the current findings, if more conclusive evidences can be generated employing transgenic animal models, which might help to understand the physiological and pathophysiolgical role of pAβ in AD.

1. INTRODUCTION

1.1. Protein misfolding, aggregation and age-related neurodegenerative diseases

Diverse human disorders, including most neurodegenerative diseases are thought to arise from misfolding and aggregation of proteins. The pathology of these diseases is believed to develop from the effect of intra- or extracellular aggregates of misfolded proteins (Agorogiannis et al., 2004; Selkoe, 2003; Soto and Estrada, 2008). The information required for a polypeptide chain to fold correctly into a three-dimensional structure ('native structure') which allows it to carry out intricate biological functions is encoded in its primary amino acid sequence (Anfinsen, 1973; Fawzi et al., 2008; Herczenik and Gebbink, 2008). The amino acid sequence that gives rise to a structural ensemble are thermodynamically stable at physiological pressures, temperatures and solution conditions existent in the normal cellular or extracellular environment. Destabilizing sequence mutations, chemical modifications or changes in protein concentration and solution environment of the protein can shift the equilibrium from the native state in favor of aggregates, i.e., misfolded states (Dobson, 2003; Goedert and Spillantini, 2006; Cellmer et al., 2007; Finder and Glockshuber, 2007; Roychaudhuri et al., 2009). The misfolded aggregates that escape the cellular quality-control mechanisms such as chaperone assisted refolding, proteosomal degradation, autophagy and ER-associated degradation (ERAD) is the underlying pathology of a wide range diseases (Kaganovich et al., 2008; Dobson, 2003; Gregersen et al., 2006). Aggregation of proteins could also impair the function of the ubiquitin–proteasome system (UPS), which in turn increases the production of aggregated proteins (Bence et al., 2001; Forloni et al., 2002; Gregersen et al., 2005). The protein aggregates can occur in various different structural appearances with intermediates (oligomers) varying from unordered amorphous aggregates to highly ordered fibrils that are called amyloid (Yoshiike et al., 2008). They are generally 'enriched with' cross-β structures (Fig. 1). These misfolded protein structures (oligomers, amorphous aggregates, protofibrils and fibrils) have been found to be associated with various disease states including age-related neurodegenerative diseases (Selkoe, 2003; Santucci et al., 2008; Winklhofer et al., 2008; Selkoe, 2004b). Insoluble protein deposits contribute to the pathology of a variety of human brain diseases (Table 1), including the amyloidoses (Fink, 1998). They can appear as amorphous structures like inclusion bodies or as ordered fibers (straight, unbranched, 10 nm wide fibrils) such as amyloid plaques and prion particles (Davies et al., 1999; Soto et al., 2006; Prusiner, 1998; McLaurin et al., 2000).

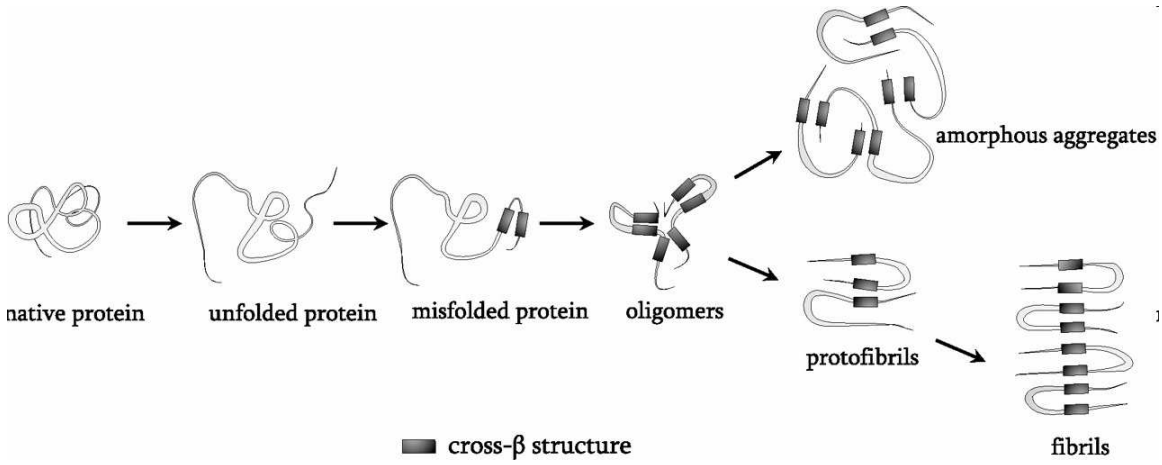

Fig. 1: Protein misfolding and aggregation.
Each protein has an ensemble of possible structures. Proteins undergo conformational changes under certain circumstances and results in unfolding and partial misfolding that is associated with the tendency to aggregate. During aggregation, proteins can obtain a range of different structural appearances, which are generally enriched with cross-β sheet structure, including intermediates varying from unordered oligomers, amorphous aggregates to ordered protofibrils and fibrils that are called amyloid (Figure adapted from Herczenik and Gebbink, 2008).

Age-related neurodegenerative diseases are some of the most debilitating disorders, affecting thinking, skilled movements, feelings, emotions, cognition, memory and other abilities (Table 1). This pathologically diverse group of diseases includes Alzheimer's disease (AD) and Parkinson's disease (PD) as well as rarer disorders such as Huntington's disease (HD), amyotrophic lateral sclerosis (ALS), spinocerebellar ataxias and transmissible spongiform encephalopathies (TSE). Despite their differences in clinical manifestation and disease progression, these disorders share some common features such as, i) their appearance in later life, ii) the neuronal loss and synaptic abnormalities and iii) the presence of cerebral deposits of misfolded protein aggregates. Compelling data from biochemical, neuropathological and genetic studies identifying the mutations in the respective disease-related proteins that are found in AD, PD, HD, ALS and TSE respectively, support the involvement of protein misfolding, aggregation and amyloid formation (Fig. 2). The fundamental cause of these diseases is the cellular inability to degrade misfolded and damaged proteins and formation of cytotoxic intracellular and extracellular oligomers and aggregates. The pathology in these diseases is predominantly determined by the cell damage associated with the aggregation process, thus exhibiting what can be considered a "gain-of-toxic function" or "loss-of-biological function" (Gregersen et al., 2006; Winklhofer et al., 2008). In support of this hypothesis, several pathological and clinical features have been observed in transgenic animal models that

develop protein aggregates (Hsiao et al., 1990; Gurney, 1994; Games et al., 1995; Schenk et al., 1995; Games et al., 1995; Mangiarini et al., 1996; Davies et al., 1997; Masliah et al., 2000; Gotz and Ittner, 2008; Sathasivam et al., 1999; Davies et al., 1999; Price DL, 2000; Chapman et al., 1999).

Table 1: Clinical, pathological and biochemical features of neurodegenerative disorders characterized by the deposition of misfolded abnormal protein aggregates.

Disease	Toxic protein involved	Cellular location of toxic aggregates	Affected brain regions	Clinical features
Alzheimer's disease (AD)	Amyloid-β (Aβ) and Tau	Extracellular Aβ plaques and Intracellular tangles	Cerebral cortex, Hippocampus, entorhinal cortex and altered vessels	Progressive dementia
Parkinson's disease (PD)	α-Synuclein	Cytoplasmic (Lewy bodies)	Substantia nigra, hypothalamus	Movement disorder and dementia
Huntington's diseases (HD)	Huntington	Nuclear and Cytoplasmic inclusions	Striatum, cerebral cortex	Dementia, motor and psychiatric problems
Amylotrophic lateral sclerosis (ALS)	Superoxide dismutase	Cytoplasmic Bunina bodies	Motor cortex, brainstem	Movement disorder
Transmissible spongiform encephalopathies (TSE)	Prion protein	Extracellular prions plaques	Various regions depending on the disease	Dementia, ataxia, psychiatric problems or insomnia
Neurodegenerative Tauopathies For eg., Progressive supranuclear palsy (PSP), Corticobasal degeneration (CBD), Pick's disease (PiD) and Frontotemporal dementia (FTD)	Tau protein	Intracellular abnormal filamentous tau inclusions	Different regions of the brain depending on the disease	Dementia, brain degeneration, movement disorder

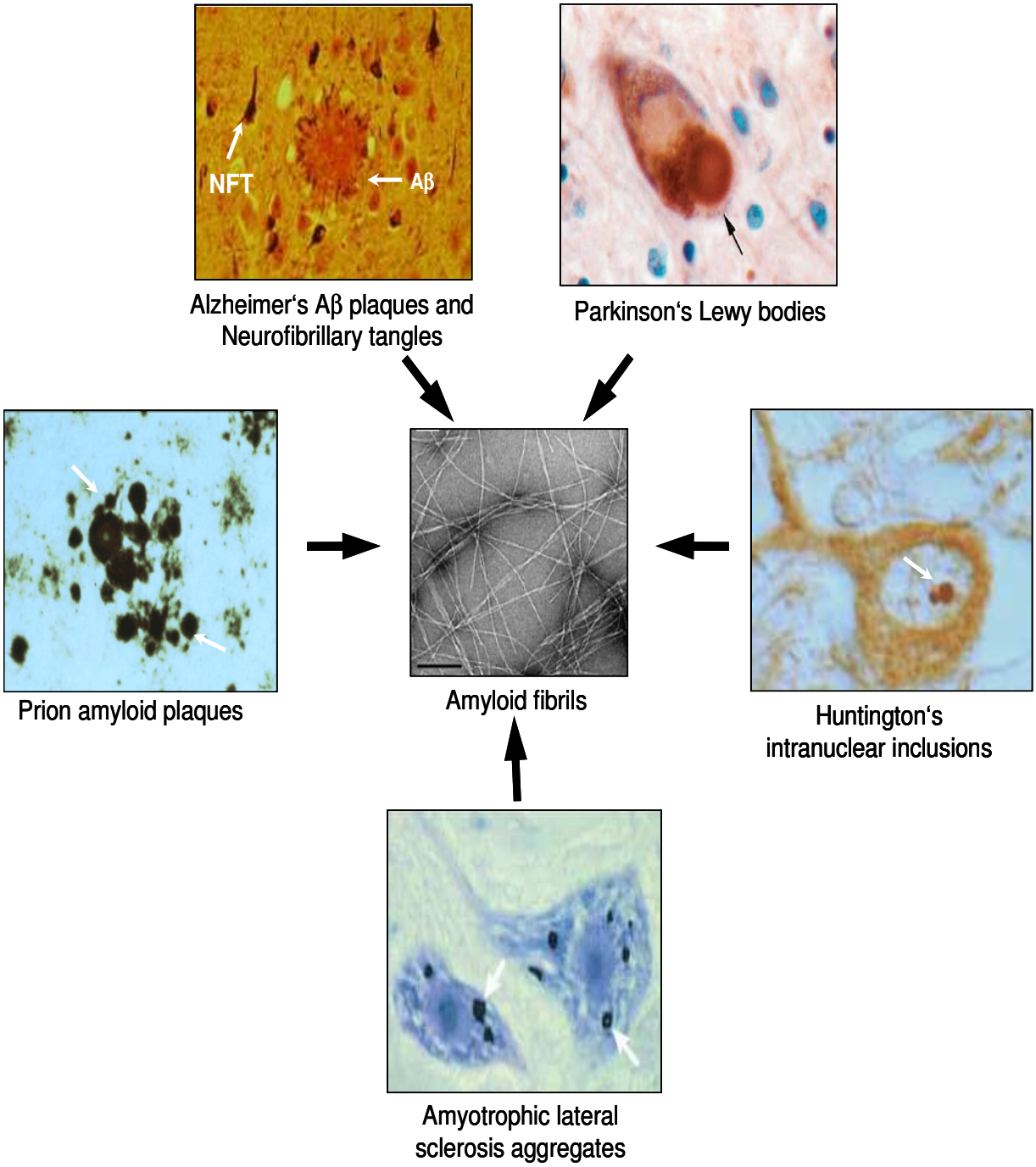

Fig. 2: Misfolded protein aggregates in various neurodegenerative diseases.
Extracellular amyloid plaques (Aβ) and intracellular neurofibrillary tangles (NFTs) are the neuropathological signature of the Alzheimer's disease. Intracytoplasmic aggregates are typically present in the neurons of people affected by Parkinson's disease and Amyotrophic lateral sclerosis. Intranuclear inclusions of Huntington protein are observed in Huntington's disease. Transmissible spongiform encephalopathy cases show extracellular prion amyloid plaques in different brain regions. In spite of the different protein compositions, the final ultra structure of these protein deposits seems to be similar and contain amyloid fibrillar structure under electron microscope (Figure modified from Soto and Estrada, 2008).

The aggregation of proteins implicated in neurodegenerative disorders have been modelled *in vitro* as well as *in vivo*. There is accumulating evidence to suggest that the aggregates formed by the different proteins have the similar morphological, structural and staining characteristics (Cohen and Calkins, 1959; Sunde and Blake, 1997; Sunde et al., 1997; Kim and Takahashi, 2006; Serpell et al., 2000; Serpell and Smith, 2000; Lyubchenko et al., 2006; Breydo et al., 2008). Despite the difficulties in high-resolution studies of aggregated proteins via conventional methods due to their insolubility and noncrystalline nature, recent studies using nuclear magnetic resonance spectroscopy, X-ray diffraction, atomic force microscopy and cryoelectron microscope studies have confirmed the cross-β sheet rich structure of protein aggregates (Dahlgren et al., 2005; Tycko, 2006; Nelson et al., 2005; Sawaya et al., 2007; Eisenberg et al., 2006; Serpell et al., 2000; Serpell and Smith, 2000; Makin and Serpell, 2002).

Aggregation is well-described as a multi-stage process involving misfolding of free monomers, along with one or more assembly steps to form soluble or insoluble protein aggregates (Fig. 3). Generally, the native monomeric protein is mainly composed of α-helical and/or unordered structure, whereas the misfolded polymers are rich in β-sheet conformation. The conformational changes leading to the formation of extended β-sheets promotes homophilic interactions and eventually leads to fibrillogenesis. The fibrils are typically 7–12 nm wide and stabilized by an extensive β-sheet structure in which the β-strands are perpendicular to the fibril axis (Sunde and Blake, 1997; Sachse et al., 2006; Takano, 2008). Amyloid fibrils share certain defining properties which include an unbranched morphology in electron microscope images, pronounced and typically green optical birefringence after Congo Red staining, fluorescence after binding to Thioflavin T dye (Kirschner et al., 1987; Inouye et al., 1993; Sunde et al., 1997; Serpell and Smith, 2000).

Kinetic studies have suggested that the protein misfolding occurs first, and then formation of protein oligomer which is a critical event. These oligomers then act as seeds/nuclei to further accelerate the protein aggregation. This nucleation-dependent polymerization is the basis for the currently accepted model of amyloid formation (Soto et al., 2006; Harper and Lansbury, Jr., 1997; Gajdusek, 1994). According to this model, aggregation into fibrils is dependent on both time and concentration of the respective protein. Amyloid fibrils formation analogues to protein crystallization are a highly ordered process. Aggregation processes are characterized by (a) a slow nucleation phase/lag phase, in which the protein undergoes a series of unfavorable association steps to form an ordered oligomeric nucleus, (b) a growth phase/elongation phase, in which the nucleus rapidly grows and forms larger polymers in the saturation phase. Interactions between monomers determine a slow phase (‘lag phase’) in

which oligomers are formed, providing an ordered nucleus to catalyze the further growth of the polymers finally resulting in mature fibrils (Fig. 3; green line). The initial, slow phase of primary nucleation can be shortened by seeding (Fig. 3; Red line), with preformed nuclei (Jarrett et al., 1993b; Jan et al., 2008).

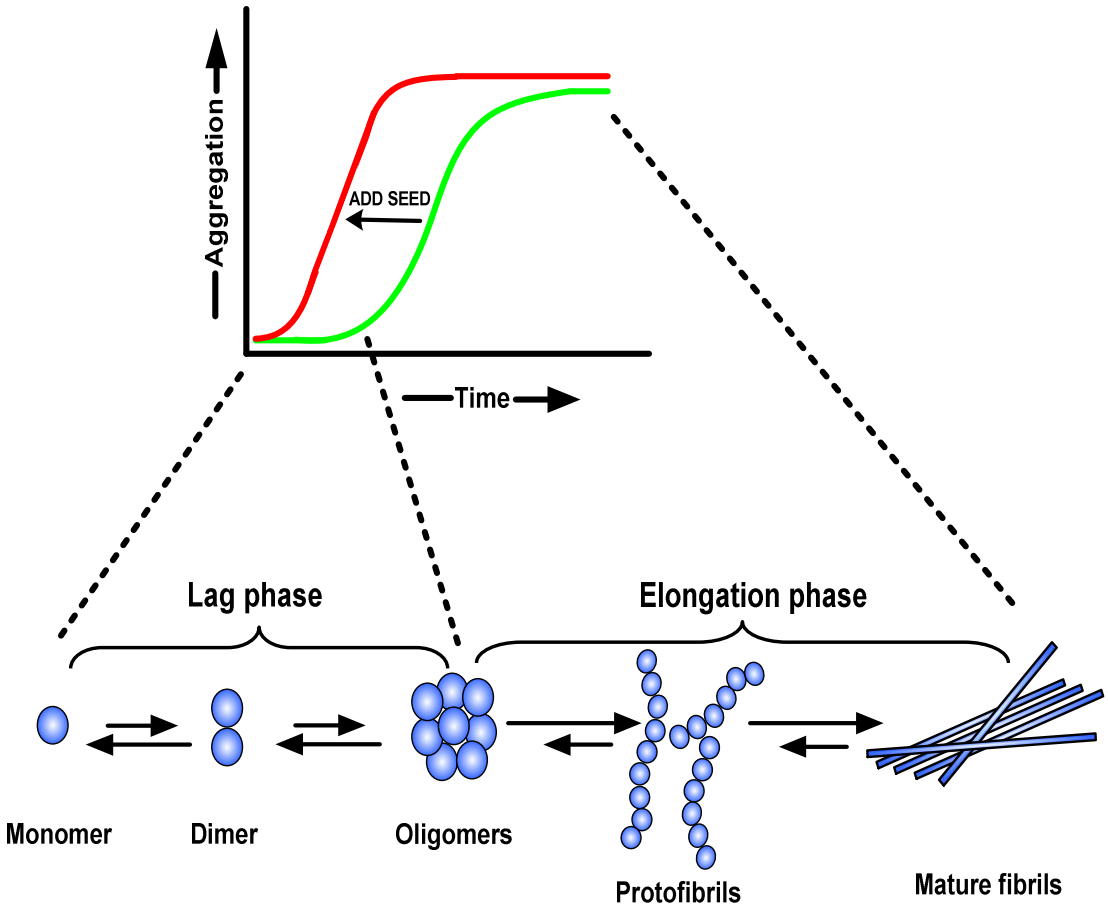

Fig. 3: Kinetics of nucleation dependent amyloid aggregation.
Amyloid formation consists of three phases; lag phase, elongation phase and saturation phase. In the 'lag phase', oligomeric nuclei are formed in a slow process that involves misfolding of the protein and unfavorable intermolecular interactions. Once these seeds are formed, a much more rapid 'elongation phase', results in amyloid aggregates formation leading to protofibrils and fibrils in saturation phase (green line). The rate limiting step in the process is the formation of seeds to direct further aggregation. Amyloid formation can be substantially speedup by the addition of preformed seeds (nuclei). The addition of seeds (nuclei) reduces the lag time and induces faster aggregate formation (red line).

1.2. Alzheimer's disease (AD)

AD is a progressive and insidious neurodegenerative disorder of the central nervous system and is the most common cause of dementia (Hof et al., 1995; Lobo et al., 2000; Schoenberg et al., 1987; Selkoe, 2001a). The German psychiatrist Alois Alzheimer (1864-1915), after whom the disease was named, first described the clinical and pathological symptoms of a case of presenile dementia in a 51 year old female patient (named Auguste Deter) almost a century ago. His first presentation of the typical clinical and morphological features of AD in a meeting was not considered to be valuable at that time, but it was published a year later (Alzheimer, 1907). Clinically, AD is characterized by progressive memory impairment, disordered cognitive function as well as altered behavior including paranoia, delusions, impairments of attention, perception, reasoning, loss of social appropriateness and a progressive decline in language function (Selkoe, 2001a; Price et al., 1993; Morris, 1996). The daily activities, mental functions and normal living become progressively impaired (Forstl and Kurz, 1999). A state of dementia is identified when these deficits undermine the capacity for independent living (Linn et al., 1995; Fox et al., 1998).

AD directly affects millions of people and indirectly affects the lives of ten millions of others who have to deal with many years of cognitive declines of their loved ones (Neet and Thinakaran, 2008). It is the most common form of dementia in the elderly accounting for over 50% of the typical, late-onset cases of dementia. There are about 28 million AD patients world wide with 4.5 million in the USA and 7 million in Europe. The numbers are expected to rise as the current population ages. Epidemiological studies indicate that AD type of dementia occurring in mid-to-late life, affects 7–10% of individuals >65 years of age and approximately 40% of persons >80 years of age (Pfeffer et al., 1987; McKhann et al., 1984; Bachman et al., 1992; Evans et al., 1989; Hy and Keller, 2000). It has been known for several decades that AD can occur in familial AD (FAD) forms which have an autosomal dominant mode of inheritance (<5%). However, the largest proportion of AD cases are sporadic (>95%), occurring without a clearly defined etiology (Selkoe, 1994; Lendon et al., 1997). FAD is clinically and pathologically indistinguishable from sporadic AD, except for the early age of onset (Lehtovirta et al., 1996; Lippa et al., 1996).

1.2.1. Neuropathological hallmarks of AD

Microscopically, the AD brain is characterized by the presence of extracellular amyloid plaques and intraneuronal neurofibrillary tangles (Fig. 4). Extracellular amyloid plaques display a broad range of morphological and biochemical characteristics and contain numerous proteins, the principle amongst them being the Aβ (Glenner and Wong, 1984a; Masters et al., 1985; Glenner et al., 1984). Classical senile or neuritic plaques are multicellular lesions containing extracellular deposits of Aβ that include abundant β-amyloid fibrils (7-12 nm) intermixed with non-fibrillar forms of the Aβ peptide. Aβ is a ~ 4 kDa protein with a common core sequence but heterogeneous N- and C-termini. The most common form of Aβ is 40 amino acids long and is called Aβ1-40. A less abundant form i.e., Aβ1-42, differs only by having two additional amino acid residues at the C-terminus, is particularly associated with the disease (Jarrett et al., 1993b; Burdick et al., 1992; Jarrett et al., 1993a; Bentahir et al., 2006). Compact, neuritic amyloid plaques stained by thioflavin T and Congo red–positive fibrillar deposits contains both Aβ1-40 and Aβ1-42 peptides (Iwatsubo et al., 1994). Neuritic plaques are surrounded by variable numbers of dystrophic neurites, both axonal terminals and dendrites. Many such plaques contain activated microglial cells situated near the amyloid core, as well as reactive astrocytes around the periphery of the plaque (Itagaki et al., 1989; Wisniewski et al., 1989; Meda et al., 2001; Farfara et al., 2008). Although many plaques with these features can be found in the AD brain, an even larger number of deposits seem to lack surrounding dystrophic neurites or glia. These lesions are called preamyloid or diffuse plaques, where the Aβ occurs in a non-fibrillar, less dense and amorphous form in the neuropil (Tagliavini et al., 1988; Yamaguchi et al., 1988; Yamaguchi et al., 1989). These immature deposits are detected in the brains of young patients with Down's syndrome before the manifestation of AD-type dementia (Lemere et al., 1996). As a result, diffuse plaques are considered to be precursors of mature neuritic plaques. Besides diffuse and compact plaques, extracellular Aβ deposits often occur in the walls of cerebral and microvascular lesions associated with cerebral amyloid angiopathy (Mandybur, 1975; Vinters et al., 1988; Kumar-Singh, 2008; Thal et al., 2008).

The second neuropathological hallmarks are the neurofibrillary tangles (NFTs). They are intracellular cytoplasmic accumulations consisting of hyperphosphorylated isoforms of the microtubule-associated protein tau and are found frequently proximate to amyloid deposits (Wood et al., 1986; Kosik et al., 1986). They are filamentous structures composed of straight filaments and paired helical filaments (PHFs) of 10 nm and are located in cell body inclusions, neuritic structures and dystrophic neurites associated with plaques (Goedert et al.,

1988; Braak et al., 1999). NFTs generally occur in large numbers in the AD brain, particularly in limbic and paralimbic structures such as the entorhinal cortex, hippocampus and amygdala. Intensive studies have shown that the tau protein, which normally enhances the polymerization of tubulin into microtubules and acts to stabilize these organelles in neurons, becomes excessively phosphorylated, which reduces binding to microtubules (Lovestone and Reynolds, 1997). The tau and tangle hypothesis argues that in AD the normal role of tau in stabilizing microtubules is impaired, and in diseased neurons microtubules are replaced by tangles (Gray et al., 1987). The resultant microtubule dysfunction in these neurons eventually leads to the degeneration of dendrites and a loss of synapses at their axonal projection targets. The observation that NFT form in some cell bodies whose axons terminate in regions containing amyloid-bearing neuritic plaques, suggests that NFT formation in some perikarya and neurites may be related to events associated with amyloid plaque formation in the AD brain (Hyman et al., 1986; Rasool et al., 1986). Indeed, a growing body of genetic and biochemical evidence suggests that NFTs are downstream of Aβ (Oddo et al., 2003). Specifically, experimental evidence suggests that abnormal Aβ accumulation triggers tau pathology (Gotz et al., 2001; Lewis et al., 2001), and tau has been proposed as an essential mediator of Aβ-induced neurotoxicity (Alexander et al., 2002). Aβ has been shown to induce the calpain-mediated cleavage of tau, leading to the generation of a toxic 17-kDa fragment (Park and Ferreira, 2005), and to induce abnormal tau phosphorylation at disease-relevant sites (Busciglio et al., 1995; Greenberg et al., 1994). However, the existence of prominent filamentous tau inclusions and brain degeneration in the absence of Aβ deposits are also shown to be the hallmarks of neurodegenerative tauopathies such as sporadic corticobasal degeneration, progressive supranuclear palsy and Pick's disease, as well as by hereditary frontotemporal dementia and parkinsonism linked to chromosome-17 (FTDP-17) (Lee et al., 2001). Tau appears to play a central role in the memory deficits in certain transgenic mouse models of AD (Roberson et al., 2007). A recent study even suggests that tau phosphorylation is the limiting factor in Aβ-induced neurotoxicity (Leschik et al., 2007). Thus, recent findings led to the proposal of a hypothesis called "dual pathway" model of causality in AD, whereby Aβ and tau can be linked by mechanisms driven by a common upstream molecular defects (Small and Duff, 2008).

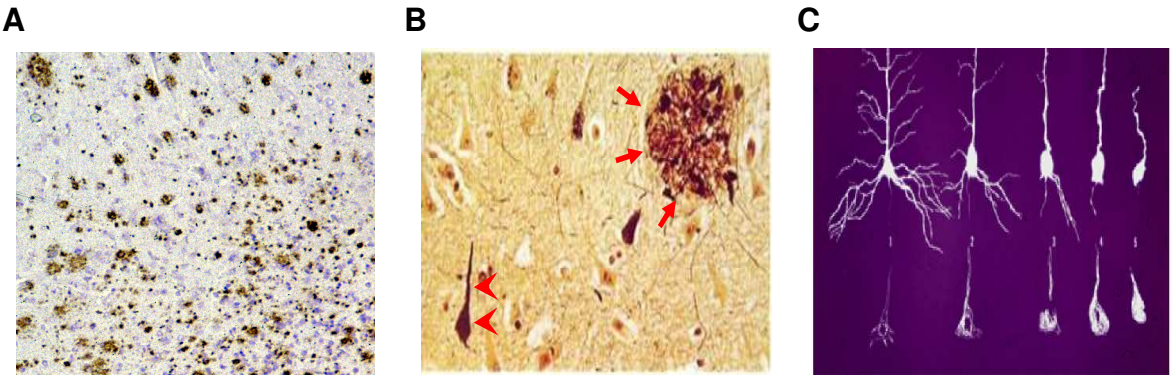

Fig. 4: Neuropathological hallmarks of AD.
A) Immunohistochemical staining of a brain section from human AD patient using anti-Aβ antibody demonstrating classic neuropathological lesions – Aβ plaques. B) Bielschowsky's silver staining of an AD brain section, depicting Aβ plaque (red arrows) and NFTs (red arrow heads) respectively. C) Drawings indicating the progressive neuronal cell loss and the related reduction of specific synaptic connections (Figure A, B and C are adapted from Selkoe et al.,1998 and http://www.alzforum.org/).

Neuronal loss, synaptic alteration and cholinergic deficits

In addition to plaques and tangles, AD is predominantly characterized by progressive neuronal loss and neuronal degeneration in the brain. AD has been suggested to be a form of neuroplasticity failure (Mesulam, 1999; Selkoe, 2002). Consistent with this, the potential neuroplasticity in the adult brain occurs unevenly in different regions, with synaptic plasticity, axonal and dendritic remodeling and synaptogenesis (Arendt, 2001). Recent research has examined the potential importance of soluble species of Aβ in synaptic dysfunction, long before fibrillary Aβ is deposited and neurodegenerative changes occur (Lue et al., 1999; McLean et al., 1999; Lacor et al., 2007). In addition, cognitive decline can also be related to the disruption of the structural integrity of synapses, with most significant decrease in presynaptic terminal densities in the frontal cortex and the hippocampus. Also in regions with many neuritic plaques, synaptic density is strongly decreased (Terry et al., 1991; West et al., 1994; Gomez-Isla et al., 1996; Scheff et al., 1990). Neuronal loss has been observed in a number of cortical and subcortical regions within the neocortex, the frontal and the temporal lobes. Further, massive neuronal loss is regularly observed in superficial enthorinal cortex and in the hippocampal efferent area, the subiculum. Neuronal loss, vulnerability of particular memory-focused synapses to degeneration (Selkoe, 2002; Scheff and Price, 2003), and synapse loss are considered to be the best correlate of AD dementia (DeKosky and Scheff, 1990; Terry et al., 1991).

Besides neuronal loss, AD has also been correlated with a synaptic dysfunction in the cholinergic system (Bowen et al., 1992). A deficit in central cholinergic transmission caused by degeneration of the basal forebrain nuclei is an important pathological and neurochemical

feature of AD. The brains of AD patients exhibit a significant loss of choline acetyltransferase (ChAT) activity and this decrease correlates with the cognitive impairments (Whitehouse et al., 1986). Selective loss of different subtypes (α7 or α4β2) of nicotinic ACh receptors (nAChRs) in AD brains have been reported (Teaktong et al., 2004; Wevers and Schroder, 1999; Pakaski and Kalman, 2008). There is evidence of a role for these receptors in the deficits in memory and cognition. Progressive loss of nicotinic receptors over the disease course of AD has also been described (Newhouse et al., 1997). Recent evidences show that cholinesterase (ChE) inhibitors can interfere with the progression of AD, proving the cholinergic hypothesis in AD (Sugimoto, 2008).

1.2.2. The Amyloid Precursor Protein (APP) and generation of Aβ

The partial purification of Aβ peptides from the microvasculature of AD brains by Glenner and Wong initiated AD research at the molecular level (Glenner and Wong, 1984a). The purification of the Aβ protein from meningovascular amyloid deposits in AD and Down's syndrome as well as its sequencing and the successive observation that Aβ was also the subunit of the plaque amyloid (Masters et al., 1985; Selkoe et al., 1986), enabled the successful cloning of the gene encoding the APP (Kang et al., 1987). APP is a type I single-transmembrane, receptor-like glycoprotein that is expressed ubiquitously in neuronal and non-neuronal cells. Aβ is derived from its large precursor protein by sequential proteolytic cleavages (Fig. 5). The heterogeneity of APP arises from alternative splicing (yielding 3 major isoforms of 695, 751, and 770 residues) as well as by a variety of posttranslational modifications, including the addition of N- and O-linked sugars, sulfation, and phosphorylation (Selkoe, 2001a). Alternatively spliced forms of the APP containing 751 or 770 amino acids are widely expressed in cells throughout the body and occur in neurons. However, neurons express much higher levels of the 695-residue isoform, which is generally observed at very low abundance in nonneuronal cells (Haass et al., 1991). The difference between the 751-, 770- and 695-residue forms is the presence of an exon that codes for a 56-amino acid motif that is homologous to the Kunitz-type of serine protease inhibitor (KPI) domain, indicating one potential function of these longer APP isoforms (751-, 770-). Indeed, the KPI domain containing forms of APP found in human platelets serve as inhibitors of factor XIa, which is a serine protease in the coagulation cascade (Smith et al., 1990).

APP has been identified in many vertebrate species and is a member of an evolutionarily conserved protein family. Search for genes implicated in AD led to the identification of the mammalian homologues, APLP1 (amyloid precursor-like proteins 1) and APLP2 (Wasco et al., 1993; Wasco et al., 1992). APP-like proteins (APPL) have also been identified in *Dro-*

sophila melanogaster (Rosen et al., 1989; Luo et al., 1990), and *Caenorhabditis elegans* (APL-1) (Daigle and Li, 1993). All of the three mammalian proteins (APP, APLP1 and APLP2) display substantial homology at the primary amino acid level, especially within a part of the ectodomain encoded by exons 1 and 2 and their intracellular domains. However, both APLPs lack the Aβ domain (Walsh et al., 2007).

A variety of physiological properties of APP and their metabolites have been described, however, a definitive cell biological role has yet to be ascribed to APP, APLP and its metabolites (Reinhard et al., 2005; Zheng and Koo, 2006). The physiological roles for APP in transmembrane signal transduction (Nishimoto et al., 1993), calcium metabolism (Mattson et al., 1993b; Mattson et al., 1993a), neuritic outgrowth (Perez et al., 1997), and synapse formation have been suggested (Priller et al., 2006). Potential functional motifs within APP, identified by the presence of consensus sequences, suggest roles in metal ion binding (Bush et al., 1993), heparin binding (Schubert et al., 1989b), cell adhesion as a receptor for a currently unrecognized ligand (Schubert et al., 1989a), and in regulating cell growth (Saitoh et al., 1989). Recently, studies have suggested that Aβ, in addition to its neurotoxic effects, also may play a beneficial role, e.g., by limiting neuronal excitation (Kamenetz et al., 2003).

Various researchers have generated APP- or APLP- knock-in and knock-out transgenic animals to better understand the *in vivo* function of these proteins (Anliker and Muller, 2006; Reinhard et al., 2005; Nikolaev et al., 2009). Single disruption of APP, APLP1 or APLP2 each cause minor abnormalities that are largely distinct for the different family members (Heber et al., 2000; Seabrook et al., 1999). The phenotypes of the single KO (knockout) mice were relatively mild, *in vivo* and *in vitro* studies suggest that APP, APLP1 and APLP2 function to promote neurite outgrowth, neural cell migration and copper homeostasis and that the rather benign phenotypes seen in KO mice may results from functional redundancy between APP, APLP1 and APLP2 (Walsh et al., 2007; Zheng and Koo, 2006). In contrast, $APLP2^{-/-}/APP^{-/-}$ mice and $APLP2^{-/-}/APLP1^{-/-}$ mice each show a lethal phenotype (postnatal day 1), where as $APLP1^{-/-}/APP^{-/-}$ mice are apparently normal. Interestingly, no detectable gross or histopathological abnormalities were observed in any of double knock-out lines, where as triple KO mice ($APP^{-/-}/APLP1^{-/-}/ APLP2^{+/-}$ and $APP^{-/-}/APLP1^{-/-}/ APLP2^{-/-}$), which die *in utero* and show cortical dysplasia resembling lissencephaly and cranial abnormalities. Recent study using knock-in mice report that APPsα domain is sufficient to rescue prominent abnormalities of APP-KO mice and suggest that APPsα is sufficient to mediate the (postnatal) physiological functions of APP (Ring et al., 2007; Tamboli et al., 2008). These results from different transgenic mice provide genetic evidence for at least some distinct physiological roles for APP and APLP2 and suggest that APLP2 might have key physiological role among

the family members. This physiological key role of APLP2 is further corroborated by the lethality of $APP^{-/-}/APLP1^{-/-}/ APLP2^{+/-}$ mice revealing haplosufficiency of a single APLP2 allele in the absence of APP and APLP1 (Herms et al., 2004).

APP is trafficked through the secretory and recycling/endocytic pathways, where it undergoes posttranslational processing including a variety of proteolytic cleavage events. The signal peptide is cleaved after the co-translational translocation to the membrane of the endoplasmic reticulum (ER). Classical N- and O-glycosylation, tyrosine sulfation, sialylation and phosphorylation occur during transit through the ER and the Golgi apparatus (Hung and Selkoe, 1994; Suzuki et al., 1994; Weidemann et al., 1989). APP is also shown to be phosphorylated in both the extracellular and intracellular domains (Hung and Selkoe, 1994; Walter et al., 1997a; Flajolet et al., 2007; da Cruz e Silva EF and da Cruz e Silva OA, 2003). In addition, some APP molecules are chondroitin-sulfated in their ectodomains (Shioi et al., 1993).

The proteolytic processing events underlying APP metabolism and Aβ generation have been studied intensely. Both during and after its transport through the secretory pathway to the cell surface, a subset of APP molecules undergoes specific endoproteolytic cleavage by the secretases termed α-, β- and γ-secretases. APP has a short half-life and is metabolized rapidly by two different pathways in all cells: the non-amyloidogenic/α-secretase pathway or the amyloidogenic/β-secretase pathway (Fig. 5). The proteolytic pathways are mediated by three distinct cleavage events. The first cleavage of APP by either α- or β-secretase is a prerequisite for the γ-secretase cut, which takes place after either of the proteolytic processing (α or β) (Walter et al., 2001b).

α-secretase cleaves APP between amino acid residues Lys^{16} and Leu^{17} of the Aβ region (Lys612 and Leu613 of full length APP695), and therefore precludes Aβ production (Esch et al., 1990). This cleavage creates a large, soluble ectodomain fragment (APPsα) which is subsequently released into vesicle lumens and eventually secreted, and a membrane-bound 83 amino acid long C-terminal fragment (CTF; CTFα; C83; α-stub). This cleavage is mediated by members of the ADAM (a disintegrin and metalloproteinases) family of zinc metalloproteases, the most relevant of which appear to be ADAM 10 (Lammich et al., 1999) and ADAM 17 (Buxbaum et al., 1998). The CTFα undergoes subsequent cleavage by γ-secretase to generate p3 and the intracellular C-terminal domains (ICDs) (Selkoe, 2001a).

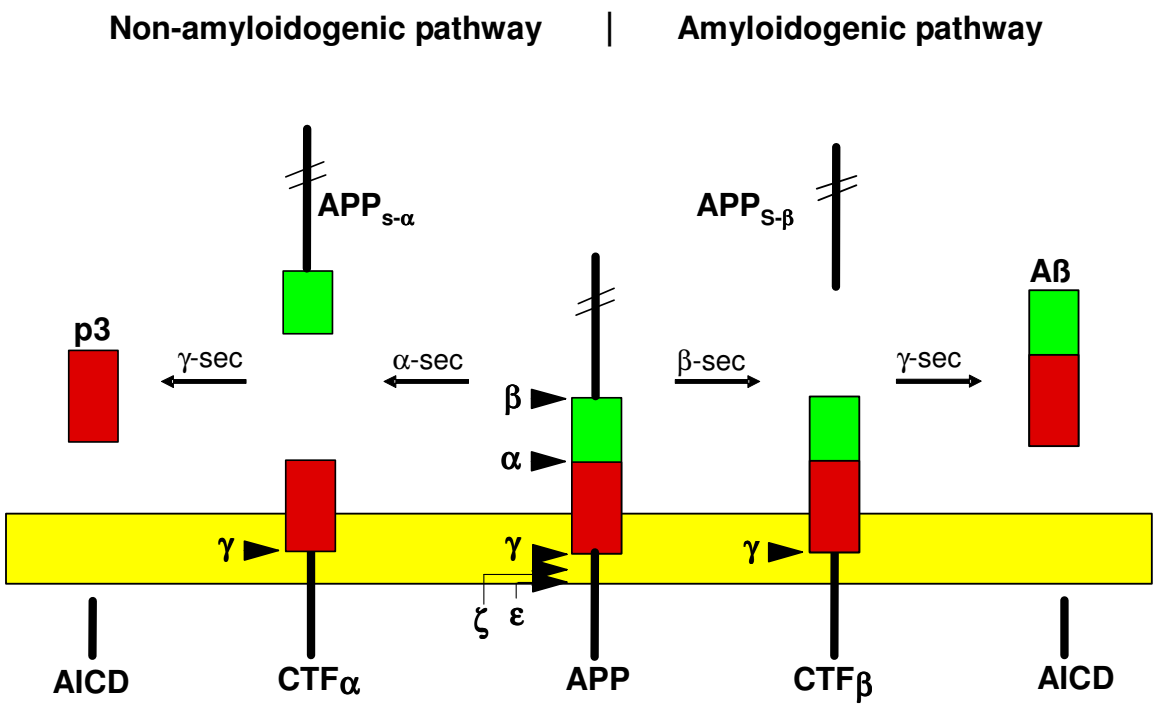

Fig. 5: Proteolytic processing of APP by secretases.
In non-amyloidogenic pathway, APP is first cleaved by α-secretase within the Aβ domain and then by γ-secretase to generate non-amyloidogenic p3 (red). In the amyloidogenic pathway APP is first cleaved by β-secretase and then by γ-secretase to generate Aβ (green and red). Additionally γ-secretase can also cleave APP at ε- and ζ-cleavage site as indicated. ε-cleavage of CTFα/β generates AICD. Arrowheads indicate the respective cleavage sites within APP molecule (Figure adapted from Walter et al., 2001b).

In contrast, the cleavage leading to Aβ production is mediated by a single aspartyl protease named BACE1 (β-site APP Cleaving Enzyme-1; β-secretase). The β-secretase cuts immediately N-terminal to the Aβ domain (Met596 and Asp597 of full length APP695). Thereby producing a slightly smaller, truncated form of soluble APP (APPsβ); which is secreted (shedding) from the cell surface (Roch et al., 1993), leaving a 99 amino acid (CTFβ; C99; β-stub) membrane bound fragment (Cai et al., 2001; Vassar et al., 1999). This C-terminal 99–amino acid stub is subsequently cleaved by γ-secretase to produce Aβ and generate AICD (Schroeter et al., 2003). In addition, BACE1 can also cleave within the Aβ domain (β′ cleavage site). This second cleavage is less-favored and takes place at a site 11 residues further C-terminal (between Tyr606 and Glu607 of full length APP695), producing C89 and a slightly longer APPsβ. γ-secretase cleaves at multiple sites within the transmembrane domain of APP, generating Aβ peptides ranging in length from 38-43 residues. Depending on the exact point of cleavage by γ-secretase, two main forms of Aβ, comprising of either 1-40 or 1-42

amino acid residues, are produced. Nearly 90% of secreted Aβ ends in residue 40 (Aβ1-40) whereas Aβ1-42 accounts for less than 10% of secreted Aβ. Moreover, minor amounts of shorter Aβ peptides such as Aβ1-38 and Aβ1-37 have also been detected. The proportion of Aβ1-42 to Aβ1-40 formed is particularly noteworthy, because the Aβ1-42 is far more prone to oligomerize and form fibrils than the more abundantly produced Aβ1-40 peptide. FAD-linked mutations in APP just beyond the C-terminus of Aβ domain increase Aβ1-42 production. Intriguingly, FAD-linked mutations in PS1 and PS2 influence γ-secretase cleavage by elusive mechanisms that variably influence the cleavage site specificity, in general favoring cleavage at position 42 relative to that of 40, thus increasing the Aβ1-42/1-40 ratio (Selkoe and Wolfe, 2007). In addition there are several N-terminal heterogenous truncated Aβ isoforms that have been detected in human brain and such heterogeneity is known to affect the toxicity of Aβ peptides (Pike et al., 1995; Thal et al., 2006; Schilling et al., 2008). For eg., several isoforms truncated at the N-terminus [Aβ4-40/42, Aβ8-40/42, Aβ12-40/42, and Aβ17-42(p3)] aggregate more readily and are more toxic than Aβ1-42 (Geddes et al., 1999; Tekirian, 2001).

1.2.3. Genetic factors of AD

AD is a genetically complex and heterogeneous disorder. In spite of the complete etiological picture of AD remaining unresolved; the inheritance of some genetic factors appears to play a major role in predisposing the disease. Three genes are currently known to cause familial early-onset AD (<65 years): the APP and the presenilins (PS1 and PS2). The mutations in these genes cause over production of total Aβ or Aβ1-42 generation, resulting in change in Aβ1-42/Aβ1-40 ratios and aggregational properties of Aβ. For the much more common late-onset disease (>65 years), only the ApoE gene has repeatedly associated to AD where the e4 allele increases disease risk and decreases the age of onset (Selkoe, 2000). The four genes are located on the chromosomes 21, 14, 1 and 19 respectively (Table 2).

Studies on the APP as a genetic determinant of AD began with the observation that individuals with Down's syndrome developed the clinical and pathological features of AD (Mann et al., 1985; Mann, 1988). These data pointed to the involvement of chromosome 21 in AD, leading to the first genetic linkage discovery between a locus on chromosome 21q and autosomal dominant early-onset FAD (St George-Hyslop et al., 1987). Sequencing of the APP gene and screening for mutations led to the discovery of several missense mutations in families with the early onset AD (Goate et al., 1991; Hendriks et al., 1992; Mullan et al., 1992). Although the APP mutations account for less than 0.1% of all AD cases (Tanzi and Bertram, 2001), they proved to be highly informative about the general mechanisms of the disease. Missense mutations in PS1 and PS2 proteins also cause early onset of AD, usually between

35 and 60 years of age (Levy-Lahad et al., 1995; Sherrington et al., 1995). Until now, more than 150 missense mutations have been identified in PS1 and at least 6 have been identified in PS2. These tend to cluster within and adjacent to the 8 transmembrane domains of PS protein (Selkoe, 2004a). The apolipoprotein E4 (ApoE4) allele was discovered as a genetic polymorphism which conferred an increased risk of Alzheimer disease (Schmechel et al., 1993; Strittmatter et al., 1993; Saunders et al., 1993). Inheritance of 1 or 2 apolipoprotein E4 alleles is a far more prevalent genetic basis for Alzheimer disease. ApoE4 hasten the disorder primarily in patients who are in their sixties and seventies, thereby lowering the typical age of onset of late-life AD (Saunders et al., 1993).

Table 2: Genetic factors predisposing to AD: Relationships to the Aβ phenotype (Adapted from Selkoe, 2004a).

Fault in the Gene	Chromosome	Age of onset (years)	Aβ phenotype
Amyloid precursor protein (APP) mutations	21	43-62	Altered APP processing, Increased $A\beta_{total}$ production and leading to aggregation. $A\beta_{1-42}/A\beta_{1-40}$ ratio increased
Presenilin 1 (PS1) mutations	14	29-62	Increased $A\beta_{1-42}$ production and reduction in $A\beta_{1-40}$ resulting increase in $A\beta_{1-42}/A\beta_{1-40}$ ratio
Presenilin 2 (PS2) mutations	1	40-88	Increased $A\beta_{1-42}$ production and reduction in $A\beta_{1-40}$ resulting increase in $A\beta_{1-42}/A\beta_{1-40}$ ratio
Apolipoprotein E4 (ApoE4) polymorphism	19	>65	Increased Aβ plaques density and vascular deposits and Aβ fibrillization

A large number of additional genes have been suggested to be associated with AD. However, most lack confirmation in independent studies or their replications have been inconsistent. AlzGene database provide a comprehensive, unbiased and regularly updated collection of genetic association studies performed on Alzheimer's disease. (http://www.alzforum.org/res/com/gen/alzgene).

1.2.4. Aβ toxicity: The importance of structure

Aβ is generated during normal cellular metabolism and is present in the brains and secreted to the extracellular space of the human brain and also found in cerebrospinal fluid (CSF) of normal humans throughout life (Haass et al., 1992; Seubert et al., 1992; Tamaoka et al., 1997; Brody et al., 2008). Several lines of evidence indicate the physiological role of Aβ in neuronal activity (Pearson and Peers, 2006). Thus, the presence of Aβ in the CSF of non-demented individuals and in the media from neuronal cell cultures during normal metabolism indicates that Aβ has a role in the central nervous system in addition to having a potential pathological role in AD (Brody et al., 2008). Therefore, the mere presence of Aβ simply does not cause neurodegeneration; rather neuronal injury appears to develop because of the ordered self-association of Aβ molecules rich in β-sheet structures and becoming neurotoxic. This self-association of Aβ may differ either quantitatively or qualitatively from its effects when the levels are elevated that are normally seen during disease conditions (Pike et al., 1991; Pike et al., 1993; Busciglio et al., 1992).

In the past decade, Pike et al., (Pike et al., 1991), in a landmark discovery established that innocuous monomers of Aβ become neurotoxic and this was further confirmed from studies by Yanker et al., (Lorenzo and Yankner, 1994), indicating that monomeric Aβ become neurotoxic only upon self-association. This is well supported by the recent research on amyloid toxicity in resolving the specific neurotoxic structures derived from Aβ's self-association and their relative contributions to AD pathogenesis (Haass and Selkoe, 2007).

Due to limitations in the characterization of the assemblies that were formed *in vitro*, it was assumed that since amyloid fibrils were detectable; these assemblies mediated the observed toxicity. Current *in vitro*, *in vivo* and *ex vivo* studies provide evidence of the involvement of soluble, non-fibrillar oligomeric Aβ in toxicity. These findings are further supported by recent studies showing the robust correlation between soluble Aβ levels and the extent of synaptic loss and severity of cognitive impairment (Lacor et al., 2007; Lacor et al., 2004; Haass and Selkoe, 2007). Both control and AD brain contain a continuous distribution of Aβ species from monomer up to oligomers of higher MW of 100 kDa, with the major contribution coming from low molecular weight (MW) oligomers ranging from dimers to octamers. Western blot analysis of AD brain extracts revealed the presence of variable proportions of monomeric, dimeric and trimeric Aβ species and showed their potential toxic nature (McLean et al., 1999). Such sodium dodecyl sulfate (SDS)-stable low MW oligomers have also been detected in human CSF by LC-MS and appear to represent highly stable non-covalently associated dimers (Vigo-Pelfrey et al., 1993). Genetically modified Chinese Hamster Ovary

(CHO) cell line expressing human APP also forms similar SDS-stable oligomers (Walsh et al., 2002a). The presence of similar SDS-stable dimers and trimers in the soluble fraction of the human brain and in extracts of amyloid plaques, suggests that SDS-stable low MW oligomers of Aβ are the fundamental building blocks of insoluble amyloid deposits and could be the earliest mediators of neuronal dysfunction (Shankar et al., 2008; Townsend et al., 2006; Roher et al., 1996).

Studies using synthetic Aβ peptides provide additional support for the role of prefibrillar and fibrillar Aβ assemblies in AD pathogenesis. The first nonfibrillar assemblies identified were protofibrils; these heterogeneous structures range from spherical assemblies of ~5 nm in diameter to short, flexible rods of up to 200 nm in length (Harper et al., 1997; Walsh et al., 1997). The protofibrils and fibrils are principally different from each other depending on their size and relative solubility. The protofibrils appear to behave as true fibrils intermediates in that they can both form fibrils and dissociate to low MW species. They are known to be neurotoxic, acute application of protofibrils *in vivo* rapidly alter the synaptic physiology, whereas chronic application causes cell death (Hartley et al., 1999; Walsh et al., 1999; Hartley et al., 2008). The second soluble, nonfibrillar assemblies of synthetic Aβ-derived diffusible ligands (ADDLs), appears in the form of spheres with a diameter of ~5nm. ADDLs are formed only under certain specific *in vitro* conditions but can cause neuronal death and block long-term potentiation in *ex vivo* preparations (Lambert et al., 1998). A recent study reported that synthetic ADDL preparations can bind excitatory synapses and cause a reduction in spine density, similar to the findings observed with soluble Aβ oligomers secreted in cell culture (Lacor et al., 2007).

Over the past decade, increasing attention has been turning towards small oligomeric aggregates before they could assemble into amyloid fibrils or plaques (Ross and Poirier, 2005; Deshpande et al., 2006). Data that have emerged from various *in vitro* (Oda et al., 1995; Walsh et al., 1997; Lambert et al., 1998; Hartley et al., 1999; Townsend et al., 2006), and *in vivo* studies suggest that oligomeric, pre-fibrillar Aβ intermediate assemblies are potent neurotoxins and are therefore thought to be the key effectors of neurotoxicity in AD (Haass and Selkoe, 2007; Selkoe, 2008; Klein et al., 2001; Walsh and Selkoe, 2007). In transgenic mice expressing the human APP, neurological deficits develop even before amyloid deposits occur (Mucke et al., 2000). It has been shown recently that oligomers of Aβ inhibit long-term potentiation *in vivo* (Walsh et al., 2002a).

Various reports indicating the conversion of peptides from their soluble monomeric functional forms to soluble oligomers later into well-defined fibrillar aggregates are a characteristic process in the AD pathogenesis (Roychaudhuri et al., 2009; El-Agnaf et al., 2003;

Walsh and Selkoe, 2007; Walsh et al., 2002b; Walsh and Selkoe, 2004). It is now recognized that the low MW soluble oligomers which are capable of forming high MW aggregates are the most toxic Aβ peptide species, found in the brains of patients with AD could contributes to the pathogenesis of the disease (Shankar et al., 2008; Klyubin et al., 2008). Dynamic soluble oligomeric Aβ pools exist in AD and are well correlated to disease severity. Thus, converging lines of evidence suggest that progressive accumulation of the Aβ and its self-association to form several different assembly forms (aggregates) plays a central role in the pathogenesis of AD (Fig. 6). The pathological accumulation of Aβ in brain includes not only the self-association and formation of toxic Aβ aggregates but also decreased capability of the body to degrade Aβ oligomers by different proteases (Tanzi et al., 2004; Selkoe, 2001b). Proteolysis of Aβ by variety of proteases is reported to be highly dependent upon aggregation state. It is shown that Aβ oligomers and aggregates tend to be resistant to variety of proteases (Betts et al., 2008; Hartley et al., 2008).

There is an increasing evidence that amyloid fibrils and soluble oligomeric intermediates have a common structure and pathway of aggregation in many of the observed degenerative diseases. Although such diseases are associated with different proteins, they share similar pathological features. Evidences have come from the discovery of antibodies that recognize generic epitopes on all types of amyloid fibril (O'Nuallain and Wetzel, 2002; Kayed et al., 2007) and soluble oligomers (Kayed and Glabe, 2006), independently of their specific amino acid sequences. These similarities might be due to underlying commonalities in the pathway of aggregation and the structures of the various aggregation products. This realization not only indicates that assemblies produced by different disease-causing amyloid proteins might initiate similar cytotoxic mechanisms, but also raises the possibility of targeting their common structures for therapeutic treatment (Glabe, 2006).

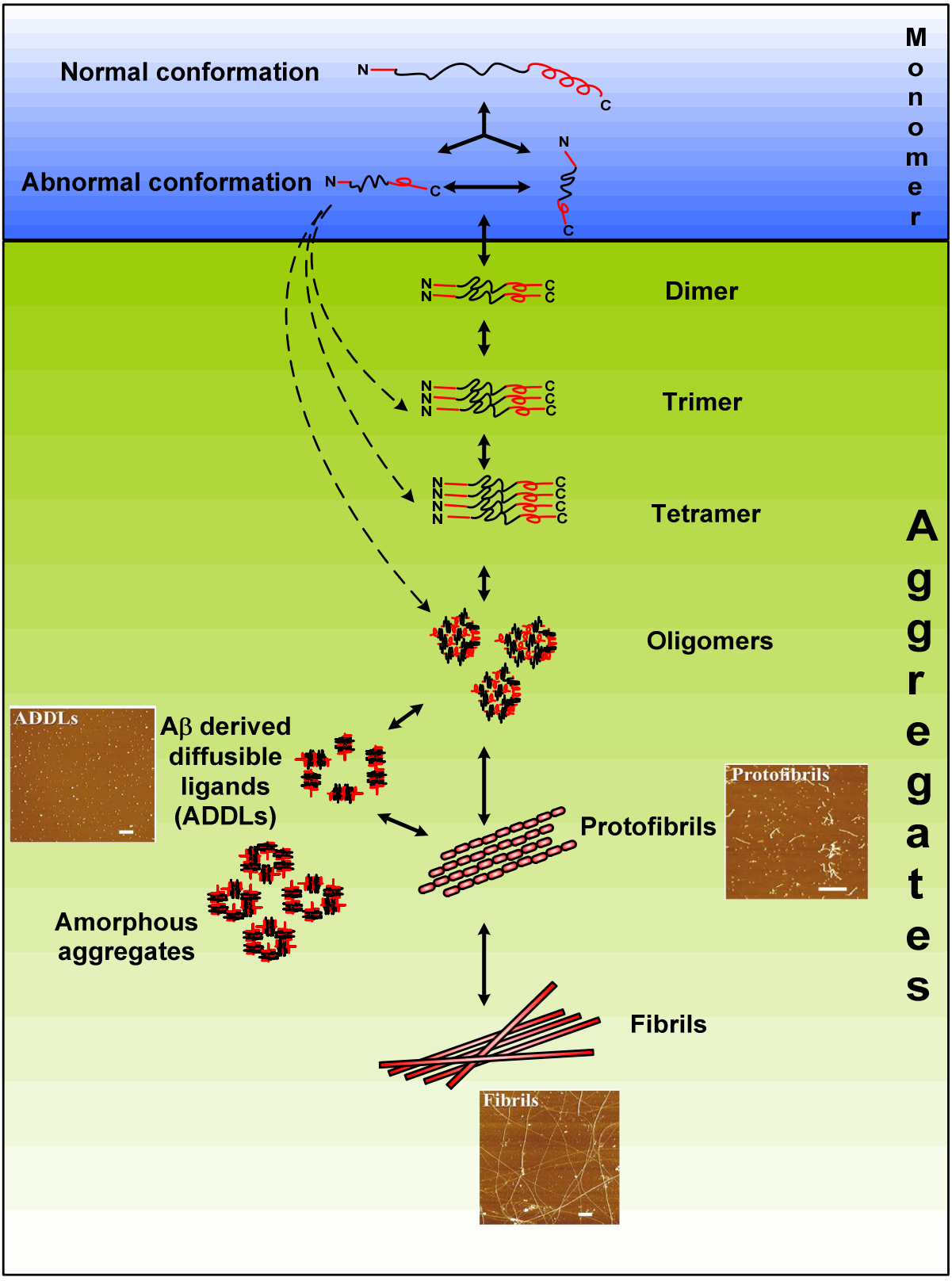

Fig. 6: The conformational alteration and formation of toxic Aβ intermediates.
Conformational change of the monomer, perhaps with several possible abnormal conformations, initiates the aggregation process. The misfolded monomer acquires the ability to self assemble into higher-order structures. Aggregation starts as soon as there is an association of two or more abnormal monomeric proteins including dimers, trimers, tetramers and larger oligomers. Fibrils are formed by the linear addition of monomers through intermediate oligomeric assemblies, or species called protofibrils. Oligomers or protofibrils might be capable of forming ADDLs. It is currently proposed that the early species in the aggregation process are more toxic than large aggregates (fibrils).

1.2.5. The "Amyloid hypothesis" or "Aβ hypothesis"

The understanding of molecular mechanisms involved in AD has increased significantly over the past two decades. This has led to the proposal of several hypotheses responsible for the AD disease pathogenesis. Especially the "Aβ hypothesis" and "neuronal cytoskeleton degeneration hypothesis", have been widely discussed, which emphasize the critical role of Aβ in neurodegeneration and tau in axonal transport respectively (Hardy and Selkoe, 2002). In spite of other hypotheses such as cholinergic system dysfunction (Francis et al., 1999), Ca^{2+} signaling deficits (Mattson, 2002), NMDA receptor hypofunction, disruption of APP signaling and cell cycle abnormalities, and mitochondrial dysfunction have been put forward (Swerdlow and Khan, 2004). However, none of the hypotheses is clinically proven. Despite the several perspectives on the deficiencies in hypotheses, a large body of evidences from neuropathological, biochemical, genetic, cell biological and even therapeutic studies in humans during the last 25 years support the "Aβ hypothesis"(Hardy, 2006).

The "Aβ hypothesis" states that AD is initiated by the accumulation, aggregation and deposition of the toxic Aβ peptide, leading to an impaired cell-cell communication, compromising the synaptic function, and eventually causing the death of the neurons in the brain (Fig. 7). The strongest evidence for the "Aβ hypothesis" comes from the studies of rare FAD cases. Based on the fact that all the identified FAD mutations in the APP gene which are found clustered around or within the Aβ region affect total Aβ production, increase Aβ1-42/Aβ1-40 ratio and increase the aggregation properties of Aβ (Levy et al., 1990; Chartier-Harlin et al., 1991; Goate et al., 1991; Citron et al., 1992). Other multiple factors which affect Aβ generation, clearance and deposition are believed to be in the onset of sporadic forms of AD. In support, experiments employing transgenic animal models such as APP *tg* mice and *Drosophila* harboring human mutant APP showed a time-dependent increase in extracellular Aβ production and aggregation and develop certain neuropathological and behavioral changes similar to those observed in AD (Gotz and Ittner, 2008). *In vivo*, seeded aggregation of Aβ is seen after injecting AD brain extracts into the brains of nonhuman primates (Ridley et al., 2006) or APP-transgenic mice (Kane et al., 2000). Finally, cerebral β-amyloidogenesis in transgenic mice was induced by exogenously injected Aβ purified from AD patients and transgenic mice (Meyer-Luehmann et al., 2006).Various factors such as the age, ischemia, higher caloric intake, head injury, inflammation, etc. either in concert with ApoE or alone could further modify Aβ metabolism and deposition (Behl, 2005). The toxicity of the Aβ peptide has been demonstrated by its ability to interfere with many physiological processes such as apoptosis, Ca^{2+} storage and release, proteosomal activity, receptor endocytosis as well as

synaptic functions such as the long-term potentiation (LTP). There are reports indicating the role of Aβ in oxidative stress and disruption of metabolism and function of various membrane proteins and lipids upon Aβ binding to membrane lipids (Marchesi, 2005).

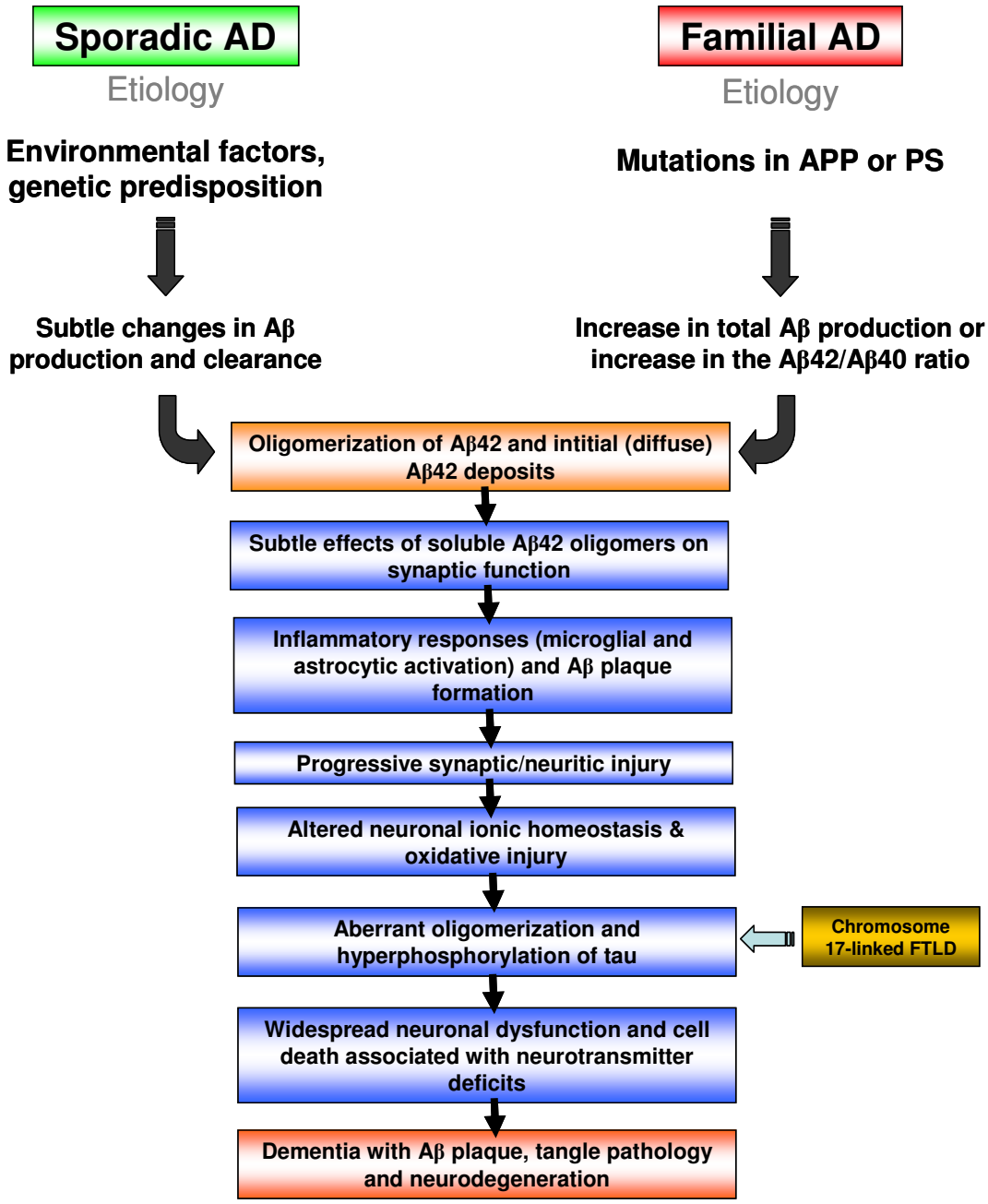

Fig. 7: The "Aβ hypothesis" cascade.
The sequence of pathogenic events leading to AD as proposed by the "Aβ hypothesis". The environmental factors, genetic predisposition and mutations in APP and PS can affect the metabolism of Aβ. Initially, small and soluble oligomeric assemblies of Aβ1-42 are produced, which then cause synaptic dysfunction as well as an induction of the Aβ cascade. Note the 'shortcut' to tau pathology and FTLD via chromosome 17-linked tau mutations (Figure modified from Winklhofer KF et al., 2008).

The "Aβ hypothesis" is further extended to accommodate more recent findings such as the predominant role of Aβ oligomers in the disease (Walsh and Selkoe, 2007), and the presence of intracellular Aβ (Ohyagi, 2008), as well as the modulation of tau phosphorylation by Aβ through regulation of kinases and phosphatases (Huang and Jiang, 2009). In its most recent iteration in supporting the formal proposal, the "Aβ hypothesis" states that the gradual accumulation and aggregation of the small hydrophobic peptide initiates a slow but deadly cascade that leads to synaptic alterations, microglial and astrocytic activation, the modification of the normally soluble tau protein into oligomers and then into insoluble PHFs, and progressive neuronal loss with multiple neurotransmitter deficiencies and cognitive failure (Haass and Selkoe, 2007). The emerging collective data from biochemical, genetic and *tg* animal models studies corroborating that Aβ plays a central role in initiating the AD.

In spite, the "Aβ hypothesis" is gaining a more widespread acceptance and it is the predominant scientific explanation for the cause of AD over the past two decades, it has also been constantly criticized and challenged by the new studies. The development of AD therapeutics has been plagued with many failed and equivocal clinical trial outcomes. Although amyloid immunotherapy has been a particular focus of almost all large pharmaceutical efforts, there has been limited progress in that area (Thakker et al., 2009; Schroeter et al., 2008; Golde et al., 2009). Thus, recent clinical findings from a growing number of Aβ-reducing drug trials in sporadic AD cases suggest the alternative models linking Aβ with tau and proposing "Dual pathway hypothesis" (Small and Duff, 2008). In addition, recent clinical trial findings regarding the outcome of passive immunization and Aβ lowering strategies in humans challenging the acceptance of "Aβ hypothesis". However, the recent new findings needs to be further investigated and validated by future studies in human patients and animal models to refute, confirm, or modify the existing "Aβ hypothesis".

1.3. Protein phosphorylation

Protein phosphorylation is a covalent post-translational modification event that is essential for regulation and maintenance of most biological processes in eukaryotes (Cohen, 1992). Since the breakthrough discoveries of reversible protein phosphorylation [Edmond H. Fischer and Edwin G. Krebs 1992 Nobel Prize in physiology or medicine (http://nobelprize.org/nobel_prizes/medicine/laureates/1992/press.html)], research on protein phosphorylation in general and on the dynamic interplay between kinases and phosphatases has been gaining increasing interest. Reversible phosphorylation can modify the function of a protein in almost every conceivable way. For example, regulating the biological activity of

proteins, by stabilizing it or marking it for destruction, by facilitating or inhibiting movement between subcellular compartments, or regulation of protein– protein interactions (Manning et al., 2002b; Manning et al., 2002a). It has extended from initial studies describing single phosphorylation events to the complex regulations involving multisite phosphorylation in signalling cascades, which are accepted as major regulatory principle of life (Cohen, 2002). In higher eukaryotes, phosphorylation occurs on serine, threonine and tyrosine residues in majority. However, phosphorylation can also take place on histidine and aspartic acid residues (Saito, 2001). In eukaryotes phosphoserine, -threonine, and -tyrosine are estimated to occur at a relative abundance of ~90 % to ~10 % to ~0.05 %, respectively.

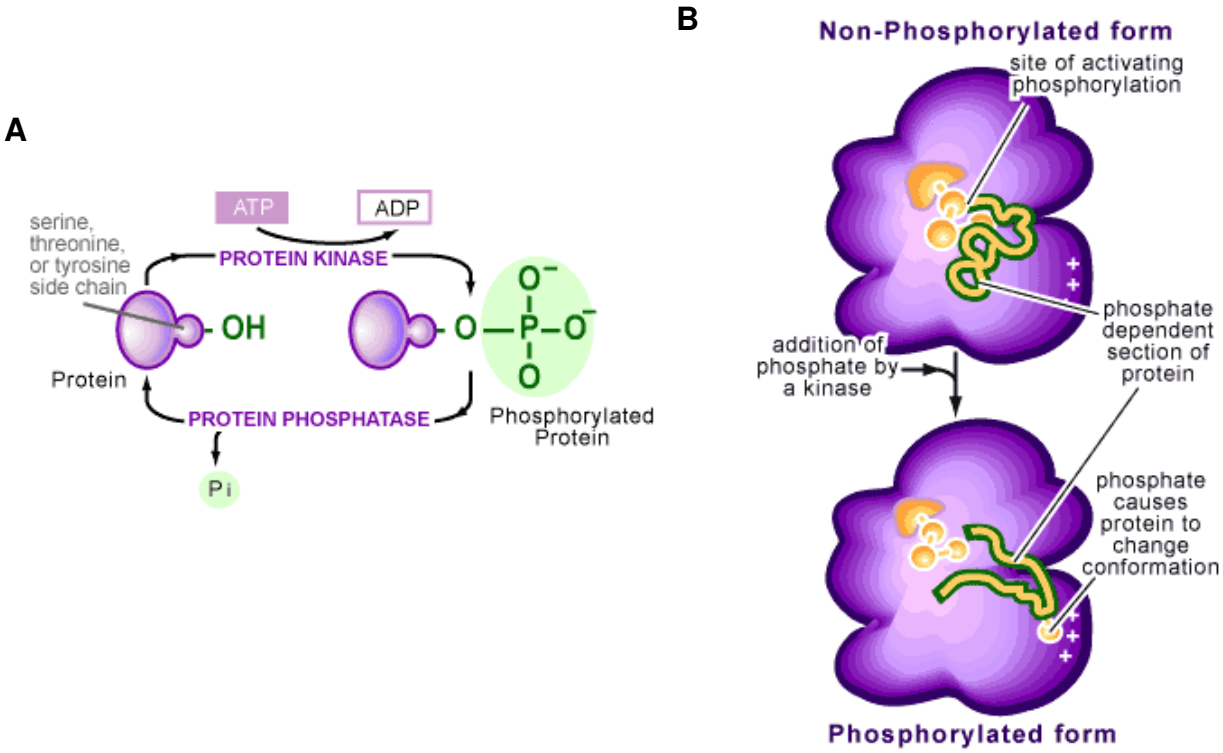

Fig. 8: Reversible protein phosphorylation and its effect.
A) Dynamic interplay between kinases and phosphatases on hydroxyl groups of amino acids in reversible protein phosphorylation. Addition of negatively charged phosphoryl group from ATP to the protein is catalyzed by protein kinases and protein phosphatases remove the phosphate group. B) Conformation changes caused by phosphorylation.
(Adapted from http://www.scq.ubc.ca/protein-phosphorylation-a-global-regulator-of-cellular-activity)

Phosphorylation refers to the addition of a phosphoryl group from ATP to one of the amino acid side chains of a protein (Fig. 8A). The reaction is catalyzed by enzymes called protein kinases (Krebs and Beavo, 1979). The phosphate group can be removed by protein phosphatase activities (Ingebritsen and Cohen, 1983a; Ingebritsen and Cohen, 1983b; Ingebritsen et al., 1983; Cohen, 1989). Phosphates are negatively charged under physiological conditions (with each phosphate group carrying two negative charges) and addition to a pro-

tein could change the characteristics of the protein (Fig. 8B). This change is presumably by alteration of structure (conformation) resulting in alteration of the protein function (Jeganathan et al., 2008; Mondragon-Rodriguez et al., 2008; Eidenmuller et al., 2000).

Many proteins could be phosphorylated at multiple sites. Multisite phosphorylation enables the cell to develop and maintain complex regulatory pathways contributing to the different levels of hierarchical organization (Soderling, 1979). In such proteins in general, phosphorylation at different sites is not completely independent. It is frequently observed that phosphorylation at one site enhances or suppresses phosphorylation at another site (Roach, 1991). Multisite phosphorylation is a key mechanism for achieving signal integration and fine-tuning of the phosphorylation events in cells (Cohen, 2000). More than 500 protein kinases, and perhaps half as many protein phosphatases, are thought to be present in the human genome (Manning et al., 2002b), and 30% of all proteins in any eukaryotic cell are thought to be phosphorylated at any time (Mann et al., 2002), many on multiple sites. Therefore, one can assume that phosphorylation is not simply used to switch on or switch off the activity of a protein, but can have many additional roles.

1.3.1. Protein phosphorylation in the human brain

In the last 25 years, substantial evidence has appeared that strongly suggesting that protein phosphorylation also plays an important role in neuronal function in the brain (Nestler and Greengard, 1983). Extensive studies indicate the implication of protein phosphorylation as the molecular mechanism by which many extracellular signals regulate brain functions. The proteins which undergo phosphorylation appear to be particularly important in neuronal function including intermediary metabolism, neuronal excitability, neurotransmitter biosynthesis and release as well as neuronal growth, differentiation, and morphology (Nestler and Greengard, 1983; Nestler et al., 1984; Walaas and Greengard, 1991). Most of the earlier studies indicated that many of the protein phosphorylation systems take place primarily in the neuronal body. Recent studies indicate protein phosphorylation also being highly concentrated in synaptic junctions, the part of the nerve cell anatomically specialized for intercellular communication.

1.3.2. Phosphorylation of proteins by extracellular protein kinases

Intracellular protein phosphorylation by protein kinases plays a significant role in the regulation of numerous biological processes (Hunter, 1987). In addition to intracellular kinases, the existence of a novel class of protein kinases, which are located extracellularly, has been shown to phosphorylate the extracellular protein substrates. In 1974, Agren and

Ronquist reported that intact glia and glioma cells can catalyze the transfer of the gamma phosphate from extracellular ATP to exogenously added protein substrates suggesting the existence of cell surface protein kinases (Agren and Ronquist, 1974). Stimulation of a protein kinase activity at the surface of glioma cells by cyclic AMP was reported soon after (Schlaeger and Kohler, 1976). Subsequent reports have provided the evidence of extracellular protein kinase activity in a variety of cellular systems. In 1982, Kubler et al., reported rigorous study of protein phosphorylation at the surface of the cloned human HeLa cells and provided convincing evidence for the existence of extracellular protein kinase in this cell line (Kubler et al., 1982). These protein kinases are termed ecto-protein kinases (ecto-PKs) and exo-protein kinases (exo-PKs). The ecto-PKs have been localized at the external surface of the plasma membrane (membrane bound) where they exert their catalytic activity. They use extracellular nucleoside triphosphate as co substrates, which can be released by intact cells in response to certain stimuli to phosphorylate membrane bound protein as well as soluble extracellular proteins (Dubyak and el-Moatassim, 1993; Gordon, 1986; el-Moatassim et al., 1992). Exo-PKs are secreted/shedded to the extracellular milieu and can phosphorylate the extracellular matrix proteins and soluble proteins (Kubler et al., 1992; Walter et al., 1996b; Rodriguez et al., 2005).

Ecto-PKs activity has also been characterized on the membrane surfaces of neuronal cells (Ehrlich et al., 1986; Tsuji et al., 1988). A critical role of these ecto-protein kinases in the regulation of the synaptic plasticity in the mammalian hippocampus has been shown (Chen et al., 1996). On the basis of their localization and substrate specificity these ecto or exo-PKs might play a significant role in the regulation of cell–cell interactions, ligand binding, and signal transduction. Phosphorylation of cell-surface proteins by exo-PKs has been implicated in the regulation of certain cellular functions, including long-term potentiation and synaptogenesis (Muramoto et al., 1994). The developments in this area of investigation contribute to the expanding understanding on the importance of extracellular protein phosphorylation systems in the regulation of cellular function of neurons (Ehrlich et al., 1990). Conclusive demonstration and further understanding of ecto-domains phosphorylation of cell membrane proteins and proteins in the extracellular milieu suggests physiological significance of an ecto-phosphorylation mechanism.

1.3.3. Altered protein phosphorylation in AD

Dysregulation of phosphorylation and dephosphorylation events is associated with several diseases and malignancies in humans. Altered signal transduction is thought to be one of the unifying aspects of a wide variety of disorders, including neurodegenerative conditions

such as AD (Mattson D, 2004). Several studies have reported abnormal protein kinase (Jin and Saitoh, 1995), and protein phosphatase expression and as well as their activities in the brains of AD patients as compared to the normal cohort (Gong et al., 1993). Such altered activities, as well as altered protein levels of specific kinases and/or phosphatases, support the hypothesis that abnormal or aberrant phosphorylation and malfunctioning of various signaling cascades results in AD pathogenesis. The overall result of such dysfunctional signaling activity would be expected to be the association of neurodegenerative conditions with abnormal phosphorylation of specific key proteins. This is well documented for tau phosphorylation, a key protein which is involved in AD. In addition to phosphorylation of tau, the kinases themselves have been shown to be affected in AD diseased brain. For example, in AD there is evidence of altered activities of the major isoforms of protein kinase C (PKC) in the vasculature and in neurons. In addition, report describe that Aβ peptide might play an essential role in the down-regulation of PKC seen in the AD cerebral vasculature and exposure of cultured brain endothelial cells to Aβ peptide stimulate the translocation of PKCα from the membrane to the cytosol (Pakaski et al., 2002). Activation of PKC was shown to lead to a relative increase in nonamyloidogenic cleavage of APP (da Cruz e Silva OA et al., 1993; Gandy et al., 1993), and a decreased Aβ production (Buxbaum et al., 1993; Buxbaum et al., 1990). It is therefore likely that a protein phosphorylation cascade is involved in Aβ toxicity (Tan et al., 1997).

1.3.4. Phosphorylation of AD related proteins

Numerous proteins having a variety of physiological functions appear to be relevant to the AD condition, and a considerable number of these are shown to be phosphorylated, including tau, BACE1, the presenilins and APP. The major pathophysiological role of phosphorylation in AD disease is confined to hyperphosphorylated tau protein. Phosphorylation of tau has been well documented in AD (Grundke-Iqbal et al., 1986; Gustke et al., 1992; Delobel et al., 2002). In AD, tau is abnormally hyperphosphorylated at several Ser/Thr sites. Indeed, hyperphosphorylation and accumulation of neurofilament (NF) subunits is a typical feature of the AD brain (Wang et al., 2001; Mi and Johnson, 2006; Chun and Johnson, 2007).

BACE1 is shown to undergo phosphorylation and plays a critical role in its trafficking, endocytosis and interaction with adapter proteins (Walter et al., 2001a; Wahle et al., 2005; Wahle et al., 2006). Phosphorylated BACE1 at serine residues are identified in the human brain suggesting the serine phosphorylation of BACE1 is a physiologically relevant post-translational modification that regulates trafficking (von Arnim et al., 2004).

Presenilins are shown to be constitutively phosphorylated in transiently transfected cells (Walter et al., 1996a; De et al., 1997; Walter et al., 1998). Phosphorylation sites and responsible kinases have been identified by *in vitro* and *in vivo* studies. It is reported that potential PKC recognition sequences are present within the Presenilin amino acid sequence (Walter et al., 1997b; Fluhrer et al., 2004). Reports indicate the PKC-dependent phosphorylation of the PS proteins in regulation of βAPP processing and Aβ generation.

APP is a phosphoprotein carrying several phosphorylatable amino acid residues in its cytoplasmic and luminal regions. The phosphorylated forms of APP present in each tissue are mAPP (mature APP) in neurons and imAPP (immature APP) in dividing cells (Suzuki and Nakaya, 2008). By using phosphorylation-state specific antibody, it is shown that mAPP695 (mature APP-695 isoform) species can undergo phosphorylation in mouse and in human brain (Iijima et al., 2000). The physiological role of the phosphorylation state of APP has been investigated in the brain, postmitotic differentiating neuronal cells, and dividing cells (Iijima et al., 2000; Suzuki et al., 1994; Ando et al., 1999; Kimberly et al., 2005).

The intracellular domain of APP can undergo phosphorylation by different kinases (Suzuki et al., 1994; Suzuki et al., 1997; Oishi et al., 1997). Using phosphorylation state-specific antibodies, Oishi et al., provided evidence for the *in vivo* phosphorylation of Thr654, Ser655 and Thr668 on the cytoplasmic domain of APP (Gandy et al., 1988; Suzuki et al., 1992). Studies are also showing the role of stress activated kinase such as c-Jun NH2-terminal kinase (JNK) in Thr668 phosphorylation in APP (Kimberly et al., 2005; Standen et al., 2001; Taru et al., 2002). APP-CTFs are also found to be phosphorylated at Thr668 and detected as phosphopeptides pC99, pC89 and pC83 (Sano et al., 2006). These pCTFs are reported to be involved in signal transduction events via interaction with Shc/Grb2 adaptor proteins in reactive astrocytes of Alzheimer's disease brain (Russo et al., 2002a; Russo et al., 2002b). Several identified phosphorylation sites are localized within known amino acid motifs such as ^{667}V**T**PEER^{672}, ^{681}G**Y**ENP**T**Y^{687} and ^{653}**YTSI**^{656} and play a critical role in APP endocytosis, polarized sorting and subcellular trafficking of APP. Furthermore, phosphorylation could regulate the interaction with cytosolic adaptor proteins such as Fe65 and probably other intracellular adapter proteins like Dab1, Dab2, Jip1b, Numb, PATI and X11 (Kerr and Small, 2005). Recent report shows the association of phosphorylated CTFs with PS1. Phosphorylated CTFs can be the substrates of the γ-secretase and an increase in the phosphorylation of APP-CTFs facilitates their processing by γ-secretase (Vingtdeux et al., 2005). Clearly, phosphorylation-dependent events are important in AD, spanning APP phosphorylation, phosphorylation-dependent interactions of APP with other proteins, and related events that affect APP trafficking and metabolism and are associated with signal transduction cascades.

In addition to phosphorylation of cytoplasmic and intracellular domain, several groups identified phosphorylatable amino acids residues in ectodomain of APP. APP undergoes phosphorylation within its ectodomain at two distinct subcellular localizations of the secretory pathway, namely in secretory vesicles and at the cell surface. The phosphorylation sites within the ectodomain of APP have been identified as serine residues 198 and 206, and protein kinases phosphorylating APP as ecto-CK1- and ecto-CK2 are known (Knops et al., 1993; Walter et al., 1997a; Walter et al., 2000). These kinases have been previously shown to be located at the cell surface (Walter et al., 1996b; Walter et al., 1994). These kinases can phosphorylate membrane-bound as well as soluble forms of APP (Walter et al., 2000).

The Aβ domain contains two serine residues at positions 8 and 26 that represent potential phosphorylation sites for different protein kinases (PK) A, (PK) C, cdc2, CK1, and CK2. Although these kinases are known to exist mainly in the cytosol, recent studies indicate that these kinases also occur at the cell surface and in extracellular fluids (Walter et al., 1996b; Walter et al., 1997b; Walter et al., 2000; Redegeld et al., 1999; Cho et al., 2000; Rodriguez et al., 2005; Kubler and Barnekow, 1986; Kubler et al., 1989). This is important because Aβ is also secreted into extracellular fluids where it could aggregate and form extracellular plaques. It is also important to note that ATP, the co substrate of protein kinases, can be secreted from neuronal and non-neuronal cell types and metabolized by different ecto-enzymes, including ecto-nucleotide kinases/phosphatases (Inoue et al., 2007). Recently, Aβ and APP have been shown to interact with an ATP synthase localized at the cell surface, thereby modulating extracellular ATP synthesis (Schmidt et al., 2007). However, whether the Aβ domain of APP or Aβ itself is also phosphorylated has not been clearly demonstrated. In spite, by using phosphoserine specific antibodies and purified kinase, it was suggested that Aβ could be phosphorylated on Ser26 by cdc2 *in vitro* (Milton, 2001; Milton, 2005). On the other hand, some kinases including CK1, CK2 and PKC failed to phosphorylate Aβ *in vitro* (Chauhan et al., 1993).

2. AIM OF THE STUDY

Genetic mutations that cause early onset familial AD, although found in at least three different genes (APP, PS1 and PS2), commonly increase the generation and/or aggregation of Aβ. Specifically, several mutations within the APP gene that lead to amino acid substitutions in the Aβ domain promote its aggregation leading to formation of extracellular amyloid plaques in the brain and cause early onset AD. However, such mutations are very rare and account for only a very small number of cases (<5%). Mechanisms that increase the aggregation of wild-type Aβ and cause the much more common sporadic forms of AD (>95%), are largely unknown. It is plausible that certain post-translational events may render the Aβ peptide amyloidogenic in sporadic AD cases. In this context, especially the impact of changed environmental conditions that can trigger these structural conversions has especially attracted the interest of many researchers in recent years. Changes in environmental conditions such as pH, ionic strength, metal ions, protein concentration, oxidative stress, proteolysis, glycosylation and transglutamination have been shown to induce a conformational transition that shifts the equilibrium from the functional, mostly unfolded or partially α-helical structure to the β-sheet rich aggregation prone structures.

Protein phosphorylation is a key post-translational modification and it plays an important role in neuronal function. Numerous proteins having a variety of physiological functions appear to be relevant to the AD condition, and a considerable number of these are shown to be phosphorylated, including APP, BACE, the presenilins, and tau. Various reports show the role of different kinases and phosphatases in the regulation of Aβ production. In addition, several lines of evidence indicated abnormal protein kinase and protein phosphatase activities in the brains of AD patients compared to the normal cohort. In spite of the major role of phosphorylation of AD related proteins and their physiological role, the role of phosphorylation is still placed downstream of Aβ deposition, i.e., the pathophysiological role of phosphorylation in AD disease is just confined to hyperphosphorylated tau protein and aggregation intermediates linked to neurodegeneration. Although, the Aβ domain contains several potential phosphorylation sites, whether the Aβ domain of APP or Aβ itself is also phosphorylated has not been clearly demonstrated. In addition, several kinases are known to present at the surface of living cells or are secreted into extracellular fluids. Thus, such kinases could potentially phosphorylate extracellular Aβ and could modulate its aggregation.

The aim of the present work was to understand the role of extracellular Aβ phosphorylation and its role in AD pathogenesis. Specifically, the following aims were followed:

1) Determination of potential phosphorylation sites of Aβ and the responsible protein kinases.
2) Identification of the role of extracellular kinases in phosphorylation of Aβ *in vivo*.
3) Elucidation of the effect of phosphorylation on Aβ conformation and its role in oligomerization and aggregation.
4) Detection of phosphorylated Aβ *in vivo*.

3. MATERIALS AND METHODS

3.1. MATERIALS

3.1.1. Chemical used

Unless otherwise stated, chemicals were purchased from Sigma (Steinheim, Germany), Roche (Basel, Switzerland), Fermentas (St.Leon-Rot, Germany), New England Biolabs GmbH (Frankfurt am Main, Germany), Merck (Darmstadt, Germany), Fluka (Deisenhofen, Germany), Invitrogen Life Technologies (Karlsruhe, Germany), or Applichem (Darmstadt, Germany).

[γ-^{32}P]ATP was obtained from Hartmann Analytic GmbH (Braunschweig, Germany).

All cell culture solutions, buffers, antibiotics were from Sigma (Deisenhofen, Germany), Invitrogen/Life technologies (Karlsruhe, Germany) & GibcoBRL (Karlsruhe, Germany).

3.1.2. Ready-to-use solutions / reagents

Acetic Acid
Acrylamide solution (37.5:1) Acrylamide/bis-acrylamide for protein-SDS-gel
Chloroform
DAB substrate (Biogenex, DC138R006)
Dimethylsulfoxide (DMSO)
Ethanol
Ethidiumbromide, 10mg/ml
Formaldehyde, 37%
Isopropanol
Methanol
TEMED for protein-SDS gel
Tween-20
Triton-X100
DPX Mountant for histology (Fluka, 44581)

3.1.3. Kits

BCA^{TM} Protein Assay Kit (Thermo Scientific)
Chemiluminescence's Kit (Amersham, GE Healthcare)

3.1.4. Buffers and Solutions for Protein Biochemistry

Name	Final Concentration	Constituents and their amounts
Stacking gel buffer (Upper Tris)	0.5 M 0.4%	Tris-base 15.1 g 1 g SDS Volume made up to 250 ml with Dist. H_20 after adjusting pH to 6.8, sterile filtered and stored at 4 °C.
Separating gel buffer (Lower Tris)	1.5 M 0.4%	181.7 g Tris 4 g SDS Volume made up to 1 L after adjusting to pH 8.8, sterile filtered and stored at 4 °C.
SDS-running buffer	23 mM 190 mM 0.1%	2.78 g Tris Base 14.26 g Glycine 5 ml 20% SDS stock The contents were mixed in 1 L Dist. H_20 and pH was adjusted to 8.8. Stored at room temperature (RT).
5x Laemmli sample buffer	50 mM 5% 40 mM 5 mM 5 mM 20% 0.01%	Sodium phosphate pH 6.8 SDS DTT EDTA EGTA Glycerol Bromophenol blue Mixed thoroughly, the solution was aliquoted, was stored at -20 °C, and freeze/thawed not more than 5 times.
APS	10%	1 g Ammonium persulphate in 10 ml water. Stored at 4 °C for not longer than 1 month.
Transfer buffer (10x)	390 mM 480 mM	96 g Tris 72 g Glycine The contents were dissolved in 1 L Dist. H_20, and pH was adjusted to 8.0. Solution was stored at 4 °C.
Transfer buffer (1x)	1 x 10%	100 ml 10 x Transfer buffer Methanol Volume was made up to 1 L with Dist. H_20.
10x Tris buffered saline (TBS)	0.1 M 1.5 M	12.1 g Tris 87.6 g NaCl Contents were dissolved in 750 ml Dist. H_20, pH was adjusted to 7.5 and the volume was made up to 1 L. Solution was sterilized by autoclaving and stored at RT.
Western blot washing buffer	1x 0.1%	100 ml 10x TBS 1 ml Tween 20 Volume was made up to 1 L with Dist. H_20.
NuPAGE Gel running buffer	1x	50 ml 20x NuPAGE MES SDS Running buffer resuspended and volume was made up to 1 L with Dist. H_20.
NuPAGE LDS Sam-	1x	2.5 µl of LDS sample buffer (4x)

ple buffer (1x)	1x	1 µl of NuPAGE reducing agent (10x) x µl of Sample and final volume made up to 10µl with Dist. H_20.
Tricine Running buffer (10x)	1 M 1 M 1%	60.5 g Tris-Base, pH 8.3 89.5 g Tricine 10 g SDS The salts were dissolved in 900 ml Dist. H_20, adjusted the pH to 8.3 and volume made up to 1.0 L with Dist. H_20.
Tricine Running buffer (1x)	1x	100 ml 10x Tricine Running buffer Volume was made up to 1 L with Dist. H_20.
Coomassie staining solution	0.4% 5% 40%	1.0 g Coomassie Brilliant Blue G-250 25 ml Acetic Acid 200 ml Methanol Volume was adjusted to 500 ml with Dist. H_20, filtered through a Whatman filter paper and stored at RT. Solution was used more than once.
Coomassie destaining solution	10% 30%	50 ml Acetic Acid 150 ml Methanol Solution made up to 500 ml with Dist. H_20.
Ponceau S staining solution	0.5% 1%	0.5 g Ponceau S 1 ml Acetic acid Contents were dissolved in 100 ml of Dist. H_20 and filtered; Solution was stored in dark at RT.
Blocking solution	5% 1x 0.5%	5 g Non-fat Skimmed milk powder 100 ml 10x TBS/PBS 1 ml Tween 20 Always prepared fresh for the usage.
Alternative blocking solution	5% 1x 0.5%	5 g BSA fraction V 100 ml 10x TBS/PBS 1 ml Tween 20 Always prepared fresh for the usage.
Protease inhibitor	1x	Complete Protease Inhibitor Cocktail Tablets. 25x stock solution was prepared by dissolving one tablet in 2 ml Dist. H_20, aliquoted and stored up to 6 months at -20 °C.
Phosphatase inhibitor	1x	Phosphatase Inhibitor Cocktail Tablets. 10 x stock solution was prepared by dissolving one tablet in 1 ml Dist. H_20, aliquoted and stored up to 6 months at -20 °C.
2% SDS Buffer	2%	2 g SDS Volume was made up to 100 ml with Dist. H_20.
Sucrose Buffer	320 mM	10.95 g Sucrose Dissolved in 100ml of sterile Dist. H_20.
STEN- Buffer (1x)	50 mM 150 mM 2 mM 0.2%	Tris-HCl pH 7.6 NaCl EDTA NP-40 (Igepal CA-630) pH 7.6 @ 25 °C
STEN-NaCl Buffer (1x)	50 mM 500 mM	Tris-HCl pH 7.6 NaCl

	2 mM 0.2%	EDTA NP-40 (Igepal CA-630) pH 7.6 @ 25 °C
STEN-Lysis Buffer with BSA (1x)	50 mM 150 mM 2 mM 1% 1% 2% 1 x	Tris-HCl pH 7.4 NaCl EDTA Triton X-100 NP-40 (Igepal CA-630) BSA Complete Protease inhibitor
Hypotone buffer	10 mM 1 mM 1 mM 100 mM 25mM 1 mM	Tris-HCl, pH 7.4 EDTA EGTA KF Glycerol phosphate Sodium Orthovandate
Phosphorylation assay buffer (P-Mix)	30 mM 70 mM 5 mM 0.5 mM 83 mM 5 mM	Tris; pH 7.3 NaCl Magnesium Acetate EDTA D(+) Glucose KH_2PO_4/K_2HPO_4 pH adjusted to 7.3 using acetic acid; Osmomolarity: 290 ± 10 mOsm.
PKA Reaction buffer (1x)	20 mM 0.5 mM 5 mM	Tris pH 7.6 Calcium Chloride Magnesium acetate
CK1 Reaction Buffer (1x)	50 mM 10 mM 5 mM	Tris-HCl Magnesium Chloride DTT pH 7.5 @ 25 °C
CK2 Reaction Buffer (1x)	20 mM 50 mM 10 mM	Tris-HCl Postassium Chloride $MgCl_2$ pH 7.5 @ 25 °C
Protein A/G sepharose suspension (Zymed)		100 mg/ml protein A/G bound sepharose beads were washed with STEN buffer and resuspended in it. If required beads were blocked with 2 mg/ml BSA to avoid non-specific binding.
10x Phosphate Buffered Saline (PBS)	137 mM 2.7 mM 10 mM 2 mM	40 g NaCl 1 g KCl 89 g $Na_2HPO_42H_2O$ 12 g KH_2PO_4 Salts were dissolved in 4.5 L Dist. H_20, pH was adjusted to 7.4 with HCl, and volume made up to 5 L with Dist. H_20 and autoclaved. Stored at RT.
Congo-Red (CR) solution	100 µM	Stock solution prepared in filtered PBS and 10% Ethanol.
Thioflavin-T (ThT) solution	20 µM	Prepared in Millipore H_20.

3.1.5. Solutions for Histochemistry and Immunofluorescence

Name	Final Concentration	Constituents and their amounts
20% PFA	20%	100 g paraformaldehyde 1.9 ml 10 N NaOH DEPC (Diethylpyrocarbonate) water to 500 ml Solution was heated to 56 °C until solution was almost clear, filtered through a Whatman filter paper and stored as 10 ml or 50 ml aliquots at -20°C. The solution was diluted to 4% in 1x PBS before use.
2.6% Phosphate buffer paraformaldehyde solution (PFA)	2.6% 0.1 M	26 g PFA 500 ml of 0.2 M PBS Dissolved above constituents in 400 ml Dist. H_20, heat to 60 ºC, neutralized with 1M NaOH, adjust pH to 7.6 and final volume adjusted to 1L.
Eosin	1%	1 g in 100 ml of distilled water. Filtered and used for a maximum of 3 weeks
Citrate buffer	0.1 M 0.1 M	10.5 g Citric acid in 500 ml water (Solution A) 14.71 g Sodium citrate in 500 ml water (Solution B). Before use, 9 ml of solution A and 41 ml of solution B was added to 450 ml distilled water. pH was adjusted to 6.0.
Reduction solution	10% 30% 0.05 M	Methanol H_2O_2 TBS, pH 7.6
Hydrogen peroxide	1% (or 3%)	3.3 ml or (10 ml) of 30% Hydrogen peroxide 100ml water. Always prepared fresh and used.
Washing solution (TBS-T)	1x 0.1%	100 ml 10x TBS 1ml Tween 20 Volume was made up to 1L with water.
Blocking solution	0.1 M 0.25% 10%	DL-Lysine Triton-X BSA

3.1.6. Solutions for eukaryotic cell culture and primary mouse neuronal cell culture

Cell lines used	Media and Constituents
HEK293	DMEM (Dulbecco's Modified Eagle Medium) Glutamax™ containing 4.5 g/L of D-Glucose supplemented with 10% FCS and 1% Pen Strep (Final concentration-Penicillin:100 units/ml; Streptomycin:100 µg/ml)
A 172 (Human neuroglioblastoma)	DMEM Glutamax™ containing 4.5 g/L of D-Glucose supplemented with 10% FCS and 1% Pen Strep (Final concentration-Penicillin:100 units/ml; Streptomycin:100 µg/ml)

SH-SY5Y	RPMI (Roswell Park Memorial Institute) Glutamax™ containing 4.5 g/L D-Glucose supplemented with 15% FCS and 1% Pen Strep.
HeLa cells (Immortalized human epithelial cells from a fatal cervical carcinoma)	DMEM Glutamax™ containing 4.5 g/L of D-Glucose supplemented with 10% FCS and 1% Pen Strep (Final concentration- Penicillin:100 units/ml; Streptomycin:100 µg/ml)
H4 cells	DMEM Glutamax™ containing 4.5 g/L of D-Glucose supplemented with 10% FCS and 1% Pen Strep (Final concentration- Penicillin:100 units/ml; Streptomycin:100 µg/ml)
Primary mouse cortical neuronal cultures	DMEM medium without Glutamine supplemented with 15% FCS and sterile filtered potassium chloride (20 mM). 2 mM of glutamine (Final concentration) was supplemented before use in the required amount of medium.

3.1.7. Antibodies

3.1.7.1 Primary antibodies

Name	Antigen	Species	Dilution		Source
			WB	IHC/IF	
4G8	Aβ17-24	mouse	1:1000		SIGNET/Covance
82E1	Aβ1-16	mouse	1:1000		IBL Corporation, Japan
2964	Fibrillar Aβ1-40	rabbit	1:500		Raised in lab
Bap-1a	Aβ 1-40	mouse	1:1000		Gift from Elan
3D6	Aβ 1-40	mouse	1:1000		Gift from Elan
β-actin	hβ-actin-CT	mouse	1:1000		Sigma
5313	MBP-hAPP$_{695}$-NT (a.a. 444-592)	rabbit	1:1000		Walter et.al., 2000
PKAβ cat (C-20)	C-terminus of PKAβ catalytic subunit	rabbit	1:1000		Santa Cruz Biotechnology, Inc.
SA5434	Aβ1-16 (pSer-8)	rabbit	1:50	1:5	Raised in lab
6E10	Aβ1-16	mouse	1:1000	1:5	SIGNET/Covance
22C11	rAPP fusion protein	mouse		1:100	Chemicon International
CD68	Anti CD-68, KP1	mouse		1:100	DakoCytomation, Denmark.
GFAP	GFAP from human brain	mouse		1:400	DakoCytomation, Denmark.

3.1.7.2 Secondary antibodies

Name	Species	Antigen	Application	Dilution	Source
anti-rabbit-HRP	goat	Rabbit IgG	WB	1:20,000	Sigma
anti-mouse-HRP	rabbit	Mouse IgG	WB	1:20,000	Sigma
Alexa Fluor 594	goat	Rabbit IgG	IHC/IF	1:1000	Molecular Probes
Alexa Fluor 594	goat	Mouse IgG	IHC/IF	1:1000	Molecular Probes
Alexa Fluor 488	goat	Rabbit IgG	IHC/IF	1:1000	Molecular Probes
Alexa Fluor 488	goat	Mouse IgG	IHC/IF	1:1000	Molecular Probes
anti-mouse Cy2	donkey	Mouse IgG	IHC/IF	1:50	Dianova, Germany
anti-rabbit Cy3	donkey	Rabbit IgG	IHC/IF	1:50	Dianova, Germany

3.1.8. Mouse lines

Genotype	Short Description	Source
C57BL/6	Wild type mice with black color for breeding and back crossing	Charles River, Germany
APP/PS1	Amyloid pathology that develops in these mice derives from the proteolytic processing of the human APP transgene product that harbors the Swedish double mutation (K595N/M596L) and ΔE9 knock-out mutation in presenilin 1, that in combination, lead to the marked overproduction and progressive accumulation of Aβ plaques (Borchelt et al., 1997).	Jax Laboratories, USA (Strain Name: B6C3-Tg, Stock # 004462)

3.1.9. General Lab Materials

All sterile cell culture plastic-ware were purchased from Corning.
Pipette Tips and tubes were purchased from Sarstedt
Fuji Medical X-Ray film (Kodak)
Phosphor Imager screens (Kodak)
Hybond-N- blotting membrane 30cm x 3m (Amersham, RPN303B)
Microscope slides 76 x 26 mm (Engelbrecht)
Sterile filters 0.45 µm, 0.2 µm, 0.1 µm (Schleicher & Schuell)
SuperFrost® Plus microscope slides (Menzel #041300)
Universal agarose
0.2 µm PROTRAN Nitrocellulose membrane (Whatman GmbH, Germany)
0.2 µm Polyvinylidene Difluoride (PVDF) membrane (Whatman GmbH, Germany)

3.1.10. Laboratory Devices

Thermomixer	Eppendorf
Block heater	Stuart Scientific
Photometer (Genesis)	ThermoSpectronic
-80 ºC freezer	ThermoForma
-20 ºC freezer	AEG Electrolux
Refrigerator	LIEBHERR
Ultrasonic Bath	Merck Eurolab
Sonicator	Bandelin Sonopuls
Weighing Balance	Metler Toledo
pH Meter	Metler Toledo
Orbital Shaker	Biometra
Autoclave	H+P
37 ºC CO_2 incubator	Binder
Cell culture hood	Thermo
Nitrogen tank	Linde
Centrifuge	Eppendorf
SpeedVac concentrator	Eppendorf
Vortexer	Scientific Industries
Cryo tubes	Nunc
Western-blotting unit	Amersham Biosciences
Electrophoresis power supply consort	Amersham Biosciences
Microwave	LG

Overhead rotor	Scientific Industries
Water bath	Medigen
Phosphor imager	Fuji Inc.
Chemiluminiscence imager	Biorad
Centrifuge	Eppendorf
Ultracentrifuge	Beckman
Ultracentrifuge rotor (SW40Ti)	Beckman
Fluorescence microscope	Leica
Cary Eclipse Fluorescence Spectrophotometer	Varian
Circular Dichroism Spectroscopy	Jasco
NMR	Brucker
DynaPro Titan	Wyatt Technology Corporation
Transmission Electron Microscope	FEI

3.2. APPLIED METHODS

A series of bioanalytical, biophysical and immunohistological techniques were applied for the characterization of phosphorylation of Aβ in *in vitro* and *in vivo*, effect of phosphorylation on biophysical properties of the Aβ peptide and finally to show the occurrence of pAβ *in vivo* in brains of AD *tg* mouse and in human AD patients. Following section will briefly summarize and describe the analytical techniques applied here. Further detailed information on the particular method can be obtained from the cited literatures.

3.2.1. *In silico* analysis of putative phospho-sites of Aβ and the responsible kinases

A variety of web-based computational prediction tools (applications) are available for the prediction of phospho-sites of a particular peptide/protein such as Scansite (Obenauer et al., 2003), NetphosK (Blom et al., 2004; Hjerrild et al., 2004), PREDIKIN (Brinkworth et al., 2003), PredPhospho (Kim et al., 2004) and idenfication of kinase specificity for the substrates such as GPS (Xue et al., 2005), PPSP (Xue et al., 2006), and KinasePhos (Wong et al., 2007). The above mentioned tools differ among each other with relation to the type of data that they use for the predictions. Basically, these web-based computational methods rely on i) experimental identification of the consensus sequence motifs recognized by the active site of kinases and ii) verified phosphorylation sites as reported in the literature as well as in curated databases (Swiss-prot database). These tools are freely available on world-wide-web (www). The predictions from these prediction tools are generally reliable while these neural networks based prediction tools evaluates the identified phosphorylation sites iteratively comparing the results with other prediction programmes, the experimentally verified phosphorylation sites as reported in the literature and the data in curated databases such as the Swiss-Prot database.

The identification of the phosphorylation sites of Aβ and responsible kinases were carried out using NetPhosK 1.0 (Blom et al., 1999), and NetPhos 2.0 sever (Blom et al., 2004). These two prediction programmes employ neural network based algorithms prediction processes which are based on the evolutionary information obtained from sequence similarity of the phosphorylation site and taxonomy. The NetPhosK 1.0 is a kinase specific eukaryotic phosphorylation site predictions server. The kinase predictions are verified with homologues phosphorylation sites obtained from other protein homologues from higher eukaryotes. The NetPhos 2.0 server is a generic (non kinase specific) phosphorylation predictions server and perform the predictions for serine, threonine and tyrosine phosphorylation sites in protein/peptides. The input sequences of any protein/peptide in the one-letter amino acid code in FASTA format can be used for carrying out the predictions. The instructions for the usage of the programme are provided with the respective tools.

3.2.2. *In vitro* Aβ phosphorylation assay

Recombinant rat CK1 (1000 u/µl; New England Biolabs), recombinant subunits of human CK2 (500 u/µl; New England Biolabs) and the catalytic subunits of PKA purified from bovine heart (gift from Dr. D. Bossemeyer) were used for *in vitro* phosphorylation assays in a respective kinase reaction buffer. The phosphorylation assay reaction mixture (28 µl kinase buffer) consisted of 1 µl synthetic Aβ 1-40 or Aβ 1-42 (Stock concentration: 1 mg/ml) and 1 µl of kinase. The phosphorylation reactions were started by addition of 3 µl of 100 µM [γ-^{32}P]ATP and allowed to proceed for 15 min at 32 °C. Reactions were stopped by the addition of 7 µl Laemmli sample buffer (5x) and boiling for 5 min. After boiling, 10 µl of sample aliquots were electrophoresed and western-blotted onto 0.2 µm Polyvinylidene Difluoride (PVDF) membranes. After blotting, the membranes were air dried and exposed to a Phoshor Imager screen/X-ray films for 1-2 days. ^{32}P Phosphate incorporation was analyzed by autoradiography and Phoshor Imaging.

3.2.3. Kinetic and Stoichiometry of Aβ phosphorylation

For Aβ phosphorylation kinetics, 1 µl of Aβ (Stock concentration: 1 mg/ml) was phosphorylated by different kinases (1 µl of PKA/CK1/CK2) at 32 °C in a reaction mixture (28 µl). In stoichiometry experiments, different concentrations of Aβ (0.05, 0.1, 0.2, 0.5, 1.0, 1.5 and 2.0 µg/µl) were phosphorylated by respective kinases for 15 min at 32 °C. *In vitro* phosphorylation and radioactive phosphate incorporation was carried out as described in 3.2.4. The K_m and V_{max} values were calculated by using phosphate incorporation data employing Michaelis-Menten and Lineweaver-Burk plots.

3.2.4. Phosphoamino acid analysis

Phosphoamino acid analysis was carried out by one-dimensional high voltage electrophoresis (Jelinek and Weber, 1993). Radiolabeled proteins electrotransferred onto 0.2 µm PVDF membrane and after the transfer the radiolabeled protein bands were cut and hydrolyzed in 6 M HCl for 90 min at 110 °C. The hydrolysates were spinned down shortly, collected the supernatants and dried in a SpeedVac concentrator. The vaccum dried pellets were dissolved in 10 µl of pH 2.5 buffer (5.9% glacial acetic acid, 0.8% formic acid, 0.3% pyridine, and 0.3mM EDTA) and spotted onto 20 x 20-cm cellulose TLC plates (Merck) together with unlabeled phosphoamino acids (1 µg each of Ser(P), Thr(P), and Tyr(P); Sigma). High voltage electrophoresis was carried out for 45 min at 20 mA. Radioactive phosphoamino acids were localized by autoradiography and identified by comparison with co migrating phosphoamino acids after ninhydrin staining.

3.2.5. *In vivo* phosphorylation of Aβ by cultured cells

Phosphorylation of Aβ by cell-surface located PKA in cultured cells was carried out as described earlier (Walter et al., 1998). Sub confluent monolayer cell cultures (HEK293, SH-SY5Y and human glioblastoma A172 cells) grown on respective medium were washed twice with prewarmed (37 °C) isotonic phosphorylation buffer mix (P-mix; 5 ml/6-cm plate) and incubated for 10 min at 37 °C in the same buffer (2ml/6-cm plate). Phosphorylation reactions were started by addition of 10 µM [γ-^{32}P]ATP and synthetic Aβ peptide (5 µg/ml) and were incubated for 30 min at 37 °C in $C0_2$ incubator (5% $C0_2$). To activate cell surface PKA during *in vivo* labeling, reactions were carried out in the presence of 2.5 µM of cAMP, a selective PKA modulator (Biomol, Germany). To inhibit PKA activities, 1 µM of H-89, a selective inhibitor (Calbiochem, USA) was added to the medium during periods of labeling. After 30 min, the phosphorylation reactions were terminated by removing cell supernatants, followed by two immediate washes of the cells with ice-cold phosphorylation buffer containing 2 mM unlabelled ATP. Subsequently, cells were lysed in the presence of 2 mM ATP for 10 min on ice using ice-cold STEN-Lysis buffer containing 1 µM Okadaic acid (Alexis Biochemicals, Switzerland). Cell lysates and cell supernatants were clarified by centrifugation (14,000 x g for 10 min). Phosphorylated Aβ from cell supernatant and in cell lysates were isolated by immunoprecipitation using polyclonal anti-Aβ specific antibody (2964). The immunoprecipitated radiolabeled Aβ was separated by SDS-PAGE and western-blotted onto 0.2 µm PVDF membranes. Radiolabeled Aβ were detected by autoradiography or by phosphorimaging. Cell viability upon Aβ addition during phosphorylation assays was evaluated by measuring the uptake of fluorescent stain ethidium bromide as described in Kubler et al., (Kubler et al., 1982).

3.2.6. Primary culture of mouse cortical neurons and phosphorylation of Aβ *in vivo*

Cortical neurons were isolated from embryonic C57BL/6J mice at the development stage of 18–19 d as previously described (Hama et al., 2001). Cells (2-2.5 x 10^6 cells) were cultured on poly-L-lysine (PLL) coated glass cover slips (12 mm/0.12–0.17 mm thickness; Marienfeld, Germany) in 6-well plate (Corning). AraC (final concentration, 10µM) was added after the first 1 day of culture, and the culture medium was changed once per week thereafter and 4 hours before treatment. After 14 days *in vitro* (DIV), cultured neurons were used for the *in vivo* phosphorylation experiment. Phosphorylation of Aβ by cell-surface located PKA by primary neuronal cultures were carried out as described in Section 3.2.5. The cell viability upon Aβ addition during phosphorylation assays was evaluated in the parallel

culture (with similar phosphorylation reaction mixture using non-radiolabeled ATP for the reaction) by microscopic observation of tryphan blue exclusion.

3.2.7. Stimulation and induced release of ecto-PKA from intact cells

Subconfluent monolayer cell cultures of HEK293, SH-SY5Y, HeLa, H4 and human glioblastoma A172 cells were grown on respective cell culture medium washed twice with prewarmed 1x PBS and adapted to and finally cultivated in serum-free DMEM medium. Stimulated release of ecto-PKA from the plasma membrane of intact cells in to the culture supernatant was carried out in the presence of 5 µM Forskolin (Calbiochem, USA) for 30 min at 37 °C. After incubation, the cell supernatant was collected and centrifuged to remove the detached cells or any other particular matter. The cleared supernatants were electophoresed to purify the released ecto-PKA and western-blotted onto 0.2 µM PROTRAN nitrocellulose membrane. The membranes were immunoprobed with rabbit polyclonal anti-PKAβ catalytic subunit antibody (PKAβ cat; Santa Cruz Biotechnology Inc, USA).

3.2.8. Cell surface biotinylation of ecto-PKA

Cell surface biotinylation using EZ-link Sulfo-NHS-Biotin was carried out according to Tamboli et al., (Tamboli et al., 2005). Cells grown on the poly-l-lysine coated dishes up to 70-80% confluence were washed with ice cold 1x PBS (5 ml/6-cm plate) for two times. Cells were then incubated with the addition of freshly prepared EZ-link Sulfo-NHS-Biotin solution (50 mg/ml in DMSO) to final concentration of 50 µg/ml and 0.2 % DMSO on ice for 30 min. After 30 min of incubation time, the cell supernatants were aspirated, and cells were washed three times (10 min each) with 20 mM Glycine (in 1x PBS) to remove or to quench the excess of biotin. After washing with Glycine, cells further washed with ice cold 1x PBS two times and then cells were lysed in STEN-lysis buffer with BSA and biotinylated cell surface proteins were isolated using streptavidin sepharose beads. The immunoprecipitated proteins were separated by SDS-PAGE and western-blotted onto nitrocellulose membrane. The detection of biotin-labeled ecto-PKA was done by incubating the membrane in primary antibody rabbit polyclonal anti-PKAβ catalytic subunit antibody (PKAβ cat; Santa Cruz Biotechnology Inc, USA). For detection of cell surface FL-APP, total FL-APP were first immunoprecipitated from lysates after biotinylation and detection of biotinylated FL-APP was performed by probing the blot with primary polyclonal antibody (5313; specific against N-terminal FL-APP).

3.2.9. Human CSF (huCSF) handling and *Ex vivo* phosphorylation

The huCSF study was approved by the local ethical committee and also rules and regulation of the university klinik Bonn. CSF samples were collected by lumbar puncture through the L3/L4 or L4/L5 interspace. The CSF were collected in a polypropylene tube, immediately transported to the laboratory for centrifugation at 5000 x g at 4 °C for 10 min and aliquoted in 2–5 ml portions that were stored at -80°C for further testing purpose. The samples were collected from patients received a diagnosis of AD using the DSM-IIIR (*Diagnostic and Statistical Manual of Mental Disorders*, third edition, revised) (American Psychiatric Association, 1987) and National Institute of Neurological and Communicative Disorders and Stroke-Alzheimer's Disease and Related Disorders Association criteria of dementia and probable AD, respectively (McKhann et al., 1984).

Ex vivo phosphorylation were carried out using CSF as a reaction assay buffer (Total reaction volume: 30 µl). For Aβ phosphorylation, 1 µl of Aβ (Stock concentration: 1 mg/ml) was phosphorylated by 1 µl of different kinases (PKA, CK1 and CK2) at 32 °C using CSF as a reaction mixture (28 µl). Phosphorylation reactions was started by addition of 3 µl of 10 µM [γ-^{32}P]ATP and allowed to proceed for respective time intervals at 32 °C. After incubation at 32 °C the reaction was stopped by the addition of 7 µl of Laemmli sample buffer (5x) and boiling for 5 min. After boiling, 10 µl of samples were electrophoresed and western-blotted onto 0.2 µm PVDF membranes. After blotting, the membranes were air dried and exposed to a Phoshor Imager screen for 1-2 days and radiolabeled Aβ were detected by phosphorimaging.

To characterize the endogenous protein kinase activity in huCSF, reactions were carried out in the presence or absence of kinase specific substrates such as Histone (Stock concentration: 0.5 µg/µl), Phosvitin (Stock concentration: 0.5 µg/µl) and Aβ (Stock concentration: 1 µg/µl) employing the huCSF as a reaction assay buffer (Reaction volume: 30 µl). As a control, 1x PBS was used as a reaction buffer. To study the modulation (activation or inhibition) of endogenous protein kinase activities in huCSF, the reactions were performed in the presence of 2.5 µM of cAMP (a selective PKA modulator) and 1 µM of H-89 (a selective inhibitor) in reaction mixture. Phosphorylation reactions was started by addition of 3 µl of 10 µM [γ-^{32}P]ATP and allowed to proceed for 15 min at 32 °C. After incubation at 32° C the reaction was stopped by the addition of 7 µl of Laemmli sample buffer (5x) and boiling for 5 min. After boiling, 10 µl of sample aliquots were electrophoresed and western-blotted onto 0.2 µm PVDF membranes. After blotting, the membranes were air dried and exposed to a Phoshor Imager screen for 1-2 days and detected the radiolabeled by phosphorimaging.

3.2.10. Preparation of Aβ stock solutions

Stock solutions (Concentration: 230 µM) of Aβ prepared by resuspending 1 mg of lyophilized Aβ peptides in 1 ml of 10 mM NaOH (sterile filtered), vortexed shortly and sonicated in Ultrasonic Bath for 1 min. After sonication, 100 µl of peptide solution aliquoted into screw cap tubes and were flash frozen using liquid nitrogen and stored at -80 °C until used. The concentration of the stock solution was checked using extinction coefficient estimation by the method of Gill and von Hippel (Gill and von Hippel, 1989). For the aggregation reactions, the stocks were diluted in respective assay buffers to the required concentrations and studies were carried out.

3.2.11. Quantifying Aβ Aggregation by CR and ThT dye binding studies

Dye binding strategies have been used as a diagnostic tool to identify amyloid fibrils in tissues more than 150 years and are still one of the most common techniques applied on a routine basis. CR and ThT are the two dyes that are widely used as a postmortem histological indicator of Aβ peptide deposition in AD brain tissue. CR and ThT undergo characteristics spectral alterations after binding to variety of amyloid fibrils, that do not occur on binding to the precursor polypeptides, monomers, or amorphous aggregates of the peptide (LeVine, III, 1999). Both the dyes have been adapted to *in vitro* measurements of amyloid aggregates formation.

Aggregation reaction solutions (Final volume: 300 µl and Final concentration: 100 µM) were made by resuspending the required amount of npAβ and pAβ stock solutions (230 µM) in filter-sterilized 2x PBS (pH 7.4) with 0.01% sodium azide. The aggregation reaction solutions was magnetically stirred at 200 rpm, incubated for 3 days at 37 °C and sample aliquots were removed at different incubation time for the CR binding assays. CR binding experiments were performed as described previously (Klunk et al., 1999). Briefly, 6 µl sample from aliquots of an aggregation reaction was added to 69 µl solution of CR (10 µM) in 1x PBS and incubated at room temperature for 15 min. After 15 min, the test solution was transferred to a quartz cuvette (Hellma, Germany) and absorbance's were read at 540 nm and 480 nm using a Spectrophotometer interfaced with computer (Varian, Australia). The amount of CR-bound (Cb) was calculated as described in Wood SJ et al., (Wood et al., 1996).

Real time ThT binding assay kinetic measurements was performed as described (Bourhim et al., 2007; Klement et al., 2007). The aggregation assay reaction mixture containing 100 µM of npAβ and pAβ peptides in 50 mM of sodium phosphate buffer (pH 7.4), 50 mM NaCl, 20 µM of ThT solution and 0.01% Sodium azide was taken in quartz fluorescence microcuvette (Hellma, Germany) with a small magnetic stirrer. The aggregation assay reac-

tion solutions was magnetically stirred at 200 rpm and incubated at 37 °C. The real time ThT fluorescence data points were recorded every 15 min by measuring fluorescence at 446 nm (Ex. Wavelength) and 482 nm (Em. Wavelength) in Cary Eclipse Fluorescence Spectrophotometer (Varian, Australia) equipped with a thermostat.

3.2.12. Circular Dichroism (CD) Spectroscopy

The structural transition from α-helix/random coil to β-sheet which usually occurs during the process of amyloid formation can be easily monitored qualitatively by CD. Secondary structure can be determined by CD spectroscopy in the far-UV spectral region (190-250 nm). At these wavelengths, the chromophore is the peptide band, and the signal arises when it is located in a regular, folded environment. Alpha (α)-helix, beta (β)-sheet, and random coil structures each give rise to a characteristics shape and magnitude of CD spectrum. This is illustrated in the Fig. 9, which shows spectra for poly-lysine in these three different conformations. Therefore, this method was employed to follow the conformational transitions of npAβ and pAβ peptides. To follow npAβ and pAβ conformational changes, a quartz cuvette of 0.2 cm path length was filled with ~500 µl of protein solution (230 µM). Temperature control with an accuracy of ± 0.5 °C was achieved with a heating/cooling accessory using a Peltier element. CD spectra were recorded in the range of 190-260 nm at regular intervals for the solution with a Jasco 810 spectropolarimeter (Jasco, Gross-Umstadt, Germany). Secondary structure calculations were made by CONTIN-LL.

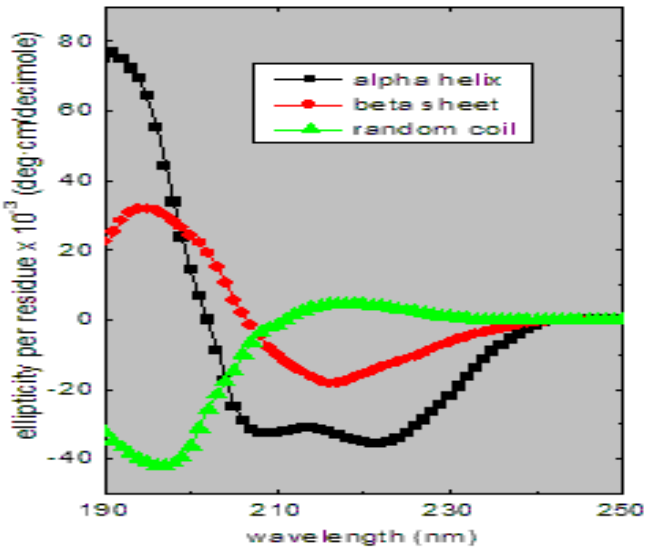

Fig. 9: Characteristics far-UV CD spectra of β-sheets (red), α-helices (black), and random coils (green). Typical bands are: β-sheet – negative at 216 nm (π-π^*), positive at 195-198 nm (n-π^*); α-helix – positive at 192-195 nm (π-π^*), negative at 208 nm (π-π^*) and 222 nm (n-π^*); random coil – negative at 200 nm (n-π^*).

3.2.13. Aggregation kinetics analysis

Aggregation kinetic measurements were carried out as described previously. The kinetic data were fitted using a logistic equation as described (Naiki and Gejyo, 1999),

$$dF/dt=kF(F_{lim}-F) \qquad (1)$$

where F is ThT fluorescence as a function of time t, F_{lim} is its limiting value when t approaches infinity and k is a tentative rate constant. This model may be physically sensible, as far as the number concentration of the growing aggregates is proportional to total concentration of proteins found in protein aggregates. Integrating equation 1 gives,

$$ln(F/(F_{lim}-F))=kF_{lim}t+C \qquad (2)$$

where C is a constant value. Employing this linear semi-logarithmic plot, the time required for F to reach at half of the maximal value, i.e. $t_{1/2}$, was conveniently obtained from the time-intercept of the line (i.e. $-C/kF_{lim}$). Also, the maximal rate of aggregation, occurring at $t=t_{1/2}$ when $F=F_{lim}/2$, was calculated as $kF^2_{lim}/4$. The lag time t_{lag} was calculated as the time-intercept of the line best fitted to the linear portion of F vs. t plot.

3.2.14. Nuclear magnetic resonance (NMR)

A novel method using solution NMR was employed to gain information about the structural information and dynamical properties of effect of phosphorylation on monomer consumption. NMR samples contained 100 μM of npAβ or pAβ in 90% H_2O /10% D_2O, 50 mM Sodium phosphate buffer at pH 7.4, 50 mM NaCl and 0.01% Sodium azide. The temperature was set at 37 °C. 1D ^{1}H-NMR spectra were acquired at the specified times on a Bruker 600 MHz NMR spectrometer equipped with a cryogenic probe. Each NMR experiment consisted of 256 scans, and 16 K complex points were obtained with a spectral width of 7200 Hz. NMR data were processed uniformly by TOPSPIN 2.0 and calibrated using the known chemical shift of water. Three signals within the aliphatic region of proton spectra (0.754, 1.258 and 2.096 ppm), which revealed an evident intensity decay with time were selected for further analysis. Relative intensities of these three peaks, as referenced by the intensity of solvent peak at each spectrum, were monitored with time and employed as a probe of peptide monomer consumption during the early phases of peptide aggregation.

3.2.15. Analysis of size of the Aβ aggregates by Dynamic Light Scattering (DLS)

The npAβ and pAβ peptide aggregation assay solution were made by diluting the stock solution (230 μM) to a concentration of 100 μM, in 50 mM sodium phosphate buffer pH 7.4, containing 50 mM NaCl and 0.01% sodium azide. The aggregation assay solutions were filtered through a Microcon-10 centrifugal device at 12,000 x g for 15 minutes. Immediately after centrifugation the peptides were transferred to a DLS cuvette and continuing for 2 hours, the intensity autocorrelation functions were automatically measured at 5 min intervals. DLS experiments were performed at 37 °C, on a DynaPro Titan DLS instrument, with a laser of 827.08 nm. The scattering angle was 90°. Each DLS measurement consisted of twelve 20 s long acquisitions, with 1 min waiting time between them. Refractive index (RI) of the solution was set at 1.333 at 589 nm and 20 °C, and the RI at the studied wavelength was obtained through Cauchy equation, with a coefficient of 3119 nm^2. The viscosity was 1.019 cp at 20 °C and the temperature-dependent variations were calculated by an aqueous model. The size distribution was determined by a constrained regularization method. Size distributions have been displayed after excluding the outlier peaks, located below 0.5 and above 2000 nm during the whole process.

3.2.16. Analysis of Aβ oligomers by Dot blot assay

Dot blotting technique was employed to monitor the appearance of oligomeric species in the fibrillization process during aggregation. The aggregation assay reaction mixture containing 100 μM of npAβ and pAβ peptide samples in 1 x PBS was incubated at 37 °C for 3 days. Sample aliquots were taken at different time intervals during incubation were flash frozen using liquid N_2. At the end of the aggregation assay, dot blot analysis was carried out. 2 μL of the respective Aβ forms in PBS was applied to a nitrocellulose membrane and allowed to dry. The membrane was blocked in 5% non-fat milk powder/BSA in Tris-buffered saline (TBS) containing 0.01% Tween 20 (TBS-T), at room temperature for 1 h. After incubation, the blots were washed three times for 5 min each with TBS-T and incubated for 1 hr at room temperature with the polyclonal rabbit anti-oligomer Aβ antibody serum (2964) in 3% non-fat milk powder/BSA in TBS-T. The membranes were washed three times for 5 min each with TBS-T, incubated with horseradish peroxidase conjugated anti-rabbit IgG (Sigma, Germany) in 3% non-fat milk powder/BSA in TBS-T and incubated for 1 hour at room temperature. The blots were washed three times with TBS-T and developed with ECL chemiluminescence's reagent.

3.2.17. Transmission Electron Microscopy (TEM)

TEM was used for the characterization of npAβ and pAβ peptide samples in the course of aggregation. Aliquots of Aβ samples used in the CR and ThT dye binding experiments collected at different time intervals during aggregation reaction were employed for the TEM studies. Samples were deposited on a carbon-coated copper grid and adsorbed for approximately for one minute. Remaining moisture was discarded by soaking with filter paper. Subsequently, the samples were covered with a droplet of 1% aqueous uranyl acetate stain. After few seconds the drop was blotted dry and the samples were analyzed with FEI CM120 transmission electron microscope (FEI, USA) operated at 120 kV.

3.2.18. Generation of phosphorylation-site specific Aβ antibody

The polyclonal phosphorylation-specific Aβ antibody (SA5434) was generated against phosphorylated Aβ (pSer-8) using a short peptide containing the phosphorylated residue (NH_2-DAEFRHD**pS**GYEVHHQK-COOH) as an immunogen. The phosphospeptide was coupled to a carrier protein such as keyhole limpet hemocyanin (KLH) and injected into rabbits to generate polyclonal antiserum. After the scheduled immunization, the rabbits were sacrificed and polyclonal serum was collected. The antibodies from serum were then purified by two step affinity chromatography. In first step, the serum was run over a protein A column containing non-phosphospecific peptide. Thus, antibodies that bind in a phosphorylation-independent fashion are retained on the column and removed while antibodies for which the phosphate is an essential part of the epitope will flow through the column. The flow through of the first column was run through a second purification step using a phosphopeptide affinity column which can further purify the phospho-specific antibodies. The polyclonal phospho-specific antibody SA5434 was generated like above with rabbit as a host (Eurogentec, Belgium). After double affinity purification, the phospho-specific antibody is first screened by ELISA to determine affinity and phospho-selectivity. After confirming the phospho-selectivity of the SA5434 by ELISA, the SA5434 antibody was tested against their pAβ specificity by SDS-PAGE and Western-blotting of npAβ and pAβ peptides.

3.2.19. Transgenic mice, protein extraction and immunohistochemistry

APPswe/PS1Δexon9 double transgenic mice (*tg*) were obtained from Jax Laboratories, USA (Strain Name: B6C3-Tg, Stock Number: 004462). Amyloid pathology that develops in these mice derives from the proteolytic processing of the human APP transgene product that harbors the Swedish double mutation (K595N/M596L) and ΔE9 knock-out mutation in presenilin 1 that, in combination, lead to the marked overproduction and progressive accumula-

tion of the Aβ (Borchelt et al., 1997). Transgenic mice and nontransgenic littermates were sacrificed at 2, 6, 9, 12, 18 and 24 months. The brains were perfused transcardially with ice-cold saline, and removed from the skull. Brain hemispheres were either frozen in liquid nitrogen until further use or fixed in 4% paraformaldehyde dissolved in PBS overnight. One half of the brain hemisphere was used for immunohistochemical studies and the other half was used for sequential protein extraction. At each step, the brains were mechanically homogenized (Eppendorf douncer; 10 repeats) followed with sonication (20 stroke, max poweroutput: 70%, 20 seconds intervals) in an appropriate buffer was followed by 30 minutes incubation on ice and centrifugation at 14,000 x g for 30 minutes at 4 °C. The supernatant was then removed, and the pellet was sonicated in the next solution used in the sequential extraction process. For two-step extraction, homogenization and sonication of the frozen brain began in 1000 µl of 0.32 M Sucrose in millipore H_2O, supplemented with complete protease inhibitor cocktail and protein phosphatase inhibitor tablet (Roche Diganostics GmbH, Germany). The next sequential extraction step used 1000 µl of 2% SDS in 50 mM Tris buffer (pH 7.3) containing protease and phosphates inhibitors (Roche Diagnostics, Germany). After each step of extraction, the respective supernatants were collected in fresh eppendorf tubes and kept on ice. After the sucrose soluble-Aβ and SDS soluble-Aβ extraction procedure, the total protein concentrations were determined with the BCA™ protein assay kit (Thermo Scientific, USA).

For immunohistochemical analysis, paraformaldehyde fixed brains were cut into 40 µm thick sagittal sections using a vibratome (LeicaVT1000S). Sections were treated with 50% methanol in PBS for 15 min, washed 3x with PBS for 10 min and blocked with 3% BSA in PBS, 0.1% Triton X-100 (blocking buffer). Next, sections were incubated with primary antibodies (6E10, SA5434) in blocking buffer overnight at 4 ºC, washed three times with blocking buffer for 10 min and incubated with Alexa Fluor 488 goat anti-mouse and 594 goat anti-rabbit antibodies (1:500). Subsequently, sections were washed three times in blocking buffer, brought onto Superfrost glasses in tap water, dried overnight and mounted in Mowiol. Immunofluorescence images of the sections were obtained with standard fluorescent microscope or spinning disk confocal microscope. Deconvoluted images of 3 µm thick stacks were obtained with standard fluorescent microscopy using Cell-P software.

3.2.20. Dephosphorylation of mouse brain lysates and synthetic pAβ samples

The reaction mixture containing (50 µl) containing 100 µg of mouse whole brain hydrolysates and 500 ng of pAβ 1-40 in 1x SAP reaction buffer were enzymatically dephosphorylated using 3 µl Shrimp-Alkaline Phosphatase (SAP) (1u/µl; Fermentas) at 37 °C for 5

hours. The samples were then electrophoresed and immunoblotted using anti-Aβ antibody (6E10). The immunoblots were quantified with Quantity One software (BioRad).

3.2.21. Immunohistochemistry and double-label confocal microscopy of human AD brain

Ten human autopsy brains were received from the University Hospital Bonn in accordance with the laws and under affirmation of the local ethical committee (Table 3). Post-mortem diagnosis of Alzheimer's disease was carried out according to the NIA-Reagan Criteria (The National Institute on Aging 1997: Neurobiol Aging, 18: S1-2.). In two cases, double-label immunohistochemistry on AD brain sections was performed using polyclonal anti-pAβ antibody (SA5434, (Eurogentec, Belgium), 1/5) combined with a monoclonal antibody directed against APP (22C11, (Chemicon, USA), 1/75). The primary antibodies were visualized with carbocyanin 2 (Cy2)-labeled antibodies directed against mouse IgG and Cy3-labeled antibodies against rabbit IgG (1:50; Cy2 and Cy3; Dianova, Hamburg, Germany). These sections were mounted in Corbit without counterstaining. The remaining eight brain sections were immunohistochemically labeled for anti-pAβ. The antibody reaction was visualized with the Biomeda ABC-Complex-kit (Biomeda, Foster City, CA). Immunolabeled sections were analyzed with a Leica DMLB fluorescence microscope. Pictures were taken digitally with a Leica DCF500 camera.

Table 3: Ten human autopsy brains were received from the University Hospital Bonn in accordance with the laws and under affirmation of the local ethical committee.

Case No.	Age	Gender	Braak-Stage	Aβ-phase	Post mortem diagnosis
1	64	Male	I	2	Normal aged brain
2	72	Male	III	2	Normal aged brain
3	83	Female	III	3	Normal aged brain
4	84	Female	III	3	Normal aged brain
5	87	Male	III	3	Normal aged brain
6	82	Male	III	3	AD
7	76	Male	IV	4	AD
8	83	Male	IV	4	AD
9	89	Female	V	4	AD
10	86	Female	VI	4	AD

3.2.22. SDS-PAGE and Western blotting

Pre-cast NuPAGE 4-12% bis-Tris Gel (Invitrogen, USA) or 16% Tris-Tricine Anamed gels (Anamed Elektrophorese GmbH, Germany) or 10% self made gels of were used for the SDS-PAGE. 50 µg of protein per sample (brain lysates) was resuspended with 4x NuPAGE LDS Sam-

ple buffer and 10x NuPAGE Reducing agent. Samples were mixed and were heated to 70 °C for 10 minutes. After heating, samples were spinned down shortly and loaded the samples in respective gels and done the electrophoresis. After electrophoresis, the proteins were transferred onto 0.2 µm nitrocellulose membranes. Membranes were boiled for 10 min in 1x PBS and blocked in PBS-T (Phosphate-Buffered Saline-Tween 20) containing 5% BSA or non-fat milk powder (ECL Advance blocking agent; GE Healthcare) and probed with appropriate antisera/antibodies diluted in 1% BSA/non-fat milk powder. Blots were developed with an Amersham ECL detection system (Amersham, GE Healthcare). Blots were quantified with Quantity One software (BioRad).

4. RESULTS

4.1. Phosphorylation of Aβ

The Aβ sequence contains two serine residues at 8th (604 aa of APP695) and 26th position (622 aa of APP695), a tyrosine (610 aa of APP695) residue at 10th position which could possibly undergo phosphorylation. The primary goal of the thesis work was to identify the role of phosphorylation in Aβ aggregation and pathogenesis of AD. Therefore, investigations were carried out to predict/identify/determine putative phosphorylation sites of Aβ.

4.1.1 *In silico* analysis of putative phosphorylation sites of Aβ

The preliminary identification of the putative phosphorylation sites of Aβ and identification of the responsible kinases were carried out by *in silico* analysis using freely available world wide web (www) based computational tools. These prediction tools are neural network-based methods for predicting potential phosphorylation sites (serine, threonine or tyrosine residues) in any given protein/peptide sequences.

The prediction of putative Aβ phosphorylation sites was performed by using the Netphos 2.0 computational tool (www.cbs.dtu.dk/services/NetPhos). The results from the *in silico* analysis indicate that Ser-8, Ser-26 and Tyr-10 residues might be potential phosphorylation sites in Aβ sequence (Fig. 10). The serine at 8th position had the highest prediction score of 0.963. The serine at 26th position had a prediction score of 0.787. The tyrosine at 10th position has a score of 0.870. In general, the higher the prediction score, the higher is the confidence level of the prediction and also the predicted sites are comparable to one or more of the already known phosphorylation consensus sequences used in neural network algorithms of the prediction tool. The phosphoprediction scores above the threshold value (>0.5) is considered to be significant according to the prediction programme and has the highest probability to undergo phosphorylation.

Method: NetPhosK 2.0 server

a) Aβ Sequence Length: 40aa

DAEFRHDSGYEVHHQKLVFFAEDVGSNKGAIIGLMVGGVV
.......S.Y..............S.............

Phosphorylation sites predicted: Ser: 2, Thr: 0 and Tyr: 1

b) Serine predictions

Name	Pos	Context	Score	Pred.
Aβ Sequence	8	FRHDSGYEV	0.963	*S*
Aβ Sequence	26	EDVGSNKGA	0.787	*S*

Tyrosine predictions

Name	Pos	Context	Score	Pred.
Aβ Sequence	10	HDSGYEVHH	0.870	*Y*

c) Graphical illustrations of the phoshopredictions

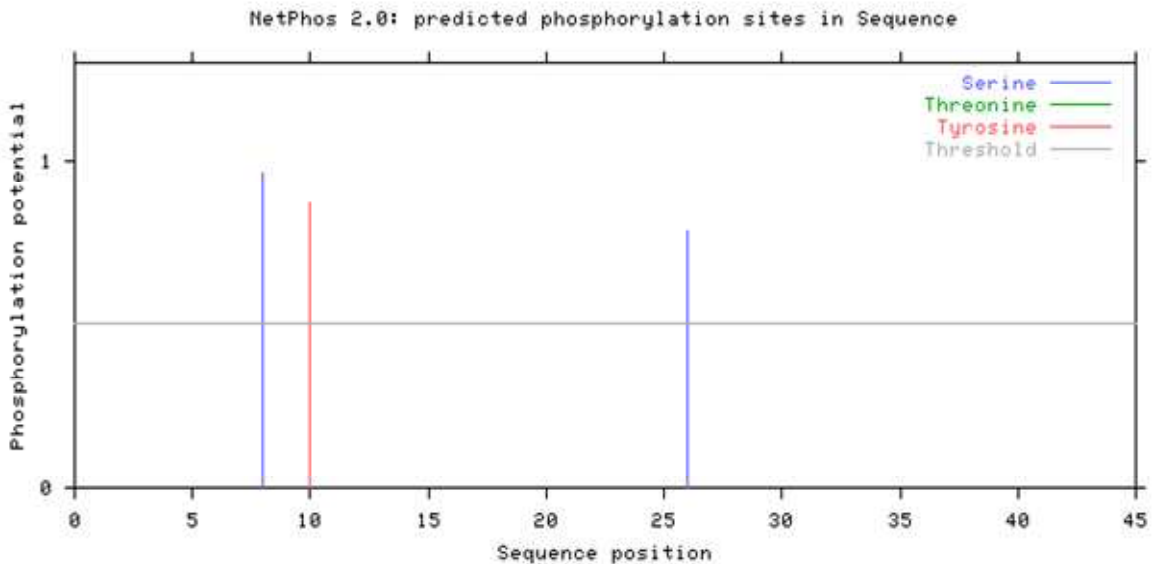

Fig. 10: *In silico* analysis of putative phosphorylation sites of Aβ.
Protein sequences of human Aβ1-40 sequences were analyzed by using NetPhos 2.0 computational prediction tool (www.cbs.dtu.dk/services/NetPhos). The result from NetPhosK contains three parts for each of the protein/peptide sequence analyzed. The first part indicates the name, length of the aa sequence and predicted phosphosites (a). The second part shows the predicted phospho residues, their positions in the sequence and the respective phospho prediction score (b). The third part shows the graphical illustrations of phosphorylation potential of predicted phosphosites (c).

4.1.2. Identification of kinase-specific consensus sequences in Aβ and responsible kinases

Consensus sequences/motifs refers to the sequence of amino acids immediately surrounding the phosphorylated site(s) by given protein kinases. They act as critical substrate recognition determinants and most probably form a reflected image of the corresponding substrate binding domains. They are considered essential for substrate recognition and phosphorylation by respective kinases (Kennelly and Krebs, 1991). KinasePhos prediction tool was used to predict the kinase-specific consensus motifs in Aβ sequence (Fig. 11).

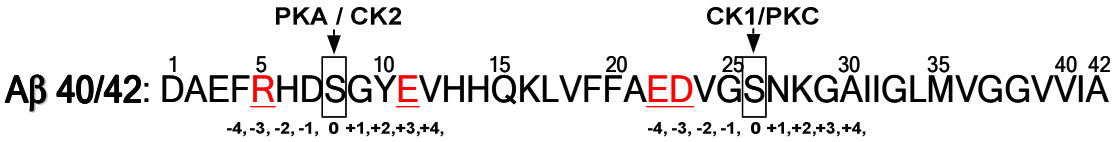

Fig. 11: Human Aβ sequence with predicted phosphosites, consensus motifs and responsible kinases.
The boxed residues (Ser-8 and Ser-26) indicate putative phosphorylation sites for the indicated protein kinases (PKA, CK1, CK2 and PKC). Residues determining the kinase-specific consensus motifs are shown in red color (underlined). The identified kinases which can conform phosphorylation consensus are indicated above the amino acid sequence. The predicted phosphosite are indicated by zero. The numbers below the Aβ sequence indicate the position of the amino acid residues towards N-terminal (-) and C-terminal (+) in the sequence.

The KinasePhos prediction tool showed the occurrence of kinsase-specific consensus sequences around the identified phosphorylation sites. Ser-8 with a consensus sequence (FRHD**S**GYEV) could undergo phosphorylation by protein kinase A (PKA) or casein kinase 2 (CK2). Likewise, Ser-26 with a consensus sequence (EDVG**S**NKGA) might undergo phosphorylation by casein kinase 1 (CK1) or protein kinase C (PKC). The resemblance of kinase-specific consensus sequences in Aβ further supports that Aβ might undergo phosphorylation by PKA, CK1, CK2 and PKC (Table 4). All of these identified kinases are reported to be implicated in AD (Chachin et al., 1996a; Jicha et al., 1999; Moore et al., 1998; Schwab et al., 2000; Su et al., 2003; Yasojima et al., 2000).

Table 4: Summary of the consensus sequences most frequently recognized by different protein kinases and resemblance of such consensus in Aβ sequence.
The amino acid indicated by an asterisks (also highlighted in red) denotes the phosphoacceptor (**S*/T***). The P in parentheses is to denote pre-existing phosphoamino acid residue. Interchangeability of two amino acids function is indicated by listing both residues with a slash (/) separating them. X is any amino acid which is neutral for the recognition sequence. The numbers in subscripts refer to the amino acid positions.

Protein Kinases	Preferred consensus sequences (motifs)	Resemblance of consensus motifs in Aβ sequence
cAMP-dependent protein kinase A (PKA)	R-R/K-X-**S*/T*** > R-X_2-**S*/T*** = R-X-**S*/T***	DAEF**R**HD**S*** (Ser-8)
Casein kinase 2 (CK2)	**S*/T***- (D/E/S(P)$_{1-3}$-X_{2-0})	DAEFRHD**S***GY**E** (Ser-8)
Casein kinase 1(CK1)	S(P)-X_2-**S*/T*** > S(P)-$X_{1\ or\ 3}$-**S*/T***>> (D/E_{2-4}, X_{2-0})- **S*/T***	**ED**VG**S***NKG (Ser-26)
Protein kinase C (PKC)	(R/K_{1-3},X_{2-0})-**S*/T***-(X_{2-0},R/K_{1-3})>**S*/T***-(X_{2-0},R/K_{1-3}) ≥ (R/K_{1-3},X_{2-0})-**S*/T***	EDVG**S***N**K**G (Ser-26)

4.1.3. *In vitro* phosphorylation of Aβ

To test the potential phosphorylation sites of Aβ, *in vitro* phosphorylation studies were carried out using synthetic Aβ1-40 peptide and purified catalytic units of PKA, CK1 and CK2. As the present study aimed at identifying the phosphorylation events taking place extracellularly, investigations were carried out with the extracellular kinases which are reported to occur at cell surfaces (PKA, CK1 and CK2) (Kubler et al., 1982; Kubler et al., 1992; Redegeld et al., 1999; Walter et al., 1996b; Walter et al., 2000).

The results of *in vitro* phosphorylation of Aβ by different kinases are shown (^{32}P) (Fig. 12A). Aβ1-40 peptide can undergo phosphorylation by PKA, CK1 and CK2. The catalytic subunits of different kinases were also found to undergo autophosphorylation. The autophosphorylation signals were observed to be reduced when the substrate (Aβ) was supplemented to the reaction indicating the authenticity of Aβ phosphorylation correspondingly by the respective kinases. This further confirms the substrate competition in the phosphorylation reaction. The amount of radiolabeled ^{32}P phosphate incorporation was quantified using phosphorimager and results indicate that phosphorylation of Aβ is in the order PKA > CK2 > CK1 (Fig. 12B).

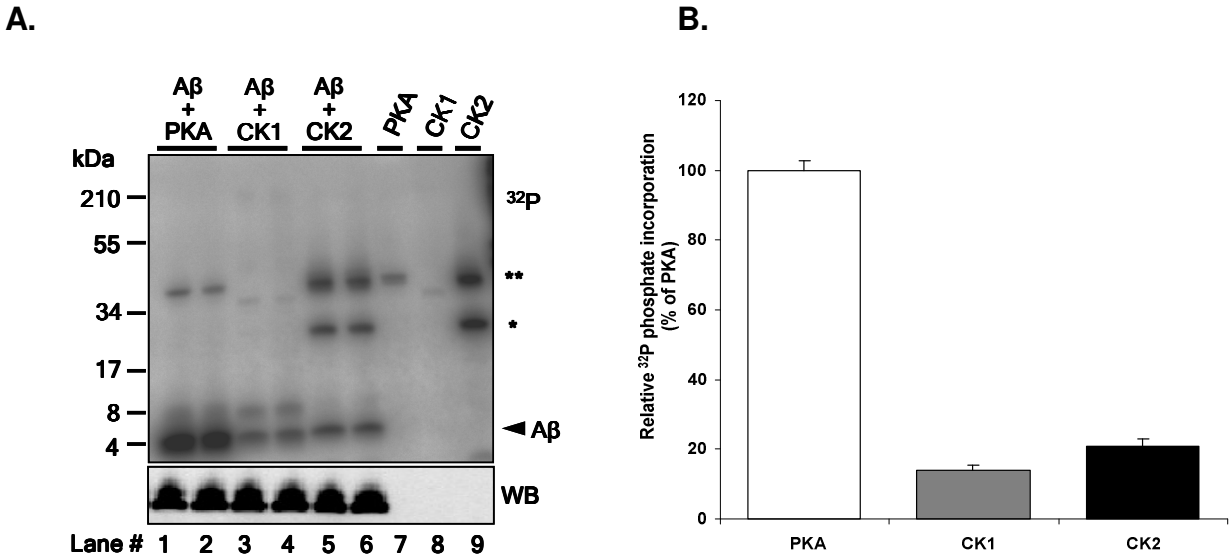

Fig. 12: *In vitro* phosphorylation of Aβ1-40 by PKA, CK1 and CK2 kinases.
In vitro phosphorylation reactions were carried out by incubating synthetic Aβ1-40 (1 µg) with radiolabeled [γ^{32}P]ATP (10 µM) in the presence of respective catalytic subunits of kinases for 15 min at 32 °C. Radiolabeled proteins were separated by SDS-PAGE and western-blotting. ^{32}P-labeled Aβ was detected by autoradiography. A) The autoradiograph showing the phosphorylation of Aβ by all the three kinases (phosphosignals at 4 kDa). The asterisks indicate autophosphorylation signals of the PKA, CK1 and CK2 kinases. The lower panel indicates immunosignals of Aβ by western-blotting confirming the equal amount of Aβ taken for the reactions (WB). B) The relative ^{32}P phosphate incorporation of Aβ by the kinases was quantified by phosphorimaging. The phosphorylation reactions were carried out in duplicates in two independent experiments. Values represent mean ± s.d. of two independent experiments.

4.1.3.1. Phosphoamino acid analysis of *in vitro* phosphorylated Aβ

To further characterize the phosphorylation site, phosphoamino acid analysis was carried out. *In vitro* phosphorylated Aβ was hydrolyzed to release the phosphoamino acids and separated them on cellulose-TLC plates. The location of the phosphoamino acid standards was mapped by ninhydrin staining and the presence of ^{32}P-amino acids by autoradiography. The results indicate the presence of only ^{32}P-labeled phospho-Ser; the same position and shape for the P-Ser (pS) spot using ninhydrin detection and autoradiography was apparent. The phosphorylation was targeted mainly on serine residues of Aβ by the used kinases (Fig. 13).

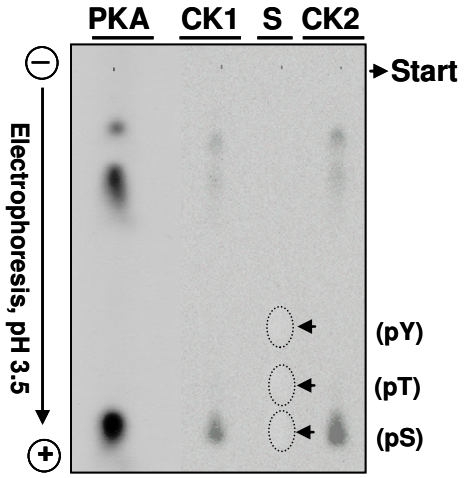

Fig. 13: Phosphoamino acid analysis of ^{32}P labeled Aβ peptide by thin-layer electrophoresis.
In vitro phosphorylated Aβ was subjected to acid hydrolysis and the released phosphoamino acids were resolved by one-dimensional thin layer electrophoresis using cellulose-TLC plates. The position of radiolabeled phosphoamino acids were detected by autoradiography. The positions of ninhydrin-stained phosphorylated amino acids are indicated by circles: phosphoserine (pS), phosphothreonine (pT), and phosphotyrosine (pY). The migration of the ^{32}P labeled serine with the ninhydrin-stained cold phosphoamino acids standards can be seen.

4.1.3.2. Stoichiometry and kinetics of phosphorylation

The stoichiometry and kinetics of phosphorylation of Aβ1-40 by PKA, CK1 and CK2 was examined. The autoradiograms show the time course of phosphorylation of Aβ1-40 by PKA, CK1 and CK2 kinases (Fig. 14A). Phosphorylation of the Aβ1-40 increased with increase in reaction time and reached saturated levels after about 15-30 min. Rapid incorporation of radiolabeled ^{32}P was observed with PKA and CK2 as compared to slower incorporation by CK1. Phosphate incorporation followed a typical hyperbolic curve. Quantitative analysis revealed that PKA mediated incorporation of ^{32}P phosphate reached plateau at ~1 mol of phosphate/mol of Aβ1-40, whereas CK2 incorporates about ~0.6 mol of phosphate/mol of Aβ1-40. The CK1 mediated ^{32}P phosphate incorporation was ~0.2 mol of phosphate/mol of Aβ1-40 respectively (Fig. 14B).

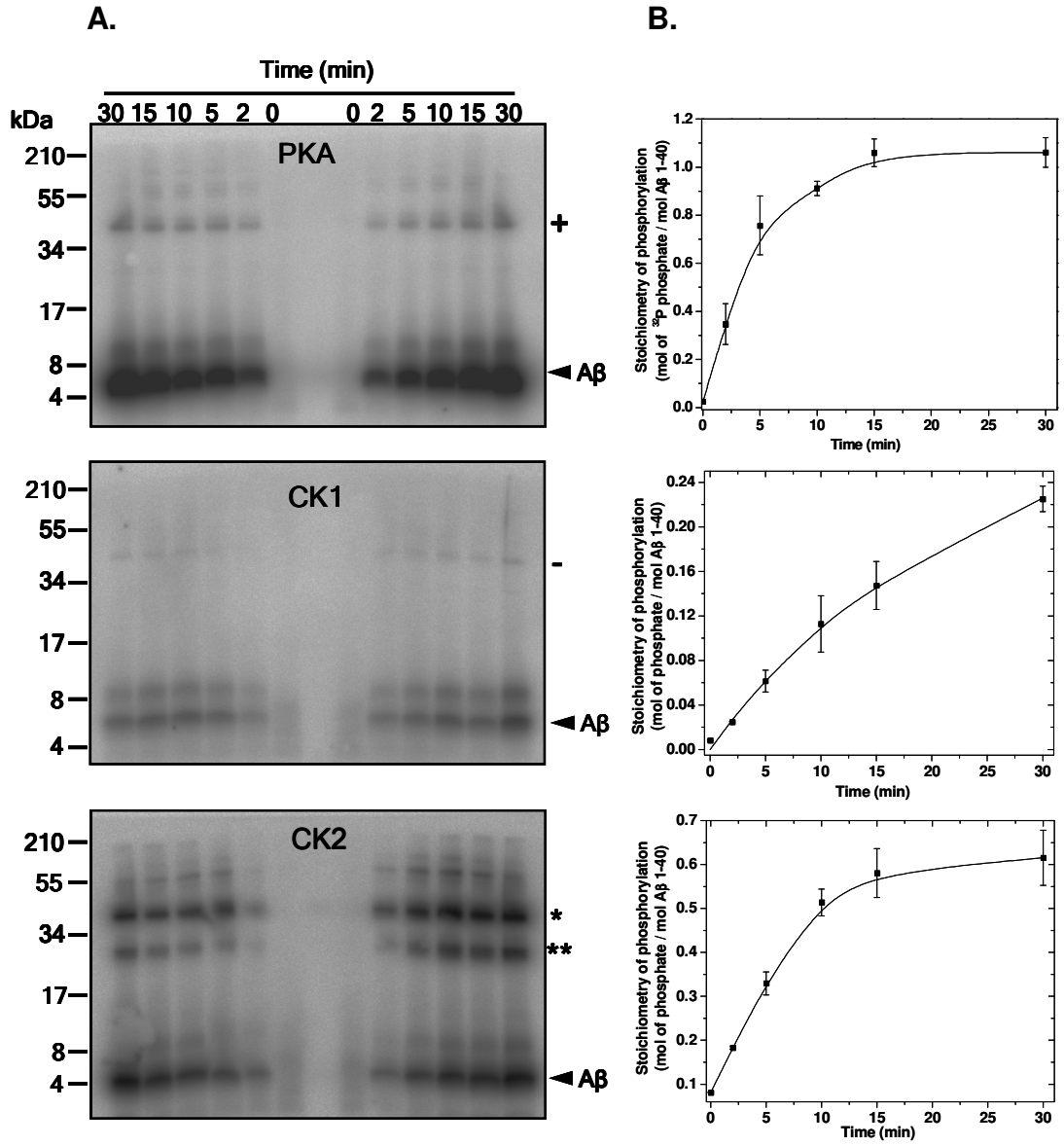

Fig. 14: Stoichiometry of Aβ1-40 phosphorylation by PKA, CK1 and CK2.
A) Synthetic Aβ1-40 (1 µg) was incubated with [γ-^{32}P]ATP (10 µM) in the presence of PKA, CK1 and CK2. *In vitro* phosphorylation reactions were carried out for the indicated time points. Phosphorylation reactions were terminated by the addition of SDS-sample buffer. The reaction products were electrophoresed and western-blotted onto PVDF (polyvinylidene difluoride) membrane. Radiolabeled proteins were detected by autoradiography. Autoradiographs show the phosphosignals of Aβ by PKA, CK1 and CK2 kinases at different time intervals (indicated by arrow head). The autophosphorylation signals of kinases are also shown (+, - and asterisks). B) The stoichiometry of the phosphorylation was calculated on the basis of the specific radioactivity of the [γ^{32}P]ATP used and the amount of Aβ (in µM) used for the reaction. Quantification by phosphorimaging revealed that PKA incorporates ~1 mol of phosphate/mol of substrate, while CK2 incorporates ~0.6 mol of phosphate/mol of substrate. The CK1 incorporates ~0.24 mol of phosphate/mol of substrate. The phosphorylation reactions were carried out in duplicates each time. The values indicate mean ± s.d. of four data points from two experiments.

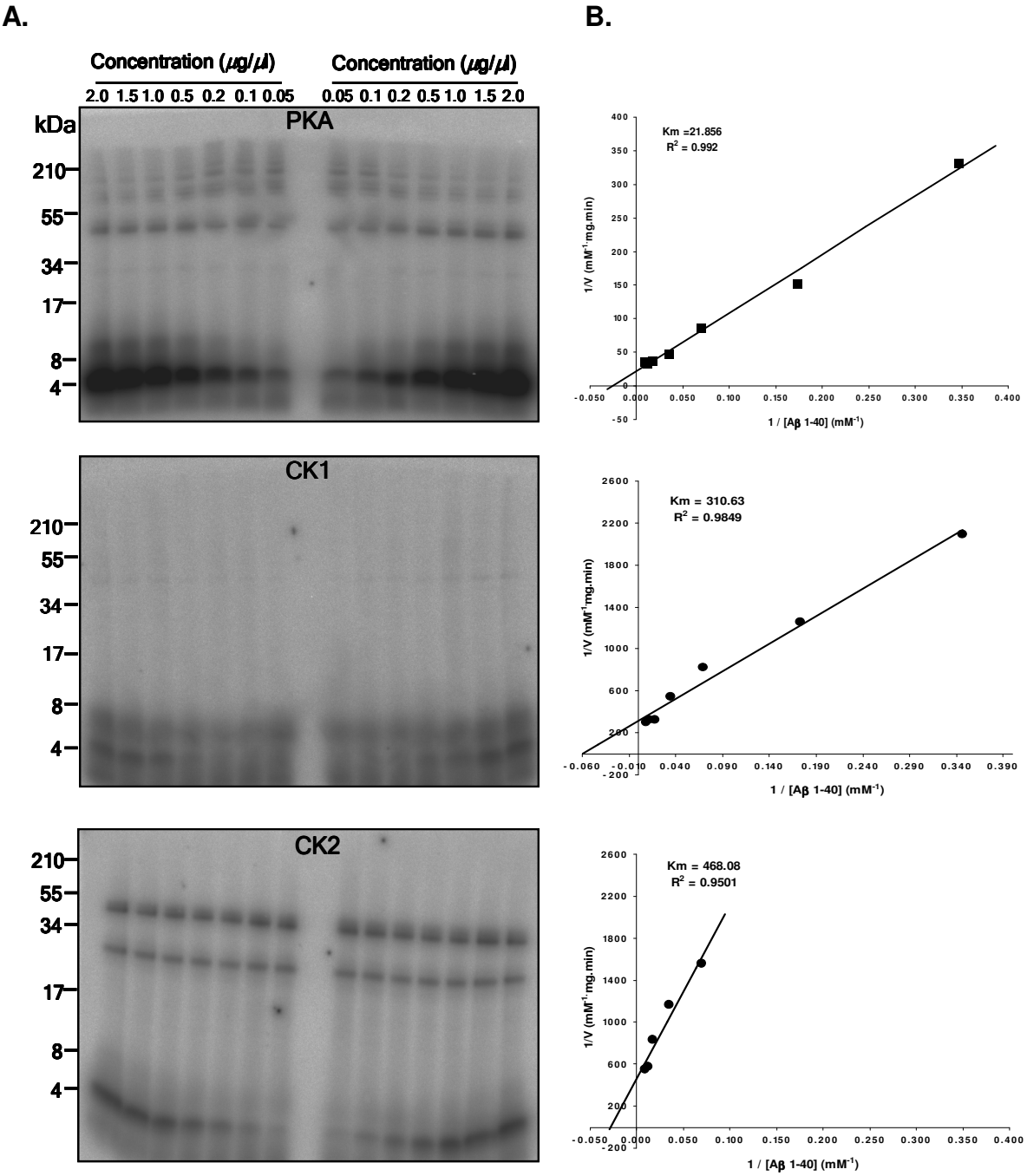

Fig. 15: Determination of Km of Aβ1-40 phosphorylation by PKA, CK1 and CK2 kinases.
A) Aβ1-40 (0.05, 0.1, 0.2, 0.5, 1.0, 1.5 and 2.0 µg) was phosphorylated by PKA, CK1 and CK2 kinases for 15 min at 32 °C. After incubation, the reactions were stopped by addition of SDS-sample buffer and aliquots of samples were electrophoresed and western-blotted onto PVDF membrane. Radiolabeled proteins were detected by autoradiography. Autoradiograph shows the phosphorylation signals of different concentrations of Aβ used for the reaction. The phosphorylation reactions were carried out in duplicates. B) Radiolabeled ^{32}P incorporation was quantified by phosphorimaging and Km was calculated by Lineweaver-Burk double reciprocal plot analysis. The calculated Km values for PKA was 21 µM and Km values for CK1 and CK2 were 310 µM and 468 µM. The assays were carried out in duplicates each time. The values indicate mean ±s.d. of four data sets from two experiments.

Different concentration of synthetic Aβ1-40 (0.05- 2.0 µg/µl) was phosphorylated by PKA, CK1 and CK2 kinases (Fig. 15A). The ^{32}P phosphate incorporation was quantified by phosphorimaging. The Km values were calculated by Lineweaver-Burk double reciprocal plot analysis. The Km value for PKA for Aβ was 21 µM and Km values for CK1 and CK2 were 310 and 468 µM respectively (Fig. 15B). Notably, the Aβ1-40 appears to be a better substrate for PKA and CK2 kinases, as indicated by the stoichiometry and kinetic analysis.

4.1.3.3. *In vitro* phosphorylation of Aβ1-42

The previous results showed that Aβ1-40 can undergo phosphorylation by PKA, CK1 and CK2. In human brain, two major forms of Aβ such as Aβ1-40 (90%) and Aβ1-42 (10%) exists (Iwatsubo et al., 1996). Therefore, phosphorylation of Aβ1-42 was also tested. Like Aβ1-40, all the three kinases phosphorylated the Aβ1-42. In addition to phosphorylation of monomeric Aβ, Aβ dimer was also found to undergo phosphorylation by PKA and CK1, little if any phosphorylation of Aβ dimer was observed with CK2 (Fig. 16). This indicates either the kinase specificity towards oligomer is different or phosphorylation by PKA or CK1 kinase could induce oligomerization of Aβ (^{32}P signals of Aβ dimer were significantly observed with PKA and CK1 as compared to CK2).

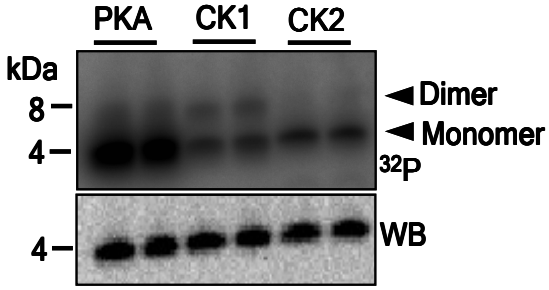

Fig. 16: *In vitro* phosphorylation of Aβ1-42 by PKA, CK1 and CK2.
In vitro phosphorylation were carried out using synthetic Aβ1-42 (1 µg) incubated with radiolabeled [γ^{32}P]ATP (10 µM) in the presence of respective kinases for 15 min at 32 °C. Radiolabeled proteins were separated by SDS-PAGE and western-blotting. ^{32}P-labeled Aβ was detected by autoradiography. The autoradiograph (^{32}P, upper panel) shows phosphorylation signal of Aβ1-42 monomer by all the three kinases (phosphosignals at 4 kDa). Significant amount of phosphorylation of Aβ1-42 dimer by PKA and CK1 are observed (phosphosignals at 8 kDa). The lower panel indicates Aβ1-42 immunosignals after western-blotting using anti Aβ1-42 specific antibody showing the equal amount of peptide employed for the assay (WB).

4.1.3.4. Localization and characterization of the PKA, CK1 and CK2 phosphorylation sites of Aβ

To identify the exact phosphorylation sites of the kinases, *in vitro* phosphorylation assays were carried out using truncated, full-length and phospho variants of synthetic peptides by PKA, CK1 and CK2 kinases (Aβ1-16, Aβ17-40, Aβ1-40, pAβ1-40 (pre-phosphorylated at Ser-8) and Aβ1-42).

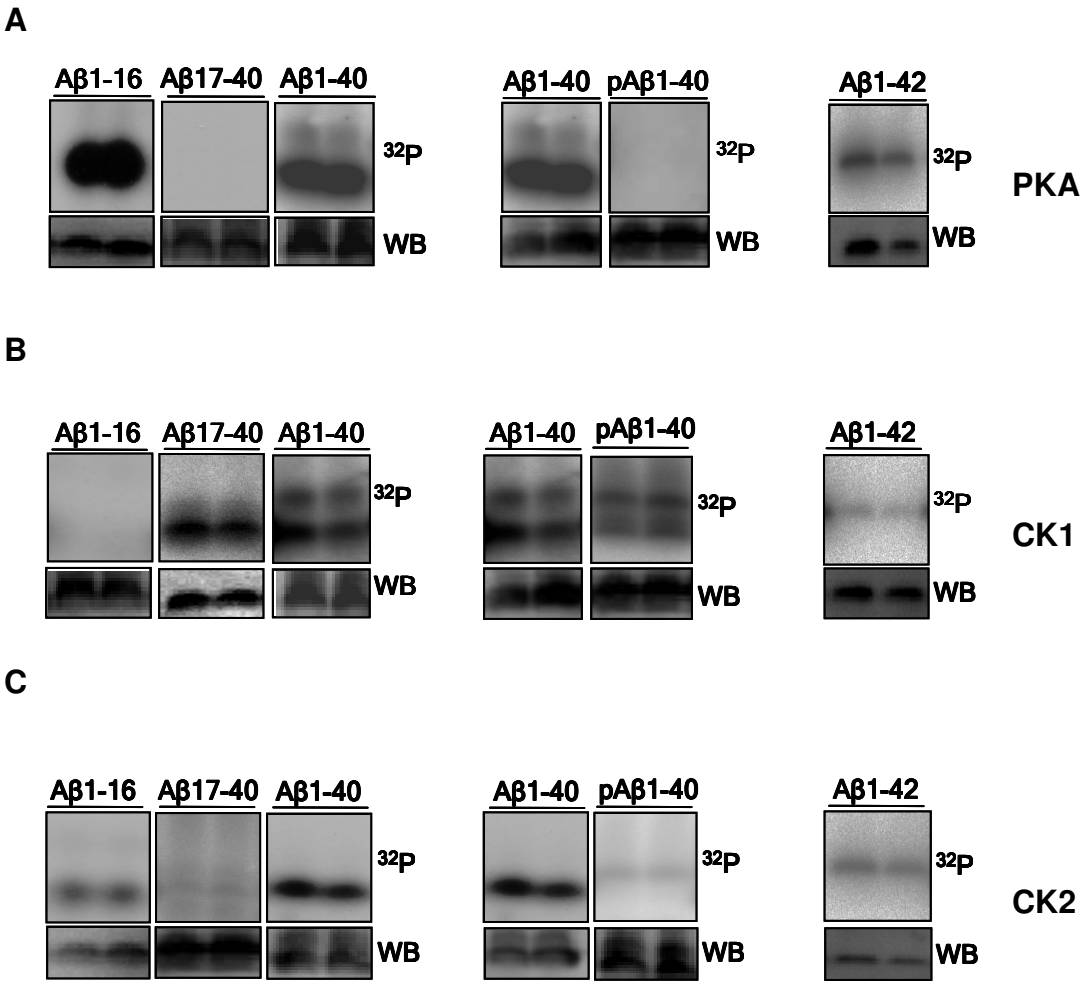

Fig. 17: Localization of PKA, CK1 and CK2 specific phosphosites of Aβ.
In vitro phosphorylation assays were carried out using different variants of synthetic Aβ peptides (1 µg), [γ-^{32}P]ATP (10 µM) and purified PKA, CK1, and CK2 (A, B and C). Radiolabeled proteins were separated by SDS-PAGE and western-blotting. ^{32}P-labeled Aβ was detected by autoradiography. A) PKA phosphorylated Aβ1-16, Aβ1-40, and Aβ1-42. No phosphosignals were observed for Aβ17-40 and pAβ1-40 (pSer-8) by PKA indicate that PKA exclusively phosphorylates Ser-8 residue in Aβ sequence. B) CK1 phosphorylated Aβ17-40, Aβ1-40, pAβ1-40 (pSer-8) and Aβ1-42 but not Aβ1-16. The results indicate that CK1 phosphorylates the Ser-26 residue in Aβ sequence. C) CK2 phosphorylated Aβ1-16, Aβ1-40, and Aβ1-42. A minor (not significant) incorporation of ^{32}P phosphate is observed for Aβ17-40 and pAβ1-40 (pSer-8). Results indicate that CK2 can phosphorylate the Ser-8 residue in Aβ sequence. The lower panel indicates immunosignals of Aβ after western blotting and confirms the equal amount of Aβ taken for the reactions (WB).

PKA readily phosphorylated the Aβ1-16, Aβ1-40 and Aβ1-42 excluding the Aβ17-40 and pAβ1-40. The use of synthetic peptide Aβ1-16 (contains Ser-8) and Aβ17-40 (contains Ser-26) showed that PKA exclusively phosphorylates Aβ at Ser-8 residue. In addition, PKA failed to phosphorylate the synthetic pAβ1-40 which was pre-phosphorylated at Ser-8 (pAβ-Ser8) further confirming the specificity of PKA to Ser-8 residue (Fig. 17A). CK1 phosphorylated the Aβ17-40, Aβ1-40, pAβ1-40 and Aβ1-42 but not Aβ1-16 indicating the specificity of CK1 to Ser-26 residue (Fig. 17B). CK2 readily phosphorylated the Aβ1-16, Aβ1-40, Aβ1-42 except Aβ17-40 and pAβ1-40 indicate that CK2 can phosphorylate Ser-8 of Aβ (Fig. 17C). Together, these data indicate that Ser-8 residue in Aβ can undergo phosphorylation by PKA and CK2 while CK1 can phosphorylate Ser-26 residue in Aβ sequence.

4.2. Characterization of extracellular kinase activity

4.2.1. Differential expression of PKA in human AD brain

The cAMP/protein kinase A (PKA) pathway is responsible for the most cAMP-mediated physiological functions in the brain and has long been known for its essential role in memory formation (Walaas and Greengard, 1991; Horiuchi et al., 2008). Biochemical analyses were carried out to check the PKA expression in human healthy (control) and diseased (AD) brain. Consistent with the results from cultured cells and human brain tissue (Orstavik et al., 2001; Orstavik et al., 2005), different catalytic subunits (Cα1; 40 kDa and Cβ2; 47 kDa) of PKA were detected in the control as well as AD human brain lysates. The expression of Cα1 catalytic subunit was predominant in AD as well as in controls as compared to Cβ2. Interestingly, the expression level of both the catalytic subunits was found to be significantly altered in AD brain as compared to controls (Fig. 18).

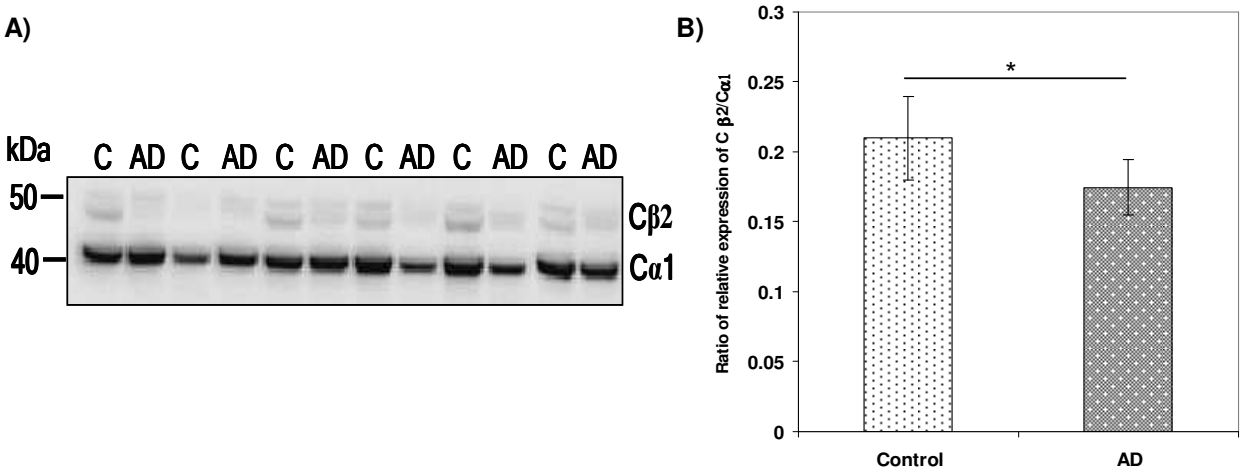

Fig. 18: Detection of endogenous PKA expression in human control and AD brain.
The brain lysates prepared from human AD patients (AD) and age-matched controls (C) brains were electrophoresed and western-blotted (50 µg of protein lysate/lane). Endogenous PKA expression was detected using anti-PKA catalytic subunit antibody. The expression of the Cα1 catalytic subunit of PKA (40kDa) is higher as compared to Cβ2 (47kDa) in AD as well as in controls. The expression of both the catalytic units are seems to be altered in AD patients brain as compared to controls (Cβ2 was more evident). B) Densitometric analysis of the alteration of different catalytic subunits. The bar graphs indicate the alteration of Cβ2/Cα1 expression in AD patients as compared to age-matched controls. The values indicate mean ± s.d (*p<0.05; n = 6). Statistical significance was evaluated by student *t*-test (n=3).The expression analysis is normalized to endogenous β-actin levels.

4.2.2. Detection of extracellular PKA in cultured cells

In addition to abundant source of intracellular kinases, existence of different extracellular PKs on the cell surface of a wide variety of cells have been reported (Nestler and Greengard, 1983; Walaas and Greengard, 1991; Redegeld et al., 1999; Walter et al., 1996). The extracellular PKs activity and the shedding of these kinases are known to be modulated by adenylate cyclase modulators. Forskolin has been used extensively to stimulate the adenylate cyclase to increase the cAMP level and to elicit cAMP-dependent physiological processes (Awad et al., 1983). Different monolayer intact cell cultures (HEK293, SH-SY5Y, HeLa, H4 and Glial cells) were used to confirm the occurrence of extracellular PKA and to check whether forskolin can modulate PKA secretion (shedding). The results indicated the expression of two catalytic subunits of PKA from the cells (Cα1 and Cβ2) and are shedded to the charged medium. The relative expression levels of PKA catalytic subunits were considerably different among the cells which were employed for the assay. The stimulation of the cells by forskolin did not alter the secretion/shedding of PKA significantly as compared to non-treated controls (Fig. 19).

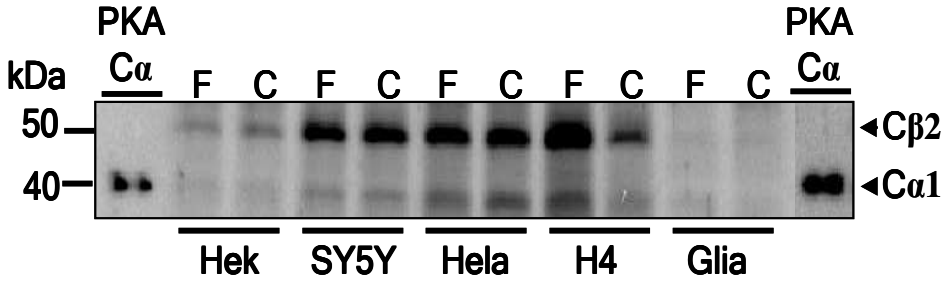

Fig. 19: Detection of extracellular PKA at the cell surface of cultured cells.
Subconfluently grown intact cell cultures (HEK293, SH-SY5Y, HeLa, H4 and Glia) were incubated with (F) or without (C) forskolin (5 µM) and incubated for 2 hours. After incubation, the conditioned medium was collected. Aliquots of conditioned medium were electrophoresed and western-blotted. The blots were detected using polyclonal anti-PKA catalytic subunit antibody. The secretion of catalytic subunit of PKA is observed to be significantly different among the cell cultures employed in the assay. The shedding of the PKA catalytic subunits was not altered in forskolin treated cells (F) as compared to non-treated cells (C). The secretion of catalytic subunit of PKA is found to be varied depending upon the cell type employed in the assay. The secretion of Cβ2 was found to be relatively higher as compared to Cα1.

4.2.3. Phosphorylation of exogenous Aβ by cell surface protein kinases of cultured cells

The ecto-PKs on the cell surface of a wide variety of cells are shown to phosphorylate both extracellular (soluble) substrates and cell-surface proteins (Hogan et al., 1995; Walter et al., 2000). Experiments were carried out to check the presence of kinases activity at the cell surface of different cultured cells and to check whether these kinases are capable of phosphorylating exogenously added Aβ1-40.

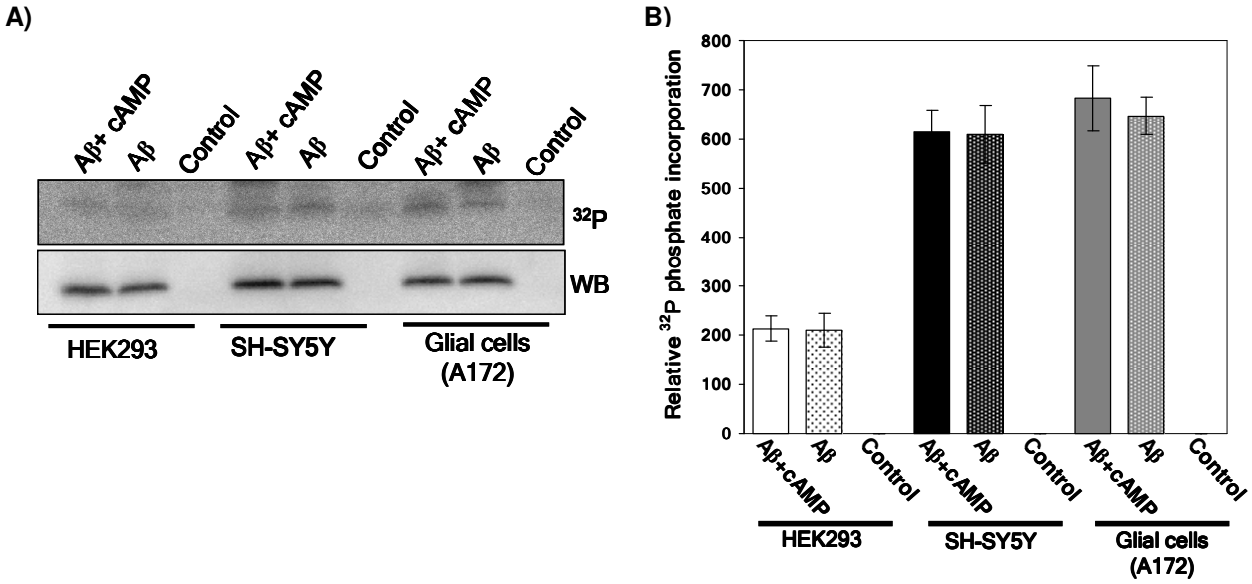

Fig. 20: *In vivo* phosphorylation of exogenous Aβ by cell surface kinases of cultured cells.
In vivo phosphorylation studies were carried out using subconfluently grown intact cultures of HEK293, SH-SY5Y and Glial cells (A172). Cultures were washed twice with the phosphorylation mix and incubated with [γ-^{32}P]ATP (10 µM) in the presence or absence of Aβ1-40 (1 µg) and cAMP (2 µM) at 37 °C with 5% CO_2 for 30 min. After incubation, the cell supernatants were collected and the Aβ was immunoprecipitated from cell supernatants using anti-Aβ antibody (2964). The immunoprecipitated Aβ was separated by SDS-PAGE and western-blotting. The radiolabeled ^{32}P Aβ was detected by phosphorimaging (^{32}P). Exogenously added Aβ was phosphorylated by the activity of cell surface located protein kinases. The phosphorylation of Aβ is found to be significantly higher in SH-SY5Y and Glial cells as compared to HEK293 cells. Addition of cAMP did not alter the phosphorylation levels of Aβ. The western-blotting (WB) signals indicate the equal amount of Aβ employed in the assay. B) The extent of ^{32}P incorporation was estimated by phosphorimaging. Values indicate the mean ± s.d. of the four data points from two sets of experiments.

The autoradiograph (Fig. 20A; ^{32}P) indicate the phosphorylation of Aβ by the cell surface kinases of different cells. The phosphorylation of Aβ was found to be relatively higher with SH-SY5Y and Glial cells as compared to HEK293 cells. The addition of cAMP did not alter the phosphorylation of Aβ. The extent of ^{32}P incorporation was calculated by phosphorimaging (Fig 20B). The plasma membrane integrity and its damage upon addition of Aβ

were checked by monitoring the uptake of tryphan blue dye. The results showed a low percentage of cells with instant uptake of tryphan blue (<2%; data not shown), indicating that there was no damage of cells and release of intracellular kinases due to addition of Aβ. These results confirm that the observed kinase activity is exclusively due to cell surface located kinases and not of the intracellular origin.

There are also reports indicating the occurrence of cell surface kinases in neuronal cells (Ehrlich et al., 1986a; Ehrlich et al., 1986b; Hogan et al., 1995). Primary cultures of mouse cerebellar neurons were used to verify whether the cell surface located kinases of neuronal cells are capable of phosphorylating the exogenously added Aβ. The radiolabeled Aβ (^{32}P) signals were observed only in the cell supernatant showing that Aβ can undergo phosphorylation by the activity of cell surface located kinases of neuronal cells (Fig. 21A). The radiolabeled Aβ signals were not observed in the corresponding cell lysates indicating that the Aβ was not internalized in the experimental paradigm (Fig. 21B). The results were further confirmed by the western-blotting (WB) showing the occurrence of Aβ in the cell supernatants and absence of Aβ signals in the cell lysates.

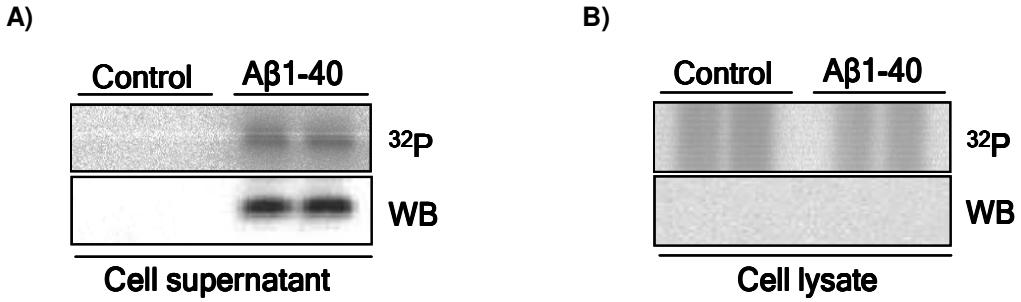

Fig. 21: *In vivo* phosphorylation of exogenous Aβ by mouse cerebellar neurons.
The primary cultures of mouse cerebellar neurons were grown in a chemically defined, serum-free medium for 14 days *in vitro* (14 Div; cell density: 2 x 10^6 cells). During the day of the analysis, the cells were rinsed twice with a phosphorylation mix. Cultures were incubated at 37 °C with 5% CO_2 for 30 min with [γ-^{32}P]ATP (10 µM) in the presence or absence of synthetic Aβ1-40 (1 µg). After incubation, the cell supernatant was collected and washed the cells twice with cold PBS. The cells were lysed with STEN-lysis buffer and collected the cell lysates. Radiolabeled Aβ was immunoprecipitated from cell supernatants (A) as well as from cell lysates (B), were electrophoresed and western-blotted. Phoshorylated Aβ was detected by autoradiography (^{32}P). The presence of Aβ in cell supernatants and absence of Aβ in cell lysates were confirmed by western-blotting (WB) and detection using anti-Aβ antibody (3D6).

4.2.4. Identification of extracellular PKA activity in primary mouse neuronal cultures

To identify whether the observed Aβ phosphorylation is mediated due to extracellular PKA, experiments were carried out with mouse primary neuronal cultures using the method of cell surface labeling with biotin. After cell surface-biotinylation, the biotinylated proteins were purified by SDS-PAGE and western-blotting. PKA was detected by immunoblotting using polyclonal anti-PKA catalytic subunit antibody. The cell surface located endogenous PKA was biotin labeled and was selectively recovered from the cell lysate by immunoprecipitation using streptavidin conjugated beads (Strep. IP). The higher PKA signals were observed in the direct loading of whole cell lysates indicating the abundant source of intracellular PKA. The biotin labeled PKA catalytic subunits were shown to migrate as similar to purified catalytic subunit of PKA. As a control, the endogenous cell surface APP was biotinylated. The biotinylated APP was immunoprecipitated with streptavidin beads and immunodetected with APP specific antibody. The biotinylated mature endogenous APP was also detected in the streptavidin immunoprecipitated samples. This result indicated the presence of extracellular PKA at the cell surface of primary neurons which can undergo biotinylation and was selectively detected in Strep. IP immunoprecipitates (Fig. 22).

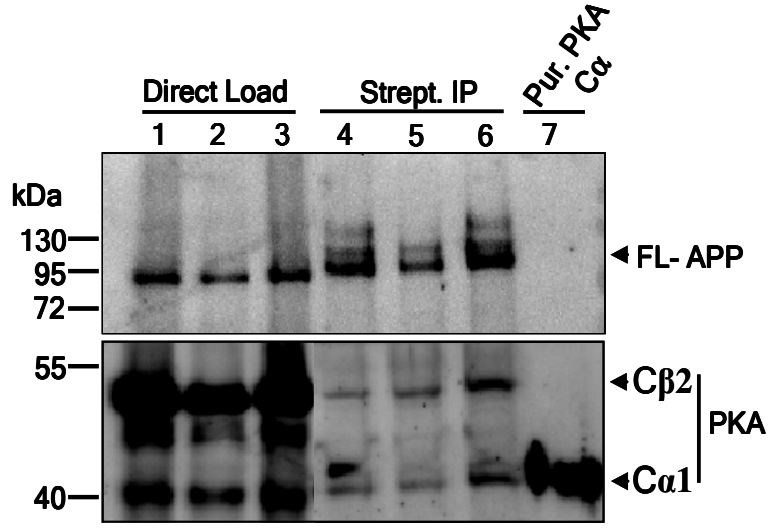

Fig. 22: Biotinylation of cell surface located PKA and APP.
Primary cultures of mouse cerebellar neurons (14 Div, Cell density: 2 x 10^6) were surface-biotinylated using sulfo-NHS-biotin for 30 min. Cell lysates (15 µl/lane) were loaded directly onto a 12 % SDS-gel (lane 1, 2 & 3) or immunoprecipitated (750 µl/immunoprecipitate) by using streptavidin-conjugated agarose beads (lane 4, 5 & 6). Biotinylated cell surface PKA and FL-APP was detected with the use of rabbit anti-PKA-catalytic subunit and anti-APP antibodies. The cell surface located catalytic subunit of PKA as well as FL-APP is biotinylated and can be observed in streptavidin immunoprecipitated samples confirming the cell surface localization (Strep. IP). Direct loading of cell lysates indicate abundant source of intracellular PKA. Purified catalytic subunit of PKA was used as loading control (lane 7).

The results from the biotinylation of cell surface PKA indicate the involvement of extracellular PKA activity in primary cultures of mouse cerebellar neurons in phosphorylation of exogenously added Aβ. To further verify whether the extracellular PKA activity can be modulated, *in vivo* phosphorylation experiments were carried out using primary neuronal cultures employing a selective PKA activator (cAMP) and inhibitor (H-89). The exogenously added Aβ can readily undergo phosphorylation by neuronal culture (Control). Significant decrease in phosphorylation signals was observed with the addition of the selective PKA inhibitor H-89. However, the addition of extracellular cAMP did not increase the phosphorylation of Aβ as compared to controls. (Fig. 23A & B).

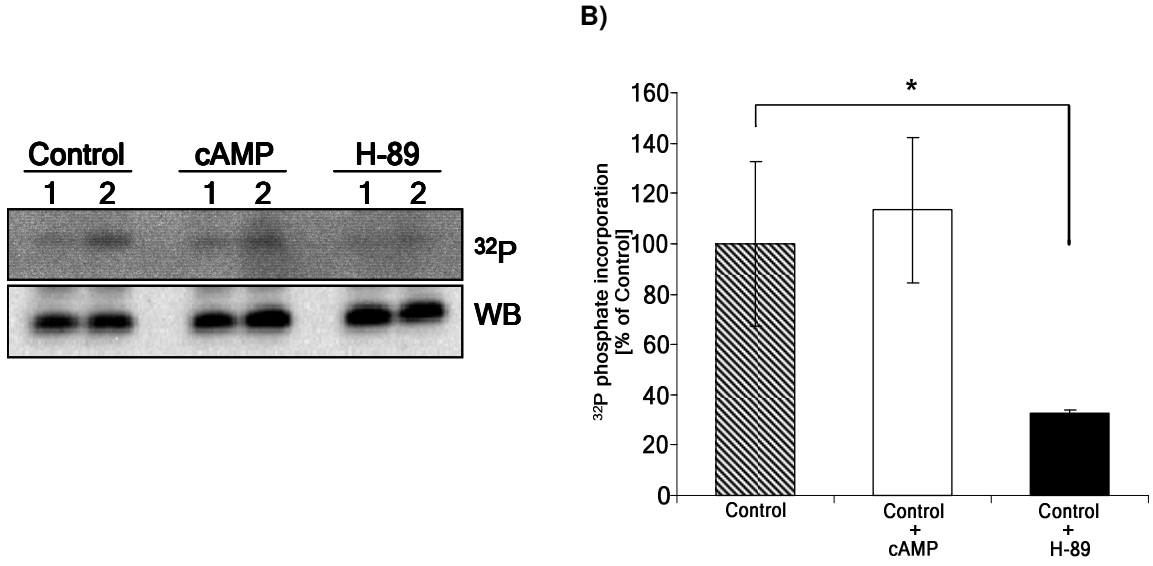

Fig. 23: Modulation of extracellular PKA activity in primary cultures of mouse cerebellar neurons.
A) The primary cultures of mouse cerebellar neurons were grown in a chemically defined, serum-free medium for 14 days *in vitro* (14 Div; 1, 1 x 10^6 cells; 2, 2 x 10^6 cells). During the day of the analysis, the cells were washed twice with phosphorylation mix. Cultures were incubated with [γ-^{32}P]ATP (10 µM), synthetic Aβ1-40 (1 µg) in the absence or presence of cAMP (2.5 µM) or H-89 (0.1 µM) at 37 °C with 5% CO_2 for 30 min. After incubation, the cell supernatant was collected and radiolabeled Aβ was immunoprecipitated from cell supernatants. The immunoprecipitates were electrophoresed and western-blotted. Phoshorylated Aβ was detected by autoradiography (^{32}P). The phosphorylation of Aβ was not increased upon addition of cAMP, however significant reduction in phosphorylation of Aβ was observed by addition of H-89. The presence of Aβ in cell supernatants was confirmed by western-blotting (WB) using anti-Aβ antibody. B) ^{32}P phosphate incorporation quantified by phosphorimaging. ^{32}P values represent mean ± s.d. of three independent experiments (*p<0.05). Statistical significance was evaluated by student *t*-test (n=3).

4.2.5. *Ex vivo* phosphorylation of Aβ

4.2.5.1. Phosphorylation of Aβ in cerebrospinal fluid (CSF) from AD patients

The CSF samples of AD patients were collected from Neurology clinic. *Ex vivo* phosphorylation was carried out to test whether Aβ phosphorylation can take place in CSF or components necessary for phosphorylation reaction exists in CSF. Aliquots of human CSF were incubated with [γ-^{32}P]ATP, Aβ and purified catalytic units of PKA, CK1 and CK2. The Aβ1-40 was found to undergo phosphorylation by PKA, CK1 and CK2 kinases in the CSF samples. In addition to phosphorylation of Aβ, several endogenous proteins were also found to undergo phosphorylation. The phosphorylation of endogenous proteins of CSF are observed to be diverse and showed different specificity among the kinases employed in the assay (Fig. 24).

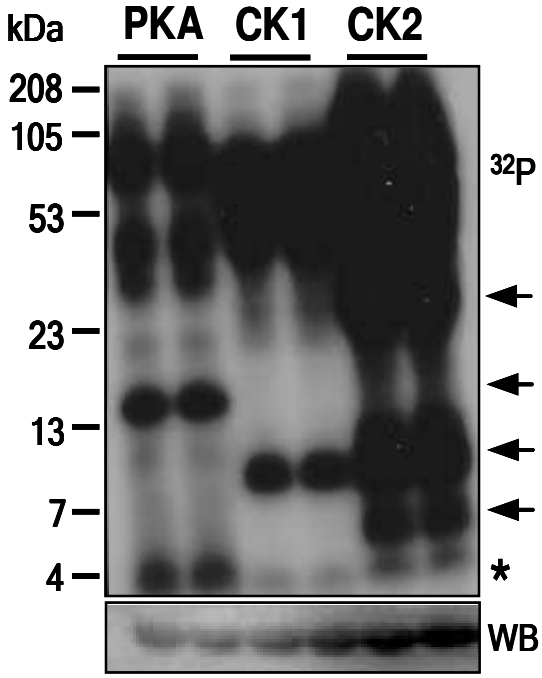

Fig. 24: *Ex vivo* phosphorylation of Aβ1-40 in human CSF of AD patients.
Human CSF from AD patients were incubated with [γ-^{32}P]ATP (10 µM), Aβ1-40 (1 µg) in the presence of different catalytic units of PKA, CK1 and CK2 at 32° C for 15 min. After incubation, the phosphorylation reaction was stopped by addition of SDS-sample buffer and boiling at 100 °C. Aliquots of samples were electrophoresed and western-blotted onto PVDF membrane. The radiolabeled proteins were detected by autoradiography. Phosphorylation of Aβ as well as endogenous CSF proteins can be seen. The asterisk indicates the phosphorylation of Aβ1-40 (4 kDa) and arrows indicate the phosphorylation of unknown endogenous phosphoproteins of CSF.

4.2.5.2. Phosphorylation of exogenous proteins by endogenous kinases of CSF

From the previous results, it was observed that CSF can serve as a buffer for the phosphorylation reactions by different kinases. Further studies were carried out to identify the presence of endogenous kinases activity in CSF. *Ex vivo* phosphorylation studies were carried out using human CSF from AD patients employing different kinase specific substrates (histone and phosvitin). The exogenously added substrates such as histone and phosvitin could undergo phosphorylation by the endogenous kinases (Fig. 25). In addition to histone and phosvitin, phosphorylation of unknown endogenous proteins of CSF was also observed. The phosphorylation signals of endogenous CSF proteins were not observed in control samples (PBS) indicating the authenticity of phosphorylation of proteins exclusively by the activity of different endogenous kinases of CSF.

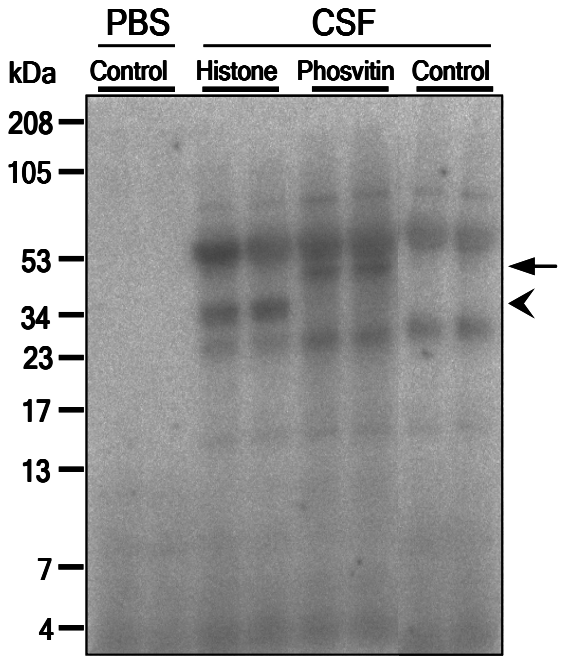

Fig. 25: Phosphorylation of exogenous kinase substrates by endogenous kinases of human CSF.
Human CSF from AD patients were incubated with [γ-^{32}P]ATP (10 µM) and kinase substrates (histone and phosvitin) at 32 °C for 15 min. After incubation, the CSF samples were separated by SDS-PAGE and western-blotting. The radiolabeled proteins were detected by autoradiography. The phosphorylation signals of histone (arrow head; 30 kDa) and phosvitin (arrow: 50 kDa) are indicated. The phosphosignals of unknown endogenous CSF proteins are only observed in CSF samples as compared to PBS (controls). Analyses were carried out in duplicates in two independent experiments.

4.2.5.3. Identification of PKA activity in CSF

To verify whether the observed endogenous kinase activity in the CSF is due to PKA like kinase, *ex vivo* phosphorylation studies were carried out using CSF from AD patients employing histone (cognate PKA substrate), cAMP (specific PKA activator) and H-89 (specific PKA inhibitor). The histone was found to undergo phosphorylation where as the phosphorylation of histone was reduced upon addition of H-89. However, the phosphorylation of histone was not increased upon addition of cAMP (Fig. 26A & B).

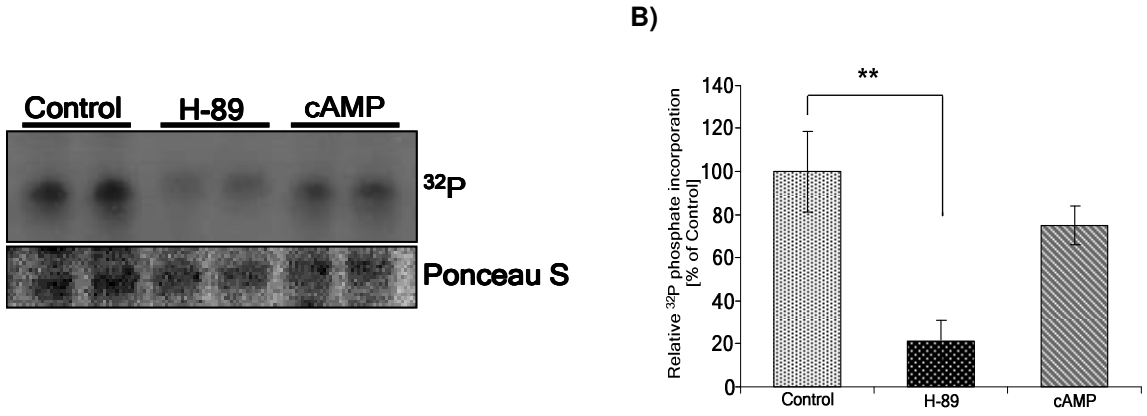

Fig. 26: Identification of the endogenous PKA activity in human CSF.
A) Human CSF from AD patients were incubated with [γ-^{32}P]ATP (10 µM) and histone (1 µg) in the absence or presence of H-89 (0.1 µM) or cAMP (2.5 µM) at 32 °C for 15 min. After incubation, the phosphorylation reactions were stopped by adding SDS-sample buffer. The aliquot of sample was electrophoresed and western-blotted onto PVDF membranes. The radiolabeled proteins were detected by autoradiography (^{32}P). The phosphorylation of histone can be observed in control samples. The phosphorylation of histone was reduced upon addition of H-89 however, the addition of cAMP do not increase the phosphorylation of histone. Ponceau-S staining (Ponceau-S) shows the histone signals in all the lanes. B) The ^{32}P phosphate incorporation was quantified by phosphorimaging. ^{32}P values represent mean ± s.d. of the four data points from two independent experiments (duplicate probes/assay). Statistical significance was evaluated by student *t*-test (*p<0.01).

3.2.5.4. *Ex vivo* phosphorylation of Aβ by endogenous PKA of CSF

The results from the previous experiments confirmed the presence of endogenous PKA activity in human CSF, and the kinase activity was inhibited upon addition of a PKA inhibitor (H-89). To check, whether this endogenous PKA of CSF can phosphorylate the exogenously added Aβ, *ex vivo* phosphorylation studies were carried out using human CSF from AD patients. The CSF samples were incubated with [γ-^{32}P]ATP and synthetic Aβ1-40 in the absence or presence of H-89. The Aβ was found to readily undergo phosphorylation by the endogenous PKA and the phosphorylation was suppressed by addition of H-89 (Fig. 27A & B).

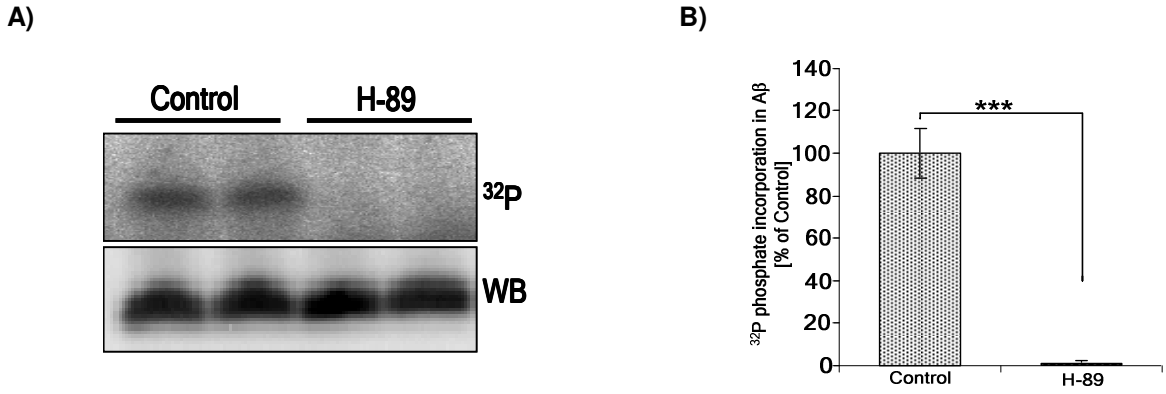

Fig. 27: *Ex vivo* phosphorylation of Aβ by human CSF.
A) Human CSF from AD patients were incubated with [γ-^{32}P]ATP (10 µM) and Aβ1-40 (1 µg) in the absence or presence of H-89 (PKA inhibitor). After phosphorylation reaction, Aβ1-40 was separated by SDS-PAGE, western-blotted onto PVDF membrane and radiolabeled Aβ was detected by autoradiography (^{32}P). Phosphorylation signals of Aβ1-40 are observed and phosphorylation was inhibited by addition of H-89. The western-blotting (WB) signals shows the equal amount of Aβ employed in the assay. B) The ^{32}P phosphate incorporation was quantified by phosphorimaging. ^{32}P values represent mean ± SD of three independent experiments (*p<0.05). Statistical significance was evaluated by student *t*-test.

Taken together, all the combined results from the biochemical, *in vivo* and *ex vivo* phosphorylation using cells and human CSF studies suggesting that, in addition to crucial role of PKA in intracellular functions, it may well have extracellular functions. The *in vivo* phosphorylation studies using cells showed that Aβ can undergo phosphorylation by extracellular surface located PKA. *Ex vivo* phosphorylation studies using CSF from AD patients further indicated the existence of endogenous PKA kinase in CSF. The endogenous PKA of CSF could phosphorylate exogenously added Aβ. Hence, one could speculate that phosphorylation of Aβ is indeed biochemically feasible at the extracellular environment in the human brain. Despite the numerous reports describing role of posttranslational modifications of Aβ in aggregation, the role of phosphorylation in Aβ aggregation has not been shown. Therefore, further studies were carried out to elucidate the role of phosphorylation in Aβ aggregation

4.3. Role of phosphorylation in the aggregation of Aβ

A series of bioanalytical, biophysical techniques were applied for investigating the role of phosphorylation on Aβ conformation and its effects on aggregation. The circular dichroism study was carried out in collaboration with Prof. Dr. Klaus Beyer, Dept. of Biochemistry, Ludwig-Maximilians-University, München. The studies such as nuclear magnetic resonance, dynamic light scattering and transmission electron microscope documented in this section was carried out in collaboration with Dr. Markus Zweckstetter of the Max Planck Institute for Biophysical Chemistry, Göttingen.

4.3.1. Effect of phosphorylation on the secondary structure of Aβ

4.3.1.1. Monitoring the conformational transition by circular dichroism (CD) spectroscopy

CD spectroscopy has been previously applied by several authors to study secondary structure transitions or to define the conformational states of different Aβ peptide variants (Barrow and Zagorski, 1991; Barrow et al., 1992; Fabian et al., 1993; Tomaselli et al., 2006). Herewith, CD spectroscopy studies were carried out to follow the kinetics of the Aβ secondary structure transition upon phosphorylation.

Conformational transition studies of npAβ (wildtype) and pAβ(pSer-8) were conducted by recording CD spectra in the range of 190-260 nm at various incubation times. The CD spectra showed the conformation transition from an unordered, random coil to a more β-sheet structure at different time intervals (0 hr, 2 hr, and 8 hr). At 0 hr, the initial conformation of npAβ and pAβ was found to be similar and is observed with no significant difference in the CD spectrum (Fig. 28 A & B). The CD spectrum of npAβ peptide sample at the early incubation time (0 hr) revealed the characteristic features of a mostly random coil state (negative peak at 200 nm). As the incubation time increased, a slight change in the CD spectrum was observed with npAβ peptide i.e., at 2 hr of incubation, the spectrum of npAβ showed a little alteration indicating the α-helical structure (with only a slight decrease in intensity in the minimum at 195 nm). The occurrence of β-sheet secondary structure was seen after 8 hr of incubation with a typical peak that is characteristic for extended β-structure (negative peak at 210-220 nm, Fig. 28A).

The initial CD spectrum of pAβ(pSer-8) peptide (at 0 hr) was also as expected for an unfolded peptide, i.e., mostly random coil state. As the incubation time increased, a significant change in the CD spectrum was observed. A pattern characteristic of extended β-sheet structure was already evident after 2 hrs of incubation (positive at 195 nm and negative at 215 nm). The dominance of β-sheet secondary structure after 8 hrs can be clearly indicated by the appearance

of a large negative peak at 215 nm and a positive peak at 195 nm with pAβ(pSer-8) peptide (Fig. 28B). Notably, the occurrence of β-sheet secondary structure can be already seen at 2 hrs of incubation with pAβ(pSer-8) peptide showing a significant difference in conformation as compared to npAβ. Together, the CD studies indicate an effect of phosphorylation on the transition from an unordered random coil soluble Aβ to the β-sheet rich conformation. Thus, phosphorylation increases the propensity of Aβ to adopt a β-sheet conformation.

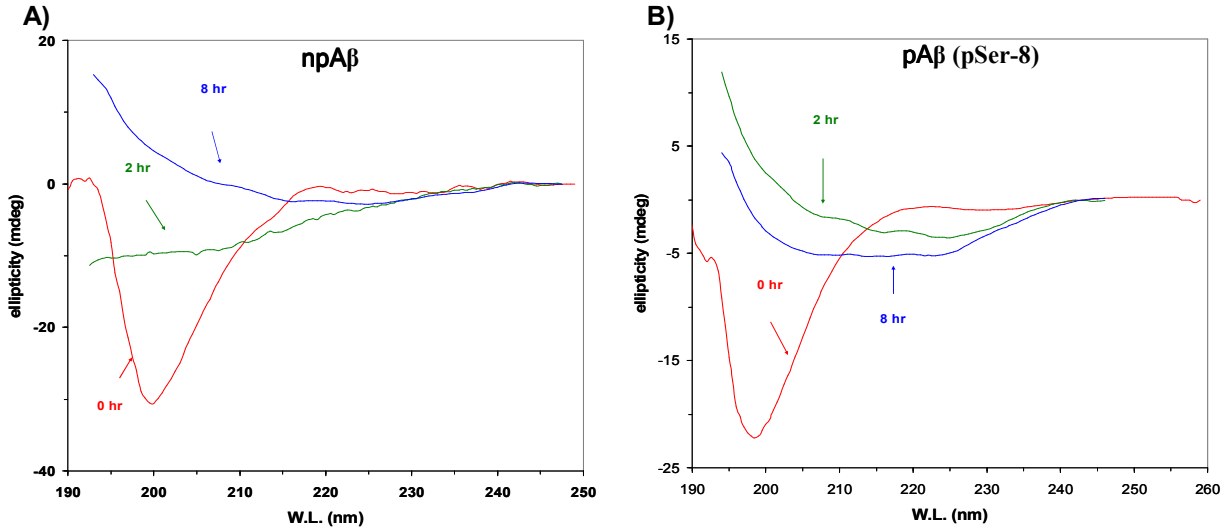

Fig. 28: Circular dichroism (CD) spectroscopy study of conformational transition of npAβ and pAβ.
The assay solution containing freshly dissolved npAβ and pAβ preparations (100 µM) was taken in quartz cuvette and incubated at 37 °C with shaking. CD spectroscopy was employed to monitor the conformational transition of secondary structures of npAβ (A) and pAβ (pSer-8) (B) samples at different incubation time points during aggregation. Graphs show the acquired CD spectra at 0 hr (red), 2 hr (green) and 8 hr (blue). At 0 hr, the curves are observed to be similar with both the peptides indicating a random coil state. The change in curve pattern is observed in later incubation times (2 hr and 8 hr). The structural conversion from a random coil structures to extended β-sheet structure is observed to be faster with pAβ and β-sheet transition is prominently observed at 8 hr of incubation with pAβ (a positive peak at 195 nm and a broad negative peak at 210-220 nm) as compared to npAβ. Typical bands are: α-helix – positive at 192-195 nm, negative at 208 nm and 222 nm; random coil – negative at 200 nm; β-sheet – negative at 216 nm, positive at 195-198 nm.

4.3.1.2. Study on thermal stability of phosphorylation induced β-sheet conformation

Many proteins and peptides aggregate or precipitate quickly after they are unfolded at high temperature ("melting"), thereby making unfolding irreversible. The structural transition of npAβ and pAβ(pSer-8) was investigated over a range of temperatures to predict the thermal stability of the phosphorylation induced conformational transition and the temperature dependence of the hydrophobic interactions (Fig. 29).

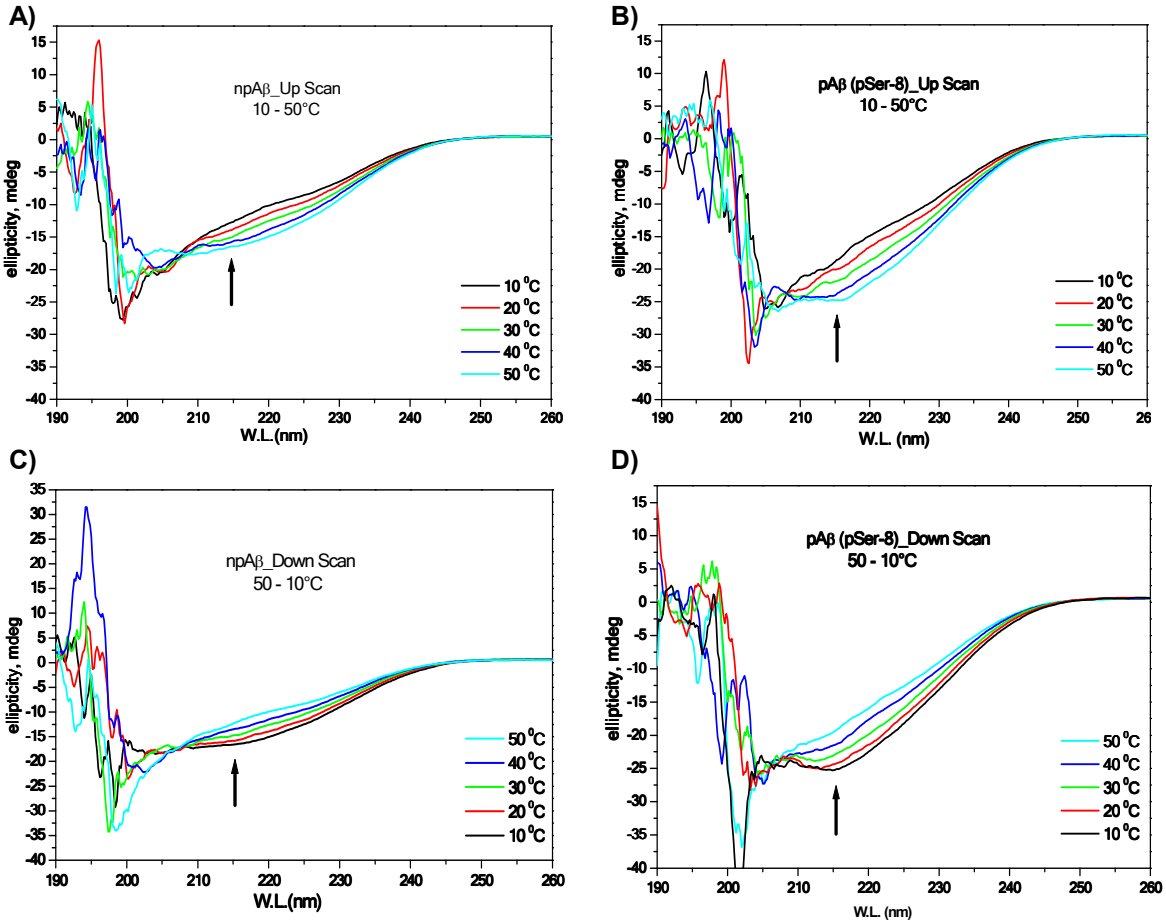

Fig. 29: Thermal-dependent CD spectroscopy study of npAβ and pAβ conformations. Aggregation assays were carried out using freshly dissolved npAβ and pAβ preparations (100 µM). The plots showing the CD spectrum of npAβ (A and C) and pAβ (B and D) that were recorded at different temperatures. The up scan spectra shows the CD spectra that were recorded at increasing in the incubation temperature (10 °C interval) step-wise from 10 - 50 °C (A and B). After up scan recordings, the temperature was decreased step-wise from 50-10 °C and down scan CD spectra were recorded at lower temperatures (C and D). At temperatures below 20 °C, the spectra of npAβ and pAβ are observed to be similar and show little β-sheet conformation. The shapes of the spectra are different for npAβ and pAβ at temperature above 20 °C. In particular, the negative peak at 210-220 nm which indicates an extended β-sheet conformation. All the scans run through isobestic points at 208 nm. The result indicate the temperature induced large structural transitions from α- to β-conformation with pAβ peptide, and further confirmed that phosphorylation of Aβ increases the propensity to adapt β-sheet conformation and this increase was reversible by subsequent decrease in temperature (down scans).

The CD spectra showed the conformation transition from an unordered to the β-sheet structure and the shape of the spectra was observed to be different for npAβ and pAβ(pSer-8) peptide at different incubation temperatures (up scan and down scans). An increase in ellipticity which is characteristic for β-sheet conformation was observed in the region of the 210-220 nm and it was more pronounced with pAβ(pSer-8) with the increase in temperature (indicated by arrows). Where as, npAβ did not show significant change in structural transition to β-sheet structure with the rise in temperature. The magnitude of the heat induced structural transition of pAβ(pSer-8) was increased at higher temperature indicating a faster unfolding state of Aβ, result-

ing in higher negative ellipticity. Interestingly, this temperature induced effect was reversible, which was seen in the down-scan measurements. The results from CD thermal scans (up scan and down scans) further demonstrated the higher propensity of pAβ(pSer-8) to adopt β-sheet structure and this increase in β-sheet conformation was largely reversible by subsequent down-shift of the incubation temperature.

4.3.2. Effect of phosphorylation on Aβ aggregation

4.3.2.1. Congo Red (CR) dye binding assay

To study the effect of phosphorylation induced β-sheet structure on Aβ aggregation, CR-Aβ spectroscopic assay was carried out using wild type (npAβ) and phosphorylated variants of Aβ (pAβ(pSer-8) and pAβ(pSer-26)). The CR dye binding was significantly increased with pAβ(pSer-8) peptide as compared to npAβ peptide (Fig. 30). In contrast, pAβ(pSer-26) peptide showed a decreased CR binding as compared to npAβ. These results indicate that phosphorylation at different phosphosites of Aβ differentially affect the aggregation of Aβ.

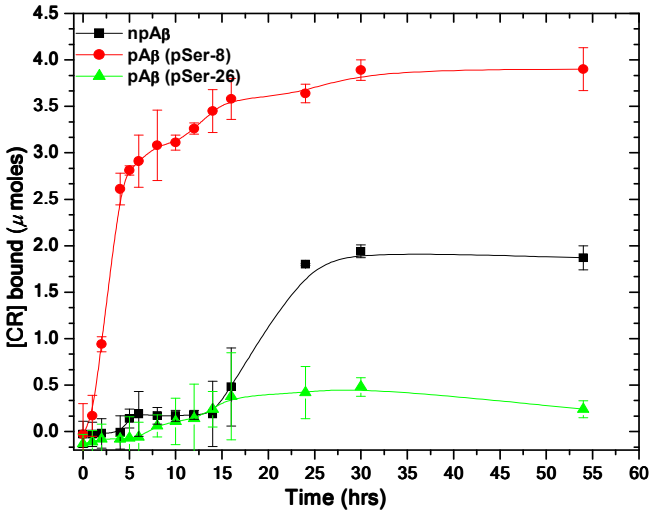

Fig. 30: Time course studies of npAβ and pAβ aggregation by Congo Red binding assay.
The aggregation reaction mixture containing 100 µM of npAβ, pAβ(pSer-8) and pAβ(pSer-26) were incubated at 37 °C with shaking and aliquots of samples were collected at different time points during aggregation. The time course of aggregation of synthetic npAβ (black), pAβ(pSer-8) (red) and pAβ(pSer-26) (green) was monitored by congo red (CR) binding assay. CR binding is expressed as µM of CR bound to the Aβ aggregates. The curves showing the differences in CR binding to the peptides employed in the assay indicating the differences in kinetics of aggregates formation upon phosphorylation. The amount of CR bound to pAβ(pSer-8) was more as compared to npAβ, while pAβ(pSer-26) showed reduced CR binding as compared to npAβ. Each data points indicate mean ± s.d. (n=3). The assays were carried out three times independently.

To investigate further regarding the observed differences with CR dye binding to different Aβ peptides, the samples from the CR-Aβ assay taken at different time points during aggregation were analyzed by SDS-PAGE electrophoresis and western-blotting (Fig. 31). The results indicated the formation of low molecular weight (M.W.) aggregates/oligomers (i.e., dimers, trimers) was faster with pAβ(pSer-8) as compared to npAβ peptide. In addition to low M.W. oligomers, pAβ(pSer-8) showed a faster formation of higher M.W. oligomeric assemblies that were detected as a smear at the upper part of the gel. The higher β-sheet structures formation in pAβ(pSer-8) peptide due to phosphorylation resulted in increased formation of different oligomeric species (dimer, trimer and higher oligomers). In contrast, pAβ(pSer-26) showed pronounced formation of low M.W. oligomers (dimer and trimer);however the larger assemblies were not observed. Together with the results from the CR dye binding assay, the SDS-PAGE analysis further suggests that phosphorylation of Ser-26 might stabilizes lower oligomeric assemblies of Aβ and thus reduce the formation of protofibrils (high M.W. oligomers).

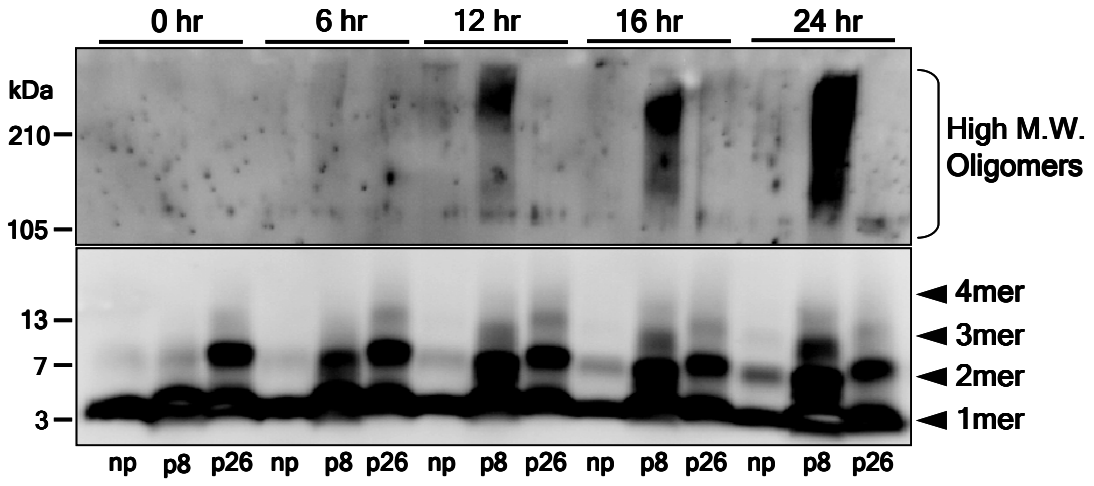

Fig. 31: SDS-PAGE and Western-blotting analysis of npAβ and pAβ aggregates formation.
The np-npAβ, p8-pAβ(pSer-8) and p26-pAβ(pSer-26) samples from CR dye binding assay taken at different time points during aggregation were analyzed by SDS-PAGE (430 ng/lane) and western-blotting. The blots were immunoprobed with anti-Aβ antibody (82E1) which can recognize all the three peptides similarly. Migrations of monomeric and low molecular weight (low M.W.) Aβ aggregates/oligomers such as dimer (2mer), trimer (3mer), tetramer (4mer) and higher molecular weight (High M.W.) oligomers are indicated. The faster formations of low and high M.W. oligomers/aggregates are observed with pAβ(pSer-8) as compared to npAβ peptide. The formation of low M.W. oligomers although increased with pAβ(pSer-26) as compared to npAβ, however the high M.W. oligomers are not observed.

4.3.2.2. Thioflavin-T (ThT) fluorescence assay

The results from the CR dye binding assay showed the increased β-sheet structure formation upon phosphorylation and faster formation of different oligomeric Aβ assemblies with pAβ as compared to npAβ. The higher β-sheet structure might induce a conformational transition, thus results in faster self-assembly. The alteration of peptide conformation due to enhanced β-sheet structures could promote aggregation and lead to faster formation of fibrils. Therefore, ThT fluorescence assays were carried out to study the effect of phosphorylation on Aβ fibrillogenesis. Increased fluorescence was observed with pAβ(pSer-8) as compared to npAβ. The fluorescence signal of pAβ(pSer-26) was observed to be much lower as compared to npAβ (Fig. 32A). Even though, it showed an increase in fluorescence signals at early incubation time (between 0.25 to 1 hour) as compared to npAβ, however the fluorescence did not further increased (Fig. 32B).

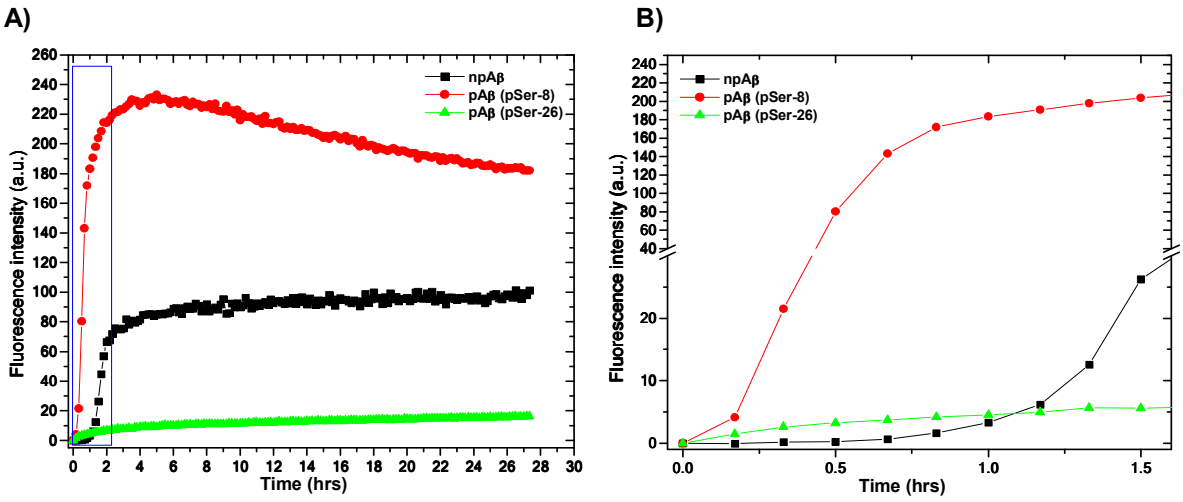

Fig. 32: Time course studies of npAβ and pAβ fibrillization by Thioflavin-T (ThT) fluorescence assay.
The aggregation assay reaction mixture containing npAβ and pAβ peptide (100 μM) with ThT dye (20 μM) was incubated at 37 °C with stirring. The real-time ThT fluorescence was monitored for every 10 min intervals with an excitation (λ_{ex}-450 nm) and emission (λ_{ex}-450 nm). Graphs show the results from the real-time ThT fluorescence measurements. Higher fluorescence is observed with pAβ(pSer-8) as compared to npAβ where as fluorescence is observed to be lower with pAβ(pSer-26). B) The enlarged image of the area indicated in image A with blue colored box. Increased fluorescence signals are observed in early phase of fibrillization with pAβ(pSer-26) as compared to npAβ (increase signals between 0.2 to 1 hr), however, the signals did not further increased. The curves clearly indicate the differences in ThT fluorescence of different peptides confirming the alteration of fibrillization kinetics after phosphorylation.

The ThT fluorescence assay indicated a faster propensity of Aβ to aggregate and speed up the fibril formation upon phosphorylation. The phosphorylation induced fibrillization was further examined by SDS-PAGE electrophoresis and western-blotting of the samples from ThT fluorescence assay (Fig. 33). Consistent with increased fluorescence as observed in ThT fluorescence

measurements, the pAβ(pSer-8) peptide also showed a faster formation of low M.W. aggregates/oligomers (dimer, trimer) and fibrils (High M.W. oligomers). Although, the formation of low M.W. aggregates/oligomers were increased in pAβ(pSer-26) peptide as compared to npAβ, however the fibrils (High M.W. oligomers) was not observed indicating the absence of fibrillization process with pAβ(pSer-26) peptide. These results further confirm the phosphorylation of Aβ at Ser-26 residue resulting in stabilization of the lower oligomeric assemblies and thus reducing the protofibril formation (High M.W. oligomers).

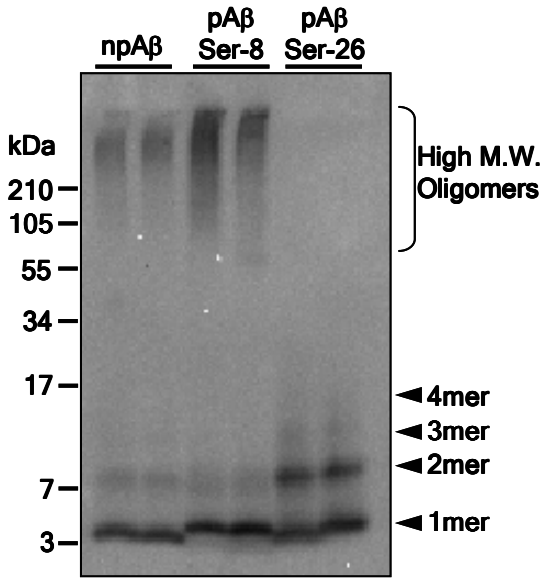

Fig. 33: SDS-PAGE and Western-blotting analysis of npAβ and pAβ fibril formation.
The npAβ, pAβ(pSer-8) and pAβ(pSer-26) sample aliquots from ThT fluorescence assay taken after 30 hrs of incubation were analyzed by SDS-PAGE electrophoresis (430 ng/lane) and western-blotting. The blots were immunodetected with anti-Aβ antibody (82E1), which recognizes all the three peptides similarly. Migrations of monomeric and different low M.W. oligomeric forms (dimer;2mer, trimer;3mer, tetramer;4mer) and high M.W. oligomeric Aβ are shown. The formation of high M.W. oligomers is significantly higher in pAβ(pSer-8) peptide as compared npAβ. While the formation of high M.W. oligomers are completely absent in pAβ(pSer-26) peptide, in spite of increased formation of low M.W. oligomers.

The results from CR and ThT binding assay indicated that the low and high M.W. Aβ aggregates/oligomer formation was accelerated with pAβ(pSer-8) as compared to npAβ and pAβ(pSer-26). Further detailed investigations on the role of phosphorylation were carried out using only npAβ and pAβ(pSer-8) peptides. Therefore, hereon npAβ represents the non-phoshorylated Aβ (wild type Aβ40) and pAβ represent to phosphorylated Aβ (pSer-8) variants.

4.3.2.3. Effect of phosphorylation on kinetics of Aβ aggregation

The aggregation assay results of npAβ and pAβ(pSer-8) using CR and ThT showed a sigmoidal curve and clearly indicated a characteristic biphasic curve containing well-resolved

lag, growth phase and saturation phase. Whereas, the pAβ(pSer-26) peptide showed feature of a hyperbolic curve. Since the ThT fluorescence measurements consisted of much more data points than CR experiments, ThT fluorescence data was selected for the kinetic analysis. The kinetic data were fitted using a logistic equation as described in methods (Naiki and Gejyo, 1999). As the first order logistic equation by Naiki et al., (1999) is applicable only to sigmoid type of aggregation kinetic curves. The kinetic analysis was carried out for npAβ and pAβ(pSer-8).

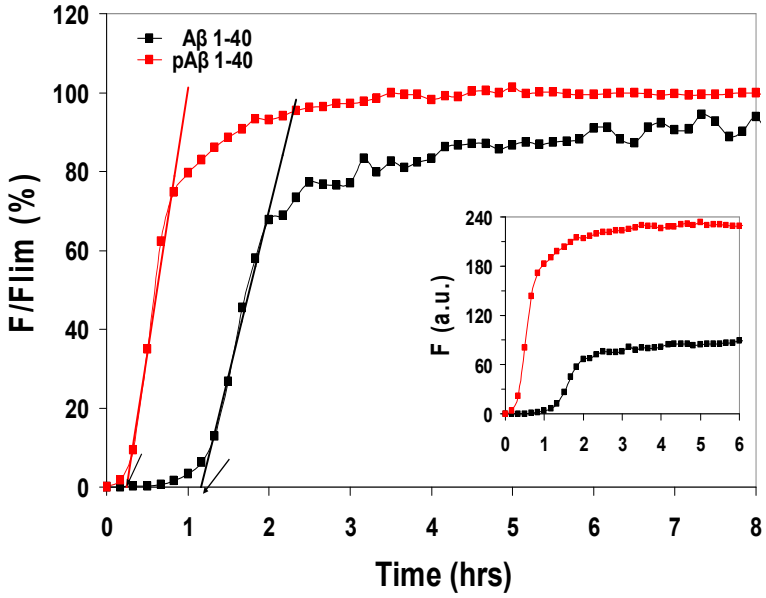

Fig. 34: Kinetic analysis of npAβ and pAβ aggregation.
Graphs show the kinetic analysis using logistic equation by Naiki et al., (1999). The graphs shows the logistic equation fitting of the data points obtained from time course of npAβ and pAβ fibrillogenesis measured by ThT fluorescence assay. The tangents are drawn after logistic fitting of the curves. The inset indicate the plot from the data points from ThT fluorescence assay indicating the change in ThT fluorescence follows a characteristic sigmoid pattern, in both wild-type and pSer8 peptides. Inset image indicating the ThT fluorescence measurements.

The results of kinetic analysis and logistic equation fitting of the ThT fluorescence assay is shown (Fig. 34). The change in ThT fluorescence followed a characteristic sigmoid pattern, with both the peptides. The lag period was prominently shorter in pAβ as compared to npAβ peptide. The rate of ThT fluorescence enhancement and its limiting value were also found to be significantly higher with pAβ peptide. While in the case of pAβ peptide, ThT fluorescence took 100 minutes to reach 90 percent of its final value, a similar event occurred for the wild-type peptide after about 3 hours (Fig. 34, inset). A closer inspection of the kinetic data revealed that, in both npAβ and pAβ peptides, ThT fluorescence data up to about 60-70 percent of the final values fitted well to the logistic equation (tangent drawn for the respective curves). However, a transition to a different regime (from log phase to stationary phase) was observed to be in much slower rate than that of expected according to the logistic model. This transition was found to be occurred

rather abruptly in both cases. Table 1 shows the kinetic parameters analyzed for ThT fluorescence assay of npAβ and pAβ peptides.

Table 5. Kinetic parameters of Thioflavin T fluorescence assay of npAβ and pAβ peptide samples.

	npAβ	pAβ
Thioflavin T fluorescence		
F_{lim} (a.u.)	98	230
$k*10^4$ ($a.u.^{-1}.min^{-1}$)	7.68	6.52
$t_{1/2}$ (min)	106	36
Maximal rate of aggregation ($a.u.^{-1}.min^{-1}$)	1.84	8.63
Lag time (min)	70	15

4.3.2.4. Effect of phosphorylation on the ensemble of Aβ fibril morphologies by transmission electron microscopy (TEM)

TEM studies were carried out to characterize the assemblies formed from npAβ and pAβ during aggregation. Sample aliquots taken at different time points from CR-Aβ aggregation assay were used for TEM studies. At 0 hr of incubation, the TEM images of both the peptide samples showed a similar morphology showing a little granular structure in both the peptide samples. In the early stages of the aggregation (2 hr), circular bodies were detected in npAβ samples. Such structures would correspond to small spherical structures of early Aβ aggregates as previously reported (Isaacs et al., 2006). Whereas in pAβ samples, a mixture of short protofibrils and larger protofibrillar aggregates were already apparent. The samples from elongation phase (16 hr) showed the circular bodies and were found to aggregate with each other as a bead of strings. Such structures would correspond to high M.W. oligomers or protofibrils as reported (Mastrangelo et al., 2006; Goldsbury et al., 2000; Lashuel et al., 2003). These high M.W. oligomeric structures were detected in greater numbers in pAβ samples. In the sample from saturation phase (24 hr), typical amyloid fibrils were clearly detected in both the peptide samples. Interestingly, in both the peptide samples the fibrils were detected together with high M.W. oli-

gomers. Notably, the high M.W. oligomers and protofibrils formation were observed to much faster and earlier in the pAβ samples (Fig. 35).

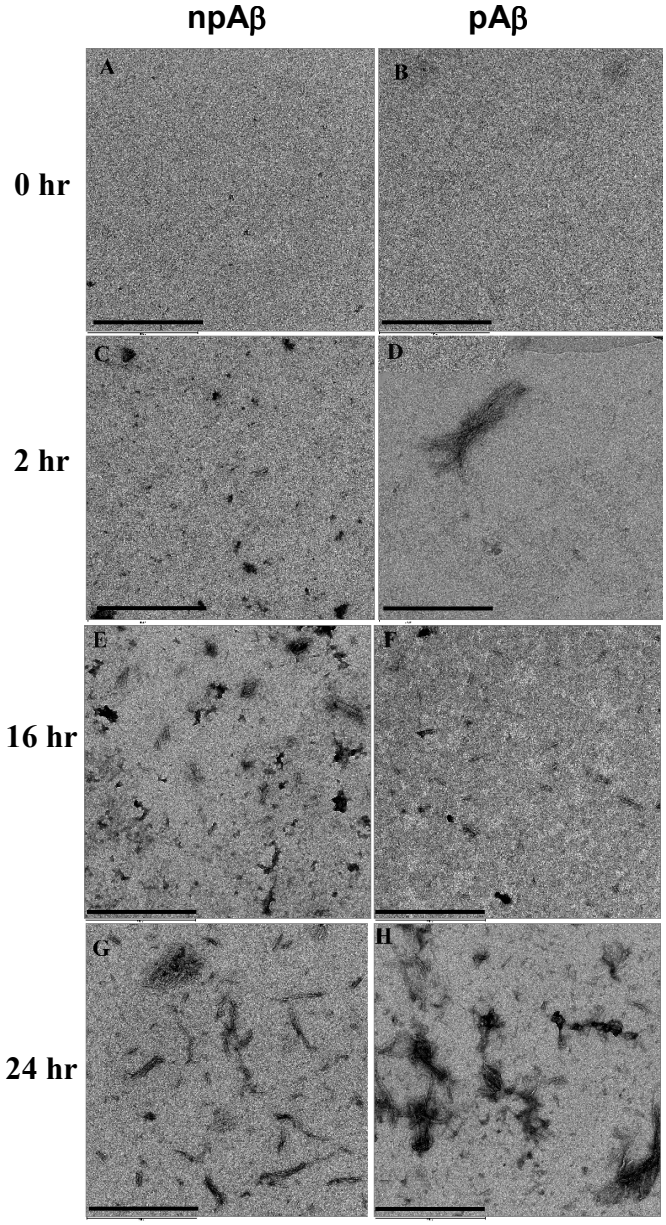

Fig. 35: Characterization of Aβ assemblies formed from npAβ and pAβ during aggregation by TEM. Sample aliquots from CR-Aβ aggregation assay taken at different time intervals were prepared and analyzed by TEM. TEM images of CR-Aβ aggregation samples taken at 0, 2, 16 and 24 hr are shown. In npAβ samples, a granular structure can be seen in 2 hr sample (C), protofibrils can be seen only after 16 hr with some longer fibril like structure (E). After 24 hr only mature fibrils are present (G). Where as in pAβ samples, at 2 hr, protofibrils are already observed (D) and they are increased at 16 hr (F). At 24 hr, the majority of the pAβ sample is fibrillar (H) (Scale bar, 200 nm).

Further studies on the overall topology of the Aβ fibrils using TEM, showed an identical granular structure in npAβ and pAβ samples at the initial stage (0 hr) of aggregation, indicating the similarity of the early aggregates among the peptides. In the saturation phase (24 hr), typical

amyloid fibrils were observed in both the peptide samples. The fibrils showed highly similar morphology and size, twisted fibrils of indefinite length and diameters of ~8 nm. The TEM studies suggest that in spite of the differences observed with kinetics of oligomerization and fibrillogenesis between two peptides, the fibrils formed at the end stage are observed to be similar in morphology (Fig. 36).

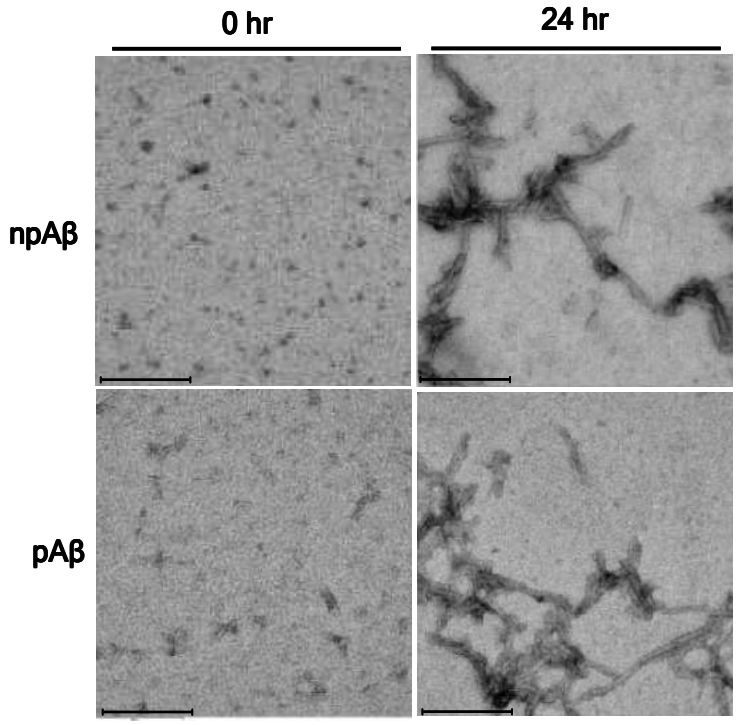

Fig. 36: Morphology of npAβ and pAβ assemblies at initial and final stages of fibrillogenesis observed by TEM.
Electron micrograph images of the npAβ and pAβ sample aliquots from ThT aggregation assay collected at 0 hr and 24 hr of incubation during the aggregation. The EM images show a granular structure in 0 hr samples. Fibrils are formed by both the peptides and show relatively similar structure (Scale bar, 200 nm).

4.3.2.5. Nuclear Magnetic Resonance (NMR) assay

The previous investigations employing variety of techniques gave insight about the phosphorylation induced effect on conformation and Aβ aggregation. Further study was carried out employing solid state NMR to study the kinetics of monomeric Aβ consumption which can precede the oligomers and fibril formation. The kinetics of monomeric Aβ consumption for the formation of Aβ intermediates in oligomerization process was studied by 1D ^{1}H-NMR spectroscopy. The relative intensities of the NMR signals of npAβ remained nearly constant while in pAβ, a rapid decrease was observed reaching about 25% of the initial value after six hours (Fig. 37). The

faster decay of the pAβ NMR signals indicates a rapid consumption of monomeric Aβ as compared to npAβ.

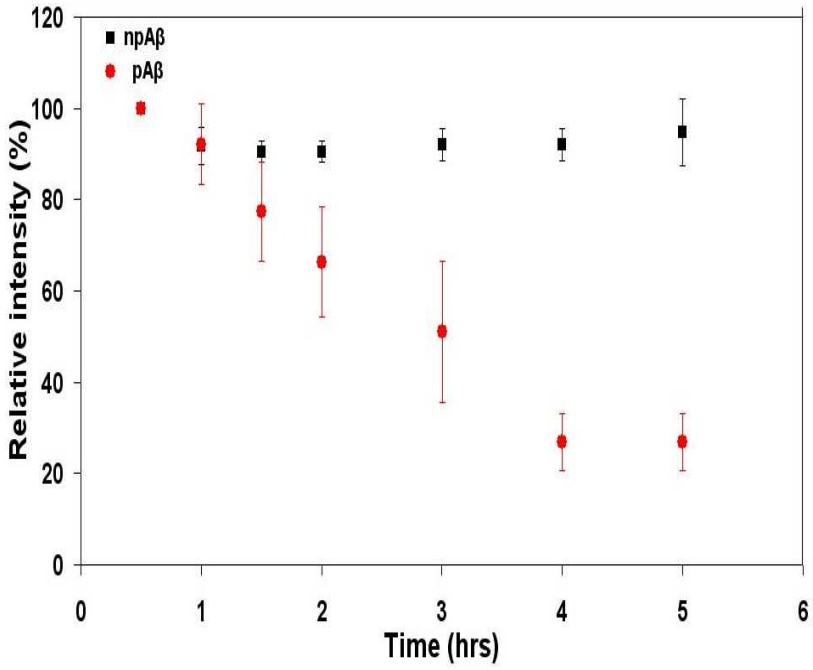

Fig. 37: Time-dependent decay of npAβ and pAβ by 1D ^{1}H-NMR.
NMR samples containing npAβ (■) and pAβ (○) peptide were incubated at 37 °C and the 1D ^{1}H-NMR spectra were recorded at different time points as indicated in the diagram. NMR data were processed by TOPSPIN 2.0 and calibrated using the known chemical shift of water. The spectrum indicates the signals of npAβ and pAβ during six hour incubation at 37°C. Three signals within the aliphatic region of the proton 1D spectra (0.754, 1.258 and 2.096 ppm) were selected for further analysis. Mean ± s.d. of the three peaks are reported. Significant increase in monomer consumption is observed with pAβ as compared to npAβ.

4.3.3. Effect of phosphorylation on Aβ oligomerization

4.3.3.1. Assessment of Aβ oligomers assembly by dynamic light scattering (DLS)

The formation of pathogenic, fibrillar protein aggregates (amyloids) requires the self-assembly of β-sheet enriched oligomeric structures. This self-association mechanism leads to different size distribution of misfolded aggregates (Janek et al., 1999). The kinetics of molecular self-assembly of npAβ and pAβ peptides and their size distribution was studied by DLS. This methodology has already been employed to characterize monomeric, oligomeric and protofibrillar Aβ aggregates (Walsh et al., 1997; Nichols et al., 2002; Janek et al., 1999). The DLS results showed the differences in distribution of the molecular size of polymerized npAβ and pAβ oligomers or aggregates in solutions (Fig. 38A & B).

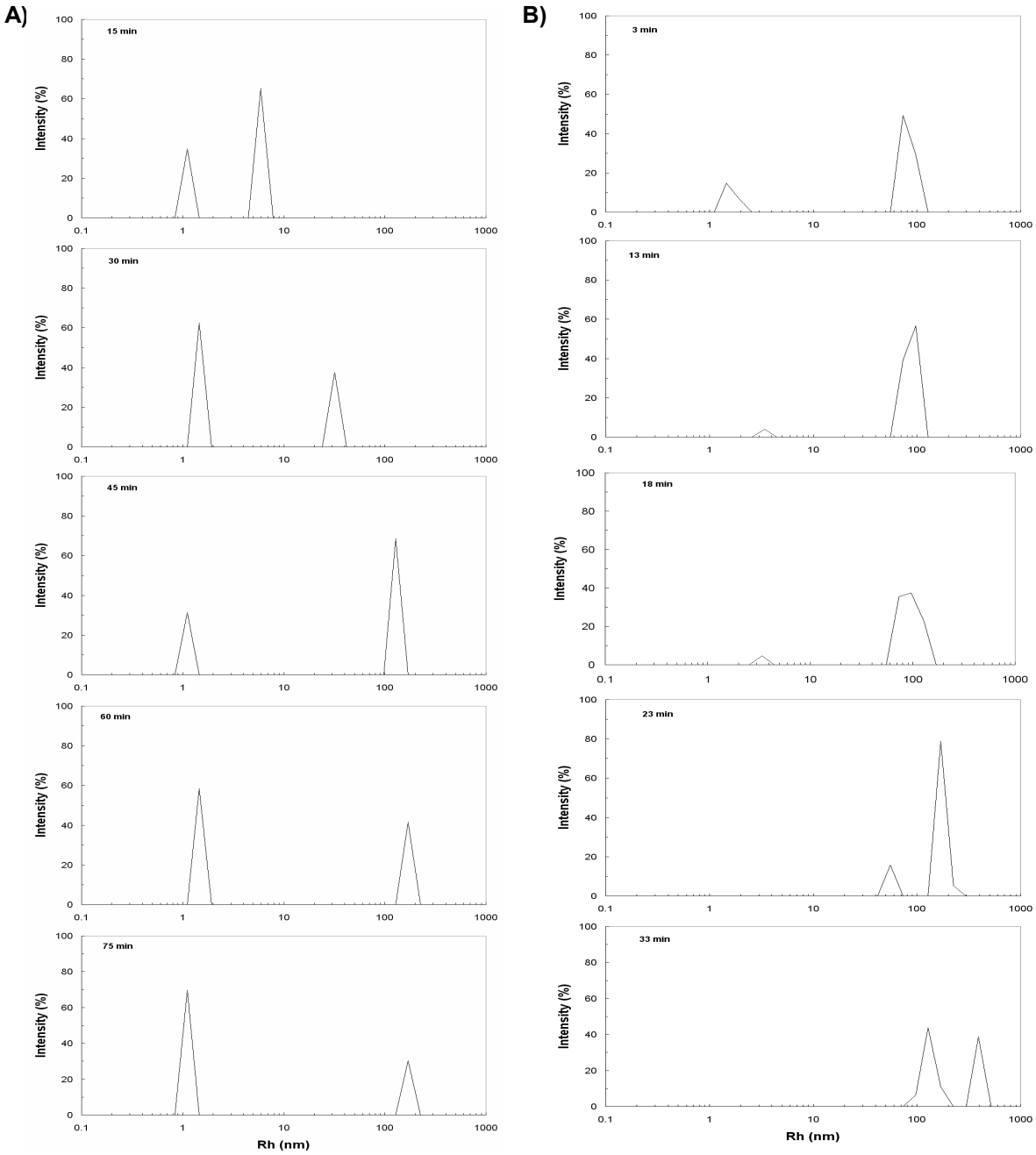

Fig. 38: Effect of phosphorylation on the size distribution of Aβ oligomers/aggregates by Dynamic Light Scattering (DLS).
The npAβ and pAβ peptide solutions (100μM) were incubated at 37 °C and the time-dependent variation in the size distribution of Aβ oligomers/aggregates were monitored by DLS. A) Size distribution of npAβ monomers and oligomers after 15, 30, 45, 60 and 75 min of incubation. Monomeric npAβ peak corresponding to the particle size between 1.1 and 1.5 nm of hydrodynamic radius (R_H) is continuously present. A second peak can be seen at a R_H value of 5.9 nm and shifted to larger values with raise in incubation time respectively (R_H of 31.7, 97.1, 128.5 nm after 30, 45, 60 and 75 min). As the intensity of scattered light was too strong, most likely due to formation of larger aggregates, the measurements were stopped at 75 min. Interestingly, during the 70 min of incubation more than 95% of the mass is associated with the monomeric peak in npAβ. B) Size distribution of pAβ monomers and oligomers after 3, 13, 18, 23 and 33 min of incubation. The peak corresponding to R_H at about 1.4 nm corresponding to monomeric pAβ is replaced by a peak of R_H at 3.4 nm after 13 min, followed by a complete disappearance of the peak. The peaks at increasingly larger sizes appeared with the increase in incubation time respectively (R_H of 82.2 nm, 87.4 nm, and 95.9 nm at 3, 13 and 18 min respectively, and R_H of 55.5 nm and 173.4 nm at 23 min, 132.6 nm and 393.2 nm after 33 minutes). The scattered light was too much due to the formation of larger aggregates after 35 minutes. Comparison of the magnitudes of intensities between npAβ and pAβ is not meaningful (i.e., it does not indicate the absolute concentration of Aβ aggregates).

At different time points during the aggregation, the size distribution of npAβ aggregates revealed mainly particles with a hydrodynamic radius (R_H) of 1-2 nm, 6-8 nm, 20-40nm and 100 nm (Fig. 38A). All the measurements after 30 min of incubation showed particles with larger R_H values >100 nm. The R_H of 1-2 nm particles observed correspond to monomeric Aβ exists in all the indicated time intervals. At 15 min of incubation, npAβ showed monomeric and dimeric Aβ peak (R_H of 6-8 nm). The particles size above R_H of 10 nm corresponds to oligomers, which were observed at 30 min of incubation. Protofibrils peak (R_H of >100 nm) was appeared after 45 min and the peak was persistent after 45 min of incubation time (until 75 min).

The size distribution of pAβ aggregates comprised peaks with a R_H of 1-2 nm 3-5 nm and above 100 nm (Fig. 38B). The monomeric pAβ peak (R_H of 1-2 nm) was observed only at 3 min of time interval. The dimer peak (R_H of 6-8 nm) was seen at 13 and 18 min but disappeared after 18 min. The protofibrils peak R_H of 100 nm size was already apparent at 3 min. After 23 min, the particle size of >100 nm was noticeable. These peaks indicate the growth of protofibrils to fibrils and this characteristic peak was observed only with pAβ. Phosphorylation induces a shift in the molecular size of the aggregates which were clearly observed during early phases of aggregation with pAβ. pAβ significantly increased the count rate as compared to npAβ. The count rates of npAβ reached plateau after 70 minutes (formation of larger aggregates) whereas the pAβ peptide reached plateau after 35 minutes. The observed particle size were in concordance with the already existing DLS data for Aβ40 (Chen et al., 2006; Bitan et al., 2003). The DLS results were very much comparable to the previously shown results indicating that the phosphorylation induces Aβ oligomerization and fibrillization.

4.3.2.2. Characterization of soluble Aβ oligomers by dot blot assay

The appearance of oligomeric Aβ species during the fibrillization process was also assessed by dot blot assay. Equal amounts of sample aliquots from Aβ aggregation assay taken at different time intervals were spotted onto the nitrocellulose membrane and the Aβ oligomers were immunodetected using an anti-oligomer specific antibody (2964;anti-oligomer antibody recognizes only the high M.W. oligomers and protofibrils). In npAβ, oligomers begin to appear after 10 hours of incubation and increased with longer incubation times (until 16 hours). Whereas, in pAβ samples the oligomer formation was found to be accelerated and oligomers were seen much earlier as compared to npAβ (at 6 hr incubation). The absolute amount of oligomer was also found to be higher in pAβ as compared to npAβ (Fig. 39A). The densitometric analysis of the dot blot showed the relative intensity of the pAβ oligomer was higher and found to be earlier as compared to npAβ. Soluble oligomer signals were observed to be decreased in

both peptide samples after longer incubation times (24 and 48 hours), which could indicate the aggregation of the higher oligomer/protofibrils to fibrils (Fig. 39B).

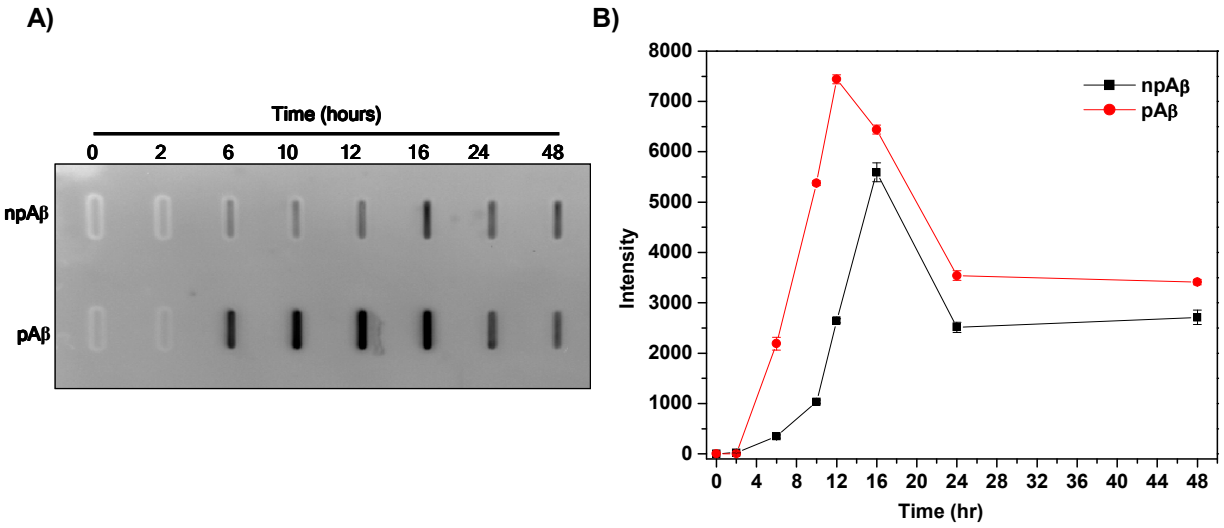

Fig. 39: Dot blot analysis of soluble Aβ oligomers and oligomerization kinetics.
A) Aggregation assays were carried out using 50 μM of npAβ and pAβ peptide solutions, incubated at 37 °C with stirring. Sample aliquots of npAβ and pAβ were collected at indicated time points and spotted onto nitrocellulose membrane (5 μl/spot) and immunodetected with oligomer-specific Aβ antibody (2964) without boiling. The incubation time of the sample aliquots are indicated above the blot. In npAβ, significant amount of oligomers begin to appear after 12 hours of incubation and increased until 16 hours, whereas in pAβ samples, oligomers are seen already at 6 hours of incubation time and increased with longer incubation (until 16 hours). The signals after 16 hours are observed to be similar in both the peptide samples. B) The densitometric analysis of the dot blots using Biorad Quantity One imaging software. Data points indicate the mean ± s.d. of three experiments.

4.3.4. Spontaneous, Nucleation-dependent aggregation by pAβ seeding

The npAβ and pAβ peptide aggregation kinetics exhibited a profile similar to that found for many amyloid fibrils, consisting of an initial lag phase followed by a rapid growth phase terminating at a plateau. The lag period was found to be prominently shorter in pAβ as compared to npAβ peptide as observed from the kinetic parameters analysis (Table 5). Reports indicate the effect of various FAD causing Aβ mutations resulting in misfolding of Aβ and forms various types of misfolded oligomers/aggregates and thus serves as a 'seed/nucleus' to accelerate the aggregation (Chiti et al., 2003; Grant et al., 2007; Cruz et al., 2005; Borreguero et al., 2005). Investigations were carried out to test whether pAβ could serve as an efficient seed as compared to npAβ. To quantify the seeding efficiency, preformed npAβ and pAβ aggregates was used to modulate the aggregation of freshly dissolved npAβ. Interestingly, both npAβ and pAβ preformed aggregates were found to serve as an effective seeds in npAβ aggregation reaction, as measured by ThT fluorescence assay. The npAβ aggregates could reduce the 1 hr lag phase of the non-seeded

reaction when added at 5% by weight of total monomeric disaggregated npAβ in the reaction. In contrast, the similar amount of pAβ aggregates can completely eliminate the 1 hr lag phase of the non-seeded reaction (Fig. 40).

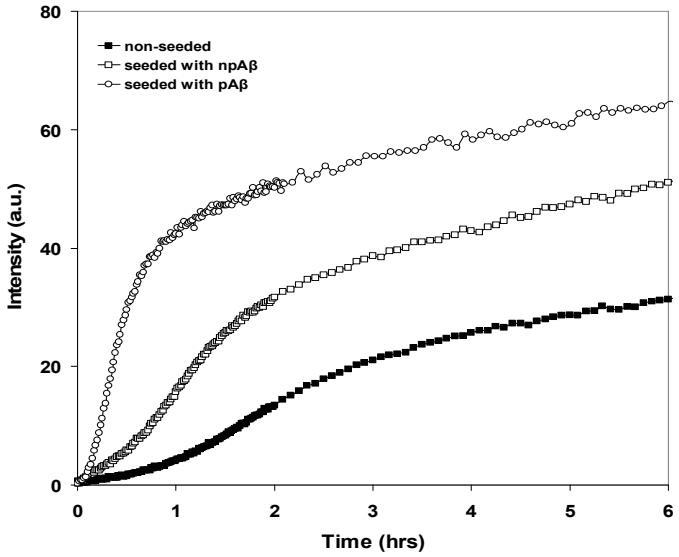

Fig. 40: *In vitro* seeding of disaggregated npAβ with preformed npAβ and pAβ seeds/aggregates. *In vitro* seeding of npAβ solution with npAβ and pAβ seeds and the seeded-aggregation was monitored by ThT fluorescence assay. Preformed npAβ and pAβ aggregates of 5% by weight of total monomeric disaggregated npAβ were used as seeds/nuclei in the aggregation reaction. The non-seeded reaction shows a ~1 hr lag phase during aggregation. However, reduction in lag phase by ~30 min is observed with npAβ seeds where as the lag phase was eliminated with the pAβ seeds/aggregates during aggregation.

4.4. Detection of pAβ *in vivo* in transgenic mouse and human AD brain

4.4.1. Generation of phosphorylation-state specific Aβ antibody and its specificity analysis against different Aβ oligomers

To facilitate the analysis of Aβ phosphorylation and identification of pAβ peptide *in vitro* or *in vivo*, it is useful to have the suitable reagent that specifically recognizes the phosphorylated forms of Aβ. Therefore, a phosphorylation-state specific Aβ antibody was generated against pAβ(pSer-8) peptide using rabbit as host as described in Methods. The polyclonal phospho-site specific Aβ antibody (SA5434) is screened by ELISA to determine the affinity and phospho-selectivity (data not shown). After confirming the phospho-selectivity of the SA5434 by ELISA, the antibody was tested for its pAβ specificity by Western-blotting.

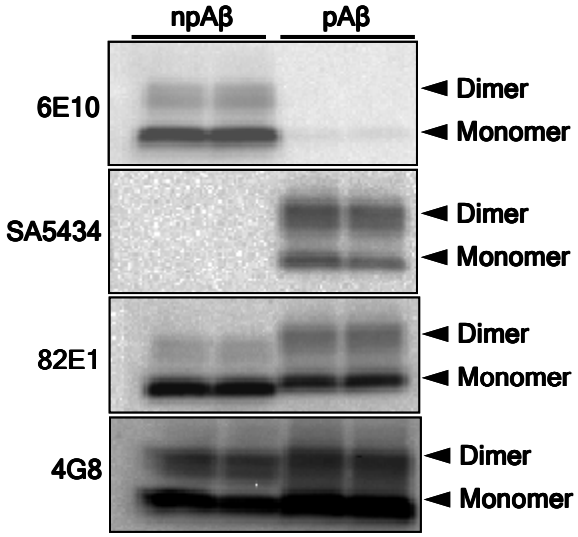

Fig. 41: Specificity assay of the phosphorylation-state specific Aβ antibody (SA5434).
Synthetic non-phosphorylated (npAβ) and phosphorylated (pAβ) peptides were electrophoresed and western-blotted. The blots were probed with polyclonal phosphorylation-state specific antibody SA5434 and commercially available monoclonal antibodies 6E10, 82E1 and 4G8 which are generally used in the AD research. SA5434 specifically recognizes monomeric and dimeric forms pAβ peptide, where as 6E10 is found to be specific for npAβ monomers and dimers. Similar detection of npAβ and pAβ monomers and dimers are observed with 82E1 and 4G8 antibodies.

Similar amounts of npAβ and pAβ peptides were electrophoresed and western-blotted. The blots were then detected with the polyclonal phospho-site specific SA5434 antibody and commercially available monoclonal Aβ antibodies such as 6E10, 82E1 and 4G8 which are generally used in AD research. The Fig. 41 shows the immunoblot results of the specificity analysis of different antibodies against monomeric and dimeric forms of npAβ and pAβ. The

SA5434 whereas 6E10 antibody is observed to be only specific to npAβ. The 6E10 antibody recognizes an epitope between amino acids 4-12 of the Aβ domain that contains the identified phosphorylation site (epitope is mapped to amino acids 4-8 at N-terminus of Aβ). The phosphorylation of Ser-8 residue makes this antibody completely insensitive to pAβ peptide. The antibodies 82E1 and 4G8 antibodies could recognize both npAβ and pAβ peptide variants similarly. The 82E1 antibody recognizes amino acids starting from 1–16 at the N-terminus of Aβ (neo-epitope specific), where as 4G8 recognizes amino acids 17–24 near the N-terminus of Aβ. As the 82E1 and 4G8 antibodies are shown to recognize the epitopes which are away from the phosphorylation site, these two antibodies could recognize both npAβ and pAβ peptides similarly. The antibody specificity analysis result clearly shows the specificity of the different antibodies to monomeric as well as dimeric forms of npAβ and pAβ peptides.

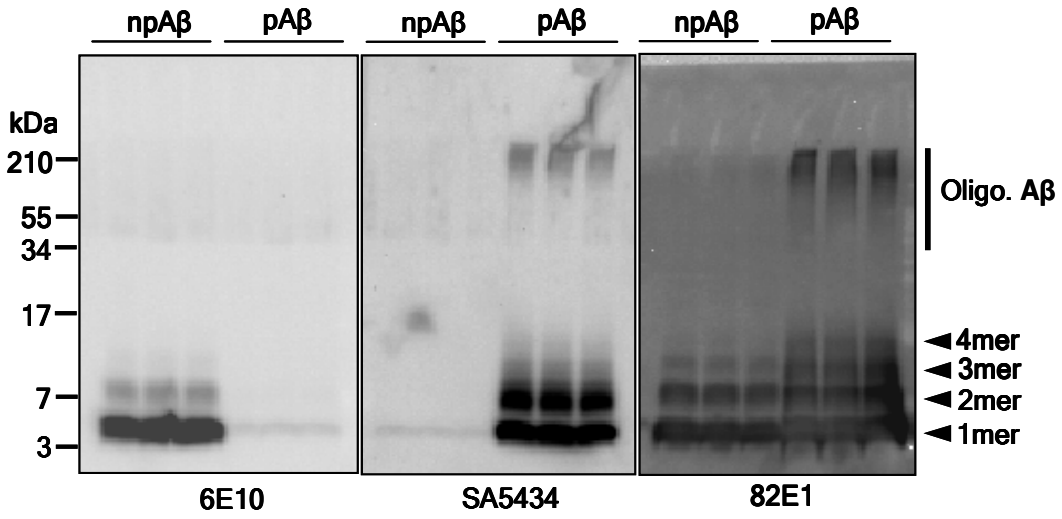

Fig. 42: Specificity analysis of pAβ specific antibody (SA5434) to Aβ oligomers.
Aliquots of npAβ and pAβ aggregates were separated by SDS-PAGE and western-immunoblotting. The blots were detected with antibodies 6E10, SA5434 and 82E1. Antibody 6E10 specifically detects the npAβ where as SA5434 selectively detects pAβ oligomers, while 82E1 detected both npAβ and pAβ oligomers. Migrations of monomeric (1mer), dimeric (2mer), trimeric (3mer), tetrameric (4mer) and higher oligomeric forms and their detection by different antibodies are shown.

Following the identification of the specificities of the polyclonal phospho-site specific antibody (SA5434) and other monoclonal antibodies (6E10, 82E1 and 4G8) against npAβ to pAβ monomeric and dimeric forms, further analysis were carried out to check whether these antibodies can recognize the different soluble low M.W. and high M.W. oligomers. The npAβ and pAβ aggregates were taken and the different Aβ oligomeric species were separated by electrophoresis and transferred onto nitrocellulose membrane. The membranes were then

immunoprobed with SA5434, 6E10 and 82E1 antibodies. The immunoblot paradigm in Fig. 42 is showing the specificity of the antibodies to different oligomeric species of npAβ and pAβ peptides. The 6E10 antibody is shown to be very specific to npAβ peptide (as indicated previously) and could recognize npAβ monomer and different oligomers. The phospho-site specific antibody SA5434 is found to be very specific to pAβ peptide and this antibody could recognize different variants of pAβ oligomers. While the 82E1 antibody is observed to recognize both npAβ and pAβ oligomers. In addition to the detection of monomer and small oligomers, these antibodies also found to recognize high M.W. oligomers that were observed as a smear in the upper part of the gels.

The antibody specificity analysis clearly indicated the specificity of 6E10 to npAβ peptide monomer and oligomers, where as SA5434 antibody is found to be highly specific for pAβ peptide monomer and oligomers. The 82E1 recognizes both npAβ and pAβ monomer and oligomers similarly. In addition to the specificity of the antibodies to npAβ and pAβ peptides, these data indicate that the antibody SA5434 recognizes also the oligomeric Aβ depending on the phosphorylation state.

4.4.2. Immunohistological and biochemical detection of pAβ in transgenic mouse brain

Immunohistological studies were carried out with APPswe/PS1ΔE9 double transgenic (*tg*) mouse brain sections to examine the occurrence of pAβ deposits *in vivo*. Consecutive sections of *tg* mouse brain were immunostained with antibodies of different specificity (pAβ specific antibody-SA5434 and npAβ specific antibody-6E10). The Fig. 43 shows the immunohistological staining of hippocampal region of the brain sections from nine-month old *tg* mice. Strong labeling of amyloid deposits with SA5434 is observed in the hippocampal region (a; Red). Most of these deposits also contain npAβ as indicated by the co-staining with antibody 6E10 (b; Green). In the merged image (c), some individual plaques show a more pronounced reactivity of SA5434 in the core region are observed and showing the co-localization of pAβ positive plaques with npAβ plaques (orange colored plaques indicated by arrows).

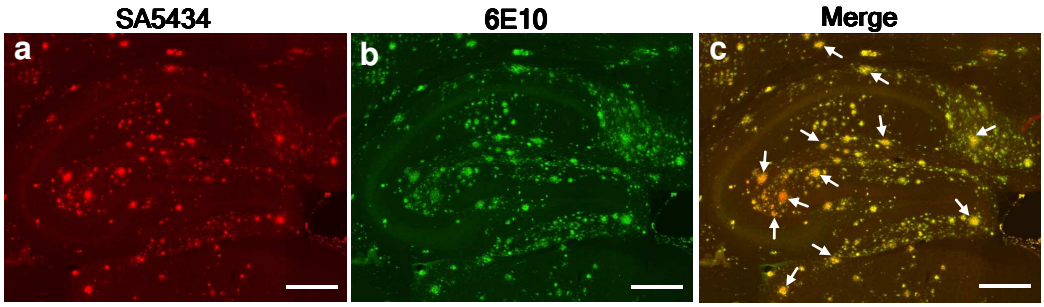

Fig. 43: Immunohistological detection of pAβ in hippocampal brain slices from transgenic mouse.
Immunohistological staining of pAβ and npAβ by antibodies SA5434 (a) and 6E10 (b) using consecutive brain sections from 9-month old APPswe/PS1ΔE9 double transgenic (*tg*) mouse. The pAβ reactive and npAβ reactive plaques are detected in hippocampal regions of *tg* brains. Co-localization of plaques with pronounced reactivity of SA5434 in the core region is indicated by arrows in the merged image (c). Scale bar, 100 µm.

After the immunohistological detection of pAβ plaques in hippocampus region, the age dependent analysis of pAβ deposition was carried out. The *tg* mice were sacrificed at 2, 6, 12, 18 months of age and immunohistological staining of the brain sections were carried out (n=3 mouse/age). The Fig. 44 shows the immunohistological staining of the cortical regions of the consecutive brain sections of *tg* mouse at different ages (2 m, 6 m, 12m, 18 m) with 6E10 and SA5434 antibodies. SA5434 reactive pAβ plaques are observed in the cortical region of *tg* mouse brain sections of all the ages (SA5434; a, b, c and d). The consecutive section from the same region which was stained with 6E10 antibody also shows the npAβ plaques in all the ages (6E10; e, f, g and h). Markedly, Aβ deposits are already observed in the cortices of 2-month old mice. Although these deposits are reactive for both the antibodies (pAβ; SA5434 and npAβ; 6E10), very few small deposits that are selectively detected with SA5434 antibody but not with 6E10 can be seen (indicated with arrow head; in image 'a' as well as in Merged image; 'i'). The pAβ associated plaque depositions are observed to be strongly increased with the increase in age. A large overlap of staining with antibodies SA5434 and 6E10 is observed (Merge; i, j, k and l) and pAβ appear to be concentrated toward the centre of individual plaques similar to a senile neuritic plaque morphology (which are indicated with arrows).

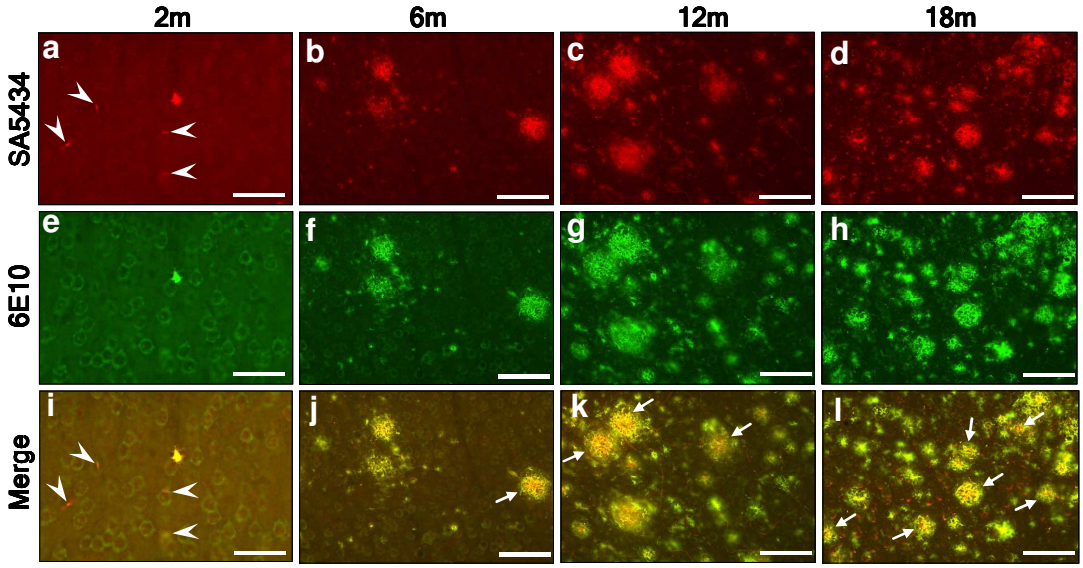

Fig. 44: Age dependent analysis of pAβ associated plaque deposition in *tg.* mouse brain. Immunohistological staining of cortical regions of brain sections from *tg* mouse of different ages (2m, 6m, 12m and 18m) by antibodies SA5434 and 6E10 respectively. At 2m age, some deposits which are reactive for both the antibodies (pAβ; SA5434 and npAβ; 6E10) are already observed, however very small deposits that are selectively detected with SA5434 antibody can be seen which are indicated with arrow head (in image a and i). At this age, we cannot observe the deposits that are selectively stained with 6E10 antibody. Plaques with pronounced reactivity of SA5434 in the core region showing the senile plaque morphology are indicated by arrows (j, k. l). Scale bars, 50 µm (2m); 200 µm (6-18m).

To further support the detection of pAβ and age dependent deposition of pAβ in the hippocampal and cortical regions of *tg* mouse brain sections, biochemical analysis was carried out. SDS-soluble Aβ containing brain lysates were prepared by sequential homogenization and centrifugation of *tg* mouse whole-brain homogenates. After the preparation, SDS-soluble Aβ containing extracts were used for the biochemical analysis by SDS-PAGE and western-blotting. Consistent with the immunohistological staining results, the pAβ and npAβ are strongly increased with age as shown in the immunoblot paradigm which was detected with SA5434, 6E10 and 82E1 antibodies respectively (Fig. 45). Strong reactivity of the oligomeric Aβ can be observed as a smear in the upper regions of the gel with SA5434 and 82E1 antibodies. These oligomeric species are seen already in two-month old mice and became prominent at six-months. At this age, SA5434 show a very little reactivity to monomeric Aβ. In contrast, monomeric Aβ is already detected in six-month old mice with mono-

clonal antibody 6E10 and it seems strongly increased with the increase in age. The reactivity of the antibody 6E10 with oligomeric Aβ assemblies is observed to be much weaker as compared to SA5434 antibody, and it is mainly observed only in 12 and 18-month old animals (Fig. 45A). Strong reactivity of the monomer and as well as oligomers are observed with 82E1 antibody. The bar graphs show the densitometric analysis of the ratio of monomeric and oligomeric Aβ detected with different antibodies (Fig. 45B).

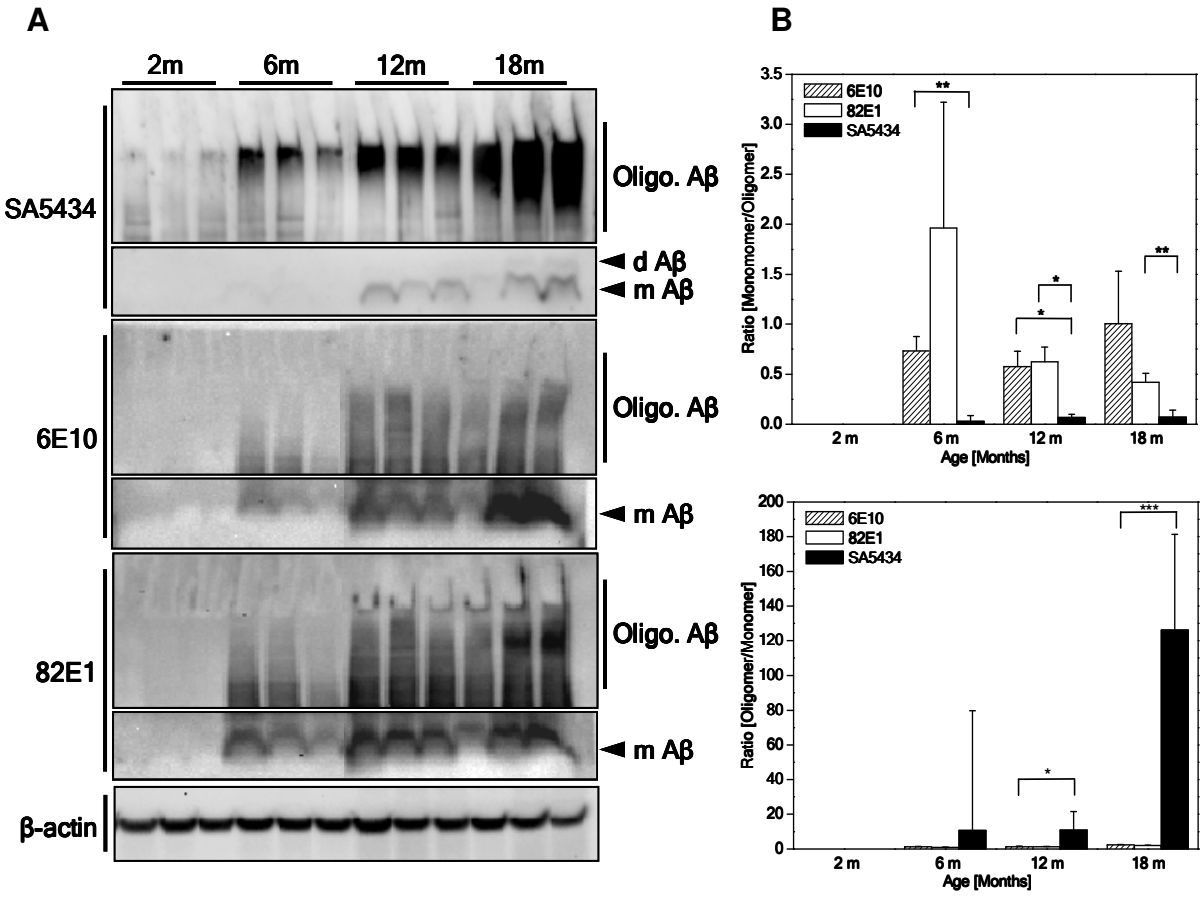

Fig. 45: Age dependent biochemical analysis of pAβ in *tg* mouse brain lysates.
A) SDS-soluble Aβ containing whole-brain homogenates of *tg* mouse from 2 to 18 months (n = 3 for each age) were analyzed by SDS-PAGE and western-blotting with antibodies SA5434, 6E10 and 82E1. Migrations of monomeric (mAβ), dimeric (dAβ and oligomeric Aβ (Oligo. Aβ) variants are indicated. Note the pronounced reactivity of SA5434 with smear in the upper part of the gels indicating the enrichment of pAβ in oligomeric assemblies signifying the increased oligomerization. B) Densitometric analysis of the ratio of monomeric/oligomeric and oligomeric/monomeric Aβ detected with different antibodies. The statistical significance was evaluated by student t-test (***p<0.001, **p<0.01 and *p<0.05; n=3).

4.4.3. Quantitative analysis of pAβ in *tg* mouse brain

After the age dependent immunohistological and biochemical analysis of phosphorylated Aβ in *tg* mice, the quantitative analysis of pAβ was carried out using *tg* mouse brain

lysates. The SDS-soluble Aβ extracts from 18 month old *tg* and non-transgenic mouse whole-brain homogenates (wt littermates; ctr) and different concentrations (10, 25, 50, 100 and 250 ng) of synthetic npAβ and pAβ peptides were electrophoresed and western-blotted. The immunoblot paradigm (Fig. 46) probed with different antibodies indicate the presence of significant amount of npAβ and pAβ in the *tg* mouse as compared to age matched control mouse (ctr.). After immunodetection of the blots, densitometric analyses of the immunoblots were carried out using Biorad Quantity One software. From the densitometric analysis, approximately 20-25% of the monomeric Aβ is in phosphorylated state in the total amount of pAβ in the SDS-soluble Aβ extracts from *tg* mice.

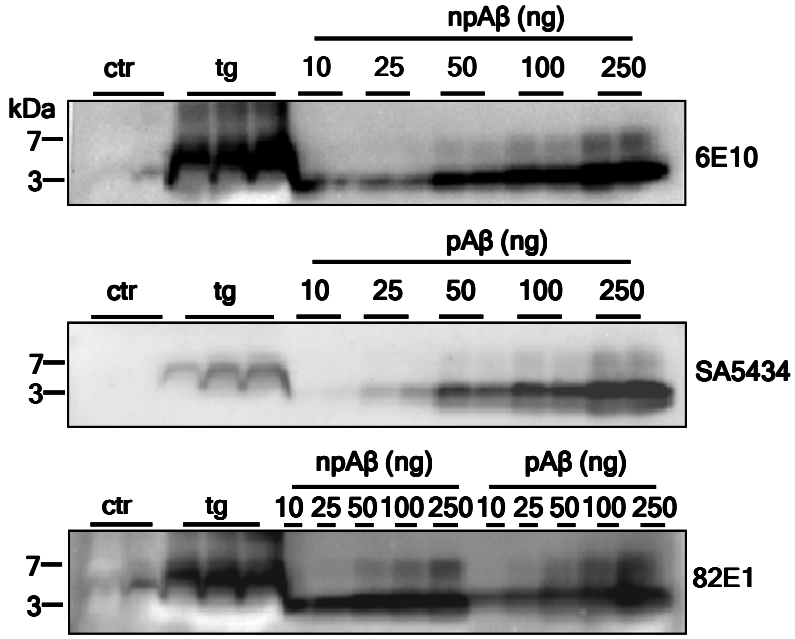

Fig. 46: Quantitative analysis of pAβ in *tg* mouse whole-brain homogenates.
Brain homogenates (total protein: 50 µg) of 18 month old non-transgenic (*ctr*) and transgenic (*tg*) mouse were separated by SDS-PAGE and western-blotted. Synthetic npAβ and pAβ were used as an internal standard. After transfer onto nitrocellulose membranes, the blots were probed with 6E10, SA5434 and 82E1 antibodies. A titration standard curve of synthetic pAβ was used to estimate the amount of pAβ. Quantitative densitometric analysis revealed that about 20-25% of extracted monomeric Aβ is in a phosphorylated state.

Additionally, the amount of pAβ was also quantified by employing the technique of dephosphorylation of the Aβ peptide by shrimp-alkaline phosphatase (SAP) and detection of the dephosphorylated Aβ peptide by phosphorylation-site sensitive antibody. This technique was already used in the detection of phosphorylated tau using phosphorylation-state sensitive antibody after dephosphorylation (Billingsley and Kincaid, 1997). To detect the pAβ as ac-

cording to this technique, the *tg* mouse brain lysates (with specific amount of proteins) were dephosphosphorylated using SAP as described in Methods. As a control for the dephosphorylation assay, 250 ng of synthetic pAβ peptide was dephosphorylated in a similar condition. After dephosphorylation of the brain lysates and synthetic pAβ peptide, the samples were electrophoresed blotted onto nitrocellulose membrane. After blotting, the blots were probed with a 6E10 antibody (Fig. 47).

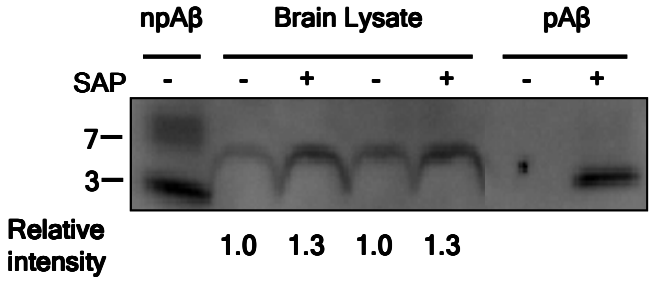

Fig. 47: Detection of pAβ in mouse whole-brain homogenates after dephosphorylation.
Brain homogenates of 18 month old *tg* mouse and synthetic pAβ were incubated in the absence or presence of SAP for 5 hrs at 37 °C. After incubation, the samples were separated by SDS-PAGE, Aβ was detected by western-blotting with 6E10 antibody. The reactivity of the 6E10 antibody is shown to be increased after dephosphorylation. The increased reactivity of antibody 6E10 after SAP treatment of synthetic pAβ demonstrates the specificity of this antibody for non-phosphorylated Aβ. The relative increased intensity after SAP treatment quantified by densitometry analysis is indicated.

The Fig. 47 shows the signals for non-dephosphorylated (-SAP) and dephosphorylated (+SAP) Aβ immunodetected with 6E10 antibody. The reactivity of the 6E10 antibody to synthetic npAβ can be clearly observed. The antibody do not show any reactivity to synthetic pAβ (due to the presence of phosphoserine, the epitope is not recognized by the 6E10 antibody), but the reactivity can be seen once it is dephosphorylated. The same was observed with the *tg* mouse whole-brain homogenates. The immunoreactivity of the Aβ from *tg* mouse brain lysates is observed to be increased after dephosphorylation (+SAP) as compared to non-dephosphorylated (-SAP). The relative increase in intensities after dephosphorylation is quantified by densitometric quantification of the signals using Quantity One software from Biorad which indicated that about 30 % of monomeric Aβ is in a phosphorylated state *in vivo* in mouse brain.

4.4.4. Detection of pAβ in human AD brain and pAβ associated neuronal alterations

The occurrence and deposition of pAβ in the human brain has not been shown so far. To detect the presence of pAβ deposits in human AD brain, immunohistochemical staining was carried out using human control and AD brains sections employing SA5434 and 6E10 antibodies. Ten human autopsy brains were received from the University Hospital Bonn in accordance with the laws and under affirmation of the local ethical committee (Table 3). Post-mortem diagnosis of Alzheimer's disease was carried out according to the NIA-Reagan Criteria (1997; Mirra, 1997). Immunolabelled sections were analyzed with a Leica DMLB fluorescence microscope. Pictures were taken digitally with a Leica DCF500 camera.

In Fig. 48, the extracellular pAβ deposition was evident in the adjacent sections that were stained with the pAβ specific antibody (SA5434; d-f and j-l) and npAβ specific (6E10; a-c and d-f) antibody. The deposition of pAβ as detected by SA5434 reveals similar patterns of staining to those observed in sections stained with the 6E10 antibody. The co-staining of pAβ and npAβ is observed in CA1 region and in entorhinal cortex of human AD brain (indicated by arrows). The reactivity of the SA5434 is found to be weaker as compared to 6E10 antibody. Largely, an overlapping pattern of the npAβ and pAβ plaques are observed. In addition to pAβ plaque staining, the staining of the vascular amyloids by SA5434 is also observed (indicated by arrow head). These immunohistochemical staining of brain sections from human AD patients indicate the occurrence of pAβ reactive plaques and staining of vascular amyloids in human AD brain. The hippocampal formation exhibits distinct diffused and core plaques staining for Aβ and pAβ in the pyramidal cell layer of the subiculum, the Ammon's horn (AH) sectors and CA1-CA4 regions as well as in the molecular layer of the dentate gyrus (indicated by arrows).

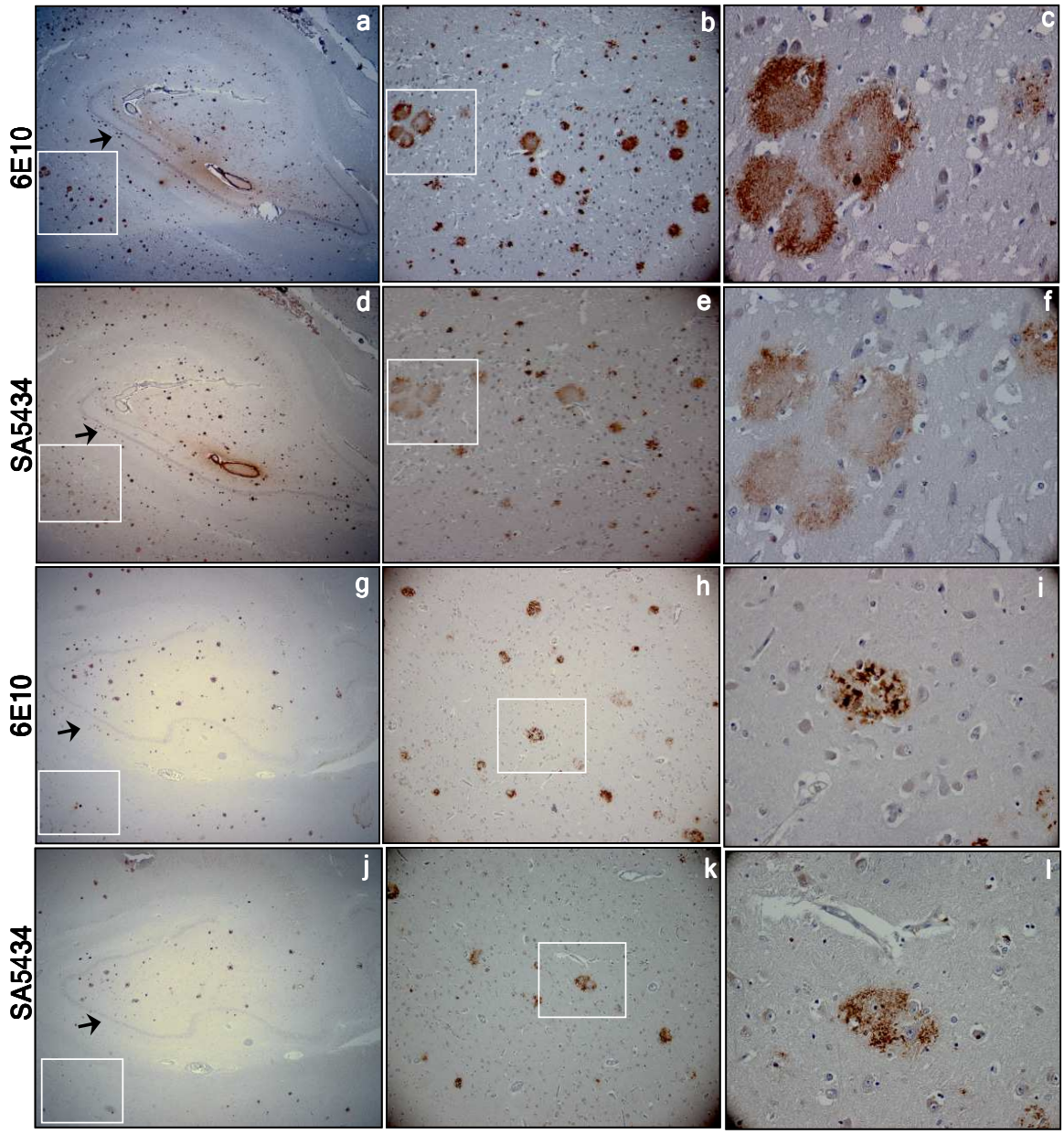

Fig. 48: Immunohistochemical staining of pAβ in human AD brain.
Detection of Aβ (a-c and g-i) and pAβ (d-f and j-l) using 6E10 and SA5434 antibody in human AD cases. The hippocampal formation exhibits distinct core and diffuse plaques staining for Aβ and pAβ of the pyramidal cell layer of the subiculum, the Ammon's horn (AH; a, d, g, j) and CA1-CA4 (b, c, e, f, h, i, k and l) as well as in the molecular layer of the dentate gyrus (arrows). Largely, an overlapping pattern of npAβ and pAβ are observed. Pictures were taken at x 2.5 (a, d, g and j), x 10 (b, e, h and k) and x 40 (c, f, i and l) magnification. The white boxes representation of the selected areas observed at higher magnifications.

Inflammatory processes have long been posited as serving integral roles in initiating and/or propagating AD-associated pathology within the human brain. It has been reported that pro-inflammatory cytokine and chemokine expressions are significantly enhanced resulting in concomitant increases in region-specific microglial cell numbers in brains of AD patients. The role of microglia and their accumulation at the sites of dense neuritic plaques has been described (D'Andrea et al., 2004; Eikelenboom et al., 2006; Gahtan and Overmier, 1999). Here in, the status of microglia cells with pAβ were assessed. Double-label immunohistochemical staining was carried out using anti-CD68 antibody specific for the microglia/macrophage surface marker and SA5434 antibody specific for pAβ. Immunohistochemical staining showed a CD68-positive microglia association with pAβ reactive plaques in the human AD brain sections. Marked distribution of CD68-positive microglia, appearing to assemble into dense pAβ positive aggregates and also found toward the edge of the plaques (Fig. 49).

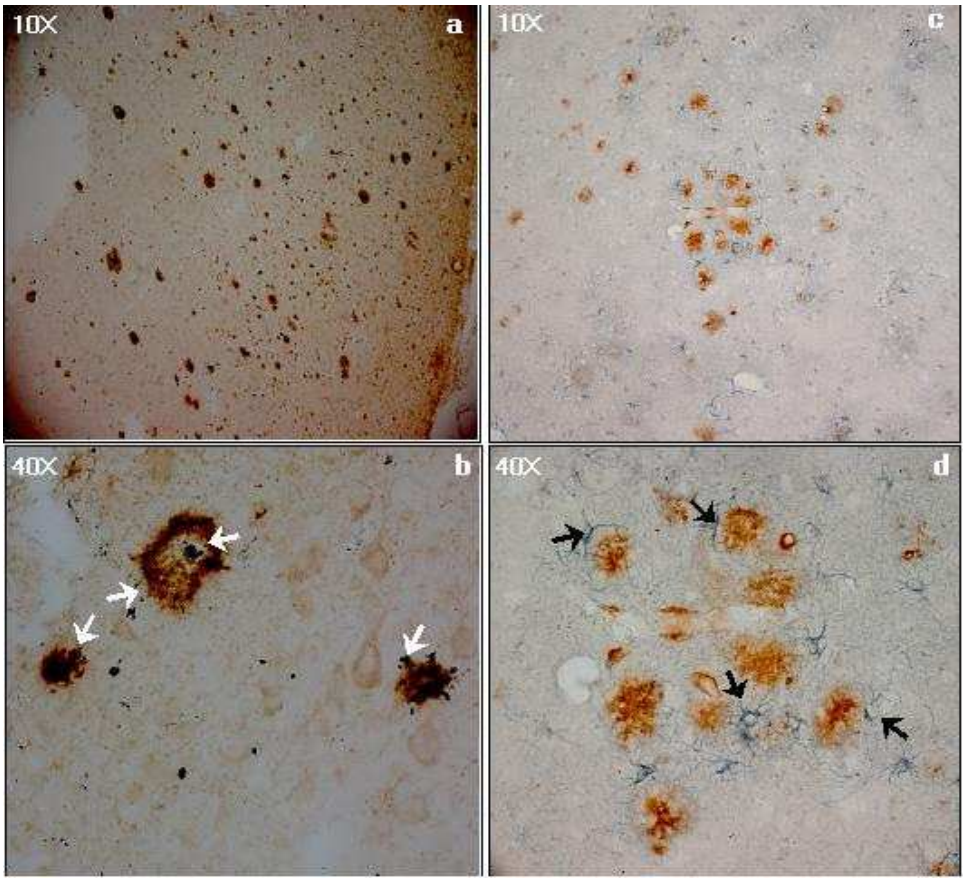

Fig. 49: Association of pAβ plaques with Microglia and Astrocytes in the human AD brain.
a, b: Double-label immunohistochemical staining of human AD brain sections with SA5434 and CD68 antibodies. Immunostaining pictures showing the pAβ plaques (brown) and CD68 (black) indicating the co-localization and association of the microglial-associated epitope CD68 with pAβ cored plaques (white arrows). **c, d:** Human AD brain sections exhibiting the association of pAβ plaques with astrocytes as indicated by double-label immunohistochemical stainings for pAβ plaques (brown) and GFAP (blue-black). Note that the astrocytes are often associated with neuritic plaques (black arrows).

Astrocytes are reported to be involved in different functions in the brain, including structural integrity of the blood brain barrier, support of neuronal synapses by ion regulation and removal of glutamate (Cotrina and Nedergaard, 2002). Although it is believed that they are not directly responsive to primary insults, astrocytes react to inflammatory events in the brain, relying upon pro-inflammatory molecules elaborated from activated microglia (Gahtan and Overmier, 1999). Glial fibrillary acidic protein (GFAP) is an intermediate filament (IF) protein that is found in glial cells such as astrocytes. GFAP is often employed as a marker of astrocytic activation. Double-label immunohistochemical stainings were carried out using anti-GFAP antibody specific for reactive astrocytes and SA5434 antibody specific for pAβ. GFAP-expressing astrocytes were readily visible in association with pAβ stained plaques throughout the hippocampus (Fig. 49). Immunohistochemical examinations of hippocampus and cortex regions of brain sections from AD patients revealed increased reactive astrogliosis (GFAP immunoreactivity) and activated microglia (CD68 immunoreactivity) in association with pAβ reactive plaques, thereby suggesting the probable reminiscent role of pAβ deposits in neuroinflammatory process.

The development of intraneuronal lesions is central to the pathological process in Alzheimer's disease (AD). The lesions consist chiefly of hyperphosphorylated tau protein and include pretangle material, neurofbrillary tangles (NFTs) in cell bodies, neuropil threads (NTs) in neuronal processes and material in dystrophic nerve cell processes of neuritic plaques (NPs). The localization of clusters of abnormal neuronal processes is referred to as dystrophic neurites (DNs) and their association with cored-neuritic Aβ plaques is a common phenomena in AD. These neuritic plaques have been considered as a pathological correlate of AD dementia (Mirra et al., 1991). Double-label immunofluorescence of AD brain sections was performed using SA5434 combined with a monoclonal antibody 22C11, directed against APP. The photomicrographs of double-label immunofluorescence labelling with SA5434 shows the pAβ immunoreactive plaques (Red) which are associated with abnormal neurites containing accumulations of neurofilaments (green) (Fig. 50). Antibody SA5434 readily stained the senile plaques in human AD brain. Importantly, strong reactivity of SA5434 is observed in the core of neuritic plaques, while antibody 22C11 against the extracellular domain of APP selectively detected dystrophic neurites in close proximity to the amyloid core of the neuritic plaques. The abnormal dystrophic neurites shows either a ring- or bulb-like morphology. These studies show the association of abnormal neurites that generally observed in AD with the pAβ-amyloid deposits.

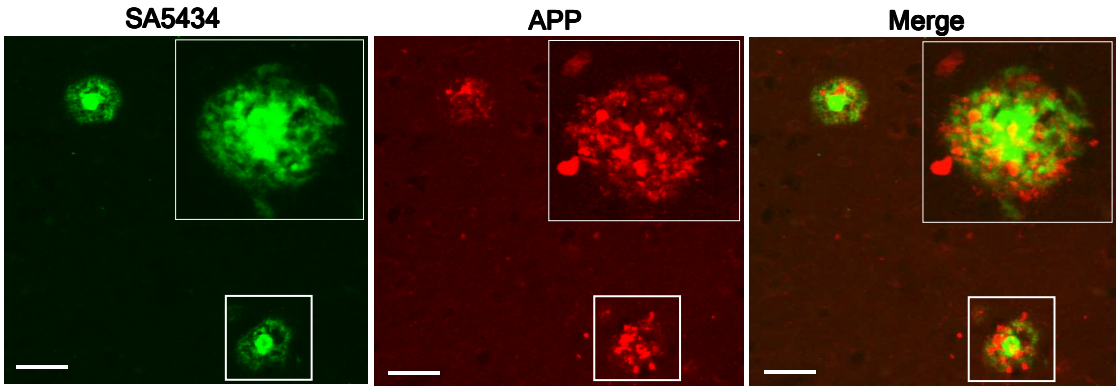

Fig. 50: Double-label immunofluorescence of pAβ associated neuronal alterations in human AD brain.
Confocal double-label immunofluorescence photo-micrographs of sections from the entorhinal cortex of a human AD brain stained with pAβ-specific antibody (SA5434; green) and APP (22C11; red). The preferential staining of the amyloid core by phosphospecific Aβ antibody (SA5434) indicates preferential deposition of pAβ in these structures. The presence of dense-cored plaque and occurrence of dystrophic neurites around plaques indicates typical morphological and neurochemical changes that are associated with AD pathogenesis. Bigger box is the magnified image of the area marked in smaller box in the image.

5. DISCUSSION

The current investigation was aimed at understanding the role of extracellular phosphorylation of Aβ peptide in aggregation. The present work demonstrates the phosphorylation of Aβ *in silico*, *in vitro* and *in vivo*. Extracellular kinases which are present at the cell surface are shown to phosphorylate the exogenous Aβ. The extracellular kinase activity was also observed in the CSF of the human brain. The biophysical data gave an insight into the role of phosphorylation at serine residues which is capable of enhancing the propensity of Aβ to adopt a β-sheet rich conformation. The phosphorylation induced β-sheet rich structures accelerated the formation of small oligomeric aggregates that could seed aggregation into larger oligomeric and fibrillar assemblies. By using phosphorylation-state specific Aβ antibody, the occurrence of phosphorylated Aβ was documented in *tg* mice and human AD patient's brains. The specific detection of phosphorylated and non-phosphorylated Aβ in *tg* mice indicate the preferential aggregation of phosphorylated Aβ *in vivo*. The phosphorylated Aβ variants are highly enriched in oligomeric species of Aβ from mouse brain, indicating the critical role of phosphorylation in the aggregation of Aβ *in vivo*. Importantly, phosphorylated Aβ is enriched in the core of amyloid plaques in the human brain that contains highly aggregated forms of Aβ peptides. These dense core plaques are associated with dystrophic neurites, indicating that these assemblies are neurotoxic and lead to degeneration of brain neurons. The phosphorylated Aβ was also found to be associated with microglia and astrocytic cells. Thus, extracellular phosphorylation of Aβ may promote aggregate formation and trigger the pathogenesis of sporadic AD.

5.1. Phosphorylation of Aβ

It is known that the activity of many kinases and phosphatases are altered in brains of patients affected by AD (da Cruz e Silva EF and da Cruz e Silva OA, 2003; Saitoh and Iimoto, 1989). In AD, aberrant activation of several kinases has been linked to hyperphosphorylation of tau and tangle formation (Jin and Saitoh, 1995; Mi and Johnson, 2006). In addition to tau phosphorylation, regulation of Aβ production and modulation of APP processing by different kinases has been shown (Buxbaum et al., 1990; Flajolet et al., 2007; Gandy et al., 1988; Marambaud et al., 1996; Xu et al., 1996). Several phosphorylation sites within the cytoplasmic domain of APP and the responsible kinases were identified both *in vitro* and *in vivo* (Ando et al., 1999; Ando et al., 2001; Aplin et al., 1996; Iijima et al., 2000; Isohara et al., 1999; Oishi et al., 1997; Standen et al., 2001; Suzuki et al., 1994; Suzuki et al., 1997; Suzuki and Nakaya, 2008). The phosphorylation of certain sites regulates the

interaction of the numerous cytoplasmic domain proteins and affects the production of Aβ in cultured cells (Ando et al., 2001; Lee et al., 2003). Notably, phosphorylation of APP has been shown to be up-regulated in AD (Lee et al., 2003). Despite vast studies on the role of phosphorylation in AD, it remains unclear if the Aβ domain of APP or Aβ can undergo phosphorylation. Using antisense peptide binding methodology, phosphoserine specific antibodies and purified kinases, it has been suggested that Aβ undergoes phosphorylation at Ser-26 by cdc2 *in vitro* (Milton, 2001; Milton, 2005). On the other hand, some kinases including CK1, CK2 and PKC failed to phosphorylate Aβ *in vitro* (Chauhan et al., 1993). Despite the above mentioned studies the phosphorylation of extracellular Aβ and its physiological role in AD remains unknown.

To ensure the fidelity of phosphorylation, the kinases must be sufficiently specific and act solely on their respective substrates (Kennelly and Krebs, 1991; Zhu et al., 2005). *In silico* analysis was carried out using computational prediction tools to predict the potential phosphorylation sites of Aβ and their kinases. *In silico* computational tools are neural network based databases that employ powerful algorithms in their predictions and the predicted phosphorylation sites are compared rigorously with previously identified phosphorylation of various proteins and their kinase specific consensus sequences. These computational tools are valuable and straightforward for prediction of phosphosites and kinases as compared to conventional procedures. The *in silico* prediction analysis indicated that Ser-8, Ser-26 and Tyr-10 residues of Aβ could be potential phosphorylation sites (Fig. 10). According to the KinasePhos computational tool the identified phosphosites of Aβ could undergo phosphorylation by PKA, CK1, CK2 and PKC (Fig. 11). Comparison of the results with already existing literature on the consensus sequences of a variety of phosphoproteins further confirmed the *in silico* analysis (Table 4).

Consensus sequences are considered essential for substrate recognition and phosphorylation by respective kinases. They act as critical substrate recognition determinants and most probably form a reflected image of the corresponding substrate domains (Kennelly & krebs, 1991). Arginine at N-terminal to the phosphoacceptor Ser-8 in Aβ sequence (at -3 position), is a key residue in substrate recognition by PKA. Arginine has been recognized as a key determinant (at -2 or -3 positions) in determining the substrate specificity of PKA (Kemp et al., 1975; Kemp et al., 1977; Ubersax and Ferrell, Jr., 2007). Thus, the consensus sequence **R**-$(X)_2$-(S^*) in Aβ could be a preferred phosphoacceptor site for PKA. Notably, a 100% conservation of the Arg-5 residue (601 aa of APP695) of Aβ sequence across all mammalian species excluding rodents, further supports a possible key role of this amino acid in the

phosphorylation of Aβ by PKA. Interestingly, mouse APP695 and human APP695 differ in only 17 amino acid residues (De et al., 1991). Three of these amino acids (Gly601 to Arg, Phe606 to Tyr and Arg609 to His) are identified in the Aβ peptide sequence, and notably, they are located between the β- and the α-cleavage sites. These three residues are identical in all species known to develop Aβ plaques with aging except rodents. This led to the hypothesis that the lack of Aβ production in rodents might reside in the amino acid differences (Johnstone et al., 1991; Selkoe et al., 1987). This hypothesis has been supported by studies involving the 'humanized' mouse APP sequence in the Aβ region by mutating these three residues and expression of the humanized mouse APP (APP/Mo/GRFYRH) in neurons (De et al., 1995). These three substitutions were sufficient to restore Aβ production to levels obtained with human APP. Interestingly, mutating the single residue Gly601 to Arg in the mouse APP sequence was alone sufficient to increase the ratio of production of Aβ peptide to p3 by 3-fold. However further investigations in to the functional aspects related to the presence of this residue were not reported. From the current observation, one could hypothesize the critical role of Arg residue in the phosphorylation of Aβ and related pathogenesis in humans.

The presence of acidic amino acid residues such as glutamate or aspartate immediately C-terminal (+1 to +3) to the phosphoacceptor conform the putative phosphorylation site for CK2 (Marin et al., 1992; Songyang et al., 1996). Hence, the consensus (S^*)-(X)$_2$-**E** found C-terminal to Ser-8 in Aβ sequence could possibly be recognized by CK2. A second serine residue at the 26th position conforms the consensus sequence for CK1 and PKC. CK1 normally target sites rich in negatively charged (i.e., acidic or phosphorylated) amino acids N-terminal to the phosphoacceptor (Marin et al., 2003). For eg., D/E-X-X-S^*/T^* for unprimed (no prior phosphorylation) substrate or S/T(p)-X-X-S^*/T^* for primed (prior phosphorylation) targets. Therefore, the **ED**-(X)$_2$-S* sequence of Aβ conforms the consensus sequence for CK1. PKC requires basic amino acid residues close to the phosphoacceptor group. Both N- and C-terminal basic residues can influence PKC. Therefore, consensus sequences such as ***ED***-(X)$_2$-S*-(X)-***K*** in the Aβ sequence can conform a PKC recognition site.

The *in silico* analysis tools indicate that other kinases such as CDK, CDC2 and GSK-3 which could phosphorylate Aβ in addition to the kinases discussed above. However, these kinases are known to be proline-directed kinases. CDK is shown to have a strong preference for proline at the +1 position (Consensus for CDK: S^*/T^*-P-X-K/R and S^*/T^*-P) whereas GSK-3 kinase prefers one or more proline residues close to the phosphoacceptor site (-3 to +3) (Ubersax et al., 2003). The CDC2 kinase whose consensus sequence is S^*/T^*-P requires a proline residue near the phosphoacceptor. Besides the prolyl residue, this kinase prefers a

basic residue at position +3. The absence of a proline residue in Aβ sequence and the lack of a basic amino acid residue at +3 positions make it unlikely that Ser-8 or Ser-26 undergoes phosphorylation by CDK, CDC2 and GSK-3. Despite the involvement of these three kinases in AD pathogenesis (Bhat et al., 2004; Guo, 2006; Hooper et al., 2008; Lee et al., 1999; Monaco, III, 2004; Monaco, III and Vallano, 2005; Vincent et al., 1997), due to the absence of consensus sequence for CDK, CDC2 and GSK-3 in Aβ, further systematic analysis were carried out only with PKA, CK1, CK2.

In vitro phosphorylation studies using synthetic Aβ1-40 and Aβ1-42, purified catalytic units of PKA, CK1, CK2 and [γ^{32}P]ATP showed that Aβ can undergo phosphorylation by these three kinases (Fig. 12 & 16). The relative ^{32}P phosphate incorporation was found to be higher with PKA as compared to CK1 and CK2. Phosphoamino acid analysis indicated that the phosphorylation was targeted mainly at serine residues (Fig. 13). Further characterization and localization of phosphosites employing a variety of full length and truncated variants of synthetic Aβ confirmed the kinase specific phosphorylation sites of Aβ. PKA was found to phosphorylate exclusively the Ser-8 residue of Aβ and the current findings were further confirmed by the complete absence of phosphorylation when the prephosphorlyated Aβ (pAβ-Ser8) was used in the *in vitro* phosphorylation analysis. CK1 exclusively phosphorylates the Ser-26 residue in Aβ. *In vitro* phosphorylation assay by CK2 employing different Aβ variants indicated that CK2 phosphorylate Serine-8 residue of Aβ. All together, the results from the *in vitro* phosphorylation studies correlate with the *in silico* phosphosite predictions.

The stoichiometry and kinetics analysis of Aβ phosphorylation indicate that the Aβ can undergo phosphorylation more efficiently by PKA as compared to CK1 and CK2. The stoichiometry of phosphorylation mediated by PKA increased with time and reached a plateau at ~1 mol of phosphate/mol of Aβ1-40. Kinetic analysis of the reaction by PKA showed that the phosphorylation was concentration dependent and Michaelis-Mentens (Km) for the phosphorylation of Aβ1-40 was 21 μM (Fig. 14 & 15). Further, *in vitro* phosphorylation assays employing Aβ1-42 peptide showed that Aβ1-42 could also undergo phosphorylation by these above mentioned three kinases. Notably, the phosphorylation of the Aβ dimer was observed and interestingly these dimers were phosphorylated only with PKA and CK1 but not with CK2 (Fig. 16). From this observation, one could speculate the distinct specificity of kinases in phosphorylation of monomeric and dimeric Aβ. As recent reports suggesting the potential role of soluble oligomers in the AD pathogenesis (Haass and Selkoe, 2007), the further in depth evaluation of the specificity of the kinases and phosphorylation induced

oligomerization might provide more insights into the functional significance of different kinases in phosphorylation and phosphorylation induced oligomerization.

The activities of different kinases have been reported to be altered in AD brain as well as in fibroblasts derived from patients with sporadic AD, familial AD, and Down's syndrome (Bernert et al., 1996; Buxbaum et al., 1990; Cole et al., 1988; Cole et al., 1991; Masliah et al., 1990; Masliah et al., 1991; Saitoh et al., 1990; Saitoh et al., 1991). Among the identified kinases, PKA, PKC, CK1 and CK2 are associated with AD and several reports indicate that they have been implicated in the AD pathology (Chachin et al., 1996b; Jicha et al., 1999; Moore et al., 1998; Schwab et al., 2000; Su et al., 2003; Yasojima et al., 2000). From the current investigation, it was found that PKA can phosphorylate Aβ more efficiently as compared to CK1 and CK2 kinase. It is reported that PKA, CK1 and CK2 kinases are present at the cell surface and are shedded to the extracellular environment (Kubler et al., 1982; Walter et al., 2000; Walter et al., 2001). Therefore, one could speculate the role of such cell surface PKA in phosphorylation of Aβ.

5.2. Expression of PKA in Human brain and phosphorylation of Aβ by extracellular PKA

PKA is one among the several kinases in the central nervous system involved in myriads of functions in the brain (Nairn et al., 1985). PKA is capable of phosphorylating a large number of substrates involved in neurotransmitter synthesis and release, gene expression, synaptic plasticity, memory, and cell growth and differentiation (Borrelli et al., 1992; Walaas and Greengard, 1991; Riccio et al., 1999; Lara et al., 2003). Furthermore, PKA participates in neurite outgrowth (Song and Poo, 1999), neuronal differentiation (Liesi et al., 1983), and cell survival (Rydel and Greene, 1988; Li et al., 2000). Intracellular PKA is a tetrameric holoenzyme consisting of two catalytic (C) subunits and two regulatory (R) subunits in the absence of cAMP (Nairn et al., 1985). Several isoforms of both C subunit (Cα, Cβ, and Cγ) and R subunit (RIα, RIβ, RIIα and RIIβ) have been found in mammalian tissue. The Cα isoform is expressed ubiquitously in most tissue, whereas the Cβ isoform is highly expressed in the brain (Cadd and McKnight, 1989) and Cγ is expressed exclusively in the testis (Foss et al., 1992). All four isoforms of the R subunits are expressed in human brain (Chang et al., 2003). The expression of both Cα1 and Cβ2 was observed to be significantly reduced in the brains of AD patients as compared to control. The altered expression levels might indicate the possible dysregulation of PKA function in AD patient's brain when compared with controls (Fig. 18). The current finding is consistent with the previous reports

demonstrating the altered mRNA expression of different PKA isoforms in the neurons of AD patients brain as compared to control (Bonkale et al., 1999; Miyamoto et al., 1969; Liang et al., 2008), as well as decreased PKA activity in AD brain (Kim et al., 2001).

Alteration of PKA expression is recognized as a key player in age-related cognitive decline including AD (Ramos et al., 2003). A recent study demonstrated the importance of cAMP/PKA signaling in age-related memory impairment (Yamazaki and Saitoe, 2008). PKA is shown to play an important role in maturation of APP and in Aβ production (Su et al., 2003). PKA is shown to phosphorylate tau at Ser-214 and Ser-409 and primes tau for further phosphorylation by another important tau kinase, glycogen synthase kinase-3β (Wang et al., 2007; Liu et al., 2006). The down-regulation of PKA in AD brain might lead to disturbance in the normal functioning of the PKA enzyme and thus in turn affects several downstream pathways. Thus, observed alteration in expressions of different C subunits could signify the possible physiological role in AD. Studies have also shown the association of the R subunits to the C subunits having other several biological roles in addition to keeping the C subunits inactive and dynamically regulating the activity, which in turn contributes to the down regulation of CREB and impaired cognition and memory (Liang et al., 2007). Further detailed studies on R subunits in AD brain might also give insights into the critical role of R subunits in the regulation of C subunits. From the current investigation, it is found that Aβ can undergo phosphorylation efficiently by PKA. Subcellular targeting of PKA has emerged as a mechanism to secure specific signalling by cAMP. The localization of catalytic subunits, promotes the specific, differentiated and appropriately timed phosphorylation of substrates. In the present context, given the importance of PKA in mediating crucial physiological function in the brain, additional studies into the characterization of the PKA subunits expression profile and their activity in different areas of brain regions in healthy and as well as AD patients might possibly give insight in to the dynamic nature of mechanism(s) underlying the PKA disturbances as important neurobiological factors and may be relevant in therapeutic intervention.

A number of reports document the presence of PKs on the external side of the cellular membrane in a wide variety of cells. These kinases were shown to phosphorylate both extracellular (soluble) substrates and cell-surface proteins primarily on ecto-domains. On the basis of the localization and substrate specificity of these PKs, they might play a significant role in the regulation of cell–cell interactions, ligand binding and signal transduction (Redegeld et al., 1999). The existence of various types of cAMP-dependent (Behrens and Mazon, 1988; Kubler et al., 1989; Kubler et al., 1992; Shaltiel et al., 1993), and cAMP-

independent types (Kubler et al., 1983; Skubitz et al., 1991; Walter et al., 1994; Walter et al., 1996) of extracellular PKs have been reported. These extracellular PKs are either plasma membrane bound (ecto-PKs) or can be released from intact cells (exo-PKs) in a process termed as secretion/shedding to the extracellular milieu and act on the outer surface of cells (Ehrlich et al., 1986a; Tsuji et al., 1988; Muramoto et al., 1994; Kubler and Barnekow, 1986; Cho et al., 2000; Walter et al., 2000; Walter et al., 1994; Kubler et al., 1989; Kubler et al., 1992; Kubler et al., 1983; Paas and Fishelson, 1995). The analysis of extracellular PKs using intact cultured cells (HEK293, SH-SY5Y, Hela, H4 and Glial cells) showed the expression of Cα1 and Cβ2 catalytic subunits of PKA and is found to be shedded to the medium. The differential expression of catalytic subunits of PKA observed amongst the various cell types tested supports the evidence of cell specific expressions of PKA among neuronal and non-neuronal cells. The observed differences in PKA expression in different cell types could suggest the involvement of PKA in the regulation of distinct physiological processes (Nairn et al., 1985). This cell type specific expression of PKA could also be due to change in specific expression of R subunits of PKA as reported previously (Liang et al., 2007). Thus, one could speculate the capacity of extracellular PKA expression, stage of maturation and its shedding be cell type specific. Further detailed studies might provide valuable information on cell-type specific extracellular PKA expression, shedding and their physiological role.

The expression, activities and shedding of intracellular and as well as extracellular PKs are known to be modulated by activation of adenylyl cyclase by external stimuli (PDBu, forskolin), and also by using kinase specific substrates (phosvitin, casein and histone) (Kubler et al., 1983; Walter et al., 1996; Jordan and Kubler, 1992; Kondrashin et al., 1999). The modulation of adenylate cyclase by forskolin (PKA agonist), increases the intracellular cAMP level, thereby activating the intracellular as well as extracellular cAMP dependent PKA (Insel and Ostrom, 2003; Insel and Ostrom, 2003; Awad et al., 1983). The shedding of the endogenously expressed PKA into the conditioned medium appeared to be different amongst the cell type studied for the assay upon forskolin treatment. However, the forskolin treatment did not further stimulate the secretion/shedding of PKA, indicating that elevation of intracellular cAMP level after forskolin treatment does not stimulate either the expression or the shedding of extracellular PKA (Fig. 19). These results might also suggest the expression of only the specific catalytic subnits of PKA on cell surface and not the PKA holoenzyme. The current observations are consistent with the previous studies showing the shedding of PKA catalytic subunits to the extracellular milieu independent of cAMP (Kubler et al., 1983; Cho et al., 2000).

In vivo phosphorylation studies using intact cultured cells of HEK 293, SH-SY5Y and glial cells showed for the first time that Aβ can undergo phosphorylation by extracellular PKs. The degree of Aβ phosphorylation was different among the cultures employed in the assay further confirming the cell-type specific differential expression of extracellular PKs and their activity as discussed earlier. The intensity of Aβ phosphorylation was stronger in SH-SY5Y and glial cells as compared to HEK 293 cells indicating the significance of extracellular PKs in brain related cells and their critical role in extracellular protein phosphorylation events. The addition of extracellular cAMP did not alter the level of Aβ phosphorylation among the cell types employed in the assay (Fig. 20). This is consistent with the previous observations showing the selective secretion of PKA catalytic subunits on the cell surface which is not stimulated by extracellular cAMP addition as observed earlier. However, one cannot exclude the role of cAMP-independent kinases in phosphorylation of Aβ under the experimental paradigm. Overall, the results showed that Aβ can undergo phosphorylation by the extracellular PKs.

It has been shown that extracellular ATP affects a diverse range of physiological as well as pathophysiological processes in neuronal and non-neuronal cells (Gordon, 1986; Inoue et al., 2007; Hubschmann and Skladchikova, 2008; Nicholls, 2008; Paas et al., 1999). The potential role of extracellular ATP acting as a cofactor for the phosphorylation in different cell type has been described (Zhang et al., 1988; Koizumi et al., 2005). There are reports suggesting a role of surface protein phosphorylation of different extracellular proteins employing kinases and ATP which are present at the cell surface in regulation of the specific functions of developing and mature neurons (Ehrlich et al., 1986b; Ehrlich et al., 1990). Conclusive evidence has been presented previously for the existence of extracellular PKs activity on the external surface of neurons (Hogan et al., 1995). Phosphorylation of cell-surface proteins by cell surface kinases (Ecto or Exo PKs), using extracellular ATP as phosphate donor, is considered to play a role in many of the cellular response (Redegeld et al., 1999). Nevertheless, the extracellular phosphorylation of Aβ by neuronal cells has not been shown. The mouse primary neuronal cultures showed the PKA activity and cell surface localization. The activity of this extracellular kinase activity was shown to be altered by employing kinase modulators. The extracellular kinases could readily phosphorylate the exogenous Aβ. Phosphorylated Aβ was not detected in the corresponding cell lysates, suggesting that Aβ was not internalized and phosphorylated by intracellular kinases under the experimental conditions (Fig. 21). The biotinylation of cell surface localized PKA further confirmed that the observed PK activity of the primary neuronal cell cultures is by ectopically

expressed PKA (Fig. 22). The current findings were further substantiated by the differences in phosphorylation of Aβ by PKA modulators (selective PKA activator; cAMP and inhibitor; H-89) further confirming the bona fide ecto-PKA activity (Fig. 23).

The current study showed the extracellular PKA-like enzyme activity on the cell surface of neuronal and non-neuronal cells. This cell surface localized PKA was able to phosphorylate the extracellularly added Aβ. Despite the findings regarding the extracellular PKA activity, there are few open questions regarding the role of other cell surface localized kinases in Aβ phosphorylation and Aβ induced shedding of extracellular kinases. In addition to PKA, CK1/CK2 like kinases and tyrosine kinases have also been identified on the cell surface(Walter et al., 1994; Paas and Fishelson, 1995). *In silico* analysis predicted the occurrence of tyrosine in addition to serine residues as potential phosphorylation sites. *In vitro* phosphorylation studies indicated that Aβ can undergo phosphorylation by PKA, CK1 and CK2. Therefore, understanding the role of other ecto-kinases in phosphorylation of Aβ in addition to PKA may be enhanced by further studies using more specific kinase modulators. Addition of kinase specific substrates has been shown to influence the shedding of variety of membrane-bound kinases (Kubler et al., 1983). Hence, further investigations regarding the Aβ induced expression, activity and shedding of extracellular kinases and different phosphatases could be of pathophysiological relevance in AD.

5.3. Extracellular kinase activity in CSF and *ex vivo* phosphorylation of Aβ

CSF is a serum-like solution that bathes the brain. CSF is produced in the brain at an approximate rate of 500 ml per day in healthy adults, the total volume being about 135 ml. With a turnover time of about 6 hr, CSF is in constant flow within the brain ventricles and subarachnoid space of the brain and spinal cord, providing buoyancy and protection (Sickmann et al., 2002; Thompson and Keir, 1990). It carries nutrients for cells, removes products of their metabolism, and serves as a transport medium for hormones. CSF is known to contain protein and peptides which pass through the blood-brain barrier or are produced in the brain. As a direct recipient of cell-shedding products, it serves as a potential indicator of abnormal CNS states such as inflammation, infection, neurodegenerative processes (Zougman et al., 2008).

Ex vivo phosphorylation studies shows that CSF could serve as a medium for the phosphorylation of Aβ by externally added PKA, CK1 and CK2. The endogenous proteins of CSF were also found to undergo phosphorylation. The phosphorylation signals of endogenous proteins were observed to be varied indicating the presence of proteins with different kinase

specificity (Fig. 24). Phosphorylation studies using different PK substrates showed the phosphorylation of exogenously added kinase specific substrates (histone and phosvitin). As histone and phosvitin are known to be a substrate for PKA-like kinase and CK1/CK2-like kinase (Fig. 25), the observed results would indicate the occurrence of endogenous PKA and CK1/CK2-like activity in CSF from AD patients. In addition to phosphorylation of exogenously added histone and phosvitin, unknown endogenous proteins of CSF were found to undergo phosphorylation. The studies using histone and a selective PKA activator (cAMP) and inhibitor (H-89) further corroborate the fact that the observed endogenous PK activity was due to PKA-like kinases (Fig. 26). The addition of H-89 led to reduction in the phosphorylation of histone. However cAMP did not alter the phosphorylation activity, suggesting the selective shedding of catalytic subunits of PKA from the neuronal cells and its secretion to the CSF. Thus, addition of cAMP had no effect on the escalation of PKA activity. Further investigations indicated that endogenous PKA-like kinase of CSF could phosphorylate the externally added Aβ. The results indeed confirm that the observed endogenous PKA-like kinases activity of CSF was adequate to phosphorylate the externally added Aβ and phosphorylation was inhibited upon addition of PKA inhibitor (Fig. 27).

CSF has been the focus of interest in AD research during recent years. Published reports concentrated on discovering potential CSF biomarkers in neurodegenerative diseases (Blennow and Nellgard, 2004; Blennow, 2004; Puchades et al., 2003; Zhang et al., 2005; Abdi et al., 2006). Currently three biomarkers, total tau (T-tau), phospho-tau (P-tau), and the Aβ1-42, have been evaluated. Recent studies have reported that several components of the signal transduction pathways including adenylate cyclase, phosphoinositides and protein kinase C, are altered in AD brain (Pascale et al., 2007; Yamazaki and Saitoe, 2008). The metabolites from various brain regions are known to be secreted into the interstitial space and passed to the CSF. CSF has been shown to contain variety of proteins/peptides that are synthesized in the brain (Zougman et al., 2008). Despite the critical role of phosphorylation in brain, analysis of the CSF for occurrences of kinases if any and their activity has not been carried out. In support to the present findings, additional detailed phosphoproteome analysis of CSF could possibly indicate the alteration of phosphorylation events in AD pathogenesis such as extracellular kinase/phosphatase activity, toxic phosphoproteins and peptides (including phosphorylated Aβ) and thus serve as additional biomarkers of AD.

To summarize, the undertaken study confirms the occurrence of endogenous PKA-like activity in CSF from AD patients and it could phosphorylate the exogenously added Aβ. These findings could substantiate the expression of various ecto-PKs in neuronal cells and

their activity at the extracellular environment of the brain (since they could be possibly secreted in to the CSF). Thus, overall, the components necessary for phosphorylation reaction such as ATP, Aβ and PKs are found to exist extracellulary in the human brain. Therefore, one could speculate the phosphorylation of Aβ is biochemically feasible, and extracellular phosphorylation of Aβ might affect the functional property of Aβ, which presumably plays a key role in pathogenesis of AD.

5.4. Effect of phosphorylation on Aβ conformation and aggregation

Conformational alteration of proteins/peptides characterized by misfolding, leads to self-assembled fibrillar inclusions or aggregates (Dobson, 1999; Rochet and Lansbury, Jr., 2000; Carrell and Gooptu, 1998; Ross and Poirier, 2004; Selkoe, 2003). The conformational transition can be triggered by mutations as well as by changes of the environmental conditions such as pH, ionic strength, metal ions, protein concentration, oxidative stress, or a small quantity of misfolded protein fragments. Numerous studies have documented all the above mentioned conditions that are shown to affect the folding of Aβ, which results in the formation of soluble and fibrillar neurotoxic aggregates rich in β-sheet structures (Tew et al., 2008; Janek et al., 1999; Herczenik and Gebbink, 2008; Finder and Glockshuber, 2007). The posttranslational modifications are known to contribute to conformational transition and protein misfolding (Rochet, 2007). Covalent modification of proteins such as oxidative modification of α-Synuclein via dopamine adducts (Conway et al., 2001), nitration of α-Synuclein (Giasson et al., 2000), ubiquitin-like modifier SUMO in huntingtin protein (Steffan et al., 2004) has shown to facilitate protein misfolding and initiate aggregation (Ross and Poirier, 2004). Phosphorylation is also an important posttranslational modification promoting protein misfolding leading to aggregates formation that are associated with pathogenesis (Schvartz et al., 2002). For e.g., α-Synuclein purified from Lewy bodies is extensively phosphorylated and phosphorylation modulate its interaction with other proteins and leads to formation of inclusions (Iwatsubo, 2003; Okochi et al., 2000). Phosphorylation is reported to be involved in aggregation of ataxin-1 and ataxin-3. Phosphorylation of ataxin-1 markedly increased inclusion body formation *in vivo* (Emamian et al., 2003; Tao et al., 2008). Phosphorylation is known to be implicated in AD, hyperphosphorylation of tau by kinases leads to the formation of neurofibrillary tangles (NFTs) and accelerates tau-induced neurodegeneration. Thus, a huge variety of factors and examples on the crucial role of different posttranslational modifications of variety of proteins, thereby influencing the destabilization of their native conformation and thus leading to aggregation.

A CD spectroscopy study indicates the effect of phosphorylation on conformational transition of Aβ. The CD spectrum of npAβ and pAβ(pSer-8) peptide samples at the start of incubation time (0 hr) revealed the characteristic features of a mostly random coil state indicating the unfolded peptide structure. The increase in incubation time resulted in significant change in the CD spectrum on going from a α-helical state to a β-sheet structure (2 hr and 8 hr). Notably, the α-to-β conformational transition was found to be faster with pAβ(pSer-8) peptide (Fig. 28). CD has been previously applied by several researchers to study secondary structure transitions or to define the conformational states of Aβ40/42 aggregates (Barrow and Zagorski, 1991; Otvos, Jr. et al., 1993; Tomaselli et al., 2006; Fabian et al., 1993). Structural transition from random coil or α-helical structures to β-sheet structures have been observed in amyloid fibrils from protein aggregates such as Aβ, poly-glutamine repeats, Huntington protein, lysozyme, prion proteins, and transthyretin repeats (Armen et al., 2004). The thermal denaturation CD spectroscopy studies showed that phosphorylation induced conformation can be easily shifted towards a α-helix or β-sheet by changing the temperature. Phosphorylation induced β-sheet conformation was observed to be very stable at extended temperature, and remarkably the phosphorylation induced α-to-β transition was reversible upon decreasing the incubation temperature (Fig. 29). The significance of conformational transition of the Aβ42 secondary structure from soluble unordered/α-helix to β-sheet rich conformers in conformational seeding and self-aggregation has been shown (Walsh et al., 1997; Walsh et al., 1999; Kirkitadze et al., 2001; Tomaselli et al., 2006; Bartolini et al., 2007). Even, some FAD causing mutations such as Flemish, Arctic, Dutch, Italian and Iowa are known to affect the conformational transition (D'Ursi et al., 2004; Murakami et al., 2002). The critical role of conformational diversity has been described for β2-microglobulin (Yamaguchi et al., 2005), prion protein (Bessen et al., 1995), tau (Frost et al., 2009) and for Aβ (Petkova et al., 2005). The flexibility of the phosphorylation induced β-sheet conformational transition might result in faster folding and unfolding of Aβ and this can result in generation of several possible soluble Aβ aggregates like the reversible nature of the toxic conformers as observed in AD (Walsh et al., 2005; Demuro et al., 2005; Lambert et al., 1998). Together, the CD results indicate an effect of phosphorylation on the structural transition from the unordered/α-helical structure to the β-sheet rich conformation. Thus, phosphorylation increases the propensity of Aβ to adopt a β-sheet conformation. This could represent the initial step of an aggregation process that can lead to toxic oligomers and fibrils formation.

Growing evidence implicates Aβ oligomerization and fibrillization in the etiology of AD. Aggregation process is thought to be initiated by protein segments with hydrophobic

amino acid residues, β-sheet predisposition, and low net charge (Linding et al., 2004; Schmittschmitt and Scholtz, 2003). Conclusive evidences are reported regarding the critical role of certain factors such as pH or temperature change, mechanical stress, glycation, oxidation and mutations in the protein which are known to affect the β-sheet conformation and modulating the aggregation of Aβ (Murakami et al., 2002; Kirkitadze et al., 2001). The structural studies on Aβ peptides suggested that a conformational transition from unordered or α-helix structure to a β-sheet rich conformation is the key to forming fibrils and inducing cytotoxic effects (Serpell, 2000). Enrichment of β-sheet structures could promote the self-assembly of β-sheet domains resulting in the formation of pathogenic, fibrillar protein aggregates (Janek et al., 1999). CR dye binding and ThT fluorescence assay assessed the predisposition of β-sheet structures due to phosphorylation. CR assay indicated the phosphorylation dependent formation of β-sheet structures. Specific binding of CR to β-sheet structures alters the absorbance spectrum (Klunk et al., 1999). The assay showed that the amount of CR dye binding was significantly higher with pAβ(pSer-8) peptide as compared to npAβ, confirming the fact that phosphorylation induces β-sheet structure formation. The phosphorylation induced effect on Aβ fibrillization was monitored by ThT fluorescence assay. ThT fluorescence is a commonly used method to monitor the Aβ fibril formation (Khurana et al., 2005). This method is particularly attractive since ThT fluoresces only when the dye binds to fibrils and more importantly ThT does not interfere with aggregation of Aβ fibrils (Ban et al., 2003). The real-time ThT fluorescence assay showed an increased fluorescence signal with pAβ(pSer-8) as compared to npAβ indicating the higher fibrillar content with pAβ(pSer-8). Immunoblot analysis of the CR and ThT assay samples indicated that the formation of low (i.e., dimers, trimers) and high M.W. aggregates/oligomers was more rapid with pAβ(pSer-8) as compared to npAβ peptide (Fig. 31 & 32). In contrast, the pAβ(pSer-26) peptide showed a faster formation of low M.W. oligomers (dimers and trimers), however larger assemblies were not observed. It is intriguing to note that although pAβ(pSer-26) showed a low CR binding value and ThT fluorescence values, immunoblot analysis showed faster formation of lower oligomers. This can be attributed to phosphorylation induced hydrophobic interaction, thereby stabilizing the lower oligomeric assemblies and reducing the formation of fibrils. Ser-26 residue is reported to be located in the β-turn of the Aβ peptide and phosphorylation of this residue might result in β-sheet independent conformation which favors the Aβ oligomerization (Luhrs et al., 2005). Current result supports the recent observation of the critical role of Ser-26 in the formation of a turn structure of Aβ and the role of turns in nucleating monomer folding and mediating oligomerization (Shankar et al., 2008; Teplow et

al., 2006). A recent finding reports the role of FAD causing mutations in this turn region altering the stability of the monomer folding nucleus and destabilization of the Aβ folding and resistant to proteolysis (Grant et al., 2007). The current findings indicate the effect of phosphorylation promoting Aβ aggregation (oligomer and fibril formation). Interestingly, phosphorylations at different sites show a variation in the oligomer and aggregates stability indicating the difference in conformation. Thus altered conformation induced by the phosphorylation of Aβ clearly had an effect on its ability to bind the dyes CR and ThT.

During Aβ oligomerization, self-association of monomeric Aβ is necessary to produce a mixture of metastable, noncovalently associated soluble oligomeric assemblies that eventually form fibrils. Recent reports have shown that soluble oligomeric Aβ assembly intermediates are potent neurotoxins, and these intermediates may be the key effectors of neurotoxicity in AD (Klein et al., 2001). Soluble Aβ oligomers extracted from Alzheimer's disease patient brains as well as from CSF are known to potently impair synapse structure and function (Gong et al., 2003; Kayed et al., 2003; Lacor et al., 2004). The ^{1}H-NMR spectroscopy indicated the rapid loss of signal intensity with pAβ(pSer-8) as compared to npAβ, indicating that signal loss is the result of rapid association of monomeric pAβ(pSer-8) in the course of oligomerization (Fig. 37). TEM images indicated the presence of small oligomers as well as protofibrils during the course of aggregation (Fig. 35). The TEM studies showed that phosphorylation indeed accelerated the formation of aggregates which was evident from the observation of rapid formation of high M.W. oligomers, and small protofibrillar aggregates in pAβ (pSer-8) samples as compared to npAβ. This observation was further corroborated by DLS studies. DLS showed the heterogeneity of the soluble Aβ oligomers and protofibrillar structures formed during the process of aggregation. The transformation of the monomeric Aβ form into protofibrils is accompanied by an increase in the apparent R_H of the different Aβ aggregates. The increase in R_H is accompanied by an increase in the oligomerization. The distribution and the size of different soluble oligomers in the population were changed with time. The observed change was significantly different upon phosphorylation. It was evident by the rapid disappearance of a peak corresponding to monomeric Aβ and appearance of soluble oligomeric peak with pAβ(pSer-8). The size of the aggregates measured were concordant with existing DLS data of monomeric and oligomeric intermediates during Aβ aggregation (Walsh et al., 1997; Tomski and Murphy, 1992; Lomakin et al., 1996; Chen et al., 2006; Bitan et al., 2003; Nichols et al., 2002). The appearance of assembled forms of soluble oligomeric Aβ species in the course of aggregation was shown by dot blotting analysis. In npAβ, oligomers begin to appear at 10 hours of incubation and

increased until 16 hours. Whereas in pAβ(pSer-8) samples, oligomers appeared already at 6 hours of incubation time and increased with longer incubations (until 16 hours). The rate and absolute amount of soluble oligomer formation was accelerated with pAβ(pSer-8) as compared to npAβ (Fig. 39). These results confirm that the phosphorylation induces oligomerization and thus results in the quick shifts in the molecular size of the aggregates that were clearly observed during early phases of aggregation. An increasing body of evidence arising in recognition of the biological importance of small misfolded assemblies and identifying and characterizing these intermediates is central to understanding the mechanism of fibril assembly and toxicity in AD (Cardinale and Biocca, 2008). Recent evidence suggests that soluble oligomers of Aβ, rather than amyloid fibrils, play a crucial role in synaptic and cognitive dysfunction in the early stages of AD. In recent years, the structures of amyloid intermediates have attracted broad attention as potential therapeutic targets, particularly at early stages of AD. Thus one can suggest that phosphorylation of Aβ could cause dementia by enhanced formation of toxic soluble Aβ oligomers. Therefore, further investigation on phosphorylation induced Aβ intermediate structures could provide insights into the molecular mechanisms of phosphorylation induced aggregation and production of toxic intermediate species.

Extensive studies have been carried out in examining the effect of FAD causing mutations (Liu et al., 2004; Soto et al., 1996; Soto and Castano, 1996; Lin et al., 2003; Ban et al., 2004), various modifications (Schilling et al., 2006; Johansson et al., 2007; Hou et al., 2004), and substitutions of different charged groups on conformational transition of Aβ (Williams et al., 2004; Morimoto et al., 2004; Wetzel et al., 2007; Williams et al., 2006; Wurth et al., 2006; Kim and Hecht, 2006; Kim and Hecht, 2005; Shanmugam et al., 2005; Kaneko et al., 2001). These studies show that any disturbance of structural properties of the Aβ is very likely to be the cause for aggregation. In support, significance of hydrophobic and electrostatic interactions is considered to be crucial in amyloid aggregation (Hilbich et al., 1991; Hilbich et al., 1992; Harper et al., 1999; Halverson et al., 1990). Protein phosphorylation has been shown to promote conformational changes that may be local to, or more remote from, the site of phosphorylation and thus could result in changes in secondary conformation (Tholey et al., 1999). These changes can influence the surface properties of the protein, thus affecting self-association (aggregation) of peptides/proteins (Johnson and Barford, 1993; Sprang et al., 1988; Barford and Johnson, 1989; Barford and Johnson, 1992; Barford et al., 1991). The physical changes introduced by covalently bound phosphoryl group are obvious and could lead to alteration of steric characteristics, charge and the ability to form

hydrogen bonds (Hurley et al., 1990; Johnson and Barford, 1994; Johnson, 1994). Recent reports showed the effect of charge by SDS, Cu^{2+} and Ca^{2+} in modulating the Aβ1-40/42 folding (Tew et al., 2008; Bush, 2003; Isaacs et al., 2006). The phosphorylation of serine introduces a negatively charged phosphate moiety and results in a structural change of Aβ peptide leading to aggregation.

The present study shows the phosphorylation of serine in facilitating the transition from unordered or α-helical to β-sheet structures. Ser-8 is located within the N-terminal side of the Aβ peptide which forms α-helical structure, while the Ser-26 is located in C-terminal part of the Aβ peptide which forms β-turn. Residues 25–29 contain a bend of the peptide backbone that brings the two β-sheets in contact through side chain-side chain interactions (Petkova et al., 2002). Previous studies only highlighted the crucial role of amino acid substitutions in C-terminal region of Aβ in aggregation. However, recently FAD mutations such as English, Tottori and a recessive mutation have been identified in the N-terminal region of the Aβ which could affect the aggregation of Aβ (Hori et al., 2007; Di et al., 2009). In support, the N-terminal region (1–28) of Aβ is reported to be involved in aggregation (Solomon et al., 1997), and the 3–6 sequential epitope EFRH of Aβ is reported to be particularly important (Frenkel et al., 1999; Frenkel et al., 2000b; Frenkel et al., 2000a). Monoclonal antibody 3D6 directed to the 1–5 sequence is shown to prevent the aggregation of Aβ *in vitro* (Solomon et al., 1997). Thus recent reports highlighting the importance of N-terminal residues and their modifications in Aβ aggregation. Passive immunization with 3D6 antibody prevented amyloidosis and vascular amyloid formation in *tg* mice further supporting the critical role of N-terminal region of Aβ in aggregation (Schroeter et al., 2008; Seubert et al., 2008; Bard et al., 2000).

The earliest step of aggregation is described as a conformational change leading to different possibilities of polypeptide self-association (Gsponer and Caflisch, 2002; Pellarin and Caflisch, 2006). This initial ensemble of aggregates is highly dynamic and aggregates are able to dissociate, reassociate and interconvert (Carulla et al., 2005; Cerda-Costa et al., 2007). Once the different Aβ conformers are formed and associated in one or the other pathway they will be further stabilized upon fibril polymerization or Aβ globulomer maturation. The current study shows the effect of phosphorylation in promoting β-sheet structure driven conformational transition. Depending upon the phosphorylation of serine either at the N-terminal (Ser-8) or at C-terminal (Ser-26) of Aβ peptide serves as a decisive conformational switch for either fibril formation or alternatively to Aβ globulomer formation (Fig. 51).

Altogether, the results indicate that phosphorylation of Aβ results in alteration of conformation and this in turn hastens the Aβ aggregation.

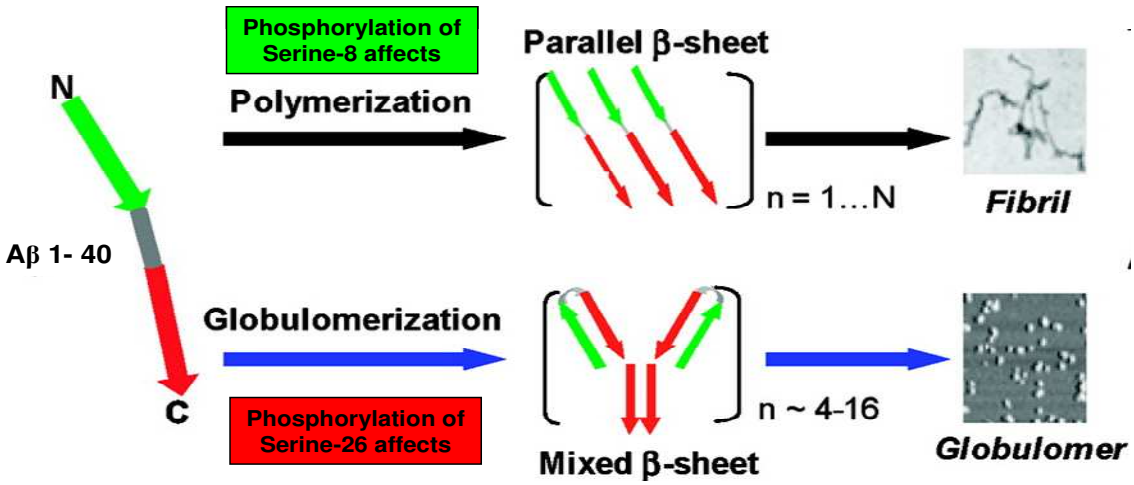

Fig. 51: Schematic drawing of effect of phosphorylation on Aβ aggregation.
The phosphorylation of Ser-8 residue may induce polymerization and formation parallel β-sheet resulting in generation of amyloid fibrils, whereas phosphorylation of Ser-26 residue can induce globulomerization and formation of mixed β-sheet globular aggregates. Modified from (Yu et al., 2009).

AD is a heterogeneous neurodegenerative disorder. Whereas only a minority is due to genetic abnormalities and mostly with early onset, the majority of all Alzheimer cases is sporadic and with late onset. Hence, in recent years the role of Aβ as a causative factor of sporadic AD is challenged. Therefore, in the sporadic AD, age-related disturbances in cellular metabolism or factors such as alteration of kinases or phosphatases expression, down regulation of neuropeptidase expression, variety of posttranslational modifications of Aβ may come into focus leading to Aβ misfolding and aggregation. From the current study, one can hypothesize that phosphorylation of Aβ results in conformational transition thus leading to rapid transition of non-aggregating structure to aggregation prone structures which serve as nuclei and accelerate the aggregation (Fig. 52). The current hypothesis is further supported by the aggregation kinetic analysis of npAβ (wildtype Aβ) and pAβ. The analysis of aggregation kinetics revealed a prominent difference in the duration of the lag phases, pAβ took 15 min whereas npAβ took 90 min and took about five times longer to exit the lag phase (Fig. 34 and Table 5). Altogether, these data suggest that the higher rate of aggregation for pAβ(pSer-8) is predominantly caused by a more efficient nucleation stage during which a higher number of small aggregates are formed.

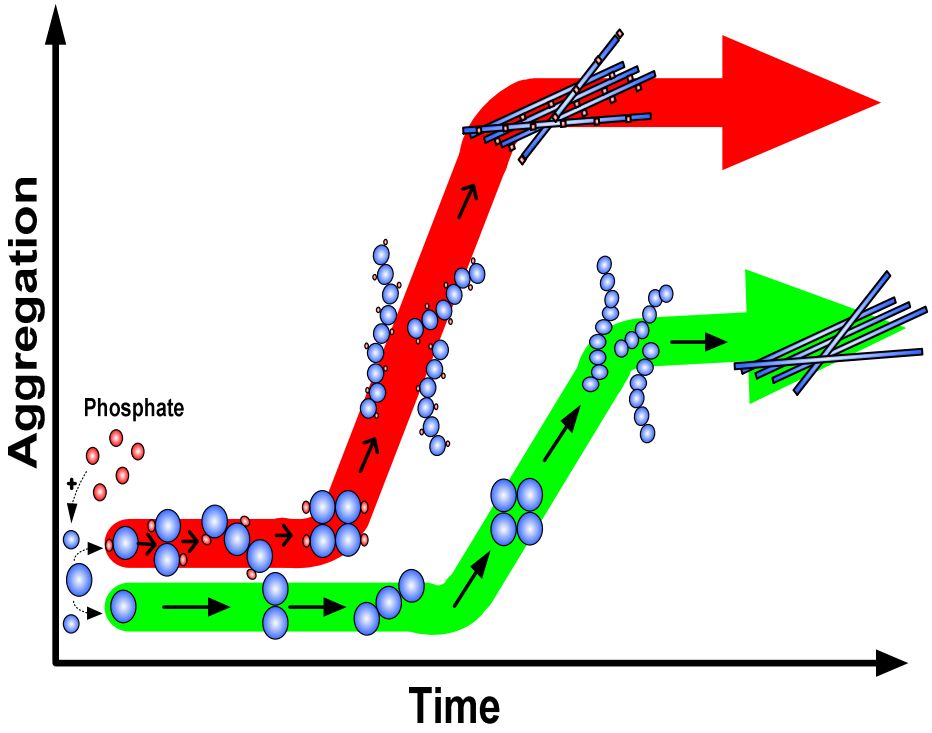

Fig. 52: The effect of phosphorylation on amyloidogenesis.
The kinetics of the amyloid assembly process of npAβ is depicted as a sigmoid curve to reflect the three distinct phases characterizing the fibril formation pathway (green curve). A lag phase with low molecular weight oligomer formation (dimer and trimer), an exponential phase with a rapid increase in high molecular weight oligomers (globular oligomer and protofibrils) and a prevailing plateau phase (mature fibrils). When npAβ can undergo phosphorylation, phosphorylation induces structural change thus in faster formation of low and high molecular weight oligomers. Oligomers serve as a nuclei and ensemble into various assemblies leading to accelerated Aβ aggregation (red curve). The reduction of lag phase as well as rate of aggregation can be clearly evident upon phosphorylation.

During aggregation, proteins can obtain a range of different structural appearances, which are generally enriched in cross-β sheet structure, including intermediates varying from unordered amorphous aggregates to ordered fibrils. According to the ‘‘nucleated conformational conversion’’ (NCC) model for aggregate formation (Serio et al., 2000), a group of monomers initially present in solution coalesces to form ‘‘molten’’ oligomers, which can propagate the aggregation process as observed in prion protein and eventually give rise to more highly organized oligomers and fibrils rich in β-sheet structure. In agreement with this hypothesis, the aggregates of pAβ(pSer-8) were capable of seeding npAβ aggregation *in vitro* much faster than npAβ aggregates clearly showing the significance of phosphorylation induced β-sheet rich oligomers in promoting aggregation. The current finding demonstrate that phosphorylation of Aβ promotes the nucleation of Aβ and the formation of oligomers by increasing the propensity to adopt β-sheet conformation. Thus, phosphorylated variants of Aβ could trigger oligomer formation and deposition of Aβ in sporadic AD cases.

Models representing several possible structures of aggregated forms have been proposed very recently. At the moment, attempts to identify regions of peptide or the conditions, prompted by surrounding medium which drive conformational transitions still represents a promising approach in understanding the molecular basis of AD. In addition, the structural characterization of a partially folded intermediate in the α-to-β transition and vice versa, opens many perspectives for the design of molecules that could able to interfere with the aggregation process. Therefore, further detailed investigations on phosphorylation induced structural transition might give more insight into the pathophysiological role of phosphorylation and even suggest the possible role of phosphorylation induced β conformation seeding in sporadic AD.

5.5. Detection of pAβ *in vivo* in *tg* mouse and human AD brain

To assess the phosphorylation of Aβ *in vivo*, phosphorylation state-specific antibodies against pAβ(pSer-8) was generated. The antibody characterization studies indicated that antibody SA5434 was found to be highly specific for Aβ phosphorylated at Ser-8 (pAβ(pSer-8)). In addition, several commercially available monoclonal antibodies showed their reactivity to pAβ(pSer-8) and non-phosphorylated Aβ (npAβ). The antibody 82E1 detected both the peptides, whereas the antibody 6E10 was found to be highly specific for npAβ (Fig. 41). The 82E1 antibody specifically reacts with the human Aβ N-terminal end (neo-epitope specific) (Horikoshi et al., 2004), whereas 6E10 antibody recognizes an epitope between amino acids 4-12 of the human Aβ domain that contains the identified phosphorylation site (Kim et al., 1988). Further evaluation of these antibodies using npAβ and pAβ aggregates indicated their specificities to soluble low M.W. and high M.W. oligomers. Notably, the SA5434 recognized oligomeric Aβ depending on the phosphorylation state (Fig. 42), and not on the specific misfolded conformations that are generally recognized by conformation-dependent antibodies (Kayed et al., 2003; Kayed et al., 2007; Kayed and Glabe, 2006).

During the past decade, various lines of transgenic mice have been generated to mimic, at least in part, some of the pathological lesions in AD. There are multiple transgenic mice lines that show Aβ deposits and neuritic plaques (Gotz et al., 2004a; Gotz et al., 2004b; Oddo et al., 2003a; Oddo et al., 2003b; Suh and Checler, 2002). To demonstrate the occurrence of pAβ deposits *in vivo*, the APPswe/PS1ΔE9 double transgenic (*tg*) mice that co-express FAD mutant human PS1-ΔE9 and a chimeric mouse-human APP695 harboring a human Aβ domain and mutations (K595N, M596L) linked to Swedish FAD pedigrees (APPswe) was used (Jankowsky et al., 2001). This transgenic mouse is a well accepted

model, as the development of Aβ amyloidosis is observed to be similar to that seen in AD and is characterized by age-associated acceleration of Aβ plaque deposition, gliosis and neuritic pathology in the hippocampus as well as in the cerebral cortex (Lazarov et al., 2002).

The immunohistological studies using *tg* mouse brain sections with pAβ antibody (SA5434) indicated the strong labeling of pAβ amyloid deposits in the hippocampal region of nine-month-old animal's brain. Most deposits also contained npAβ as indicated by the co-staining with antibody 6E10. In individual plaques, however, a more pronounced reactivity of SA5434 in the core was evident, suggesting preferential deposition of pAβ (Fig. 43). Further age-dependent analyses showed the pAβ seeded nucleation-dependent oligomerization. The deposits containing pAβ and npAβ were already detectable in the cortices of 2 months old mice (2m), a very early stage of plaque formation. The detection of very small deposits that were selectively detected with the SA5434 at this early age suggests the likelihood of plaques with pAβ as seeding agents for the amyloidogenesis. The Aβ deposition was observed to be strongly increased with the age of these mice (2m, 6m, 12m and 18m) and a large overlap of stainings with antibodies SA5434 and 6E10 was found, indicating co-deposition of pAβ together with npAβ in extracellular plaques (Fig. 44). The pAβ appeared to be concentrated toward the centre of individual plaques which are similar in morphology to compact plaques and characteristics of CR staining (Dickey et al., 2005). Compact Aβ plaques are shown to be positive for CR and ThT dyes and are known to be rich in fibrillar β-pleated sheet conformation of Aβ, and these extracellular compact plaques were found to induce neuritic changes and neuronal loss (Armstrong, 1998). *In vivo* imaging in transgenic models have shown the neuritic dystrophy and distortion in direct apposition with fibrillar deposits of compact plaques (Spires et al., 2005; Tsai et al., 2004), which cause alterations in neocortical synaptic responses (Stern et al., 2004). Altogether, immunohistological analysis of brain sections of *tg* mice indicated the pAβ deposits in the hippocampus as well as in the cerebral cortex which were readily stained with SA5434. Early onset/appearance of pAβ deposition in the cortex was observed already at the age of 2 months and was strongly increased with the age of these mice.

The observations of age-dependent deposition of pAβ in the brains of *tg* mice was further substantiated with biochemical detection of both pAβ and npAβ in the brain extract from *tg* mice by immunoblot analysis. Consistent with the immunohistochemical data, both pAβ and npAβ were strongly increased with age. Importantly, SA5434 showed strong reactivity to high M.W. oligomeric assemblies of Aβ in brain extracts. These oligomeric species were already detected in two-month old mice and became prominent at six-months. At

this age, SA5434 detected very little monomeric Aβ. In contrast, npAβ which was detected with 6E10 antibody was observed in six-month old mice and they increased further with age. As compared to antibody SA5434, the reactivity of antibody 6E10 with oligomeric Aβ assemblies was much weaker and was mainly detected in 12 and 18 months old animals. Oligomeric assemblies of Aβ have been isolated from young *tg* mice (Cheng et al., 2007; Lesne et al., 2006; Oddo et al., 2006). These soluble Aβ aggregates have been implicated in the rapid interference of memory of learned behaviors inhibiting LTP (Cleary et al., 2005). The soluble Aβ exhibit potent toxic effects capable of inducing neuronal cell death in hippocampal slices (Lambert et al., 1998), and also induces ectopic neuronal cell cycle events (Varvel et al., 2008; Yang et al., 2006). In summary, the specific detection of pAβ high M.W. oligomers in mouse brain indicates an enrichment of pAβ in oligomeric assemblies and suggests that phosphorylation could increase oligomerization of Aβ and could become potentially toxic (Fig. 45).

In support to the above, the quantitative analysis of pAβ in mouse brain extract revealed that about 20-25% of extracted monomeric Aβ in 18 months old tg mice was in a phosphorylated state (Fig. 46). This was further supported by the detection of pAβ using phosphorylation-sensitive monoclonal antibody 6E10 after dephosphorylation. Notably, the relative reactivity of monomeric Aβ with antibody 6E10 was markedly increased after dephosphorylation with alkaline phosphatase, also indicating that about 30% of monomeric Aβ is in a phosphorylated state *in vivo* (Fig. 47). Biochemical analysis of the Aβ isolated from AD brain indicates that Aβ1-42 is the principal species associated with senile plaques and accumulates in neurons of AD brain. Expression of FAD mutations in APP or PS has been shown to increase the levels of Aβ1-42 production and results in increased levels of the Aβ oligomers, further supporting its pathological relevance (Suzuki et al., 1994; Xia et al., 1997). Although the relative amount of Aβ1-42 expression is 10% as compared to 90% of Aβ1-40 in the human brain, Aβ1-42 is known to be enriched in neuritic plaques, rich in β-sheet conformers, appears to seed further amyloid deposition, and seems to be toxic *in vitro* and *in vivo* (Garzon-Rodriguez et al., 1997; Iwatsubo et al., 1996; Lambert et al., 1998; Nagele et al., 2002). Thus, robust association of Aβ1-42 with FAD even argues strongly in favor of a causative role for Aβ1-42 in the etiology of AD. Altogether, from the current immunohistochemical and quantitative analysis of pAβ in *tg* mice, one could consider the role of phosphorylation and pAβ seeded oligomerization, toxicity and neurodegeneration. The recent observation on the rapid appearance of amyloid plaques within brains of *tg* mice might hint the possibility and role of phosphorylation dependent Aβ misfolding and seeded growth

in vivo (Meyer-Luehmann et al., 2008). Further studies employing other *tg* mouse models to show the occurrence of pAβ might support and validate the current findings regarding the crucial role of pAβ in Aβ aggregation *in vivo*.

In recent years, various mechanisms have been proposed which could contribute to the pathogenesis of AD. However, cerebral β-amyloid deposition and related toxicity effect is considered to be one of the key mechanism in the development of AD, which results in neurodegeneration, plaque induced neurite abnormalities and disturbing the synaptic plasticity (Braak and Braak, 1991; Knowles et al., 1998; Knowles et al., 1999; Mirra et al., 1991; Selkoe, 2008; Vickers et al., 2000). Previous studies have reported that various posttranslational modifications of Aβ that takes place in the human brain and it contributes to the development of AD (Atwood et al., 2002; Piccini et al., 2005; Saido et al., 1995; Saido et al., 1996; Saido, 1998; Schilling et al., 2008; Zhang et al., 2004). Such post-translationally modified Aβ peptides have also been identified in the CSF and plasma of individuals (Bahl et al., 2008; Bibl et al., 2006; Vanderstichele et al., 2005). Immunohistochemical studies using SA5434 indicated the occurrence of different isoforms of pAβ plaques in the hippocampus and entorhinal cortex regions in brain sections from AD patients. However, majority of the identified plaques were observed to be dense-cored in morphology. A range of hypotheses have been proposed which are based on the presence of different morphological isoforms of Aβ plaques (diffuse, dense-cored and fibrillar) and their toxicological properties in the development of AD (Armstrong, 1998; Dickson and Vickers, 2001). Antibody SA5434 readily detected pAβ in senile plaques in the human brain. Importantly, strong reactivity with SA5434 was observed in the core of neuritic plaques. Numerous reports indicated the critical role of senile plaques in neurodegeneration in AD (Braak et al., 1993; Cruz et al., 1997; Dickson and Vickers, 2001). Senile plaques are known to be composed mainly of Aβ peptide in its fibrillar form and triggers a variety of pathological changes including tau hyperphosphorylation, leading to neuronal dysfunction and degeneration contributing to cognitive dysfunction (Duyckaerts et al., 2008; Nakada et al., 2008; Spires-Jones et al., 2009). Immunohistochemical stainings from AD human brain demonstrates that pAβ is highly enriched in the amyloid core and these pAβ-positive plaques may cause neurodegeneration of plaque-associated neurites in the human brain. In addition, the deposition of the pAβ within cerebral blood vessel walls was observed similar to cerebral amyloid angiopathy (CAA) (Fig. 48). CAA is accepted as an early and integral part of AD pathogenesis. Rare forms of hereditary cerebral amyloidosis caused by mutations within the Aβ domain have been

identified, where mutant Aβ preferably deposits in vessels (Dickson and Vickers, 2001; Kumar-Singh, 2008; Thal et al., 2008; Wegiel et al., 2001).

The Aβ is known to activate a variety of cells including microglia (D'Andrea et al., 2004), and astrocytes in the brains to produce cytokines and neurotoxins (Nagele et al., 2004), hence promoting neurodegeneration (Coraci et al., 2002; El Khoury et al., 2003; El et al., 1996; El and Luster, 2008; Meda et al., 1995). Microglial cells surround aggregated Aβ are known to restrict senile plaques formation by phagocytosing Aβ (Simard et al., 2006), and are believed to play a role in AD pathogenesis (Streit, 2004; Streit et al., 2004). In the brains of AD patients, senile plaques are known to trigger increased level of pro-inflammatory factors (cytokines and chemokines) and the activation of the complement cascade which are known to contribute to the local inflammatory response. (Farfara et al., 2008). It was imperative to continue to monitor any possible association of pAβ positive senile plaques with microglia or to astrocytes (Fig. 49). The immunohistochemical stainings of human AD brain indicated the association of inflammatory responsible microglia and GFAP-positive astrocytes clustering around pAβ deposits. In human AD brain, microglia and astrocytes accumulation with senile plaques is an integral part of the disease processes. The present observation might suggest the additional role of pAβ in the pathogenesis of AD such as neuroinflammation in addition to seeded aggregation. It is also possible that small soluble pAβ aggregates may trigger local activation of glial cells as suggested by a recent study of the young APP *tg* mice that has not yet developed Aβ deposits (Heneka et al., 2005). These results suggest that pAβ oligomers could initiate the activation of microglia, astrocytes and subsequent release of proinflammatory molecules in the AD brain which can lead to neuroinflammation.

Senile or neuritic plaques are known to damage the surrounding tissue physically and lead to neurofibrillar pathology and are found to be associated with abnormal neuronal processes known as dystrophic neurites in human AD brain (Cruz et al., 1997; Vickers et al., 2000). These dystrophic neurites, in addition to neurofibrillary tangles (NFT) and neuropil threads has been proposed to consist of abnormal filamentous structures derived from a transformation of normal cytoskeletal proteins (Masliah et al., 1993; Su et al., 1996; Vickers et al., 1994; Vickers et al., 2000). The double-label immunofluorescence photomicrographs showed a widespread neuronal degeneration and pAβ reactive plaques. Antibody SA5434 readily detected pAβ in senile plaques and strong reactivity was observed in the core of neuritic plaques; while antibody 22C11 against the extracellular domain of APP selectively detected dystrophic neurites in close proximity to the amyloid core of the neuritic plaques (Fig. 50). These studies confirmed the occurrence of pAβ reactive senile neuritic plaques that

causes a physical damage resulting in ring and bulb-like accumulations of neurofilaments (Vickers, 1997).

In summary, the pAβ exists *in vivo* and is found in extracellular plaques and in vessels in *tg* mouse brain as well as in human AD brain. pAβ is found to be present at a very early age in *tg* mice and appears to be enriched in oligomeric and aggregated forms. Furthermore, pAβ also occurs in senile plaques of *tg* mice and recent studies have shown that such Aβ deposits induce dendritic and plaque-associated neuritic degeneration (Spires et al., 2005; Tsai et al., 2004). The importance of the present finding is further supported by the detection of pAβ in neuritic plaques of AD patients which highlight the critical role of pAβ in AD-related neurodegeneration (Braak and Braak, 1991; Mirra et al., 1991). From these findings, one can speculate that pAβ might acts as a seed and trigger aggregation. In agreement with this hypothesis, the aggregates of pAβ were capable of seeding npAβ aggregation *in vitro* much faster than aggregates of npAβ. These data suggest that AD pathogenesis in sporadic cases may be influenced by extracellular phosphorylation of Aβ which modulate the Aβ aggregation leading to assembly of the Aβ into soluble oligomers and insoluble β-sheet rich Aβ fibrillar aggregates and their subsequent accumulation in affected neurons, eventually resulting in neurodegeneration. From the current findings, one can hypothesize that phosphorylated variants of Aβ could trigger oligomer formation and deposition of Aβ in the pathogenesis of sporadic AD (Fig. 53).

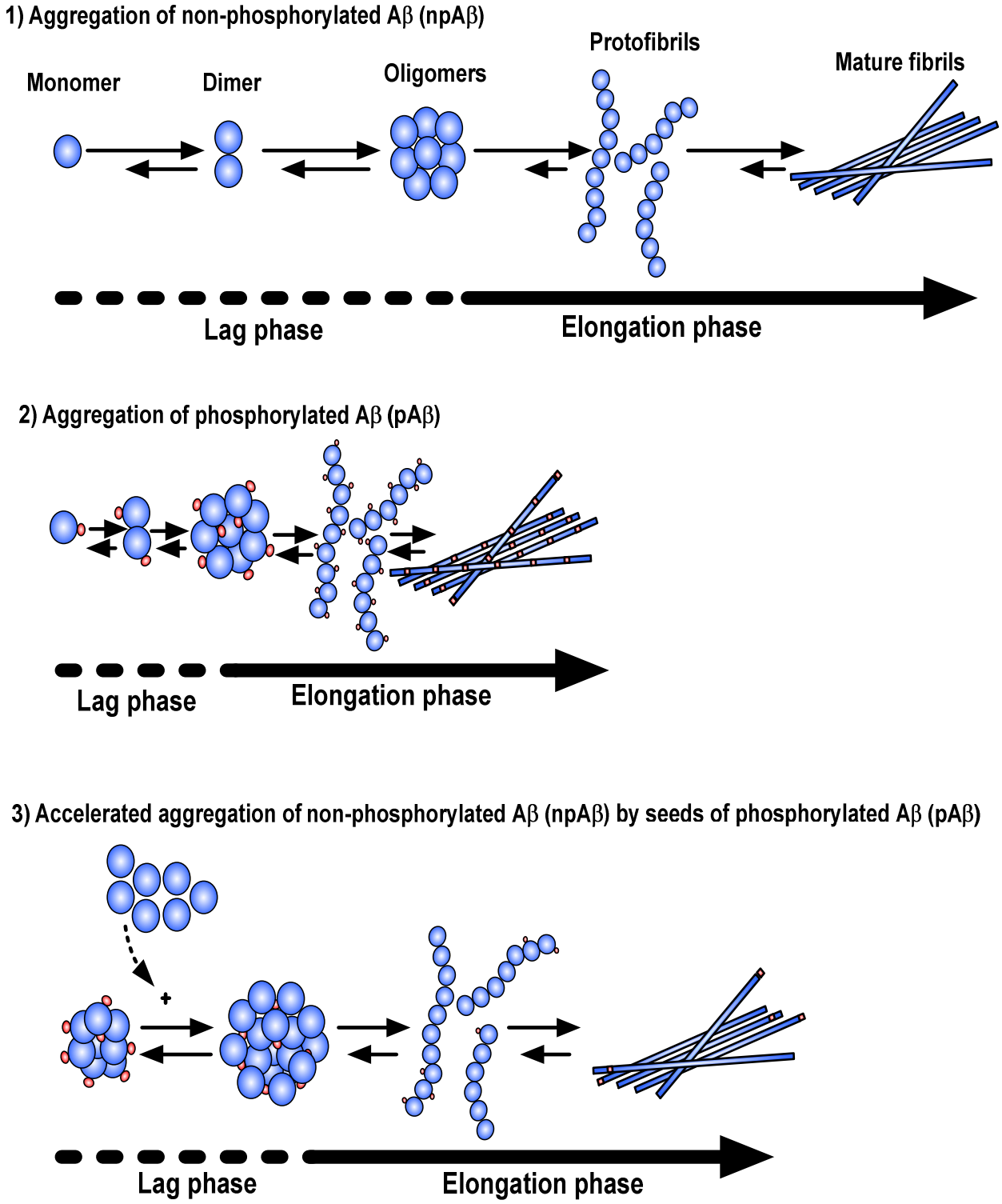

Fig. 53: Model for the phosphorylation-dependent aggregation of Aβ.
1) Aggregation of npAβ peptide having two kinetic phases. In the 'lag phase', oligomeric nuclei are formed in a slow process. In the 'elongation phase', the oligomeric nuclei-seed promotes fibril formation, 2) Phosphorylation of Aβ reduces the lag phase of nucleation. 3) Nuclei of pAβ could serve as seeds to accelerate the aggregation of npAβ.

6. FUTURE OUTLOOK

Amyloid formation in AD is conceptualized as a complex process of aggregation. In recent years our understanding of the nature and significance of amyloid formation and deposition and the role that these play in AD have taken dramatic leaps forward. Further advances in understanding the mechanisms that control extracellular Aβ aggregation and their toxic nature are likely to identify new strategies for effective disease therapies. The current work is focused on what is unknown about the role of extracellular phosphorylation of Aβ and its role in aggregation.

The operation of powerful regulatory machinery, the protein phosphorylation exists in the human brain. Although the intracellular kinase activities in neurons have been widely described, extracellular protein kinase activities and their biological relevance with respect to phosphorylation of extracellular Aβ is not known. This is the first investigation reporting an important role of extracellular or cell surface-localised protein kinases in the pathogenesis of AD. This study identified a modification of Aβ by phosphorylation that strongly promotes its aggregation and is found in neurotoxic amyloid deposits in sporadic AD. Thus, the phosphorylated Aβ might play a major role in the pathogenesis of the most common, sporadic forms of AD. Therefore, pharmacological manipulation by targeting extracellular phosphorylation of Aβ could be explored for therapeutic or preventive strategies to decrease Aβ aggregation and toxicity in AD.

The current biophysical analyses highlighted the importance of structural transition of Aβ upon phosphorylation. They indicate the role of phosphorylation at serine residues, which is capable of increasing the propensity to adopt β-sheet conformation and promote oligomerization and aggregation. Recent reports highlight the existence of highly toxic intermediates with high β-sheet structure in AD brain. Phosphorylation induced the misfolding of Aβ and thus in turn coalesces to form small soluble oligomers and fibrillar aggregates. The aggregation property of Aβ oligomers observed upon phosphorylation is consistent with the recent two-pathway model showing the production of soluble and insoluble Aβ aggregates. Phosphorylation seems to act as a conformational switch for Aβ peptide to proceed to form fibrils or soluble globular oligomers. This could result in changes in the ratio of soluble and insoluble forms of the peptide which may then influence the disease. Of further interest, is determining which pathway is critical for the pathogenesis of AD might help to shape the therapeutic strategy that should be used to block the pathogenic Aβ assembly process.

Interestingly, phosphorylation of Ser-26 residue showed rapid formation of soluble oligomers. Therefore, further detailed investigation on the role of Ser-26 phosphorylation and

its detection *in vivo* could give much more insight in to the pathogenesis of AD. The relevance of soluble oligomers for AD pathology has been underlined by their detection in AD patient's brain. This suggests that phosphorylation induced formation of soluble oligomers of Aβ may be pathogenic. If oligomerization indeed causes neuronal impairment, then detection of oligomers may facilitate the early diagnosis and treatment. Assays for detection of oligomers could be used for high-throughput screening to identify small molecules that specifically bind to, and disrupt, the oligomer specific conformation. The detection of phosphorylated (pAβ) and non-phosphorylated Aβ (npAβ) in biological fluids could also be explored for evaluation as biomarkers. Finally, the demonstration of protein kinases in human CSF might also stimulate further studies on the physiological and pathophysiological implications of the extracellular phosphorylation of peptides and proteins in the human brain.

In addition to Aβ aggregation, the time-dependent accumulation of Aβ in the brain is another invariable component observed in AD. Proposed mechanisms for the pathological accumulation of Aβ include not only the formation of Aβ aggregates but also an inability of the body to degrade and clear Aβ. Thus, identifying the effects of phosphorylation on the clearance of pAβ could help to understand the initial pathogenic accumulation of pAβ in AD pathogenesis.

Certainly, it will be important to evaluate the role of phosphorylation-dependent aggregation of Aβ in a variety of *in vivo* models. Generation and analysis of phosphomimicking-Aβ mutants could offer an excellent platform to study the physiological and pathological behaviour of pAβ *in vivo*. The expression and detailed analysis of role of phosphomimicking-Aβ in transgenic animal models could exemplify the toxic role of pAβ in the brain. It may facilitate our understanding of pAβ and elucidate the physiological mechanism (s) and may lead to development of novel therapeutic agents.

7. REFERENCES

Abdi F, et al. (2006) Detection of biomarkers with a multiplex quantitative proteomic platform in cerebrospinal fluid of patients with neurodegenerative disorders. J Alzheimers Dis 9:293-348.

Agorogiannis EI, Agorogiannis GI, Papadimitriou A, Hadjigeorgiou GM (2004) Protein misfolding in neurodegenerative diseases. Neuropathol Appl Neurobiol 30:215-224.

Agren G, Ronquist G (1974) (32-P) Phosphoryl transfer by endogenous protein kinase at the glia and glioma cell surface in culture into extrinsic acceptor proteins. Acta Physiol Scand 92:430-432.

Alexander GE, Chen K, Pietrini P, Rapoport SI, Reiman EM (2002) Longitudinal PET Evaluation of Cerebral Metabolic Decline in Dementia: A Potential Outcome Measure in Alzheimer's Disease Treatment Studies. Am J Psychiatry 159:738-745.

Ando K, Iijima KI, Elliott JI, Kirino Y, Suzuki T (2001) Phosphorylation-dependent regulation of the interaction of amyloid precursor protein with Fe65 affects the production of beta-amyloid. J Biol Chem 276:40353-40361.

Ando K, Oishi M, Takeda S, Iijima K, Isohara T, Nairn AC, Kirino Y, Greengard P, Suzuki T (1999) Role of phosphorylation of Alzheimer's amyloid precursor protein during neuronal differentiation. J Neurosci 19:4421-4427.

Anfinsen CB (1973) Principles that govern the folding of protein chains. Science 181:223-230.

Anliker B, Muller U (2006) The functions of mammalian amyloid precursor protein and related amyloid precursor-like proteins. Neurodegener Dis 3:239-246.

Aplin AE, Gibb GM, Jacobsen JS, Gallo JM, Anderton BH (1996) In vitro phosphorylation of the cytoplasmic domain of the amyloid precursor protein by glycogen synthase kinase-3beta. J Neurochem 67:699-707.

Arendt T (2001) Disturbance of neuronal plasticity is a critical pathogenetic event in Alzheimer's disease. Int J Dev Neurosci 19:231-245.

Armen RS, DeMarco ML, Alonso DO, Daggett V (2004) Pauling and Corey's alpha-pleated sheet structure may define the prefibrillar amyloidogenic intermediate in amyloid disease. Proc Natl Acad Sci U S A 101:11622-11627.

Armstrong RA (1998) Beta-amyloid plaques: stages in life history or independent origin? Dement Geriatr Cogn Disord 9:227-238.

Atwood CS, Martins RN, Smith MA, Perry G (2002) Senile plaque composition and posttranslational modification of amyloid-beta peptide and associated proteins. Peptides 23:1343-1350.

Awad JA, Johnson RA, Jakobs KH, Schultz G (1983) Interactions of forskolin and adenylate cyclase. Effects on substrate kinetics and protection against inactivation by heat and N-ethylmaleimide. J Biol Chem 258:2960-2965.

Bachman DL, Wolf PA, Linn R, Knoefel JE, Cobb J, Belanger A, D'Agostino RB, White LR (1992) Prevalence of dementia and probable senile dementia of the Alzheimer type in the Framingham Study. Neurology 42:115-119.

Bahl JM, Jensen SS, Larsen MR, Heegaard NH (2008) Characterization of the human cerebrospinal fluid phosphoproteome by titanium dioxide affinity chromatography and mass spectrometry. Anal Chem 80:6308-6316.

Ban T, Hamada D, Hasegawa K, Naiki H, Goto Y (2003) Direct observation of amyloid fibril growth monitored by thioflavin T fluorescence. J Biol Chem 278:16462-16465.

Ban T, Hoshino M, Takahashi S, Hamada D, Hasegawa K, Naiki H, Goto Y (2004) Direct observation of Abeta amyloid fibril growth and inhibition. J Mol Biol 344:757-767.

Bard F, et al. (2000) Peripherally administered antibodies against amyloid beta-peptide enter the central nervous system and reduce pathology in a mouse model of Alzheimer disease. Nat Med 6:916-919.

Barford D, Hu SH, Johnson LN (1991) Structural mechanism for glycogen phosphorylase control by phosphorylation and AMP. J Mol Biol 218:233-260.

Barford D, Johnson LN (1989) The allosteric transition of glycogen phosphorylase. Nature 340:609-616.

Barford D, Johnson LN (1992) The molecular mechanism for the tetrameric association of glycogen phosphorylase promoted by protein phosphorylation. Protein Sci 1:472-493.

Barrow CJ, Yasuda A, Kenny PT, Zagorski MG (1992) Solution conformations and aggregational properties of synthetic amyloid beta-peptides of Alzheimer's disease. Analysis of circular dichroism spectra. J Mol Biol 225:1075-1093.

Barrow CJ, Zagorski MG (1991) Solution structures of beta peptide and its constituent fragments: relation to amyloid deposition. Science 253:179-182.

Bartolini M, Bertucci C, Bolognesi ML, Cavalli A, Melchiorre C, Andrisano V (2007) Insight into the kinetic of amyloid beta (1-42) peptide self-aggregation: elucidation of inhibitors' mechanism of action. Chembiochem 8:2152-2161.

Behl C (2005) Oxidative stress in Alzheimer's disease: implications for prevention and therapy. Subcell Biochem 38:65-78.

Behrens MM, Mazon MJ (1988) Yeast cAMP-dependent protein kinase can be associated to the plasma membrane. Biochem Biophys Res Commun 151:561-567.

Bence NF, Sampat RM, Kopito RR (2001) Impairment of the ubiquitin-proteasome system by protein aggregation. Science 292:1552-1555.

Bentahir M, Nyabi O, Verhamme J, Tolia A, Horre K, Wiltfang J, Esselmann H, De SB (2006) Presenilin clinical mutations can affect gamma-secretase activity by different mechanisms. J Neurochem 96:732-742.

Bernert G, Nemethova M, Herrera-Marschitz M, Cairns N, Lubec G (1996) Decreased cyclin dependent kinase in brain of patients with Down syndrome. Neurosci Lett 216:68-70.

Bessen RA, Kocisko DA, Raymond GJ, Nandan S, Lansbury PT, Caughey B (1995) Non-genetic propagation of strain-specific properties of scrapie prion protein. Nature 375:698-700.

Betts V, Leissring MA, Dolios G, Wang R, Selkoe DJ, Walsh DM (2008) Aggregation and catabolism of disease-associated intra-Abeta mutations: reduced proteolysis of AbetaA21G by neprilysin. Neurobiol Dis 31:442-450.

Bhat RV, Budd Haeberlein SL, Avila J (2004) Glycogen synthase kinase 3: a drug target for CNS therapies. J Neurochem 89:1313-1317.

Bibl M, Mollenhauer B, Esselmann H, Lewczuk P, Trenkwalder C, Brechlin P, Ruther E, Kornhuber J, Otto M, Wiltfang J (2006) CSF diagnosis of Alzheimer's disease and dementia with Lewy bodies. J Neural Transm 113:1771-1778.

Billingsley ML, Kincaid RL (1997) Regulated phosphorylation and dephosphorylation of tau protein: effects on microtubule interaction, intracellular trafficking and neurodegeneration. Biochem J 323 (Pt 3):577-591.

Bitan G, Kirkitadze MD, Lomakin A, Vollers SS, Benedek GB, Teplow DB (2003) Amyloid beta - protein (Abeta) assembly: Abeta 40 and Abeta 42 oligomerize through distinct pathways. Proc Natl Acad Sci U S A 100:330-335.

Blennow K (2004) CSF biomarkers for mild cognitive impairment. J Intern Med 256:224-234.

Blennow K, Nellgard B (2004) Amyloid beta 1-42 and tau in cerebrospinal fluid after severe traumatic brain injury. Neurology 62:159-160.

Bonkale WL, Cowburn RF, Ohm TG, Bogdanovic N, Fastbom J (1999) A quantitative autoradiographic study of [3H]cAMP binding to cytosolic and particulate protein kinase A in post-mortem brain staged for Alzheimer's disease neurofibrillary changes and amyloid deposits. Brain Res 818:383-396.

Borchelt DR, Ratovitski T, van LJ, Lee MK, Gonzales V, Jenkins NA, Copeland NG, Price DL, Sisodia SS (1997) Accelerated amyloid deposition in the brains of transgenic mice coexpressing mutant presenilin 1 and amyloid precursor proteins. Neuron 19:939-945.

Borreguero JM, Urbanc B, Lazo ND, Buldyrev SV, Teplow DB, Stanley HE (2005) Folding events in the 21-30 region of amyloid beta-protein (Abeta) studied in silico. Proc Natl Acad Sci U S A 102:6015-6020.

Borrelli E, Montmayeur JP, Foulkes NS, Sassone-Corsi P (1992) Signal transduction and gene control: the cAMP pathway. Crit Rev Oncog 3:321-338.

Bourhim M, Kruzel M, Srikrishnan T, Nicotera T (2007) Linear quantitation of Abeta aggrega-tion using Thioflavin T: reduction in fibril formation by colostrinin. J Neurosci Methods 160:264-268.

Bowen DM, Francis PT, Pangalos MN, Stephens PH, Procter AW (1992) Treatment strategies for Alzheimer's disease. Lancet 339:132-133.
Braak H, Braak E (1991) Neuropathological stageing of Alzheimer-related changes. Acta Neuropathol 82:239-259.

Braak H, Braak E, Bohl J (1993) Staging of Alzheimer-related cortical destruction. Eur Neurol 33:403-408.

Braak H, Sandmann-Keil D, Gai W, Braak E (1999) Extensive axonal Lewy neurites in Parkinson's disease: a novel pathological feature revealed by alpha-synuclein immunocytochemistry. Neurosci Lett 265:67-69.

Breydo L, Makarava N, Baskakov IV (2008) Methods for conversion of prion protein into amyloid fibrils. Methods Mol Biol 459:105-115.

Brody DL, Magnoni S, Schwetye KE, Spinner ML, Esparza TJ, Stocchetti N, Zipfel GJ, Holtzman DM (2008) Amyloid-beta dynamics correlate with neurological status in the injured human brain. Science 321:1221-1224.

Burdick D, Soreghan B, Kwon M, Kosmoski J, Knauer M, Henschen A, Yates J, Cotman C, Glabe C (1992) Assembly and aggregation properties of synthetic Alzheimer's A4/beta amyloid peptide analogs. J Biol Chem 267:546-554.

Busciglio J, Lorenzo A, Yankner BA (1992) Methodological variables in the assessment of beta amyloid neurotoxicity. Neurobiol Aging 13:609-612.

Busciglio J, Lorenzo A, Yeh J, Yankner BA (1995) beta-amyloid fibrils induce tau phosphorylation and loss of microtubule binding. Neuron 14:879-888.

Bush AI (2003) The metallobiology of Alzheimer's disease. Trends Neurosci 26:207-214.

Bush AI, Multhaup G, Moir RD, Williamson TG, Small DH, Rumble B, Pollwein P, Beyreuther K, Masters CL (1993) A novel zinc(II) binding site modulates the function of the beta A4 amyloid protein precursor of Alzheimer's disease. J Biol Chem 268:16109-16112.

Buxbaum JD, Gandy SE, Cicchetti P, Ehrlich ME, Czernik AJ, Fracasso RP, Ramabhadran TV, Unterbeck AJ, Greengard P (1990) Processing of Alzheimer beta/A4 amyloid precursor protein: modulation by agents that regulate protein phosphorylation. Proc Natl Acad Sci U S A 87:6003-6006.

Buxbaum JD, Koo EH, Greengard P (1993) Protein phosphorylation inhibits production of Alzheimer amyloid beta/A4 peptide. Proc Natl Acad Sci U S A 90:9195-9198.

Buxbaum JD, Liu KN, Luo Y, Slack JL, Stocking KL, Peschon JJ, Johnson RS, Castner BJ, Cerretti DP, Black RA (1998) Evidence that tumor necrosis factor alpha converting enzyme is involved in regulated alpha-secretase cleavage of the Alzheimer amyloid protein precursor. J Biol Chem 273:27765-27767.

Cadd G, McKnight GS (1989) Distinct patterns of cAMP-dependent protein kinase gene expression in mouse brain. Neuron 3:71-79.

Cai H, Wang Y, McCarthy D, Wen H, Borchelt DR, Price DL, Wong PC (2001) BACE1 is the major beta-secretase for generation of Abeta peptides by neurons. Nat Neurosci 4:233-234.

Cardinale A, Biocca S (2008) Combating protein misfolding and aggregation by intracellular antibodies. Curr Mol Med 8:2-11.

Carrell RW, Gooptu B (1998) Conformational changes and disease--serpins, prions and Alzheimer's. Curr Opin Struct Biol 8:799-809.

Carulla N, Caddy GL, Hall DR, Zurdo J, Gairi M, Feliz M, Giralt E, Robinson CV, Dobson CM (2005) Molecular recycling within amyloid fibrils. Nature 436:554-558.

Cellmer T, Douma R, Huebner A, Prausnitz J, Blanch H (2007) Kinetic studies of protein L aggregation and disaggregation. Biophys Chem 125:350-359.
Cerda-Costa N, Esteras-Chopo A, Aviles FX, Serrano L, Villegas V (2007) Early kinetics of amyloid fibril formation reveals conformational reorganisation of initial aggregates. J Mol Biol 366:1351-1363.

Chachin M, Shimohama S, Kunugi YU, Taniguchi T (1996) Assessment of protein kinase C mRNA levels in Alzheimer's disease brains. Jpn J Pharmacol 71:175-177.

Chang A, Li PP, Warsh JJ (2003) Altered cAMP-dependent protein kinase subunit immunolabeling in post-mortem brain from patients with bipolar affective disorder. J Neurochem 84:781-791.

Chapman PF, White GL, Jones MW, Cooper-Blacketer D, Marshall VJ, Irizarry M, Younkin L, Good MA, Bliss TV, Hyman BT, Younkin SG, Hsiao KK (1999) Impaired synaptic plasticity and learning in aged amyloid precursor protein transgenic mice. Nat Neurosci 2:271-276.

Chartier-Harlin MC, Crawford F, Houlden H, Warren A, Hughes D, Fidani L, Goate A, Rossor M, Roques P, Hardy J, . (1991) Early-onset Alzheimer's disease caused by mutations at codon 717 of the beta-amyloid precursor protein gene. Nature 353:844-846.

Chauhan A, Chauhan VP, Murakami N, Brockerhoff H, Wisniewski HM (1993) Amyloid beta-protein stimulates casein kinase I and casein kinase II activities. Brain Res 629:47-52.

Chen K, Maley J, Yu PH (2006) Potential inplications of endogenous aldehydes in beta-amyloid misfolding, oligomerization and fibrillogenesis. J Neurochem 99:1413-1424.

Chen W, Wieraszko A, Hogan MV, Yang HA, Kornecki E, Ehrlich YH (1996) Surface protein phosphorylation by ecto-protein kinase is required for the maintenance of hippocampal long-term potentiation. Proc Natl Acad Sci U S A 93:8688-8693.

Cheng IH, Scearce-Levie K, Legleiter J, Palop JJ, Gerstein H, Bien-Ly N, Puolivali J, Lesne S, Ashe KH, Muchowski PJ, Mucke L (2007) Accelerating amyloid-beta fibrillization reduces oligomer levels and functional deficits in Alzheimer disease mouse models. J Biol Chem 282:23818-23828.

Chiti F, Stefani M, Taddei N, Ramponi G, Dobson CM (2003) Rationalization of the effects of mutations on peptide and protein aggregation rates. Nature 424:805-808.

Cho YS, Park YG, Lee YN, Kim MK, Bates S, Tan L, Cho-Chung YS (2000) Extracellular protein kinase A as a cancer biomarker: its expression by tumor cells and reversal by a myristate-lacking Calpha and RIIbeta subunit overexpression. Proc Natl Acad Sci U S A 97:835-840.

Chun W, Johnson GV (2007) The role of tau phosphorylation and cleavage in neuronal cell death. Front Biosci 12:733-756.

Citron M, Oltersdorf T, Haass C, McConlogue L, Hung AY, Seubert P, Vigo-Pelfrey C, Lieberburg I, Selkoe DJ (1992) Mutation of the beta-amyloid precursor protein in familial Alzheimer's disease increases beta-protein production. Nature 360:672-674.

Cleary JP, Walsh DM, Hofmeister JJ, Shankar GM, Kuskowski MA, Selkoe DJ, Ashe KH (2005) Natural oligomers of the amyloid-beta protein specifically disrupt cognitive function. Nat Neurosci 8:79-84.

Cohen AS, Calkins E (1959) Electron microscopic observations on a fibrous component in amyloid of diverse origins. Nature 183:1202-1203.

Cohen P (1989) The structure and regulation of protein phosphatases. Annu Rev Biochem 58:453-508.

Cohen P (1992) Signal integration at the level of protein kinases, protein phosphatases and their substrates. Trends Biochem Sci 17:408-413.

Cohen P (2000) The regulation of protein function by multisite phosphorylation--a 25 year update. Trends Biochem Sci 25:596-601.

Cohen P (2002) The origins of protein phosphorylation. Nat Cell Biol 4:E127-E130.

Cole G, Dobkins KR, Hansen LA, Terry RD, Saitoh T (1988) Decreased levels of protein kinase C in Alzheimer brain. Brain Res 452:165-174.

Cole GM, Masliah E, Shelton ER, Chan HW, Terry RD, Saitoh T (1991) Accumulation of amyloid precursor fragment in Alzheimer plaques. Neurobiol Aging 12:85-91.

Conway KA, Rochet JC, Bieganski RM, Lansbury PT, Jr. (2001) Kinetic stabilization of the alpha-synuclein protofibril by a dopamine-alpha-synuclein adduct. Science 294:1346-1349.

Coraci IS, Husemann J, Berman JW, Hulette C, Dufour JH, Campanella GK, Luster AD, Silverstein SC, El-Khoury JB (2002) CD36, a class B scavenger receptor, is expressed on microglia in Alzheimer's disease brains and can mediate production of reactive oxygen species in response to beta-amyloid fibrils. Am J Pathol 160:101-112.

Cotrina ML, Nedergaard M (2002) Astrocytes in the aging brain. J Neurosci Res 67:1-10.

Cruz L, Urbanc B, Borreguero JM, Lazo ND, Teplow DB, Stanley HE (2005) Solvent and mutation effects on the nucleation of amyloid beta-protein folding. Proc Natl Acad Sci U S A 102:18258-18263.

Cruz L, Urbanc B, Buldyrev SV, Christie R, Gomez-Isla T, Havlin S, McNamara M, Stanley HE, Hyman BT (1997) Aggregation and disaggregation of senile plaques in Alzheimer disease. Proc Natl Acad Sci U S A 94:7612-7616.

da Cruz e Silva EF, da Cruz e Silva OA (2003) Protein phosphorylation and APP metabolism. Neurochem Res 28:1553-1561.

da Cruz e Silva OA, Iverfeldt K, Oltersdorf T, Sinha S, Lieberburg I, Ramabhadran TV, Suzuki T, Sisodia SS, Gandy S, Greengard P (1993) Regulated cleavage of Alzheimer beta-amyloid precursor protein in the absence of the cytoplasmic tail. Neuroscience 57:873-877.

Dahlgren PR, Karymov MA, Bankston J, Holden T, Thumfort P, Ingram VM, Lyubchenko YL (2005) Atomic force microscopy analysis of the Huntington protein nanofibril formation. Dis Mon 51:374-385.

Daigle I, Li C (1993) apl-1, a Caenorhabditis elegans gene encoding a protein related to the human beta-amyloid protein precursor. Proc Natl Acad Sci U S A 90:12045-12049.

D'Andrea MR, Cole GM, Ard MD (2004) The microglial phagocytic role with specific plaque types in the Alzheimer disease brain. Neurobiol Aging 25:675-683.
Davies SW, Sathasivam K, Hobbs C, Doherty P, Mangiarini L, Scherzinger E, Wanker EE, Bates GP (1999) Detection of polyglutamine aggregation in mouse models. Methods Enzymol 309:687-701.

Davies SW, Turmaine M, Cozens BA, DiFiglia M, Sharp AH, Ross CA, Scherzinger E, Wanker EE, Mangiarini L, Bates GP (1997) Formation of neuronal intranuclear inclusions underlies the neurological dysfunction in mice transgenic for the HD mutation. Cell 90:537-548.

De SB, Beullens M, Contreras B, Levesque L, Craessaerts K, Cordell B, Moechars D, Bollen M, Fraser P, George-Hyslop PS, Van LF (1997) Phosphorylation, subcellular localization, and membrane orientation of the Alzheimer's disease-associated presenilins. J Biol Chem 272:3590-3598.

De SB, Simons M, Multhaup G, Van LF, Beyreuther K, Dotti CG (1995) Production of intracellular amyloid-containing fragments in hippocampal neurons expressing human amyloid precursor protein and protection against amyloidogenesis by subtle amino acid substitutions in the rodent sequence. EMBO J 14:4932-4938.

De SB, Van LF, Van den BH (1991) The amyloid beta protein precursor or proteinase nexin II from mouse is closer related to its human homolog than previously reported. Biochim Biophys Acta 1129:141-143.

DeKosky ST, Scheff SW (1990) Synapse loss in frontal cortex biopsies in Alzheimer's disease: correlation with cognitive severity. Ann Neurol 27:457-464.

Delobel P, Flament S, Hamdane M, Mailliot C, Sambo AV, Begard S, Sergeant N, Delacourte A, Vilain JP, Buee L (2002) Abnormal Tau phosphorylation of the Alzheimer-type also occurs during mitosis. J Neurochem 83:412-420.

Demuro A, Mina E, Kayed R, Milton SC, Parker I, Glabe CG (2005) Calcium dysregulation and membrane disruption as a ubiquitous neurotoxic mechanism of soluble amyloid oligomers. J Biol Chem 280:17294-17300.

Deshpande A, Mina E, Glabe C, Busciglio J (2006) Different conformations of amyloid beta induce neurotoxicity by distinct mechanisms in human cortical neurons. J Neurosci 26:6011-6018.
Di FG, et al. (2009) A recessive mutation in the APP gene with dominant-negative effect on amyloidogenesis. Science 323:1473-1477.

Dickey CA, Gordon MN, Wilcock DM, Herber DL, Freeman MJ, Morgan D (2005) Dysregulation of Na+/K+ ATPase by amyloid in APP+PS1 transgenic mice. BMC Neurosci 6:7.

Dickson TC, Vickers JC (2001) The morphological phenotype of beta-amyloid plaques and associated neuritic changes in Alzheimer's disease. Neuroscience 105:99-107.

Dobson CM (1999) Protein misfolding, evolution and disease. Trends Biochem Sci 24:329-332.

Dobson CM (2003) Protein folding and misfolding. Nature 426:884-890.

Dubyak GR, el-Moatassim C (1993) Signal transduction via P2-purinergic receptors for extracellular ATP and other nucleotides. Am J Physiol 265:C577-C606.

D'Ursi AM, Armenante MR, Guerrini R, Salvadori S, Sorrentino G, Picone D (2004) Solution structure of amyloid beta-peptide (25-35) in different media. J Med Chem 47:4231-4238.

Duyckaerts C, Perruchini C, Lebouvier T, Potier MC (2008) [The lesions of Alzheimer's disease: which therapeutic perspectives?]. Bull Acad Natl Med 192:303-318.

Ehrlich YH, Davis TB, Bock E, Kornecki E, Lenox RH (1986) Ecto-protein kinase activity on the external surface of neural cells. Nature 320:67-70.

Ehrlich YH, Davis TB, Bock E, Kornecki E, Lenox RH (1986a) Ecto-protein kinase activity on the external surface of neural cells. Nature 320:67-70.

Ehrlich YH, Garfield MG, Davis TB, Kornecki E, Chaffee JE, Lenox RH (1986b) Extracellular protein phosphorylation systems in the regulation of neuronal function. Prog Brain Res 69:197-208.

Ehrlich YH, Hogan MV, Pawlowska Z, Naik U, Kornecki E (1990) Ectoprotein kinase in the regulation of cellular responsiveness to extracellular ATP. Ann N Y Acad Sci 603:401-416.

Eidenmuller J, Fath T, Hellwig A, Reed J, Sontag E, Brandt R (2000) Structural and functional implications of tau hyperphosphorylation: information from phosphorylation-mimicking mutated tau proteins. Biochemistry 39:13166-13175.

Eikelenboom P, Veerhuis R, Scheper W, Rozemuller AJ, van Gool WA, Hoozemans JJ (2006) The significance of neuroinflammation in understanding Alzheimer's disease. J Neural Transm 113:1685-1695.

Eisenberg D, Nelson R, Sawaya MR, Balbirnie M, Sambashivan S, Ivanova MI, Madsen AO, Riekel C (2006) The structural biology of protein aggregation diseases: Fundamental questions and some answers. Acc Chem Res 39:568-575.

El Khoury JB, Moore KJ, Means TK, Leung J, Terada K, Toft M, Freeman MW, Luster AD (2003) CD36 mediates the innate host response to beta-amyloid. J Exp Med 197:1657-1666.

El KJ, Hickman SE, Thomas CA, Cao L, Silverstein SC, Loike JD (1996) Scavenger receptor-mediated adhesion of microglia to beta-amyloid fibrils. Nature 382:716-719.

El KJ, Luster AD (2008) Mechanisms of microglia accumulation in Alzheimer's disease: therapeutic implications. Trends Pharmacol Sci 29:626-632.

El-Agnaf OM, Walsh DM, Allsop D (2003) Soluble oligomers for the diagnosis of neurodegenerative diseases. Lancet Neurol 2:461-462.

el-Moatassim C, Dornand J, Mani JC (1992) Extracellular ATP and cell signalling. Biochim Biophys Acta 1134:31-45.

Emamian ES, Kaytor MD, Duvick LA, Zu T, Tousey SK, Zoghbi HY, Clark HB, Orr HT (2003) Serine 776 of ataxin-1 is critical for polyglutamine-induced disease in SCA1 transgenic mice. Neuron 38:375-387.

Esch FS, Keim PS, Beattie EC, Blacher RW, Culwell AR, Oltersdorf T, McClure D, Ward PJ (1990) Cleavage of amyloid beta peptide during constitutive processing of its precursor. Science 248:1122-1124.

Evans DA, Funkenstein HH, Albert MS, Scherr PA, Cook NR, Chown MJ, Hebert LE, Hennekens CH, Taylor JO (1989) Prevalence of Alzheimer's disease in a community population of older persons. Higher than previously reported. JAMA 262:2551-2556.

Fabian H, Szendrei GI, Mantsch HH, Otvos L, Jr. (1993) Comparative analysis of human and Dutch-type Alzheimer beta-amyloid peptides by infrared spectroscopy and circular dichroism. Biochem Biophys Res Commun 191:232-239.

Farfara D, Lifshitz V, Frenkel D (2008) Neuroprotective and neurotoxic properties of glial cells in the pathogenesis of Alzheimer's disease. J Cell Mol Med 12:762-780.

Fawzi NL, Yap EH, Okabe Y, Kohlstedt KL, Brown SP, Head-Gordon T (2008) Contrasting disease and nondisease protein aggregation by molecular simulation. Acc Chem Res 41:1037-1047.

Finder VH, Glockshuber R (2007) Amyloid-beta aggregation. Neurodegener Dis 4:13-27.

Fink AL (1998) Protein aggregation: folding aggregates, inclusion bodies and amyloid. Fold Des 3:R9-23.

Flajolet M, He G, Heiman M, Lin A, Nairn AC, Greengard P (2007) Regulation of Alzheimer's disease amyloid-beta formation by casein kinase I. Proc Natl Acad Sci U S A 104:4159-4164.

Fluhrer R, Friedlein A, Haass C, Walter J (2004) Phosphorylation of presenilin 1 at the caspase recognition site regulates its proteolytic processing and the progression of apoptosis. J Biol Chem 279:1585-1593.

Forloni G, Terreni L, Bertani I, Fogliarino S, Invernizzi R, Assini A, Ribizzi G, Negro A, Calabrese E, Volonte MA, Mariani C, Franceschi M, Tabaton M, Bertoli A (2002) Protein misfolding in Alzheimer's and Parkinson's disease: genetics and molecular mechanisms. Neurobiol Aging 23:957-976.

Forstl H, Kurz A (1999) Clinical features of Alzheimer's disease. Eur Arch Psychiatry Clin Neurosci 249:288-290.

Foss KB, Simard J, Berube D, Beebe SJ, Sandberg M, Grzeschik KH, Gagne R, Hansson V, Jahnsen T (1992) Localization of the catalytic subunit C gamma of the cAMP-dependent protein kinase gene (PRKACG) to human chromosome region 9q13. Cytogenet Cell Genet 60:22-25.

Fox NC, Warrington EK, Seiffer AL, Agnew SK, Rossor MN (1998) Presymptomatic cognitive deficits in individuals at risk of familial Alzheimer's disease. A longitudinal prospective study. Brain 121 (Pt 9):1631-1639.

Francis PT, Palmer AM, Snape M, Wilcock GK (1999) The cholinergic hypothesis of Alzheimer's disease: a review of progress. J Neurol Neurosurg Psychiatry 66:137-147.

Frenkel D, Balass M, Katchalski-Katzir E, Solomon B (1999) High affinity binding of monoclonal antibodies to the sequential epitope EFRH of beta-amyloid peptide is essential for modulation of fibrillar aggregation. J Neuroimmunol 95:136-142.

Frenkel D, Katz O, Solomon B (2000a) Immunization against Alzheimer's beta -amyloid plaques via EFRH phage administration. Proc Natl Acad Sci U S A 97:11455-11459.

Frenkel D, Solomon B, Benhar I (2000b) Modulation of Alzheimer's beta-amyloid neurotoxicity by site-directed single-chain antibody. J Neuroimmunol 106:23-31.

Frost B, Ollesch J, Wille H, Diamond MI (2009) Conformational Diversity of Wild-type Tau Fibrils Specified by Templated Conformation Change. J Biol Chem 284:3546-3551.

Gahtan E, Overmier JB (1999) Inflammatory pathogenesis in Alzheimer's disease: biological mechanisms and cognitive sequeli. Neurosci Biobehav Rev 23:615-633.

Gajdusek DC (1994) Nucleation of amyloidogenesis in infectious and noninfectious amyloidoses of brain. Ann N Y Acad Sci 724:173-190.

Games D, Adams D, Alessandrini R, Barbour R, Berthelette P, Blackwell C, Carr T, Clemens J, Donaldson T, Gillespie F, . (1995) Alzheimer-type neuropathology in transgenic mice overexpressing V717F beta-amyloid precursor protein. Nature 373:523-527.

Gandy S, Czernik AJ, Greengard P (1988) Phosphorylation of Alzheimer disease amyloid precursor peptide by protein kinase C and Ca2+/calmodulin-dependent protein kinase II. Proc Natl Acad Sci U S A 85:6218-6221.

Gandy SE, Caporaso GL, Buxbaum JD, de Cruz SO, Iverfeldt K, Nordstedt C, Suzuki T, Czernik AJ, Nairn AC, Greengard P (1993) Protein phosphorylation regulates relative utilization of processing pathways for Alzheimer beta/A4 amyloid precursor protein. Ann N Y Acad Sci 695:117-121.

Garzon-Rodriguez W, Sepulveda-Becerra M, Milton S, Glabe CG (1997) Soluble amyloid Abeta-(1-40) exists as a stable dimer at low concentrations. J Biol Chem 272:21037-21044.

Geddes JW, Tekirian TL, Mattson MP (1999) N-terminus truncated beta-amyloid peptides and C-terminus truncated secreted forms of amyloid precursor protein: distinct roles in the pathogenesis of Alzheimer's disease. Neurobiol Aging 20:75-79.

Giasson BI, Duda JE, Murray IV, Chen Q, Souza JM, Hurtig HI, Ischiropoulos H, Trojanowski JQ, Lee VM (2000) Oxidative damage linked to neurodegeneration by selective alpha-synuclein nitration in synucleinopathy lesions. Science 290:985-989.

Gill SC, von Hippel PH (1989) Calculation of protein extinction coefficients from amino acid sequence data. Anal Biochem 182:319-326.

Glabe CG (2006) Common mechanisms of amyloid oligomer pathogenesis in degenerative disease. Neurobiol Aging 27:570-575.

Glenner GG, Wong CW (1984a) Alzheimer's disease: initial report of the purification and characterization of a novel cerebrovascular amyloid protein. Biochem Biophys Res Commun 120:885-890.

Glenner GG, Wong CW, Quaranta V, Eanes ED (1984) The amyloid deposits in Alzheimer's disease: their nature and pathogenesis. Appl Pathol 2:357-369.

Goate A, Chartier-Harlin MC, Mullan M, Brown J, Crawford F, Fidani L, Giuffra L, Haynes A, Irving N, James L, . (1991) Segregation of a missense mutation in the amyloid precursor protein gene with familial Alzheimer's disease. Nature 349:704-706.

Goedert M, Spillantini MG (2006) A century of Alzheimer's disease. Science 314:777-781.

Goedert M, Wischik CM, Crowther RA, Walker JE, Klug A (1988) Cloning and sequencing of the cDNA encoding a core protein of the paired helical filament of Alzheimer disease: identification as the microtubule-associated protein tau. Proc Natl Acad Sci U S A 85:4051-4055.

Golde TE, Das P, Levites Y (2009) Quantitative and mechanistic studies of abeta immunotherapy. CNS Neurol Disord Drug Targets 8:31-49.

Goldsbury CS, Wirtz S, Muller SA, Sunderji S, Wicki P, Aebi U, Frey P (2000) Studies on the in vitro assembly of a beta 1-40: implications for the search for a beta fibril formation inhibitors. J Struct Biol 130:217-231.

Gomez-Isla T, Price JL, McKeel DW, Jr., Morris JC, Growdon JH, Hyman BT (1996) Profound loss of layer II entorhinal cortex neurons occurs in very mild Alzheimer's disease. J Neurosci 16:4491-4500.

Gong CX, Singh TJ, Grundke-Iqbal I, Iqbal K (1993) Phosphoprotein phosphatase activities in Alzheimer disease brain. J Neurochem 61:921-927.

Gong Y, Chang L, Viola KL, Lacor PN, Lambert MP, Finch CE, Krafft GA, Klein WL (2003) Alzheimer's disease-affected brain: presence of oligomeric A beta ligands (ADDLs) suggests a molecular basis for reversible memory loss. Proc Natl Acad Sci U S A 100:10417-10422.

Gordon JL (1986) Extracellular ATP: effects, sources and fate. Biochem J 233:309-319.

Gotz J, Chen F, van DJ, Nitsch RM (2001) Formation of neurofibrillary tangles in P301l tau transgenic mice induced by Abeta 42 fibrils. Science 293:1491-1495.

Gotz J, Ittner LM (2008) Animal models of Alzheimer's disease and frontotemporal dementia. Nat Rev Neurosci 9:532-544.

Gotz J, Schild A, Hoerndli F, Pennanen L (2004a) Amyloid-induced neurofibrillary tangle formation in Alzheimer's disease: insight from transgenic mouse and tissue-culture models. Int J Dev Neurosci 22:453-465.

Gotz J, Streffer JR, David D, Schild A, Hoerndli F, Pennanen L, Kurosinski P, Chen F (2004b) Transgenic animal models of Alzheimer's disease and related disorders: histopathology, behavior and therapy. Mol Psychiatry 9:664-683.

Grant MA, Lazo ND, Lomakin A, Condron MM, Arai H, Yamin G, Rigby AC, Teplow DB (2007) Familial Alzheimer's disease mutations alter the stability of the amyloid beta-protein monomer folding nucleus. Proc Natl Acad Sci U S A 104:16522-16527.

Gray EG, Paula-Barbosa M, Roher A (1987) Alzheimer's disease: paired helical filaments and cytomembranes. Neuropathol Appl Neurobiol 13:91-110.

Greenberg SM, Koo EH, Selkoe DJ, Qiu WQ, Kosik KS (1994) Secreted beta-amyloid precursor protein stimulates mitogen-activated protein kinase and enhances tau phosphorylation. Proc Natl Acad Sci U S A 91:7104-7108.

Gregersen N, Bolund L, Bross P (2005) Protein misfolding, aggregation, and degradation in disease. Mol Biotechnol 31:141-150.

Gregersen N, Bross P, Vang S, Christensen JH (2006) Protein misfolding and human disease. Annu Rev Genomics Hum Genet 7:103-124.

Grundke-Iqbal I, Iqbal K, Tung YC, Quinlan M, Wisniewski HM, Binder LI (1986) Abnormal phosphorylation of the microtubule-associated protein tau (tau) in Alzheimer cytoskeletal pathology. Proc Natl Acad Sci U S A 83:4913-4917.

Gsponer J, Caflisch A (2002) Molecular dynamics simulations of protein folding from the transition state. Proc Natl Acad Sci U S A 99:6719-6724.

Guo Q (2006) When good Cdk5 turns bad. Sci Aging Knowledge Environ 2006:e5.

Gurney ME (1994) Transgenic-mouse model of amyotrophic lateral sclerosis. N Engl J Med 331:1721-1722.

Gustke N, Steiner B, Mandelkow EM, Biernat J, Meyer HE, Goedert M, Mandelkow E (1992) The Alzheimer-like phosphorylation of tau protein reduces microtubule binding and involves Ser-Pro and Thr-Pro motifs. FEBS Lett 307:199-205.

Haass C, Hung AY, Selkoe DJ (1991) Processing of beta-amyloid precursor protein in microglia and astrocytes favors an internal localization over constitutive secretion. J Neurosci 11:3783-3793.

Haass C, Schlossmacher MG, Hung AY, Vigo-Pelfrey C, Mellon A, Ostaszewski BL, Lieberburg I, Koo EH, Schenk D, Teplow DB, . (1992) Amyloid beta-peptide is produced by cultured cells during normal metabolism. Nature 359:322-325.

Haass C, Selkoe DJ (2007) Soluble protein oligomers in neurodegeneration: lessons from the Alzheimer's amyloid beta-peptide. Nat Rev Mol Cell Biol 8:101-112.

Halverson K, Fraser PE, Kirschner DA, Lansbury PT, Jr. (1990) Molecular determinants of amyloid deposition in Alzheimer's disease: conformational studies of synthetic beta-protein fragments. Biochemistry 29:2639-2644.

Hama E, Shirotani K, Masumoto H, Sekine-Aizawa Y, Aizawa H, Saido TC (2001) Clearance of extracellular and cell-associated amyloid beta peptide through viral expression of neprilysin in primary neurons. J Biochem 130:721-726.

Hardy J (2006) Has the amyloid cascade hypothesis for Alzheimer's disease been proved? Curr Alzheimer Res 3:71-73.

Hardy J, Selkoe DJ (2002) The amyloid hypothesis of Alzheimer's disease: progress and problems on the road to therapeutics. Science 297:353-356.

Harper JD, Lansbury PT, Jr. (1997) Models of amyloid seeding in Alzheimer's disease and scrapie: mechanistic truths and physiological consequences of the time-dependent solubility of amyloid proteins. Annu Rev Biochem 66:385-407.

Harper JD, Wong SS, Lieber CM, Lansbury PT (1997) Observation of metastable Abeta amyloid protofibrils by atomic force microscopy. Chem Biol 4:119-125.

Harper JD, Wong SS, Lieber CM, Lansbury PT, Jr. (1999) Assembly of A beta amyloid protofibrils: an in vitro model for a possible early event in Alzheimer's disease. Biochemistry 38:8972-8980.

Hartley DM, Walsh DM, Ye CP, Diehl T, Vasquez S, Vassilev PM, Teplow DB, Selkoe DJ (1999) Protofibrillar intermediates of amyloid beta-protein induce acute electrophysiological changes and progressive neurotoxicity in cortical neurons. J Neurosci 19:8876-8884.

Hartley DM, Zhao C, Speier AC, Woodard GA, Li S, Li Z, Walz T (2008) Transglutaminase induces protofibril-like amyloid beta-protein assemblies that are protease-resistant and inhibit long-term potentiation. J Biol Chem 283:16790-16800.

Heber S, Herms J, Gajic V, Hainfellner J, Aguzzi A, Rulicke T, von KH, von KC, Sisodia S, Tremml P, Lipp HP, Wolfer DP, Muller U (2000) Mice with combined gene knock-outs reveal essential and partially redundant functions of amyloid precursor protein family members. J Neurosci 20:7951-7963.

Hendriks L, van Duijn CM, Cras P, Cruts M, Van HW, van HF, Warren A, McInnis MG, Antonarakis SE, Martin JJ, . (1992) Presenile dementia and cerebral haemorrhage linked to a mutation at codon 692 of the beta-amyloid precursor protein gene. Nat Genet 1:218-221.

Heneka MT, Sastre M, Dumitrescu-Ozimek L, Dewachter I, Walter J, Klockgether T, Van LF (2005) Focal glial activation coincides with increased BACE1 activation and precedes amyloid plaque deposition in APP[V717I] transgenic mice. J Neuroinflammation 2:22.

Herczenik E, Gebbink MF (2008) Molecular and cellular aspects of protein misfolding and disease. FASEB J 22:2115-2133.

Herms J, Anliker B, Heber S, Ring S, Fuhrmann M, Kretzschmar H, Sisodia S, Muller U (2004) Cortical dysplasia resembling human type 2 lissencephaly in mice lacking all three APP family members. EMBO J 23:4106-4115.

Hilbich C, Kisters-Woike B, Reed J, Masters CL, Beyreuther K (1991) Aggregation and secondary structure of synthetic amyloid beta A4 peptides of Alzheimer's disease. J Mol Biol 218:149-163.

Hilbich C, Kisters-Woike B, Reed J, Masters CL, Beyreuther K (1992) Substitutions of hydrophobic amino acids reduce the amyloidogenicity of Alzheimer's disease beta A4 peptides. J Mol Biol 228:460-473.

Hof PR, Giannakopoulos P, Vickers JC, Bouras C, Morrison JH (1995) The morphologic and neurochemical basis of dementia: aging, hierarchical patterns of lesion distribution and vulnerable neuronal phenotype. Rev Neurosci 6:97-124.

Hogan MV, Pawlowska Z, Yang HA, Kornecki E, Ehrlich YH (1995) Surface phosphorylation by ecto-protein kinase C in brain neurons: a target for Alzheimer's beta-amyloid peptides. J Neurochem 65:2022-2030.

Hooper C, Killick R, Lovestone S (2008) The GSK3 hypothesis of Alzheimer's disease. J Neurochem 104:1433-1439.

Hori Y, Hashimoto T, Wakutani Y, Urakami K, Nakashima K, Condron MM, Tsubuki S, Saido TC, Teplow DB, Iwatsubo T (2007) The Tottori (D7N) and English (H6R) familial Alzheimer disease mutations accelerate Abeta fibril formation without increasing protofibril formation. J Biol Chem 282:4916-4923.

Horikoshi Y, Sakaguchi G, Becker AG, Gray AJ, Duff K, Aisen PS, Yamaguchi H, Maeda M, Kinoshita N, Matsuoka Y (2004) Development of Abeta terminal end-specific antibodies and sensitive ELISA for Abeta variant. Biochem Biophys Res Commun 319:733-737.

Horiuchi J, Yamazaki D, Naganos S, Aigaki T, Saitoe M (2008) Protein kinase A inhibits a consolidated form of memory in Drosophila. Proc Natl Acad Sci U S A 105:20976-20981.

Hou L, Shao H, Zhang Y, Li H, Menon NK, Neuhaus EB, Brewer JM, Byeon IJ, Ray DG, Vitek MP, Iwashita T, Makula RA, Przybyla AB, Zagorski MG (2004) Solution NMR studies of the A beta(1-40) and A beta(1-42) peptides establish that the Met35 oxidation state affects the mechanism of amyloid formation. J Am Chem Soc 126:1992-2005.

Hsiao KK, Scott M, Foster D, Groth DF, DeArmond SJ, Prusiner SB (1990) Spontaneous neurodegeneration in transgenic mice with mutant prion protein. Science 250:1587-1590.

Huang HC, Jiang ZF (2009) Accumulated amyloid-beta peptide and hyperphosphorylated tau protein: relationship and links in Alzheimer's disease. J Alzheimers Dis 16:15-27.

Hubschmann MV, Skladchikova G (2008) The Role of ATP in the Regulation of NCAM Function. Neurochem Res.

Hung AY, Selkoe DJ (1994) Selective ectodomain phosphorylation and regulated cleavage of beta-amyloid precursor protein. EMBO J 13:534-542.

Hunter T (1987) A thousand and one protein kinases. Cell 50:823-829.

Hurley JH, Dean AM, Sohl JL, Koshland DE, Jr., Stroud RM (1990) Regulation of an enzyme by phosphorylation at the active site. Science 249:1012-1016.

Hy LX, Keller DM (2000) Prevalence of AD among whites: a summary by levels of severity. Neurology 55:198-204.

Hyman BT, Van Hoesen GW, Kromer LJ, Damasio AR (1986) Perforant pathway changes and the memory impairment of Alzheimer's disease. Ann Neurol 20:472-481.

Iijima K, Ando K, Takeda S, Satoh Y, Seki T, Itohara S, Greengard P, Kirino Y, Nairn AC, Suzuki T (2000) Neuron-specific phosphorylation of Alzheimer's beta-amyloid precursor protein by cyclin-dependent kinase 5. J Neurochem 75:1085-1091.

Ingebritsen TS, Cohen P (1983a) Protein phosphatases: properties and role in cellular regulation. Science 221:331-338.

Ingebritsen TS, Cohen P (1983b) The protein phosphatases involved in cellular regulation. 1. Classification and substrate specificities. Eur J Biochem 132:255-261.

Ingebritsen TS, Stewart AA, Cohen P (1983) The protein phosphatases involved in cellular regulation. 6. Measurement of type-1 and type-2 protein phosphatases in extracts of mammalian tissues; an assessment of their physiological roles. Eur J Biochem 132:297-307.

Inoue K, Koizumi S, Tsuda M (2007) The role of nucleotides in the neuron--glia communication responsible for the brain functions. J Neurochem 102:1447-1458.

Inouye H, Fraser PE, Kirschner DA (1993) Structure of beta-crystallite assemblies formed by Alzheimer beta-amyloid protein analogues: analysis by x-ray diffraction. Biophys J 64:502-519.

Insel PA, Ostrom RS (2003) Forskolin as a tool for examining adenylyl cyclase expression, regulation, and G protein signaling. Cell Mol Neurobiol 23:305-314.

Isaacs AM, Senn DB, Yuan M, Shine JP, Yankner BA (2006) Acceleration of amyloid beta-peptide aggregation by physiological concentrations of calcium. J Biol Chem 281:27916-27923.

Isohara T, Horiuchi A, Watanabe T, Ando K, Czernik AJ, Uno I, Greengard P, Nairn AC, Suzuki T (1999) Phosphorylation of the cytoplasmic domain of Alzheimer's beta-amyloid precursor protein at Ser655 by a novel protein kinase. Biochem Biophys Res Commun 258:300-305.

Itagaki S, McGeer PL, Akiyama H, Zhu S, Selkoe D (1989) Relationship of microglia and astrocytes to amyloid deposits of Alzheimer disease. J Neuroimmunol 24:173-182.

Iwatsubo T (2003) Aggregation of alpha-synuclein in the pathogenesis of Parkinson's disease. J Neurol 250 Suppl 3:III11-III14.

Iwatsubo T, Odaka A, Suzuki N, Mizusawa H, Nukina N, Ihara Y (1994) Visualization of A beta 42(43) and A beta 40 in senile plaques with end-specific A beta monoclonals: evidence that an initially deposited species is A beta 42(43). Neuron 13:45-53.

Iwatsubo T, Saido TC, Mann DM, Lee VM, Trojanowski JQ (1996) Full-length amyloid-beta (1-42(43)) and amino-terminally modified and truncated amyloid-beta 42(43) deposit in diffuse plaques. Am J Pathol 149:1823-1830.

Jan A, Gokce O, Luthi-Carter R, Lashuel HA (2008) The Ratio of Monomeric to Aggregated Forms of A{beta}40 and A{beta}42 Is an Important Determinant of Amyloid-{beta} Aggregation, Fibrillogenesis, and Toxicity. J Biol Chem 283:28176-28189.

Janek K, Behlke J, Zipper J, Fabian H, Georgalis Y, Beyermann M, Bienert M, Krause E (1999) Water-soluble beta-sheet models which self-assemble into fibrillar structures. Biochemistry 38:8246-8252.

Jankowsky JL, Slunt HH, Ratovitski T, Jenkins NA, Copeland NG, Borchelt DR (2001) Co-expression of multiple transgenes in mouse CNS: a comparison of strategies. Biomol Eng 17:157-165.

Jarrett JT, Berger EP, Lansbury PT, Jr. (1993a) The C-terminus of the beta protein is critical in amyloidogenesis. Ann N Y Acad Sci 695:144-148.

Jarrett JT, Berger EP, Lansbury PT, Jr. (1993b) The carboxy terminus of the beta amyloid protein is critical for the seeding of amyloid formation: implications for the pathogenesis of Alzheimer's disease. Biochemistry 32:4693-4697.

Jeganathan S, Hascher A, Chinnathambi S, Biernat J, Mandelkow EM, Mandelkow E (2008) Proline-directed pseudo-phosphorylation at AT8 and PHF1 epitopes induces a compaction of the paperclip folding of Tau and generates a pathological (MC-1) conformation. J Biol Chem 283:32066-32076.

Jelinek T, Weber MJ (1993) Optimization of the resolution of phosphoamino acids by one-dimensional thin-layer electrophoresis. Biotechniques 15:628, 630.

Jicha GA, Weaver C, Lane E, Vianna C, Kress Y, Rockwood J, Davies P (1999) cAMP-dependent protein kinase phosphorylations on tau in Alzheimer's disease. J Neurosci 19:7486-7494.

Jin LW, Saitoh T (1995) Changes in protein kinases in brain aging and Alzheimer's disease. Implications for drug therapy. Drugs Aging 6:136-149.

Johansson AS, Bergquist J, Volbracht C, Paivio A, Leist M, Lannfelt L, Westlind-Danielsson A (2007) Attenuated amyloid-beta aggregation and neurotoxicity owing to methionine oxidation. Neuroreport 18:559-563.

Johnson LN (1994) Control by protein phosphorylation. Nat Struct Biol 1:657-659.

Johnson LN, Barford D (1993) The effects of phosphorylation on the structure and function of proteins. Annu Rev Biophys Biomol Struct 22:199-232.

Johnson LN, Barford D (1994) Electrostatic effects in the control of glycogen phosphorylase by phosphorylation. Protein Sci 3:1726-1730.

Johnstone EM, Chaney MO, Norris FH, Pascual R, Little SP (1991) Conservation of the sequence of the Alzheimer's disease amyloid peptide in dog, polar bear and five other mammals by cross-species polymerase chain reaction analysis. Brain Res Mol Brain Res 10:299-305.

Jordan P, Kubler D (1992) Ecto-protein kinase release differs from cleavage by phospholipases of a glycosyl-phosphatidylinositol membrane anchor. Biochem Int 26:97-104.

Kaganovich D, Kopito R, Frydman J (2008) Misfolded proteins partition between two distinct quality control compartments. Nature 454:1088-1095.

Kamenetz F, Tomita T, Hsieh H, Seabrook G, Borchelt D, Iwatsubo T, Sisodia S, Malinow R (2003) APP processing and synaptic function. Neuron 37:925-937.

Kane MD, Lipinski WJ, Callahan MJ, Bian F, Durham RA, Schwarz RD, Roher AE, Walker LC (2000) Evidence for seeding of beta -amyloid by intracerebral infusion of Alzheimer brain extracts in beta -amyloid precursor protein-transgenic mice. J Neurosci 20:3606-3611.

Kaneko I, Morimoto K, Kubo T (2001) Drastic neuronal loss in vivo by beta-amyloid racemized at Ser(26) residue: conversion of non-toxic [D-Ser(26)]beta-amyloid 1-40 to toxic and proteinase-resistant fragments. Neuroscience 104:1003-1011.

Kang J, Lemaire HG, Unterbeck A, Salbaum JM, Masters CL, Grzeschik KH, Multhaup G, Beyreuther K, Muller-Hill B (1987) The precursor of Alzheimer's disease amyloid A4 protein resembles a cell-surface receptor. Nature 325:733-736.

Kayed R, Glabe CG (2006) Conformation-dependent anti-amyloid oligomer antibodies. Methods Enzymol 413:326-344.

Kayed R, Head E, Sarsoza F, Saing T, Cotman CW, Necula M, Margol L, Wu J, Breydo L, Thompson JL, Rasool S, Gurlo T, Butler P, Glabe CG (2007) Fibril specific, conformation dependent antibodies recognize a generic epitope common to amyloid fibrils and fibrillar oligomers that is absent in prefibrillar oligomers. Mol Neurodegener 2:18.

Kayed R, Head E, Thompson JL, McIntire TM, Milton SC, Cotman CW, Glabe CG (2003) Common structure of soluble amyloid oligomers implies common mechanism of pathogenesis. Science 300:486-489.

Kemp BE, Bylund DB, Huang TS, Krebs EG (1975) Substrate specificity of the cyclic AMP-dependent protein kinase. Proc Natl Acad Sci U S A 72:3448-3452.

Kemp BE, Graves DJ, Benjamini E, Krebs EG (1977) Role of multiple basic residues in determining the substrate specificity of cyclic AMP-dependent protein kinase. J Biol Chem 252:4888-4894.

Kennelly PJ, Krebs EG (1991) Consensus sequences as substrate specificity determinants for protein kinases and protein phosphatases. J Biol Chem 266:15555-15558.

Kerr ML, Small DH (2005) Cytoplasmic domain of the beta-amyloid protein precursor of Alzheimer's disease: function, regulation of proteolysis, and implications for drug development. J Neurosci Res 80:151-159.

Khurana R, Coleman C, Ionescu-Zanetti C, Carter SA, Krishna V, Grover RK, Roy R, Singh S (2005) Mechanism of thioflavin T binding to amyloid fibrils. J Struct Biol 151:229-238.

Kim KS, D.L.Miller, V.J.Sapienza, C.-M.Chen, C.Bai, I.Grundke-Iqbal, J.R.Currie, H.M.Wisniewski (1988) Production and characterization of monoclonal antibodies reactive to synthetic cerebrovascular amyloid peptide. Neurosci Res Commun 2:121-130.

Kim SH, Nairn AC, Cairns N, Lubec G (2001) Decreased levels of ARPP-19 and PKA in brains of Down syndrome and Alzheimer's disease. J Neural Transm Suppl263-272.

Kim W, Hecht MH (2005) Sequence determinants of enhanced amyloidogenicity of Alzheimer A{beta}42 peptide relative to A{beta}40. J Biol Chem 280:35069-35076.

Kim W, Hecht MH (2006) Generic hydrophobic residues are sufficient to promote aggregation of the Alzheimer's Abeta42 peptide. Proc Natl Acad Sci U S A 103:15824-15829.

Kim YJ, Takahashi R (2006) Role of polyunsaturated fatty acids for misfolding protein aggregations: implication for neurodegenerative diseases. Ann N Y Acad Sci 1086:11-20.

Kimberly WT, Zheng JB, Town T, Flavell RA, Selkoe DJ (2005) Physiological regulation of the beta-amyloid precursor protein signaling domain by c-Jun N-terminal kinase JNK3 during neuronal differentiation. J Neurosci 25:5533-5543.

Kirkitadze MD, Condron MM, Teplow DB (2001) Identification and characterization of key kinetic intermediates in amyloid beta-protein fibrillogenesis. J Mol Biol 312:1103-1119.

Kirschner DA, Inouye H, Duffy LK, Sinclair A, Lind M, Selkoe DJ (1987) Synthetic peptide homologous to beta protein from Alzheimer disease forms amyloid-like fibrils in vitro. Proc Natl Acad Sci U S A 84:6953-6957.

Klein WL, Krafft GA, Finch CE (2001) Targeting small Abeta oligomers: the solution to an Alzheimer's disease conundrum? Trends Neurosci 24:219-224.

Klement K, Wieligmann K, Meinhardt J, Hortschansky P, Richter W, Fandrich M (2007) Effect of different salt ions on the propensity of aggregation and on the structure of Alzheimer's abeta(1-40) amyloid fibrils. J Mol Biol 373:1321-1333.

Klunk WE, Jacob RF, Mason RP (1999) Quantifying amyloid beta-peptide (Abeta) aggregation using the Congo red-Abeta (CR-abeta) spectrophotometric assay. Anal Biochem 266:66-76.

Klunk WE, Jacob RF, Mason RP (1999) Quantifying amyloid by congo red spectral shift assay. Methods Enzymol 309:285-305.

Klyubin I, Betts V, Welzel AT, Blennow K, Zetterberg H, Wallin A, Lemere CA, Cullen WK, Peng Y, Wisniewski T, Selkoe DJ, Anwyl R, Walsh DM, Rowan MJ (2008) Amyloid beta protein dimer-containing human CSF disrupts synaptic plasticity: prevention by systemic passive immunization. J Neurosci 28:4231-4237.

Knops J, Gandy S, Greengard P, Lieberburg I, Sinha S (1993) Serine phosphorylation of the secreted extracellular domain of APP. Biochem Biophys Res Commun 197:380-385.

Knowles RB, Gomez-Isla T, Hyman BT (1998) Abeta associated neuropil changes: correlation with neuronal loss and dementia. J Neuropathol Exp Neurol 57:1122-1130.

Knowles RB, Wyart C, Buldyrev SV, Cruz L, Urbanc B, Hasselmo ME, Stanley HE, Hyman BT (1999) Plaque-induced neurite abnormalities: implications for disruption of neural networks in Alzheimer's disease. Proc Natl Acad Sci U S A 96:5274-5279.

Koizumi S, Fujishita K, Inoue K (2005) Regulation of cell-to-cell communication mediated by astrocytic ATP in the CNS. Purinergic Signal 1:211-217.

Kondrashin A, Nesterova M, Cho-Chung YS (1999) Cyclic adenosine 3':5'-monophosphate-dependent protein kinase on the external surface of LS-174T human colon carcinoma cells. Biochemistry 38:172-179.

Kosik KS, Joachim CL, Selkoe DJ (1986) Microtubule-associated protein tau (tau) is a major antigenic component of paired helical filaments in Alzheimer disease. Proc Natl Acad Sci U S A 83:4044-4048.

Krebs EG, Beavo JA (1979) Phosphorylation-dephosphorylation of enzymes. Annu Rev Biochem 48:923-959.

Kubler D, Barnekow A (1986) Ecto-protein kinase activities in normal and transformed cells. Eur J Cell Biol 40:58-63.

Kubler D, Pyerin W, Bill O, Hotz A, Sonka J, Kinzel V (1989) Evidence for ecto-protein kinase activity that phosphorylates Kemptide in a cyclic AMP-dependent mode. J Biol Chem 264:14549-14555.

Kubler D, Pyerin W, Burow E, Kinzel V (1983) Substrate-effected release of surface-located protein kinase from intact cells. Proc Natl Acad Sci U S A 80:4021-4025.

Kubler D, Pyerin W, Kinzel V (1982) Protein kinase activity and substrates at the surface of intact HeLa cells. J Biol Chem 257:322-329.

Kubler D, Reinhardt D, Reed J, Pyerin W, Kinzel V (1992) Atrial natriuretic peptide is phosphorylated by intact cells through cAMP-dependent ecto-protein kinase. Eur J Biochem 206:179-186.

Kumar-Singh S (2008) Cerebral amyloid angiopathy: pathogenetic mechanisms and link to dense amyloid plaques. Genes Brain Behav 7 Suppl 1:67-82.

Lacor PN, Buniel MC, Chang L, Fernandez SJ, Gong Y, Viola KL, Lambert MP, Velasco PT, Bigio EH, Finch CE, Krafft GA, Klein WL (2004) Synaptic targeting by Alzheimer's-related amyloid beta oligomers. J Neurosci 24:10191-10200.

Lacor PN, Buniel MC, Furlow PW, Clemente AS, Velasco PT, Wood M, Viola KL, Klein WL (2007) Abeta oligomer-induced aberrations in synapse composition, shape, and density provide a molecular basis for loss of connectivity in Alzheimer's disease. J Neurosci 27:796-807.

Lambert MP, Barlow AK, Chromy BA, Edwards C, Freed R, Liosatos M, Morgan TE, Rozovsky I, Trommer B, Viola KL, Wals P, Zhang C, Finch CE, Krafft GA, Klein WL (1998) Diffusible, nonfibrillar ligands derived from Abeta1-42 are potent central nervous system neurotoxins. Proc Natl Acad Sci U S A 95:6448-6453.

Lammich S, Kojro E, Postina R, Gilbert S, Pfeiffer R, Jasionowski M, Haass C, Fahrenholz F (1999) Constitutive and regulated alpha-secretase cleavage of Alzheimer's amyloid precursor protein by a disintegrin metalloprotease. Proc Natl Acad Sci U S A 96:3922-3927.

Lara J, Kusano K, House S, Gainer H (2003) Interactions of cyclic adenosine monophosphate, brain-derived neurotrophic factor, and glial cell line-derived neurotrophic factor treatment on the survival and growth of postnatal mesencephalic dopamine neurons in vitro. Exp Neurol 180:32-45.

Lashuel HA, Hartley DM, Petre BM, Wall JS, Simon MN, Walz T, Lansbury PT, Jr. (2003) Mixtures of wild-type and a pathogenic (E22G) form of Abeta40 in vitro accumulate protofibrils, including amyloid pores. J Mol Biol 332:795-808.

Lazarov O, Lee M, Peterson DA, Sisodia SS (2002) Evidence that synaptically released beta-amyloid accumulates as extracellular deposits in the hippocampus of transgenic mice. J Neurosci 22:9785-9793.

Lee KY, Clark AW, Rosales JL, Chapman K, Fung T, Johnston RN (1999) Elevated neuronal Cdc2-like kinase activity in the Alzheimer disease brain. Neurosci Res 34:21-29.

Lee MS, Kao SC, Lemere CA, Xia W, Tseng HC, Zhou Y, Neve R, Ahlijanian MK, Tsai LH (2003) APP processing is regulated by cytoplasmic phosphorylation. J Cell Biol 163:83-95.
Lee VM, Goedert M, Trojanowski JQ (2001) Neurodegenerative tauopathies. Annu Rev Neurosci 24:1121-1159.

Lehtovirta M, Soininen H, Helisalmi S, Mannermaa A, Helkala EL, Hartikainen P, Hanninen T, Ryynanen M, Riekkinen PJ (1996) Clinical and neuropsychological characteristics in familial and sporadic Alzheimer's disease: relation to apolipoprotein E polymorphism. Neurology 46:413-419.

Lemere CA, Blusztajn JK, Yamaguchi H, Wisniewski T, Saido TC, Selkoe DJ (1996) Sequence of deposition of heterogeneous amyloid beta-peptides and APO E in Down syndrome: implications for initial events in amyloid plaque formation. Neurobiol Dis 3:16-32.

Lendon CL, Ashall F, Goate AM (1997) Exploring the etiology of Alzheimer disease using molecular genetics. JAMA 277:825-831.

Leschik J, Welzel A, Weissmann C, Eckert A, Brandt R (2007) Inverse and distinct modulation of tau-dependent neurodegeneration by presenilin 1 and amyloid-beta in cultured cortical neurons: evidence that tau phosphorylation is the limiting factor in amyloid-beta-induced cell death. J Neurochem 101:1303-1315.

Lesne S, Koh MT, Kotilinek L, Kayed R, Glabe CG, Yang A, Gallagher M, Ashe KH (2006) A specific amyloid-beta protein assembly in the brain impairs memory. Nature 440:352-357.

LeVine H, III (1999) Quantification of beta-sheet amyloid fibril structures with thioflavin T. Methods Enzymol 309:274-284.

Levy E, Carman MD, Fernandez-Madrid IJ, Power MD, Lieberburg I, van Duinen SG, Bots GT, Luyendijk W, Frangione B (1990) Mutation of the Alzheimer's disease amyloid gene in hereditary cerebral hemorrhage, Dutch type. Science 248:1124-1126.

Levy-Lahad E, Wasco W, Poorkaj P, Romano DM, Oshima J, Pettingell WH, Yu CE, Jondro PD, Schmidt SD, Wang K, . (1995) Candidate gene for the chromosome 1 familial Alzheimer's disease locus. Science 269:973-977.

Lewis J, Dickson DW, Lin WL, Chisholm L, Corral A, Jones G, Yen SH, Sahara N, Skipper L, Yager D, Eckman C, Hardy J, Hutton M, McGowan E (2001) Enhanced neurofibrillary degeneration in transgenic mice expressing mutant tau and APP. Science 293:1487-1491.

Li M, Wang X, Meintzer MK, Laessig T, Birnbaum MJ, Heidenreich KA (2000) Cyclic AMP promotes neuronal survival by phosphorylation of glycogen synthase kinase 3beta. Mol Cell Biol 20:9356-9363.

Liang WS, Dunckley T, Beach TG, Grover A, Mastroeni D, Ramsey K, Caselli RJ, Kukull WA, McKeel D, Morris JC, Hulette CM, Schmechel D, Reiman EM, Rogers J, Stephan DA (2008) Altered neuronal gene expression in brain regions differentially affected by Alzheimer's disease: a reference data set. Physiol Genomics 33:240-256.

Liang Z, Liu F, Grundke-Iqbal I, Iqbal K, Gong CX (2007) Down-regulation of cAMP-dependent protein kinase by over-activated calpain in Alzheimer disease brain. J Neurochem 103:2462-2470.

Liesi P, Rechardt L, Wartiovaara J (1983) Nerve growth factor induces adrenergic neuronal differentiation in F9 teratocarcinoma cells. Nature 306:265-267.

Lin SY, Chu HL, Wei YS (2003) Secondary conformations and temperature effect on structural transformation of amyloid beta (1-28), (1-40) and (1-42) peptides. J Biomol Struct Dyn 20:595-601.

Linding R, Schymkowitz J, Rousseau F, Diella F, Serrano L (2004) A comparative study of the relationship between protein structure and beta-aggregation in globular and intrinsically disordered proteins. J Mol Biol 342:345-353.

Linn RT, Wolf PA, Bachman DL, Knoefel JE, Cobb JL, Belanger AJ, Kaplan EF, D'Agostino RB (1995) The 'preclinical phase' of probable Alzheimer's disease. A 13-year prospective study of the Framingham cohort. Arch Neurol 52:485-490.

Lippa CF, Saunders AM, Smith TW, Swearer JM, Drachman DA, Ghetti B, Nee L, Pulaski-Salo D, Dickson D, Robitaille Y, Bergeron C, Crain B, Benson MD, Farlow M, Hyman BT, George-Hyslop SP, Roses AD, Pollen DA (1996) Familial and sporadic Alzheimer's disease: neuropathology cannot exclude a final common pathway. Neurology 46:406-412.

Liu F, Liang Z, Shi J, Yin D, El-Akkad E, Grundke-Iqbal I, Iqbal K, Gong CX (2006) PKA modulates GSK-3beta- and cdk5-catalyzed phosphorylation of tau in site- and kinase-specific manners. FEBS Lett 580:6269-6274.

Liu R, McAllister C, Lyubchenko Y, Sierks MR (2004) Residues 17-20 and 30-35 of beta-amyloid play critical roles in aggregation. J Neurosci Res 75:162-171.

Lobo A, Launer LJ, Fratiglioni L, Andersen K, Di CA, Breteler MM, Copeland JR, Dartigues JF, Jagger C, Martinez-Lage J, Soininen H, Hofman A (2000) Prevalence of dementia and major subtypes in Europe: A collaborative study of population-based cohorts. Neurologic Diseases in the Elderly Research Group. Neurology 54:S4-S9.

Lomakin A, Chung DS, Benedek GB, Kirschner DA, Teplow DB (1996) On the nucleation and growth of amyloid beta-protein fibrils: detection of nuclei and quantitation of rate constants. Proc Natl Acad Sci U S A 93:1125-1129.

Lorenzo A, Yankner BA (1994) Beta-amyloid neurotoxicity requires fibril formation and is inhibited by congo red. Proc Natl Acad Sci U S A 91:12243-12247.

Lovestone S, Reynolds CH (1997) The phosphorylation of tau: a critical stage in neurodevelopment and neurodegenerative processes. Neuroscience 78:309-324.

Lue LF, Kuo YM, Roher AE, Brachova L, Shen Y, Sue L, Beach T, Kurth JH, Rydel RE, Rogers J (1999) Soluble amyloid beta peptide concentration as a predictor of synaptic change in Alzheimer's disease. Am J Pathol 155:853-862.

Luhrs T, Ritter C, Adrian M, Riek-Loher D, Bohrmann B, Dobeli H, Schubert D, Riek R (2005) 3D structure of Alzheimer's amyloid-beta(1-42) fibrils. Proc Natl Acad Sci U S A 102:17342-17347.

Luo LQ, Martin-Morris LE, White K (1990) Identification, secretion, and neural expression of APPL, a Drosophila protein similar to human amyloid protein precursor. J Neurosci 10:3849-3861.

Lyubchenko YL, Sherman S, Shlyakhtenko LS, Uversky VN (2006) Nanoimaging for protein misfolding and related diseases. J Cell Biochem 99:52-70.

Makin OS, Serpell LC (2002) Examining the structure of the mature amyloid fibril. Biochem Soc Trans 30:521-525.

Mandybur TI (1975) The incidence of cerebral amyloid angiopathy in Alzheimer's disease. Neurology 25:120-126.

Mangiarini L, Sathasivam K, Seller M, Cozens B, Harper A, Hetherington C, Lawton M, Trottier Y, Lehrach H, Davies SW, Bates GP (1996) Exon 1 of the HD gene with an expanded CAG repeat is sufficient to cause a progressive neurological phenotype in transgenic mice. Cell 87:493-506.

Mann DM (1988) Alzheimer's disease and Down's syndrome. Histopathology 13:125-137.

Mann DM, Yates PO, Marcyniuk B (1985) Some morphometric observations on the cerebral cortex and hippocampus in presenile Alzheimer's disease, senile dementia of Alzheimer type and Down's syndrome in middle age. J Neurol Sci 69:139-159.

Mann M, Ong SE, Gronborg M, Steen H, Jensen ON, Pandey A (2002) Analysis of protein phosphorylation using mass spectrometry: deciphering the phosphoproteome. Trends Biotechnol 20:261-268.

Manning G, Plowman GD, Hunter T, Sudarsanam S (2002a) Evolution of protein kinase signaling from yeast to man. Trends Biochem Sci 27:514-520.

Manning G, Whyte DB, Martinez R, Hunter T, Sudarsanam S (2002b) The protein kinase complement of the human genome. Science 298:1912-1934.

Marambaud P, Wilk S, Checler F (1996) Protein kinase A phosphorylation of the proteasome: a contribution to the alpha-secretase pathway in human cells. J Neurochem 67:2616-2619.

Marchesi VT (2005) An alternative interpretation of the amyloid Abeta hypothesis with regard to the pathogenesis of Alzheimer's disease. Proc Natl Acad Sci U S A 102:9093-9098.

Marin O, Bustos VH, Cesaro L, Meggio F, Pagano MA, Antonelli M, Allende CC, Pinna LA, Allende JE (2003) A noncanonical sequence phosphorylated by casein kinase 1 in beta-catenin may play a role in casein kinase 1 targeting of important signaling proteins. Proc Natl Acad Sci U S A 100:10193-10200.

Marin O, Meggio F, Draetta G, Pinna LA (1992) The consensus sequences for cdc2 kinase and for casein kinase-2 are mutually incompatible. A study with peptides derived from the beta-subunit of casein kinase-2. FEBS Lett 301:111-114.

Masliah E, Cole G, Shimohama S, Hansen L, DeTeresa R, Terry RD, Saitoh T (1990) Differential involvement of protein kinase C isozymes in Alzheimer's disease. J Neurosci 10:2113-2124.

Masliah E, Cole GM, Hansen LA, Mallory M, Albright T, Terry RD, Saitoh T (1991) Protein kinase C alteration is an early biochemical marker in Alzheimer's disease. J Neurosci 11:2759-2767.

Masliah E, Mallory M, Deerinck T, DeTeresa R, Lamont S, Miller A, Terry RD, Carragher B, Ellisman M (1993) Re-evaluation of the structural organization of neuritic plaques in Alzheimer's disease. J Neuropathol Exp Neurol 52:619-632.

Masliah E, Rockenstein E, Veinbergs I, Mallory M, Hashimoto M, Takeda A, Sagara Y, Sisk A, Mucke L (2000) Dopaminergic loss and inclusion body formation in alpha-synuclein mice: implications for neurodegenerative disorders. Science 287:1265-1269.

Masters CL, Simms G, Weinman NA, Multhaup G, McDonald BL, Beyreuther K (1985) Amyloid plaque core protein in Alzheimer disease and Down syndrome. Proc Natl Acad Sci U S A 82:4245-4249.

Mastrangelo IA, Ahmed M, Sato T, Liu W, Wang C, Hough P, Smith SO (2006) High-resolution atomic force microscopy of soluble Abeta42 oligomers. J Mol Biol 358:106-119.
Mattson MP (2002) Oxidative stress, perturbed calcium homeostasis, and immune dysfunction in Alzheimer's disease. J Neurovirol 8:539-550.

Mattson MP, Barger SW, Cheng B, Lieberburg I, Smith-Swintosky VL, Rydel RE (1993a) beta-Amyloid precursor protein metabolites and loss of neuronal Ca2+ homeostasis in Alzheimer's disease. Trends Neurosci 16:409-414.

Mattson MP, Cheng B, Culwell AR, Esch FS, Lieberburg I, Rydel RE (1993b) Evidence for excitoprotective and intraneuronal calcium-regulating roles for secreted forms of the beta-amyloid precursor protein. Neuron 10:243-254.

McKhann G, Drachman D, Folstein M, Katzman R, Price D, Stadlan EM (1984) Clinical diagnosis of Alzheimer's disease: report of the NINCDS-ADRDA Work Group under the auspices of Department of Health and Human Services Task Force on Alzheimer's Disease. Neurology 34:939-944.

McLaurin J, Yang D, Yip CM, Fraser PE (2000) Review: modulating factors in amyloid-beta fibril formation. J Struct Biol 130:259-270.

McLean CA, Cherny RA, Fraser FW, Fuller SJ, Smith MJ, Beyreuther K, Bush AI, Masters CL (1999) Soluble pool of Abeta amyloid as a determinant of severity of neurodegeneration in Alzheimer's disease. Ann Neurol 46:860-866.

Meda L, Baron P, Scarlato G (2001) Glial activation in Alzheimer's disease: the role of Abeta and its associated proteins. Neurobiol Aging 22:885-893.

Meda L, Cassatella MA, Szendrei GI, Otvos L, Jr., Baron P, Villalba M, Ferrari D, Rossi F (1995) Activation of microglial cells by beta-amyloid protein and interferon-gamma. Nature 374:647-650.

Mesulam MM (1999) Neuroplasticity failure in Alzheimer's disease: bridging the gap between plaques and tangles. Neuron 24:521-529.

Meyer-Luehmann M, Coomaraswamy J, Bolmont T, Kaeser S, Schaefer C, Kilger E, Neuenschwander A, Abramowski D, Frey P, Jaton AL, Vigouret JM, Paganetti P, Walsh DM, Mathews PM, Ghiso J, Staufenbiel M, Walker LC, Jucker M (2006) Exogenous induction of cerebral beta-amyloidogenesis is governed by agent and host. Science 313:1781-1784.

Meyer-Luehmann M, Spires-Jones TL, Prada C, Garcia-Alloza M, de CA, Rozkalne A, Koenigsknecht-Talboo J, Holtzman DM, Bacskai BJ, Hyman BT (2008) Rapid appearance and local toxicity of amyloid-beta plaques in a mouse model of Alzheimer's disease. Nature 451:720-724.

Mi K, Johnson GV (2006) The role of tau phosphorylation in the pathogenesis of Alzheimer's disease. Curr Alzheimer Res 3:449-463.

Milton NG (2001) Phosphorylation of amyloid-beta at the serine 26 residue by human cdc2 kinase. Neuroreport 12:3839-3844.

Milton NG (2005) Phosphorylated amyloid-beta: the toxic intermediate in alzheimer's disease neurodegeneration. Subcell Biochem 38:381-402.

Mirra SS (1997) The CERAD neuropathology protocol and consensus recommendations for the postmortem diagnosis of Alzheimer's disease: a commentary. Neurobiol Aging 18:S91-S94.

Mirra SS, Heyman A, McKeel D, Sumi SM, Crain BJ, Brownlee LM, Vogel FS, Hughes JP, van BG, Berg L (1991) The Consortium to Establish a Registry for Alzheimer's Disease (CERAD). Part II. Standardization of the neuropathologic assessment of Alzheimer's disease. Neurology 41:479-486.

Miyamoto E, Kuo JF, Greengard P (1969) Adenosine 3',5'-Monophosphate-Dependent Protein Kinase from Brain. Science 165:63-65.

Monaco EA, III (2004) Recent evidence regarding a role for Cdk5 dysregulation in Alzheimer's disease. Curr Alzheimer Res 1:33-38.

Monaco EA, III, Vallano ML (2005) Role of protein kinases in neurodegenerative disease: cyclin-dependent kinases in Alzheimer's disease. Front Biosci 10:143-159.

Mondragon-Rodriguez S, Basurto-Islas G, Santa-Maria I, Mena R, Binder LI, Avila J, Smith MA, Perry G, Garcia-Sierra F (2008) Cleavage and conformational changes of tau protein follow phosphorylation during Alzheimer's disease. Int J Exp Pathol 89:81-90.

Moore P, White J, Christiansen V, Grammas P (1998) Protein kinase C-zeta activity but not level is decreased in Alzheimer's disease microvessels. Neurosci Lett 254:29-32.

Morimoto A, Irie K, Murakami K, Masuda Y, Ohigashi H, Nagao M, Fukuda H, Shimizu T, Shirasawa T (2004) Analysis of the secondary structure of beta-amyloid (Abeta42) fibrils by systematic proline replacement. J Biol Chem 279:52781-52788.

Morris JC (1996) Classification of dementia and Alzheimer's disease. Acta Neurol Scand Suppl 165:41-50.

Mucke L, Masliah E, Yu GQ, Mallory M, Rockenstein EM, Tatsuno G, Hu K, Kholodenko D, Johnson-Wood K, McConlogue L (2000) High-level neuronal expression of abeta 1-42 in wild-type human amyloid protein precursor transgenic mice: synaptotoxicity without plaque formation. J Neurosci 20:4050-4058.

Mullan M, Crawford F, Axelman K, Houlden H, Lilius L, Winblad B, Lannfelt L (1992) A pathogenic mutation for probable Alzheimer's disease in the APP gene at the N-terminus of beta-amyloid. Nat Genet 1:345-347.

Murakami K, Irie K, Morimoto A, Ohigashi H, Shindo M, Nagao M, Shimizu T, Shirasawa T (2002) Synthesis, aggregation, neurotoxicity, and secondary structure of various A beta 1-42 mutants of familial Alzheimer's disease at positions 21-23. Biochem Biophys Res Commun 294:5-10.

Muramoto K, Taniguchi H, Kawahara M, Kobayashi K, Nonomura Y, Kuroda Y (1994) A substrate of ecto-protein kinase is microtubule-associated protein 1B in cortical cell cultures undergoing synaptogenesis. Biochem Biophys Res Commun 205:1467-1473.

Nagele RG, D'Andrea MR, Anderson WJ, Wang HY (2002) Intracellular accumulation of beta-amyloid(1-42) in neurons is facilitated by the alpha 7 nicotinic acetylcholine receptor in Alzheimer's disease. Neuroscience 110:199-211.

Nagele RG, Wegiel J, Venkataraman V, Imaki H, Wang KC, Wegiel J (2004) Contribution of glial cells to the development of amyloid plaques in Alzheimer's disease. Neurobiol Aging 25:663-674.

Naiki H, Gejyo F (1999) Kinetic analysis of amyloid fibril formation. Methods Enzymol 309:305-318.

Nairn AC, Hemmings HC, Jr., Greengard P (1985) Protein kinases in the brain. Annu Rev Biochem 54:931-976.

Nakada T, Matsuzawa H, Igarashi H, Fujii Y, Kwee IL (2008) In vivo visualization of senile-plaque-like pathology in Alzheimer's disease patients by MR microscopy on a 7T system. J Neuroimaging 18:125-129.

National Institute on Aging, and Reagan Institute Working Group on Diagnostic Criteria for the Neuropathological Assessment of Alzheimer's Disease (1997) Consensus recommendations for the postmortem diagnosis of Alzheimer's disease. The Neurobiol Aging 18:S1-S2.

Neet KE, Thinakaran G (2008) Thematic minireview series on the molecular basis of Alzheimer's disease. J Biol Chem.

Nelson R, Sawaya MR, Balbirnie M, Madsen AO, Riekel C, Grothe R, Eisenberg D (2005) Structure of the cross-beta spine of amyloid-like fibrils. Nature 435:773-778.

Nestler EJ, Greengard P (1983) Protein phosphorylation in the brain. Nature 305:583-588.

Nestler EJ, Walaas SI, Greengard P (1984) Neuronal phosphoproteins: physiological and clinical implications. Science 225:1357-1364.

Newhouse PA, Potter A, Levin ED (1997) Nicotinic system involvement in Alzheimer's and Parkinson's diseases. Implications for therapeutics. Drugs Aging 11:206-228.

Nicholls DG (2008) Oxidative stress and energy crises in neuronal dysfunction. Ann N Y Acad Sci 1147:53-60.

Nichols MR, Moss MA, Reed DK, Lin WL, Mukhopadhyay R, Hoh JH, Rosenberry TL (2002) Growth of beta-amyloid(1-40) protofibrils by monomer elongation and lateral association. Characterization of distinct products by light scattering and atomic force microscopy. Biochemistry 41:6115-6127.

Nikolaev A, McLaughlin T, O'Leary DD, Tessier-Lavigne M (2009) APP binds DR6 to trigger axon pruning and neuron death via distinct caspases. Nature 457:981-989.

Nishimoto I, Okamoto T, Matsuura Y, Takahashi S, Okamoto T, Murayama Y, Ogata E (1993) Alzheimer amyloid protein precursor complexes with brain GTP-binding protein G(o). Nature 362:75-79.
Oda T, Wals P, Osterburg HH, Johnson SA, Pasinetti GM, Morgan TE, Rozovsky I, Stine WB, Snyder SW, Holzman TF, . (1995) Clusterin (apoJ) alters the aggregation of amyloid beta-peptide (A beta 1-42) and forms slowly sedimenting A beta complexes that cause oxidative stress. Exp Neurol 136:22-31.

Oddo S, Caccamo A, Kitazawa M, Tseng BP, LaFerla FM (2003) Amyloid deposition precedes tangle formation in a triple transgenic model of Alzheimer's disease. Neurobiol Aging 24:1063-1070.

Oddo S, Caccamo A, Shepherd JD, Murphy MP, Golde TE, Kayed R, Metherate R, Mattson MP, Akbari Y, LaFerla FM (2003b) Triple-transgenic model of Alzheimer's disease with plaques and tangles: intracellular Abeta and synaptic dysfunction. Neuron 39:409-421.

Oddo S, Caccamo A, Tran L, Lambert MP, Glabe CG, Klein WL, LaFerla FM (2006) Temporal profile of amyloid-beta (Abeta) oligomerization in an in vivo model of Alzheimer disease. A link between Abeta and tau pathology. J Biol Chem 281:1599-1604.

Ohyagi Y (2008) Intracellular amyloid beta-protein as a therapeutic target for treating Alzheimer's disease. Curr Alzheimer Res 5:555-561.

Oishi M, Nairn AC, Czernik AJ, Lim GS, Isohara T, Gandy SE, Greengard P, Suzuki T (1997) The cytoplasmic domain of Alzheimer's amyloid precursor protein is phosphorylated at Thr654, Ser655, and Thr668 in adult rat brain and cultured cells. Mol Med 3:111-123.

Okochi M, Walter J, Koyama A, Nakajo S, Baba M, Iwatsubo T, Meijer L, Kahle PJ, Haass C (2000) Constitutive phosphorylation of the Parkinson's disease associated alpha-synuclein. J Biol Chem 275:390-397.

O'Nuallain B, Wetzel R (2002) Conformational Abs recognizing a generic amyloid fibril epitope. Proc Natl Acad Sci U S A 99:1485-1490.

Orstavik S, Funderud A, Hafte TT, Eikvar S, Jahnsen T, Skalhegg BS (2005) Identification and characterization of novel PKA holoenzymes in human T lymphocytes. FEBS J 272:1559-1567.

Orstavik S, Reinton N, Frengen E, Langeland BT, Jahnsen T, Skalhegg BS (2001) Identification of novel splice variants of the human catalytic subunit Cbeta of cAMP-dependent protein kinase. Eur J Biochem 268:5066-5073.

Otvos L, Jr., Szendrei GI, Lee VM, Mantsch HH (1993) Human and rodent Alzheimer beta-amyloid peptides acquire distinct conformations in membrane-mimicking solvents. Eur J Biochem 211:249-257.

Paas Y, Bohana-Kashtan O, Fishelson Z (1999) Phosphorylation of the complement component, C9, by an ecto-protein kinase of human leukemic cells. Immunopharmacology 42:175-185.

Paas Y, Fishelson Z (1995) Shedding of tyrosine and serine/threonine ecto-protein kinases from human leukemic cells. Arch Biochem Biophys 316:780-788.

Pakaski M, Balaspiri L, Checler F, Kasa P (2002) Human amyloid-beta causes changes in the levels of endothelial protein kinase C and its alpha isoform in vitro. Neurochem Int 41:409-414.

Pakaski M, Kalman J (2008) Interactions between the amyloid and cholinergic mechanisms in Alzheimer's disease. Neurochem Int 53:103-111.

Park SY, Ferreira A (2005) The generation of a 17 kDa neurotoxic fragment: an alternative mechanism by which tau mediates beta-amyloid-induced neurodegeneration. J Neurosci 25:5365-5375.
Pascale A, Amadio M, Govoni S, Battaini F (2007) The aging brain, a key target for the future: the protein kinase C involvement. Pharmacol Res 55:560-569.

Pearson HA, Peers C (2006) Physiological roles for amyloid beta peptides. J Physiol 575:5-10.

Pellarin R, Caflisch A (2006) Interpreting the aggregation kinetics of amyloid peptides. J Mol Biol 360:882-892.

Perez RG, Zheng H, Van der Ploeg LH, Koo EH (1997) The beta-amyloid precursor protein of Alzheimer's disease enhances neuron viability and modulates neuronal polarity. J Neurosci 17:9407-9414.

Petkova AT, Ishii Y, Balbach JJ, Antzutkin ON, Leapman RD, Delaglio F, Tycko R (2002) A structural model for Alzheimer's beta -amyloid fibrils based on experimental constraints from solid state NMR. Proc Natl Acad Sci U S A 99:16742-16747.

Petkova AT, Leapman RD, Guo Z, Yau WM, Mattson MP, Tycko R (2005) Self-propagating, molecular-level polymorphism in Alzheimer's beta-amyloid fibrils. Science 307:262-265.

Pfeffer RI, Afifi AA, Chance JM (1987) Prevalence of Alzheimer's disease in a retirement community. Am J Epidemiol 125:420-436.

Piccini A, Russo C, Gliozzi A, Relini A, Vitali A, Borghi R, Giliberto L, Armirotti A, D'Arrigo C, Bachi A, Cattaneo A, Canale C, Torrassa S, Saido TC, Markesbery W, Gambetti P, Tabaton M (2005) beta-amyloid is different in normal aging and in Alzheimer disease. J Biol Chem 280:34186-34192.

Pike CJ, Burdick D, Walencewicz AJ, Glabe CG, Cotman CW (1993) Neurodegeneration induced by beta-amyloid peptides in vitro: the role of peptide assembly state. J Neurosci 13:1676-1687.

Pike CJ, Overman MJ, Cotman CW (1995) Amino-terminal deletions enhance aggregation of beta-amyloid peptides in vitro. J Biol Chem 270:23895-23898.

Pike CJ, Walencewicz AJ, Glabe CG, Cotman CW (1991) In vitro aging of beta-amyloid protein causes peptide aggregation and neurotoxicity. Brain Res 563:311-314.

Price BH, Gurvit H, Weintraub S, Geula C, Leimkuhler E, Mesulam M (1993) Neuropsychological patterns and language deficits in 20 consecutive cases of autopsy-confirmed Alzheimer's disease. Arch Neurol 50:931-937.

Price DL WPMALMTGCDSSBDR (2000) The Value of Transgenic Models for the Study of Neurodegenerative Diseases. Ann N Y Acad Sci 920:179-191.

Priller C, Bauer T, Mitteregger G, Krebs B, Kretzschmar HA, Herms J (2006) Synapse formation and function is modulated by the amyloid precursor protein. J Neurosci 26:7212-7221.

Prusiner SB (1998) Prions. Proc Natl Acad Sci U S A 95:13363-13383.

Puchades M, Hansson SF, Nilsson CL, Andreasen N, Blennow K, Davidsson P (2003) Proteomic studies of potential cerebrospinal fluid protein markers for Alzheimer's disease. Brain Res Mol Brain Res 118:140-146.

Ramos BP, Birnbaum SG, Lindenmayer I, Newton SS, Duman RS, Arnsten AF (2003) Dysregulation of protein kinase a signaling in the aged prefrontal cortex: new strategy for treating age-related cognitive decline. Neuron 40:835-845.

Rasool CG, Svendsen CN, Selkoe DJ (1986) Neurofibrillary degeneration of cholinergic and noncholinergic neurons of the basal forebrain in Alzheimer's disease. Ann Neurol 20:482-488.

Redegeld FA, Caldwell CC, Sitkovsky MV (1999) Ecto-protein kinases: ecto-domain phosphorylation as a novel target for pharmacological manipulation? Trends Pharmacol Sci 20:453-459.

Reinhard C, Hebert SS, De SB (2005) The amyloid-beta precursor protein: integrating structure with biological function. EMBO J 24:3996-4006.

Riccio A, Ahn S, Davenport CM, Blendy JA, Ginty DD (1999) Mediation by a CREB family transcription factor of NGF-dependent survival of sympathetic neurons. Science 286:2358-2361.

Ridley RM, Baker HF, Windle CP, Cummings RM (2006) Very long term studies of the seeding of beta-amyloidosis in primates. J Neural Transm 113:1243-1251.

Ring S, Weyer SW, Kilian SB, Waldron E, Pietrzik CU, Filippov MA, Herms J, Buchholz C, Eckman CB, Korte M, Wolfer DP, Muller UC (2007) The secreted beta-amyloid precursor protein ectodomain APPs alpha is sufficient to rescue the anatomical, behavioral, and electrophysiological abnormalities of APP-deficient mice. J Neurosci 27:7817-7826.

Roach PJ (1991) Multisite and hierarchal protein phosphorylation. J Biol Chem 266:14139-14142.
Roberson ED, Scearce-Levie K, Palop JJ, Yan F, Cheng IH, Wu T, Gerstein H, Yu GQ, Mucke L (2007) Reducing endogenous tau ameliorates amyloid beta-induced deficits in an Alzheimer's disease mouse model. Science 316:750-754.

Roch JM, Jin LW, Ninomiya H, Schubert D, Saitoh T (1993) Biologically active domain of the secreted form of the amyloid beta/A4 protein precursor. Ann N Y Acad Sci 695:149-157.

Rochet JC (2007) Novel therapeutic strategies for the treatment of protein-misfolding diseases. Expert Rev Mol Med 9:1-34.

Rochet JC, Lansbury PT, Jr. (2000) Amyloid fibrillogenesis: themes and variations. Curr Opin Struct Biol 10:60-68.

Rodriguez F, Allende CC, Allende JE (2005) Protein kinase casein kinase 2 holoenzyme produced ectopically in human cells can be exported to the external side of the cellular membrane. Proc Natl Acad Sci U S A 102:4718-4723.

Roher AE, Chaney MO, Kuo YM, Webster SD, Stine WB, Haverkamp LJ, Woods AS, Cotter RJ, Tuohy JM, Krafft GA, Bonnell BS, Emmerling MR (1996) Morphology and toxicity of Abeta-(1-42) dimer derived from neuritic and vascular amyloid deposits of Alzheimer's disease. J Biol Chem 271:20631-20635.

Rosen DR, Martin-Morris L, Luo LQ, White K (1989) A Drosophila gene encoding a protein resembling the human beta-amyloid protein precursor. Proc Natl Acad Sci U S A 86:2478-2482.

Ross CA, Poirier MA (2004) Protein aggregation and neurodegenerative disease. Nat Med 10 Suppl:S10-S17.

Ross CA, Poirier MA (2005) Opinion: What is the role of protein aggregation in neurodegeneration? Nat Rev Mol Cell Biol 6:891-898.

Roychaudhuri R, Yang M, Hoshi MM, Teplow DB (2009) Amyloid beta-protein assembly and Alzheimer disease. J Biol Chem 284:4749-4753.

Russo C, Dolcini V, Salis S, Venezia V, Violani E, Carlo P, Zambrano N, Russo T, Schettini G (2002a) Signal transduction through tyrosine-phosphorylated carboxy-terminal fragments of APP via an enhanced interaction with Shc/Grb2 adaptor proteins in reactive astrocytes of Alzheimer's disease brain. Ann N Y Acad Sci 973:323-333.

Russo C, Dolcini V, Salis S, Venezia V, Zambrano N, Russo T, Schettini G (2002b) Signal transduction through tyrosine-phosphorylated C-terminal fragments of amyloid precursor protein via an enhanced interaction with Shc/Grb2 adaptor proteins in reactive astrocytes of Alzheimer's disease brain. J Biol Chem 277:35282-35288.

Rydel RE, Greene LA (1988) cAMP analogs promote survival and neurite outgrowth in cultures of rat sympathetic and sensory neurons independently of nerve growth factor. Proc Natl Acad Sci U S A 85:1257-1261.

Sachse C, Xu C, Wieligmann K, Diekmann S, Grigorieff N, Fandrich M (2006) Quaternary structure of a mature amyloid fibril from Alzheimer's Abeta(1-40) peptide. J Mol Biol 362:347-354.

Saido TC (1998) Alzheimer's disease as proteolytic disorders: anabolism and catabolism of beta-amyloid. Neurobiol Aging 19:S69-S75.

Saido TC, Iwatsubo T, Mann DM, Shimada H, Ihara Y, Kawashima S (1995) Dominant and differential deposition of distinct beta-amyloid peptide species, A beta N3(pE), in senile plaques. Neuron 14:457-466.

Saido TC, Yamao-Harigaya W, Iwatsubo T, Kawashima S (1996) Amino- and carboxyl-terminal heterogeneity of beta-amyloid peptides deposited in human brain. Neurosci Lett 215:173-176.

Saito H (2001) Histidine phosphorylation and two-component signaling in eukaryotic cells. Chem Rev 101:2497-2509.

Saitoh T, Cole G, Huynh TV (1990) Aberrant protein kinase C cascades in Alzheimer's disease. Adv Exp Med Biol 265:301-310.

Saitoh T, Iimoto D (1989) Aberrant protein phosphorylation and cytoarchitecture in Alzheimer's disease. Prog Clin Biol Res 317:769-780.

Saitoh T, Masliah E, Jin LW, Cole GM, Wieloch T, Shapiro IP (1991) Protein kinases and phosphorylation in neurologic disorders and cell death. Lab Invest 64:596-616.

Saitoh T, Sundsmo M, Roch JM, Kimura N, Cole G, Schubert D, Oltersdorf T, Schenk DB (1989) Secreted form of amyloid beta protein precursor is involved in the growth regulation of fibroblasts. Cell 58:615-622.

Sano Y, Nakaya T, Pedrini S, Takeda S, Iijima-Ando K, Iijima K, Mathews PM, Itohara S, Gandy S, Suzuki T (2006) Physiological mouse brain Abeta levels are not related to the phosphorylation state of threonine-668 of Alzheimer's APP. PLoS ONE 1:e51.

Santucci R, Sinibaldi F, Fiorucci L (2008) Protein folding, unfolding and misfolding: role played by intermediate States. Mini Rev Med Chem 8:57-62.

Sathasivam K, Hobbs C, Mangiarini L, Mahal A, Turmaine M, Doherty P, Davies SW, Bates GP (1999) Transgenic models of Huntington's disease. Philos Trans R Soc Lond B Biol Sci 354:963-969.

Saunders AM, Strittmatter WJ, Schmechel D, George-Hyslop PH, Pericak-Vance MA, Joo SH, Rosi BL, Gusella JF, Crapper-MacLachlan DR, Alberts MJ, . (1993) Association of apolipoprotein E allele epsilon 4 with late-onset familial and sporadic Alzheimer's disease. Neurology 43:1467-1472.
Sawaya MR, Sambashivan S, Nelson R, Ivanova MI, Sievers SA, Apostol MI, Thompson MJ, Balbirnie M, Wiltzius JJ, McFarlane HT, Madsen AO, Riekel C, Eisenberg D (2007) Atomic structures of amyloid cross-beta spines reveal varied steric zippers. Nature 447:453-457.

Scheff SW, DeKosky ST, Price DA (1990) Quantitative assessment of cortical synaptic density in Alzheimer's disease. Neurobiol Aging 11:29-37.

Scheff SW, Price DA (2003) Synaptic pathology in Alzheimer's disease: a review of ultrastructural studies. Neurobiol Aging 24:1029-1046.

Schenk D, Games KD, McConlogue L (1995) The potential utility of transgenic mice harboring beta-amyloid precursor protein. Neurobiol Aging 16:711-713.

Schilling S, Lauber T, Schaupp M, Manhart S, Scheel E, Bohm G, Demuth HU (2006) On the seeding and oligomerization of pGlu-amyloid peptides (in vitro). Biochemistry 45:12393-12399.

Schilling S, Zeitschel U, Hoffmann T, Heiser U, Francke M, Kehlen A, Holzer M, Hutter-Paier B, Prokesch M, Windisch M, Jagla W, Schlenzig D, Lindner C, Rudolph T, Reuter G, Cynis H, Montag D, Demuth HU, Rossner S (2008) Glutaminyl cyclase inhibition attenuates pyroglutamate Abeta and Alzheimer's disease-like pathology. Nat Med 14:1106-1111.

Schlaeger E, Kohler G (1976) External cyclic AMP-dependent protein kinase activity in rat C-6 glioma cells. Nature 260:705-707.

Schmechel DE, Saunders AM, Strittmatter WJ, Crain BJ, Hulette CM, Joo SH, Pericak-Vance MA, Goldgaber D, Roses AD (1993) Increased amyloid beta-peptide deposition in cerebral cortex as a consequence of apolipoprotein E genotype in late-onset Alzheimer disease. Proc Natl Acad Sci U S A 90:9649-9653.

Schmidt C, Lepsverdize E, Chi SL, Das AM, Pizzo SV, Dityatev A, Schachner M (2007) Amyloid precursor protein and amyloid beta-peptide bind to ATP synthase and regulate its activity at the surface of neural cells. Mol Psychiatry.

Schmittschmitt JP, Scholtz JM (2003) The role of protein stability, solubility, and net charge in amyloid fibril formation. Protein Sci 12:2374-2378.

Schoenberg BS, Kokmen E, Okazaki H (1987) Alzheimer's disease and other dementing illnesses in a defined United States population: incidence rates and clinical features. Ann Neurol 22:724-729.

Schroeter EH, Ilagan MX, Brunkan AL, Hecimovic S, Li YM, Xu M, Lewis HD, Saxena MT, De SB, Coonrod A, Tomita T, Iwatsubo T, Moore CL, Goate A, Wolfe MS, Shearman M, Kopan R (2003) A presenilin dimer at the core of the gamma-secretase enzyme: insights from parallel analysis of Notch 1 and APP proteolysis. Proc Natl Acad Sci U S A 100:13075-13080.

Schroeter S, Khan K, Barbour R, Doan M, Chen M, Guido T, Gill D, Basi G, Schenk D, Seubert P, Games D (2008) Immunotherapy reduces vascular amyloid-beta in PDAPP mice. J Neurosci 28:6787-6793.

Schubert D, Jin LW, Saitoh T, Cole G (1989a) The regulation of amyloid beta protein precursor secretion and its modulatory role in cell adhesion. Neuron 3:689-694.

Schubert D, LaCorbiere M, Saitoh T, Cole G (1989b) Characterization of an amyloid beta precursor protein that binds heparin and contains tyrosine sulfate. Proc Natl Acad Sci U S A 86:2066-2069.

Schvartz I, Kreizman T, Brumfeld V, Gechtman Z, Seger D, Shaltiel S (2002) The PKA phosphorylation of vitronectin: effect on conformation and function. Arch Biochem Biophys 397:246-252.

Schwab C, DeMaggio AJ, Ghoshal N, Binder LI, Kuret J, McGeer PL (2000) Casein kinase 1 delta is associated with pathological accumulation of tau in several neurodegenerative diseases. Neurobiol Aging 21:503-510.

Seabrook GR, Smith DW, Bowery BJ, Easter A, Reynolds T, Fitzjohn SM, Morton RA, Zheng H, Dawson GR, Sirinathsinghji DJ, Davies CH, Collingridge GL, Hill RG (1999) Mechanisms contributing to the deficits in hippocampal synaptic plasticity in mice lacking amyloid precursor protein. Neuropharmacology 38:349-359.

Selkoe DJ (1994) Amyloid beta-protein precursor: new clues to the genesis of Alzheimer's disease. Curr Opin Neurobiol 4:708-716.

Selkoe DJ (1998) The cell biology of beta-amyloid precursor protein and presenilin in Alzheimer's disease. Trends Cell Biol. 8.11: 447-53.

Selkoe DJ (2000) The genetics and molecular pathology of Alzheimer's disease: roles of amyloid and the presenilins. Neurol Clin 18:903-922.

Selkoe DJ (2001a) Alzheimer's disease: genes, proteins, and therapy. Physiol Rev 81:741-766.

Selkoe DJ (2001b) Clearing the brain's amyloid cobwebs. Neuron 32:177-180.

Selkoe DJ (2002) Alzheimer's disease is a synaptic failure. Science 298:789-791.

Selkoe DJ (2003) Folding proteins in fatal ways. Nature 426:900-904.

Selkoe DJ (2004a) Alzheimer disease: mechanistic understanding predicts novel therapies. Ann Intern Med 140:627-638.

Selkoe DJ (2004b) Cell biology of protein misfolding: the examples of Alzheimer's and Parkinson's diseases. Nat Cell Biol 6:1054-1061.

Selkoe DJ (2008) Soluble oligomers of the amyloid beta-protein impair synaptic plasticity and behavior. Behav Brain Res 192:106-113.

Selkoe DJ, Abraham CR, Podlisny MB, Duffy LK (1986) Isolation of low-molecular-weight proteins from amyloid plaque fibers in Alzheimer's disease. J Neurochem 46:1820-1834.

Selkoe DJ, Bell DS, Podlisny MB, Price DL, Cork LC (1987) Conservation of brain amyloid proteins in aged mammals and humans with Alzheimer's disease. Science 235:873-877.

Selkoe DJ, Wolfe MS (2007) Presenilin: running with scissors in the membrane. Cell 131:215-221.

Serio TR, Cashikar AG, Kowal AS, Sawicki GJ, Moslehi JJ, Serpell L, Arnsdorf MF, Lindquist SL (2000) Nucleated conformational conversion and the replication of conformational information by a prion determinant. Science 289:1317-1321.

Serpell LC (2000) Alzheimer's amyloid fibrils: structure and assembly. Biochim Biophys Acta 1502:16-30.

Serpell LC, Berriman J, Jakes R, Goedert M, Crowther RA (2000) Fiber diffraction of synthetic alpha-synuclein filaments shows amyloid-like cross-beta conformation. Proc Natl Acad Sci U S A 97:4897-4902.

Serpell LC, Smith JM (2000) Direct visualisation of the beta-sheet structure of synthetic Alzheimer's amyloid. J Mol Biol 299:225-231.

Seubert P, Barbour R, Khan K, Motter R, Tang P, Kholodenko D, Kling K, Schenk D, Johnson-Wood K, Schroeter S, Gill D, Jacobsen JS, Pangalos M, Basi G, Games D (2008) Antibody capture of soluble Abeta does not reduce cortical Abeta amyloidosis in the PDAPP mouse. Neurodegener Dis 5:65-71.

Seubert P, Vigo-Pelfrey C, Esch F, Lee M, Dovey H, Davis D, Sinha S, Schlossmacher M, Whaley J, Swindlehurst C, . (1992) Isolation and quantification of soluble Alzheimer's beta-peptide from biological fluids. Nature 359:325-327.

Shaltiel S, Schvartz I, Korc-Grodzicki B, Kreizman T (1993) Evidence for an extra-cellular function for protein kinase A. Mol Cell Biochem 127-128:283-291.

Shankar GM, Li S, Mehta TH, Garcia-Munoz A, Shepardson NE, Smith I, Brett FM, Farrell MA, Rowan MJ, Lemere CA, Regan CM, Walsh DM, Sabatini BL, Selkoe DJ (2008) Amyloid-beta protein dimers isolated directly from Alzheimer's brains impair synaptic plasticity and memory. Nat Med 14:837-842.

Shanmugam G, Polavarapu PL, Hallgas B, Majer Z (2005) Effect of D-amino acids at Asp23 and Ser26 residues on the conformational preference of Abeta20-29 peptides. Biochem Biophys Res Commun 335:712-722.

Sherrington R, Rogaev EI, Liang Y, Rogaeva EA, Levesque G, Ikeda M, Chi H, Lin C, Li G, Holman K, . (1995) Cloning of a gene bearing missense mutations in early-onset familial Alzheimer's disease. Nature 375:754-760.

Shioi J, Refolo LM, Efthimiopoulos S, Robakis NK (1993) Chondroitin sulfate proteoglycan form of cellular and cell-surface Alzheimer amyloid precursor. Neurosci Lett 154:121-124.

Sickmann A, Dormeyer W, Wortelkamp S, Woitalla D, Kuhn W, Meyer HE (2002) Towards a high resolution separation of human cerebrospinal fluid. J Chromatogr B Analyt Technol Biomed Life Sci 771:167-196.

Simard AR, Soulet D, Gowing G, Julien JP, Rivest S (2006) Bone marrow-derived microglia play a critical role in restricting senile plaque formation in Alzheimer's disease. Neuron 49:489-502.

Skubitz KM, Ehresmann DD, Ducker TP (1991) Characterization of human neutrophil ecto-protein kinase activity released by kinase substrates. J Immunol 147:638-650.

Small SA, Duff K (2008) Linking Abeta and tau in late-onset Alzheimer's disease: a dual pathway hypothesis. Neuron 60:534-542.

Smith RP, Higuchi DA, Broze GJ, Jr. (1990) Platelet coagulation factor XIa-inhibitor, a form of Alzheimer amyloid precursor protein. Science 248:1126-1128.

Soderling TR (1979) Regulatory functions of protein multisite phosphorylation. Mol Cell Endocrinol 16:157-179.

Solomon B, Koppel R, Frankel D, Hanan-Aharon E (1997) Disaggregation of Alzheimer beta-amyloid by site-directed mAb. Proc Natl Acad Sci U S A 94:4109-4112.

Song HJ, Poo MM (1999) Signal transduction underlying growth cone guidance by diffusible factors. Curr Opin Neurobiol 9:355-363.

Songyang Z, Lu KP, Kwon YT, Tsai LH, Filhol O, Cochet C, Brickey DA, Soderling TR, Bartleson C, Graves DJ, DeMaggio AJ, Hoekstra MF, Blenis J, Hunter T, Cantley LC (1996) A structural basis for substrate specificities of protein Ser/Thr kinases: primary sequence preference of casein kinases I and II, NIMA, phosphorylase kinase, calmodulin-dependent kinase II, CDK5, and Erk1. Mol Cell Biol 16:6486-6493.

Soto C, Castano EM (1996) The conformation of Alzheimer's beta peptide determines the rate of amyloid formation and its resistance to proteolysis. Biochem J 314 (Pt 2):701-707.

Soto C, Estrada L, Castilla J (2006) Amyloids, prions and the inherent infectious nature of misfolded protein aggregates. Trends Biochem Sci 31:150-155.

Soto C, Estrada LD (2008) Protein misfolding and neurodegeneration. Arch Neurol 65:184-189.

Soto C, Kindy MS, Baumann M, Frangione B (1996) Inhibition of Alzheimer's amyloidosis by peptides that prevent beta-sheet conformation. Biochem Biophys Res Commun 226:672-680.

Spires TL, Meyer-Luehmann M, Stern EA, McLean PJ, Skoch J, Nguyen PT, Bacskai BJ, Hyman BT (2005) Dendritic spine abnormalities in amyloid precursor protein transgenic mice demonstrated by gene transfer and intravital multiphoton microscopy. J Neurosci 25:7278-7287.

Spires-Jones TL, Mielke ML, Rozkalne A, Meyer-Luehmann M, de CA, Bacskai BJ, Schenk D, Hyman BT (2009) Passive immunotherapy rapidly increases structural plasticity in a mouse model of Alzheimer disease. Neurobiol Dis 33:213-220.

Sprang SR, Acharya KR, Goldsmith EJ, Stuart DI, Varvill K, Fletterick RJ, Madsen NB, Johnson LN (1988) Structural changes in glycogen phosphorylase induced by phosphorylation. Nature 336:215-221.

St George-Hyslop PH, Tanzi RE, Polinsky RJ, Neve RL, Pollen D, Drachman D, Growdon J, Cupples LA, Nee L, Myers RH, . (1987) Absence of duplication of chromosome 21 genes in familial and sporadic Alzheimer's disease. Science 238:664-666.

Standen CL, Brownlees J, Grierson AJ, Kesavapany S, Lau KF, McLoughlin DM, Miller CC (2001) Phosphorylation of thr(668) in the cytoplasmic domain of the Alzheimer's disease amyloid precursor protein by stress-activated protein kinase 1b (Jun N-terminal kinase-3). J Neurochem 76:316-320.

Steffan JS, Agrawal N, Pallos J, Rockabrand E, Trotman LC, Slepko N, Illes K, Lukacsovich T, Zhu YZ, Cattaneo E, Pandolfi PP, Thompson LM, Marsh JL (2004) SUMO modification of Huntingtin and Huntington's disease pathology. Science 304:100-104.

Stern EA, Bacskai BJ, Hickey GA, Attenello FJ, Lombardo JA, Hyman BT (2004) Cortical synaptic integration in vivo is disrupted by amyloid-beta plaques. J Neurosci 24:4535-4540.

Streit WJ (2004) Microglia and Alzheimer's disease pathogenesis. J Neurosci Res 77:1-8.

Streit WJ, Mrak RE, Griffin WS (2004) Microglia and neuroinflammation: a pathological perspective. J Neuroinflammation 1:14.

Strittmatter WJ, Saunders AM, Schmechel D, Pericak-Vance M, Enghild J, Salvesen GS, Roses AD (1993) Apolipoprotein E: high-avidity binding to beta-amyloid and increased frequency of type 4 allele in late-onset familial Alzheimer disease. Proc Natl Acad Sci U S A 90:1977-1981.

Su JH, Cummings BJ, Cotman CW (1996) Plaque biogenesis in brain aging and Alzheimer's disease. I. Progressive changes in phosphorylation states of paired helical filaments and neurofilaments. Brain Res 739:79-87.
Su Y, Ryder J, Ni B (2003) Inhibition of Abeta production and APP maturation by a specific PKA inhibitor. FEBS Lett 546:407-410.

Sugimoto H (2008) The new approach in development of anti-Alzheimer's disease drugs via the cholinergic hypothesis. Chem Biol Interact 175:204-208.

Suh YH, Checler F (2002) Amyloid precursor protein, presenilins, and alpha-synuclein: molecular pathogenesis and pharmacological applications in Alzheimer's disease. Pharmacol Rev 54:469-525.

Sunde M, Blake C (1997) The structure of amyloid fibrils by electron microscopy and X-ray diffraction. Adv Protein Chem 50:123-159.

Sunde M, Serpell LC, Bartlam M, Fraser PE, Pepys MB, Blake CC (1997) Common core structure of amyloid fibrils by synchrotron X-ray diffraction. J Mol Biol 273:729-739.

Suzuki N, Cheung TT, Cai XD, Odaka A, Otvos L, Jr., Eckman C, Golde TE, Younkin SG (1994) An increased percentage of long amyloid beta protein secreted by familial amyloid beta protein precursor (beta APP717) mutants. Science 264:1336-1340.

Suzuki T, Ando K, Isohara T, Oishi M, Lim GS, Satoh Y, Wasco W, Tanzi RE, Nairn AC, Greengard P, Gandy SE, Kirino Y (1997) Phosphorylation of Alzheimer beta-amyloid precursor-like proteins. Biochemistry 36:4643-4649.

Suzuki T, Nairn AC, Gandy SE, Greengard P (1992) Phosphorylation of Alzheimer amyloid precursor protein by protein kinase C. Neuroscience 48:755-761.

Suzuki T, Nakaya T (2008) Regulation of amyloid beta-protein precursor by phosphorylation and protein interactions. J Biol Chem 283:29633-29637.

Suzuki T, Oishi M, Marshak DR, Czernik AJ, Nairn AC, Greengard P (1994) Cell cycle-dependent regulation of the phosphorylation and metabolism of the Alzheimer amyloid precursor protein. EMBO J 13:1114-1122.

Swerdlow RH, Khan SM (2004) A "mitochondrial cascade hypothesis" for sporadic Alzheimer's disease. Med Hypotheses 63:8-20.

Tagliavini F, Giaccone G, Frangione B, Bugiani O (1988) Preamyloid deposits in the cerebral cortex of patients with Alzheimer's disease and nondemented individuals. Neurosci Lett 93:191-196.

Takano K (2008) Amyloid beta conformation in aqueous environment. Curr Alzheimer Res 5:540-547.

Tamaoka A, Sawamura N, Fukushima T, Shoji S, Matsubara E, Shoji M, Hirai S, Furiya Y, Endoh R, Mori H (1997) Amyloid beta protein 42(43) in cerebrospinal fluid of patients with Alzheimer's disease. J Neurol Sci 148:41-45.

Tamboli IY, Prager K, Barth E, Heneka M, Sandhoff K, Walter J (2005) Inhibition of glycosphingolipid biosynthesis reduces secretion of the beta-amyloid precursor protein and amyloid beta-peptide. J Biol Chem 280:28110-28117.

Tamboli IY, Prager K, Thal DR, Thelen KM, Dewachter I, Pietrzik CU, St George-Hyslop P, Sisodia SS, De SB, Heneka MT, Filippov MA, Muller U, Van LF, Lutjohann D, Walter J (2008) Loss of

gamma-secretase function impairs endocytosis of lipoprotein particles and membrane cholesterol homeostasis. J Neurosci 28:12097-12106.

Tan S, Maher P, Schubert D (1997) The role of protein phosphorylation in beta amyloid toxicity. Brain Res 765:159-163.

Tanzi RE, Bertram L (2001) New frontiers in Alzheimer's disease genetics. Neuron 32:181-184.
Tanzi RE, Moir RD, Wagner SL (2004) Clearance of Alzheimer's Abeta peptide: the many roads to perdition. Neuron 43:605-608.

Tao RS, Fei EK, Ying Z, Wang HF, Wang GH (2008) Casein kinase 2 interacts with and phosphorylates ataxin-3. Neurosci Bull 24:271-277.

Taru H, Iijima K, Hase M, Kirino Y, Yagi Y, Suzuki T (2002) Interaction of Alzheimer's beta - amyloid precursor family proteins with scaffold proteins of the JNK signaling cascade. J Biol Chem 277:20070-20078.

Teaktong T, Graham AJ, Court JA, Perry RH, Jaros E, Johnson M, Hall R, Perry EK (2004) Nicotinic acetylcholine receptor immunohistochemistry in Alzheimer's disease and dementia with Lewy bodies: differential neuronal and astroglial pathology. J Neurol Sci 225:39-49.

Tekirian TL (2001) Commentary: Abeta N- Terminal Isoforms: Critical contributors in the course of AD pathophysiology. J Alzheimers Dis 3:241-248.

Teplow DB, Lazo ND, Bitan G, Bernstein S, Wyttenbach T, Bowers MT, Baumketner A, Shea JE, Urbanc B, Cruz L, Borreguero J, Stanley HE (2006) Elucidating amyloid beta-protein folding and assembly: A multidisciplinary approach. Acc Chem Res 39:635-645.

Terry RD, Masliah E, Salmon DP, Butters N, DeTeresa R, Hill R, Hansen LA, Katzman R (1991) Physical basis of cognitive alterations in Alzheimer's disease: synapse loss is the major correlate of cognitive impairment. Ann Neurol 30:572-580.

Tew DJ, Bottomley SP, Smith DP, Ciccotosto GD, Babon J, Hinds MG, Masters CL, Cappai R, Barnham KJ (2008) Stabilization of neurotoxic soluble beta-sheet-rich conformations of the Alzheimer's disease amyloid-beta peptide. Biophys J 94:2752-2766.

Thakker DR, Weatherspoon MR, Harrison J, Keene TE, Lane DS, Kaemmerer WF, Stewart GR, Shafer LL (2009) Intracerebroventricular amyloid-beta antibodies reduce cerebral amyloid angiopathy and associated micro-hemorrhages in aged Tg2576 mice. Proc Natl Acad Sci U S A 106:4501-4506.

Thal DR, Capetillo-Zarate E, Del TK, Braak H (2006) The development of amyloid beta protein deposits in the aged brain. Sci Aging Knowledge Environ 2006:re1.

Thal DR, Griffin WS, de Vos RA, Ghebremedhin E (2008) Cerebral amyloid angiopathy and its relationship to Alzheimer's disease. Acta Neuropathol 115:599-609.

Tholey A, Lindemann A, Kinzel V, Reed J (1999) Direct effects of phosphorylation on the preferred backbone conformation of peptides: a nuclear magnetic resonance study. Biophys J 76:76-87.

Thompson EJ, Keir G (1990) Laboratory investigation of cerebrospinal fluid proteins. Ann Clin Biochem 27 (Pt 5):425-435.

Tomaselli S, Esposito V, Vangone P, van Nuland NA, Bonvin AM, Guerrini R, Tancredi T, Temussi PA, Picone D (2006) The alpha-to-beta conformational transition of Alzheimer's Abeta-(1-42) peptide in aqueous media is reversible: a step by step conformational analysis suggests the location of beta conformation seeding. Chembiochem 7:257-267.

Tomski SJ, Murphy RM (1992) Kinetics of aggregation of synthetic beta-amyloid peptide. Arch Biochem Biophys 294:630-638.
Townsend M, Shankar GM, Mehta T, Walsh DM, Selkoe DJ (2006) Effects of secreted oligomers of amyloid beta-protein on hippocampal synaptic plasticity: a potent role for trimers. J Physiol 572:477-492.

Tsai J, Grutzendler J, Duff K, Gan WB (2004) Fibrillar amyloid deposition leads to local synaptic abnormalities and breakage of neuronal branches. Nat Neurosci 7:1181-1183.

Tsuji S, Yamashita T, Nagai Y (1988) A novel, carbohydrate signal-mediated cell surface protein phosphorylation: ganglioside GQ1b stimulates ecto-protein kinase activity on the cell surface of a human neuroblastoma cell line, GOTO. J Biochem 104:498-503.

Tycko R (2006) Molecular structure of amyloid fibrils: insights from solid-state NMR. Q Rev Biophys 39:1-55.

Ubersax JA, Ferrell JE, Jr. (2007) Mechanisms of specificity in protein phosphorylation. Nat Rev Mol Cell Biol 8:530-541.

Ubersax JA, Woodbury EL, Quang PN, Paraz M, Blethrow JD, Shah K, Shokat KM, Morgan DO (2003) Targets of the cyclin-dependent kinase Cdk1. Nature 425:859-864.

Vanderstichele H, De MG, Andreasen N, Kostanjevecki V, Wallin A, Olsson A, Blennow K, Vanmechelen E (2005) Amino-truncated beta-amyloid42 peptides in cerebrospinal fluid and prediction of progression of mild cognitive impairment. Clin Chem 51:1650-1660.

Varvel NH, Bhaskar K, Patil AR, Pimplikar SW, Herrup K, Lamb BT (2008) Abeta oligomers induce neuronal cell cycle events in Alzheimer's disease. J Neurosci 28:10786-10793.

Vassar R, et al. (1999) Beta-secretase cleavage of Alzheimer's amyloid precursor protein by the transmembrane aspartic protease BACE. Science 286:735-741.

Vickers JC (1997) A cellular mechanism for the neuronal changes underlying Alzheimer's disease. Neuroscience 78:629-639.

Vickers JC, Dickson TC, Adlard PA, Saunders HL, King CE, McCormack G (2000) The cause of neuronal degeneration in Alzheimer's disease. Prog Neurobiol 60:139-165.

Vickers JC, Riederer BM, Marugg RA, Buee-Scherrer V, Buee L, Delacourte A, Morrison JH (1994) Alterations in neurofilament protein immunoreactivity in human hippocampal neurons related to normal aging and Alzheimer's disease. Neuroscience 62:1-13.

Vigo-Pelfrey C, Lee D, Keim P, Lieberburg I, Schenk DB (1993) Characterization of beta-amyloid peptide from human cerebrospinal fluid. J Neurochem 61:1965-1968.

Vincent I, Jicha G, Rosado M, Dickson DW (1997) Aberrant expression of mitotic cdc2/cyclin B1 kinase in degenerating neurons of Alzheimer's disease brain. J Neurosci 17:3588-3598.

Vingtdeux V, Hamdane M, Gompel M, Begard S, Drobecq H, Ghestem A, Grosjean ME, Kostanjevecki V, Grognet P, Vanmechelen E, Buee L, Delacourte A, Sergeant N (2005) Phosphorylation of amyloid precursor carboxy-terminal fragments enhances their processing by a gamma-secretase-dependent mechanism. Neurobiol Dis 20:625-637.

Vinters HV, Pardridge WM, Yang J (1988) Immunohistochemical study of cerebral amyloid angiopathy: use of an antiserum to a synthetic 28-amino-acid peptide fragment of the Alzheimer's disease amyloid precursor. Hum Pathol 19:214-222.

von Arnim CA, Tangredi MM, Peltan ID, Lee BM, Irizarry MC, Kinoshita A, Hyman BT (2004) Demonstration of BACE (beta-secretase) phosphorylation and its interaction with GGA1 in cells by fluorescence-lifetime imaging microscopy. J Cell Sci 117:5437-5445.

Wahle T, Prager K, Raffler N, Haass C, Famulok M, Walter J (2005) GGA proteins regulate retrograde transport of BACE1 from endosomes to the trans-Golgi network. Mol Cell Neurosci 29:453-461.

Wahle T, Thal DR, Sastre M, Rentmeister A, Bogdanovic N, Famulok M, Heneka MT, Walter J (2006) GGA1 is expressed in the human brain and affects the generation of amyloid beta-peptide. J Neurosci 26:12838-12846.

Walaas SI, Greengard P (1991) Protein phosphorylation and neuronal function. Pharmacol Rev 43:299-349.

Walsh DM, Hartley DM, Kusumoto Y, Fezoui Y, Condron MM, Lomakin A, Benedek GB, Selkoe DJ, Teplow DB (1999) Amyloid beta-protein fibrillogenesis. Structure and biological activity of protofibrillar intermediates. J Biol Chem 274:25945-25952.

Walsh DM, Klyubin I, Fadeeva JV, Cullen WK, Anwyl R, Wolfe MS, Rowan MJ, Selkoe DJ (2002a) Naturally secreted oligomers of amyloid beta protein potently inhibit hippocampal long-term potentiation in vivo. Nature 416:535-539.

Walsh DM, Klyubin I, Fadeeva JV, Rowan MJ, Selkoe DJ (2002b) Amyloid-beta oligomers: their production, toxicity and therapeutic inhibition. Biochem Soc Trans 30:552-557.

Walsh DM, Klyubin I, Shankar GM, Townsend M, Fadeeva JV, Betts V, Podlisny MB, Cleary JP, Ashe KH, Rowan MJ, Selkoe DJ (2005) The role of cell-derived oligomers of Abeta in Alzheimer's disease and avenues for therapeutic intervention. Biochem Soc Trans 33:1087-1090.

Walsh DM, Lomakin A, Benedek GB, Condron MM, Teplow DB (1997) Amyloid beta-protein fibrillogenesis. Detection of a protofibrillar intermediate. J Biol Chem 272:22364-22372.

Walsh DM, Minogue AM, Sala FC, Fadeeva JV, Wasco W, Selkoe DJ (2007) The APP family of proteins: similarities and differences. Biochem Soc Trans 35:416-420.

Walsh DM, Selkoe DJ (2004) Oligomers on the brain: the emerging role of soluble protein aggregates in neurodegeneration. Protein Pept Lett 11:213-228.

Walsh DM, Selkoe DJ (2007) A beta oligomers - a decade of discovery. J Neurochem 101:1172-1184.

Walter J, Capell A, Grunberg J, Pesold B, Schindzielorz A, Prior R, Podlisny MB, Fraser P, Hyslop PS, Selkoe DJ, Haass C (1996a) The Alzheimer's disease-associated presenilins are differentially phosphorylated proteins located predominantly within the endoplasmic reticulum. Mol Med 2:673-691.

Walter J, Capell A, Hung AY, Langen H, Schnolzer M, Thinakaran G, Sisodia SS, Selkoe DJ, Haass C (1997a) Ectodomain phosphorylation of beta-amyloid precursor protein at two distinct cellular locations. J Biol Chem 272:1896-1903.

Walter J, Fluhrer R, Hartung B, Willem M, Kaether C, Capell A, Lammich S, Multhaup G, Haass C (2001a) Phosphorylation regulates intracellular trafficking of beta-secretase. J Biol Chem 276:14634-14641.

Walter J, Grunberg J, Capell A, Pesold B, Schindzielorz A, Citron M, Mendla K, George-Hyslop PS, Multhaup G, Selkoe DJ, Haass C (1997b) Proteolytic processing of the Alzheimer disease-associated presenilin-1 generates an in vivo substrate for protein kinase C. Proc Natl Acad Sci U S A 94:5349-5354.

Walter J, Grunberg J, Schindzielorz A, Haass C (1998) Proteolytic fragments of the Alzheimer's disease associated presenilins-1 and -2 are phosphorylated in vivo by distinct cellular mechanisms. Biochemistry 37:5961-5967.

Walter J, Kaether C, Steiner H, Haass C (2001b) The cell biology of Alzheimer's disease: uncovering the secrets of secretases. Curr Opin Neurobiol 11:585-590.

Walter J, Kinzel V, Kubler D (1994) Evidence for CKI and CKII at the cell surface. Cell Mol Biol Res 40:473-480.

Walter J, Schindzielorz A, Hartung B, Haass C (2000) Phosphorylation of the beta-amyloid precursor protein at the cell surface by ectocasein kinases 1 and 2. J Biol Chem 275:23523-23529.

Walter J, Schnolzer M, Pyerin W, Kinzel V, Kubler D (1996b) Induced release of cell surface protein kinase yields CK1- and CK2-like enzymes in tandem. J Biol Chem 271:111-9.

Wang J, Tung YC, Wang Y, Li XT, Iqbal K, Grundke-Iqbal I (2001) Hyperphosphorylation and accumulation of neurofilament proteins in Alzheimer disease brain and in okadaic acid-treated SY5Y cells. FEBS Lett 507:81-87.

Wang JZ, Grundke-Iqbal I, Iqbal K (2007) Kinases and phosphatases and tau sites involved in Alzheimer neurofibrillary degeneration. Eur J Neurosci 25:59-68.

Wasco W, Bupp K, Magendantz M, Gusella JF, Tanzi RE, Solomon F (1992) Identification of a mouse brain cDNA that encodes a protein related to the Alzheimer disease-associated amyloid beta protein precursor. Proc Natl Acad Sci U S A 89:10758-10762.

Wasco W, Gurubhagavatula S, Paradis MD, Romano DM, Sisodia SS, Hyman BT, Neve RL, Tanzi RE (1993) Isolation and characterization of APLP2 encoding a homologue of the Alzheimer's associated amyloid beta protein precursor. Nat Genet 5:95-100.

Wegiel J, Bobinski M, Tarnawski M, Dziewiatkowski J, Popovitch E, Miller DC, Wisniewski T, Golomb J, de Leon MJ, Reisberg B (2001) Fibrillar amyloid-beta affects neurofibrillary changes but only in neurons already involved in neurofibrillary degeneration. Acta Neuropathol 101:585-590.

Weidemann A, Konig G, Bunke D, Fischer P, Salbaum JM, Masters CL, Beyreuther K (1989) Identification, biogenesis, and localization of precursors of Alzheimer's disease A4 amyloid protein. Cell 57:115-126.

West MJ, Coleman PD, Flood DG, Troncoso JC (1994) Differences in the pattern of hippocampal neuronal loss in normal ageing and Alzheimer's disease. Lancet 344:769-772.

Wetzel R, Shivaprasad S, Williams AD (2007) Plasticity of amyloid fibrils. Biochemistry 46:1-10.
Wevers A, Schroder H (1999) Nicotinic acetylcholine receptors in Alzheimer's disease. J Alzheimers Dis 1:207-219.

Whitehouse PJ, Martino AM, Antuono PG, Lowenstein PR, Coyle JT, Price DL, Kellar KJ (1986) Nicotinic acetylcholine binding sites in Alzheimer's disease. Brain Res 371:146-151.

Williams AD, Portelius E, Kheterpal I, Guo JT, Cook KD, Xu Y, Wetzel R (2004) Mapping abeta amyloid fibril secondary structure using scanning proline mutagenesis. J Mol Biol 335:833-842.

Williams AD, Shivaprasad S, Wetzel R (2006) Alanine scanning mutagenesis of Abeta(1-40) amyloid fibril stability. J Mol Biol 357:1283-1294.

Winklhofer KF, Tatzelt J, Haass C (2008) The two faces of protein misfolding: gain- and loss-of-function in neurodegenerative diseases. EMBO J 27:336-349.

Wisniewski HM, Wegiel J, Wang KC, Kujawa M, Lach B (1989) Ultrastructural studies of the cells forming amyloid fibers in classical plaques. Can J Neurol Sci 16:535-542.

Wood JG, Mirra SS, Pollock NJ, Binder LI (1986) Neurofibrillary tangles of Alzheimer disease share antigenic determinants with the axonal microtubule-associated protein tau (tau). Proc Natl Acad Sci U S A 83:4040-4043.

Wood SJ, Maleeff B, Hart T, Wetzel R (1996) Physical, morphological and functional differ-ences between ph 5.8 and 7.4 aggregates of the Alzheimer's amyloid peptide Abeta. J Mol Biol 256:870-877.

Wurth C, Kim W, Hecht MH (2006) Combinatorial approaches to probe the sequence determinants of protein aggregation and amyloidogenicity. Protein Pept Lett 13:279-286.

Xia W, Zhang J, Kholodenko D, Citron M, Podlisny MB, Teplow DB, Haass C, Seubert P, Koo EH, Selkoe DJ (1997) Enhanced production and oligomerization of the 42-residue amyloid beta-protein by Chinese hamster ovary cells stably expressing mutant presenilins. J Biol Chem 272:7977-7982.

Xu H, Sweeney D, Greengard P, Gandy S (1996) Metabolism of Alzheimer beta-amyloid precursor protein: regulation by protein kinase A in intact cells and in a cell-free system. Proc Natl Acad Sci U S A 93:4081-4084.

Yamaguchi H, Hirai S, Morimatsu M, Shoji M, Ihara Y (1988) A variety of cerebral amyloid deposits in the brains of the Alzheimer-type dementia demonstrated by beta protein immunostaining. Acta Neuropathol 76:541-549.

Yamaguchi H, Nakazato Y, Hirai S, Shoji M, Harigaya Y (1989) Electron micrograph of diffuse plaques. Initial stage of senile plaque formation in the Alzheimer brain. Am J Pathol 135:593-597.

Yamaguchi K, Takahashi S, Kawai T, Naiki H, Goto Y (2005) Seeding-dependent propagation and maturation of amyloid fibril conformation. J Mol Biol 352:952-960.

Yamazaki D, Saitoe M (2008) [cAMP/PKA signaling underlies age-related memory impairment]. Brain Nerve 60:717-724.

Yang Y, Varvel NH, Lamb BT, Herrup K (2006) Ectopic cell cycle events link human Alzheimer's disease and amyloid precursor protein transgenic mouse models. J Neurosci 26:775-784.

Yasojima K, Kuret J, DeMaggio AJ, McGeer E, McGeer PL (2000) Casein kinase 1 delta mRNA is upregulated in Alzheimer disease brain. Brain Res 865:116-120.

Yoshiike Y, Minai R, Matsuo Y, Chen YR, Kimura T, Takashima A (2008) Amyloid oligomer conformation in a group of natively folded proteins. PLoS ONE 3:e3235.

Yu L, Edalji R, Harlan JE, Holzman TF, Lopez AP, Labkovsky B, Hillen H, Barghorn S, Ebert U, Richardson PL, Miesbauer L, Solomon L, Bartley D, Walter K, Johnson RW, Hajduk PJ, Olejniczak ET (2009) Structural Characterization of a Soluble Amyloid beta-Peptide Oligomer. Biochemistry.

Zhang J, Goodlett DR, Quinn JF, Peskind E, Kaye JA, Zhou Y, Pan C, Yi E, Eng J, Wang Q, Aebersold RH, Montine TJ (2005) Quantitative proteomics of cerebrospinal fluid from patients with Alzheimer disease. J Alzheimers Dis 7:125-133.
Zhang J, Kornecki E, Jackman J, Ehrlich YH (1988) ATP secretion and extracellular protein phosphorylation by CNS neurons in primary culture. Brain Res Bull 21:459-464.

Zhang Q, Powers ET, Nieva J, Huff ME, Dendle MA, Bieschke J, Glabe CG, Eschenmoser A, Wentworth P, Jr., Lerner RA, Kelly JW (2004) Metabolite-initiated protein misfolding may trigger Alzheimer's disease. Proc Natl Acad Sci U S A 101:4752-4757.

Zheng H, Koo EH (2006) The amyloid precursor protein: beyond amyloid. Mol Neurodegener 1:5.

Zhu G, Liu Y, Shaw S (2005) Protein kinase specificity. A strategic collaboration between kinase peptide specificity and substrate recruitment. Cell Cycle 4:52-56.

Zougman A, Pilch B, Podtelejnikov A, Kiehntopf M, Schnabel C, Kumar C, Mann M (2008) Integrated analysis of the cerebrospinal fluid peptidome and proteome. J Proteome Res 7:386-399.

ACKNOWLEDGEMENTS

This work was carried out during February 2005 to April 2009 at the department of Neurology/Molecular Cell Biology, University Clinic Bonn, Germany. I would like extend my deepest gratitude to my mentor, Prof. Dr. Jochen Walter for his excellent guidance, valuable discussions and for all the support rendered throughout the study. Most of all I thank him for giving me an opportunity to carry out this study and grooming my research capabilities.

I am grateful to Prof. Dr. Michael Hoch for his willingness, support and accepting himself has my Ph.D thesis examiner. I am also thankful to Prof. Dr. Jörg Höhfeld and PD. Dr. Gerhild van Echten-Deckert for their valuable time.

I would like to thank Prof. Dr. Klaus Beyer, Dr. Markus Zweckstetter and his colleagues who were instrumental in assisting me in carrying out the biophysical studies. I thank Prof. Dr. Michael Heneka and his team for the help rendered in conducting experiments with mice and Prof. Dr. Dietmar Thal for his help with immunohistopathological studies. I thank Prof. Dr. Michael Hoch for giving me an opportunity to work in his laboratory and his team for the help and assistance in developing transgenic *Drosophila* which is currently under in progress. I deeply appreciate their time, invaluable discussions and support. I am also grateful to Prof. Dr. Elmar Heinzle for his support and guidance in helping me pursue my career goals.

Many people have contributed to the development my academic career over the years. I want to thank all my teachers from school till university who encouraged me and had faith in my capabilities and endeavor. I am also grateful to wider scientific community, their intriguing research which motivated me and helped me in directing my work in a right way.

Working in the lab would not have been easier for me if not the charm and support of my fellow colleagues. I deeply appreciate the help of my former colleagues Dr. Kai Prager, Dr. Natasa Kukoc, Dr. Tina Wahle, Dr. Magdalene Sastre and present colleagues Heike, Esther, Martin, Patrick, Julieta, Jessica, Leonie, Sonja, Dr. Irfan Tamboli and Dr. Thorsten Muller. I sincerely thank all of them for their discussions, advice, critical comments and time and for offering a very conducive environment in the lab, making it a home away from home. Special thanks also goes to my all my friends who have lent their helping hands whenever needed.

I owe my sincere gratitude to Mr. Peter Steinbach and Mrs. Genoveva Steinbach for their moral support, guidance, unwavering love and constant encouragements and making my stay at Germany unforgettable.

Last but not the least, I would like to extend my deepest gratitude to my family, especially my father, mother, sister and my relatives for their boundless love, moral support, endurance and encouragement to pursue my interests. Without the support of all the above, this work would not have been possible.

Declaration

I solemnly declare that the work in this thesis is original results of my own investigation, except where otherwise stated. I have carried out the work at the department of Neurology, Molecular Cell Biology, University Clinic Bonn, under the supervision of Prof. Dr. Jochen Walter and in partial fulfillment of the requirements of the Doctor of Philosophy degree of the University of Bonn. I further declare that this work has not been submitted to any university or institution towards the partial fulfillment of any degree.

Sathish Kumar H.S.
April, 2009